STUDIES ON SOLID-LIQUID INTERFACIAL PARAMETERS OF ZIRCON IN RELATION TO ITS FLOTATION RESPONSE

A Thesis Submitted
In Partial Fulfilment of the Requirements
for the Degree of

DOCTOR OF PHILOSOPHY

BY

SHARAD GOVINDRAO DIXIT

to the

DEPARTMENT OF METALLURGICAL ENGINEERING

INDIAN INSTITUTE OF TECHNOLOGY KANPUR

MAY 1971

CERTIFICATE

Certified that the work reported in this thesis has been carried out under my supervision and has not been submitted elsewhere for the degree.

A.K. Biswas

(A.K. Biswas)
Associate Professor
Department of Metallurgical Engg.
Indian Institute of Technology, Kanpur

ACKNOWLEDGEMENTS

I express my deep gratitude and appreciation for Prof. A.K. Biswas under whom this work destined to successful completion. His lively interest, constructive criticism and all round guidance have gone a long way in shaping this dissertation in its present form. His constant encouragement and amiable counsel were the sustaining factors throughout the course of these investigations.

I greatfully acknowledge the help rendered by Dr. S.D. Phatak, Mr.V.K. Bansal and Mr. Kapil Deo from time to time.

I am pleased to mention with thanks the cooperative spirit exhibited by Mr. S.P. Nigam of the Physics Department during the course of tracer studies.

I appreciate Mr. Siddiqui of the Department of Chemistry for his willing assistance in recording infrared spectra, Mr. J.K. Misra for elegant typing and Mr. B.B. Srivastava for his graphic skills.

I express my fascination for all my colleagues in the Metallurgical Engineering Department whose love and affection for me had always been overwhelming.

S.G. DIXIT

CONTENTS

LIST OF TABLES

LIST OF FIGURES

Figure No. Page

Figure No. Page

Figure No. Page

SYNOPSIS

STUDIES ON THE SOLID-LIQUID INTERFACIAL PARAMETERS OF ZIRCON IN RELATION TO ITS FLOTATION RESPONSE

A Thesis Submitted
In Partial Fulfilment of the Requirements
For the Degree of
DOCTOR OF PHILOSOPHY
by
S.G. DIXIT
to the
Department of Metallurgical Engineering
INDIAN INSTITUTE OF TECHNOLOGY, KANPUR
May, 1971

The investigations on the flotation behaviour of zircon ($ZrSiO_4$) with sodium oleate as the collector and NaF, Na_2SiO_3 and Na_2SiF_6 as moderators are being reported in this dissertation.

With the help of adsorption and electrokinetic measurements and infrared spectra, it has been concluded that the sodium oleate adsorption on the zircon surface is mainly due to van der waal's attractive forces between the hydrocarbon chains.

A mathematical model to quantitatively characterise the pH dependence of flotation recovery has been given.

An equation to express the functional relationship between oleate adsorption density (Γ_{01}) and pH (or $[H^+]$) has been obtained. It fits the experimental data remarkably well.

The correlation between the flotation recovery and adsorption as well as zeta potential in the zircon-sodium oleate system has been illustrated. It has been shown that the two phase solid-liquid interfacial parameters such as the adsorption density and zeta potential are in general correlative with the flotation recovery values.

The critical contact phenomenon is illustrated with the help of Γ_{OH} vs. pH and ζ vs. pH plots. The critical significance of the $[Ol^-]/[OH^-]$ ratio has been brought out.

In case of zircon-sodium oleate-moderator system, small additions of NaF, Na_2SiO_3 and Na_2SiF_6 induce distinct activation. It is proposed that the adsorption of Na^+ ion causes greater adsorption of collector species by decreasing the repulsion between the ionic heads of the hydrocarbon chains. This results in enhanced flotation recovery.

At relatively large additions of Na_2SiO_3 and Na_2SiF_6, the usual depression effect is obtained. However, NaF has been found to be a very poor depressor for zircon.

From the constancy of $(\Gamma_{Ol} + \Gamma_{NaF})$ and $(\Gamma_{Ol} + \Gamma_{Na_2SiO_3})$, it has been concluded that over a limited range of NaF and Na_2SiO_3 concentration, the absorption sites on the zircon surface are common for the collector and the moderator species.

CHAPTER I

INTRODUCTION

Froth flotation has become one of the most important and useful separation processes in the mineral industry, since its advent during the beginning of this century. In essence, it consists of the attachment of air bubbles to the mineral particles in the pulp and their subsequent removal with the froth formed on the surface of the pulp. This bubble attachment is effected by certain surface active reagents which render the naturally hydrophillic surface of the minerals hydrophobic. Thus, separation of solids by flotation is characterised by the establishment of contact among three phases. These three phases are the solid to be floated, an aqueous electrolyte solution and a gas, mostly air.

It is necessary to study the chemical and physical properties of the three interfaces solid-liquid, solid-gas and liquid-gas in order to gain a full understanding of the process. This has been aptly brought out by P. Som Sundaran (1) in one of his recent papers. However, it is the solid-liquid interface that has attracted more attention; and the flotation results are often explained on the basis of solid-liquid interfacial parameters. In fact, D.W. Fuerstenau (2) has shown that the two phase interfacial properties such as adsorption density and zeta

potential are correlative with the three phase contact processes such as contact angle and flotation. This parallelism between solid-liquid interfacial parameters and flotation behaviour was subsequently brought out by many other workers for different flotation systems (3,4). Naturally, studies concentrated on solid-liquid interfacial measurements have special significance in flotation research.

During the last forty years, considerable efforts have been put in to selectively float different minerals with the help of a variety of collectors and modifiers and also to understand the mechanism of collection and modulation. Simultaneously, advances have been made in other branches of surface chemistry and in the development of a series of experimental techniques such as contact angle, radioactive tracers, infrared spectra, electron diffraction and electrochemical methods of investigation. Outstanding success has been achieved through these studies as regards the fundamental aspects of the sulphide flotation (5, 6). However, the progress made in the selective flotation of nonmetallic minerals and the scientific understanding of the processes involved has been rather slow.

I-1 FLOTATION OF NONMETALLIC MINERALS:

This class of minerals include metal oxides, silicates, carbonates, phosphates, sulphates etc. F.F.Aplan and D.W. Fuerstenau (7) have tried to rationalise the available body of information upto 1962 on the flotation behaviour of

nonmetallic minerals in terms of crystal structure, surface properties and adsorption mechanisms. It has been maintained that a study of the effect of electrical forces superimposed on the chemical adsorptive forces leads to better understanding of the flotation behaviour of non-metallic minerals.

Both the hydrocarbon chain and the ionic head determine the collection abilities of the anionic collectors (7) while the ionic head determines the ionisation properties as also the closeness of approach to the mineral surface, the hydrocarbon chain determines the extent of hydrophobicity that a collector is capable of imparting when adsorbed on the mineral surface. P.F. Pilpel(8) has reviewed recently the role of fatty acid soaps as flotation collectors. These collectors are very common in nonmetallic mineral flotation.

The nature of the mineral surface and the crystal structure of the minerals affect the flotability of the minerals. A.M. Gaudin et.al. (9) systematically studied the structural attributes of flotability and concluded that the intrinsic hydrophillic nature of most of the minerals is due to the presence of ionic sites at the surface above a certain threshold value.

T.W. Healy et. al.(10) have interpreted differences in the zero point of charge (zpc) in terms of the atomic packings of various crystals in case of manganese dioxide.

The electrochemical nature of the flotation process was realised quite earlier (11,12) and there have been many systematic studies on particular systems (13,14,15).

A complete description of the physical chemistry of flotation also involves the solubility relationships and the complex ionic equilibria. Since the work of Garrels (16) and Pourbaix (17) on the pH-concentration diagrams the equilibrium data have been increasingly made use of in the interpretation of the flotation results (18, 19).

The charged condition of the mineral surface when brought in contact with aqueous solutions plays an important role as to the nature of the collector to be used. G.A. Parks (20,21) has studied the zero point of charge and potential determining role of H^+ and OH^- ions for many oxides, silicates and carbonates. In general, below the zpc, an anionic collector is efficient since the surface is positively charged, whereas a cationic collector is desirable above zpc.

The nature of compounds, if any, formed at the surface has been investigated by infrared spectroscopy since 1956. The work of M.E. Wadsworth and coworkers (22,23,24) has been pacesetter in this regard.

A few systematic studies have been made on the modulation of collection of non-metallic minerals (25,26). Since the number of modifiers used is quite large, much remains to be done to gain some insight into the action of the modulators. Also,

as far as, the quantification of the results is concerned, little progress has been achieved so far.

Experimental correlation between zeta potential and adsorption density has been clearly brought out in many cases (2,15,27). However, no suitable quantitative relationship has been proposed.

Also, very few studies on the quantitative aspect of variation of flotation recovery and adsorption density with respect to pH have been conducted. The work on graphite-fatty acid soap system (28) using Langmuirian approach is worth noting in this regard.

I-2 FLOTATION BEHAVIOUR OF SILICATE MINERALS:

Silicates are quite conspicuous by their ubiquitousness. Silicon is one of the most abundant elements in the earth's crust, and it is invariably present in the form of numerous silicates possessing variety of structures. The basic structural unit of all the silicates is the SiO_4 tetrahedron in which the silicon atom is located in the centre of the four tetrahedrally coordinating oxygen atoms. The linkage of silica tetrahedra which occurs in a number of ways in different silicate types, determine the breakage characteristics of the minerals.

Joy and coworkers (29) have classified the silicate minerals according to their flotation response into two classes.

In the first are included the framework structures with —Si—O—Si— links extending in three dimensions. These silicates do not have good cleavage properties and when cleaved, Si—O bonds are invariably broken thus presenting >Si—O^- sites. These sites invite cationic collectors which get adsorbed on the mineral surface. Anionic reagents on the other hand induce very poor flotation response. Quartz and Feldspar belong to this category. In the second type of silicates, the SiO_4 tetrahedra form separate groups rings or chains. The breakage mode of these silicates is such that polysilicate groups are preserved as far as possible. This means that other M—O bonds are broken in preference to Si—O bonds. As a result, high energy cationic sites (M^{+z}) are exposed on which anionic reagents get adsorbed. Andalusite, Beryl and Spodumene represent this class of silicates.

D.W. Fuerstenau et. al.(30) have studied three different aluminosilicates: sillimanite, andalusite and kyanite having the same chemical composition (Al_2O_3, SiO_2) but different crystal structures and varying ratio of the number of Si—O and Al—O bonds. The authors found that the ratio determined the surface properties of the above minerals. The crystallographic properties of the mineral, determine the coordination numbers of Al and Si, cleavage characteristics and density of various solids as also the Al to Si atom ratios on the surfaces of different minerals. The surface properties could be altered by procedures

that altered the Al to Si ratio at the surface. Thus, the zero point of charge shifts to lower pH values when the Al_2O_3 is preferentially leached out of the surface.

R.A. Deju and R.B. Bhappu (31,32) have studied the surface properties of the silicates with respect to zpc and H^+ ion adsorption. They have established that higher the oxygen to silicon ratio in the silicate the more is the hydrogen ion adsorption in acidic pH and the more is the zpc. A chemical interpretation of these results in terms of exchange of metal cations and hydrogen ions has been given to account for the above findings.

I-3 FLOTATION STUDIES ON ZIRCON ($ZrSiO_4$):

As far as zircon is concerned, there have been quite a few investigations regarding its flotation behaviour with various collectors and moderators. The earlier studies were mostly confined to selectively float zircon from its companion minerals in the beach sands which is their natural abode. Thus in 1934, zircon was separated by soap solution in Australia and elsewhere (33,34). In 1939, W.R. Poole (35) gave a flotation scheme to separate zircon from rutile and ilmenite. G. Gutzeit and P. Kovalive (36) introduced sodium silicate as a depressor in the flotation of the beach sand minerals including zircon. G.V. Subramanya (37) suggested an alkaline circuit (pH 11.5) instead of usual acid circuit and employed mixed collectors (sodium oleate + sodium stearate) at elevated temperatures from 65°C to 95°C.

In India, work has been done on sand deposits of Travancore in Kerala, which contained amongst others 4-6 percent zircon (38). Nayak (39) studied the flotation behaviour of zircon with sodium oleate as collector and alizarin red-S as depressant. K.M. Pai et.al. (40) employed sodium linoleate and linolinate as collectors and sodium silicate as depressor. T.R. Madhavan et.al. (41) further continued these studies to develop schemes for flotation of beach sand deposits.

In Russia, I.N. Plaksin and coworkers (42,43,44,45,46) conducted the studies on the flotation of zircon. The role of oxygen as activator, sodium fluosilicate as depressor, influence of halide ions on the state of emulsified oleic acid in conditions of flotation were investigated. It was found that oxygen activates the mineral surface of the titanium and zirconium minerals and significantly accelerated mineral conditioning for flotation. Emulsified oleic acid improves the flotation activity but decreases the selectivity. Halides were used to change the stability of the emulsion. The stability was decreased with the addition of halides.

Of late, there have been some studies on the physicochemical aspects of zircon in relation to its flotation response. J.M. Cases (47,48) has shown that in case of sodium dodecyl sulfate and dodecyl ammonium chloride of zircon, the chemical affinity of collector ions for the surface is negligible. The interaction is predominantly electrostatic in nature.

D. Salatic (49) has studied the zeta potential and flotability of zircon with dodecyl amine acetate in the presence of modifiers Na_2SO_4, Na_2SiO_3, and $Na_4P_2O_7$. D.V. Salatic (50) attempted to explain the mechanism of amyl xanthate action on zircon preactivated by sulphuric acid in terms of the following reactions.

For activation with sulphuric acid, the reaction

$$Zr^{4+} + HSO_4^- = ZrSO_4^{2+} + H^+$$

was suggested. When amyl xanthate ions are adsorbed at the activated surface the following reaction was believed to occur.

$$Zr^{4+}\ SO_4^{2-} + nK^+nAX^- = (ZrAX_n)^{n-4} + K_2SO_4 + (n-2)K^+$$

This type of mechanism was supported by the reversal of the sign of the zeta potential from the positive to the negative side on addition of xanthate. However, the above mechanism does not explain the similar case of monazite flotation investigated by the above author. No charge reversal on xanthate addition was observed in case of monazite.

The present author (51) has studied the pH dependence of flotation and collector adsorption on zircon and other beach sand minerals. The experimental behaviour was seen to be adequately explicable in terms of oleate ion adsorption and competition of oleate and hydroxyl ions for getting adsorbed on the mineral surface.

From the literature survey it is evident that no detailed investigation has been made on the role of sodium oleate as a collector for zircon and the effect of modifiers like NaF, Na_2SiO_3 and Na_2SiF_6.

I-4 PHILOSOPHY OF THE PROBLEM:

The present investigations are inspired by the need to rationalise the flotation behaviour of a vast majority of silicates in terms of their crystal structure as also the reagent types. This in its entirety is a big task and requires studies on a number of individual silicates before the problem can be tackled with sufficient scientific maturity. However, as a part of this stupendous task, an attempt has been made to study the physicochemical parameters affecting the flotation of zircon which represents the class of orthosilicates. It is hoped that this would add to our understanding of the flotability of zircon in particular and silicates in general. Similar studies on individual beach sand minerals associated with zircon, are likely to establish rational procedures for beneficiation by flotation.

I-5 STATEMENT OF THE PROBLEM:

Solid-liquid interfacial parameters e.g. adsorption density, electrokinetic properties etc. of zircon in relation to its flotation response have been investigated on the following points:

1. Electrokinetic behaviour of zircon in aqueous solutions of variable and constant total ionic concentrations.

2. Flotation, adsorption, electrokinetic and infrared investigations on the zircon - sodium oleate system and their mutual correlation.

3. Effect of pH and temperature on the adsorption of sodium oleate on zircon.

4. Mathematical models for the pH-dependence of flotation recovery and adsorption density.

5. Critical contact phenomena in the zircon-sodium oleate system.

6. Modulation of collection of zircon by Na_2SiO_3, NaF and Na_2SiF_6.

7. Effect of the moderators on the adsorption, electrokinetic and flotation behaviour of zircon and their mutual correlation.

In brief, determination of the flotation properties of zircon in various collector-moderator systems and correlation of the same with the fundamental solid-liquid interfacial properties of the above systems were contemplated to be the objectives for this dissertation.

CHAPTER II

EXPERIMENTAL TECHNIQUES

In the present work, the surface chemical properties of zircon in the presence of different aqueous solutions have been investigated with the help of flotation experiments, adsorption measurements using tracer technique, electrophoretic mobility studies and infrared spectroscopy. In this chapter, a short resume of these experimental techniques along with the details of the equipments is given.

II-1 FLOTATION CELL ASSEMBLY:

Flotation experiments were conducted in an all glass laboratory flotation cell shown in Fig. 1. It consists of a tapered glass vessel. Near the bottom of the vessel is fixed a sintered glass disc which admits air coming through the inlet at the bottom. In the lower part of the cell below the disc, an outlet for the liquid that might trickle down on long standing is provided. In the upper part of the cell is provided an outer vessel for collecting the overflowing froth which could subsequently be removed through the froth outlet. A glass stirrer is provided from the top for efficient stirring. Air is drawn to the cell from a compressor through a gas regulator. Performance of the cell for reproducibility was tested with the calcite flotation under regulated conditions. The results are

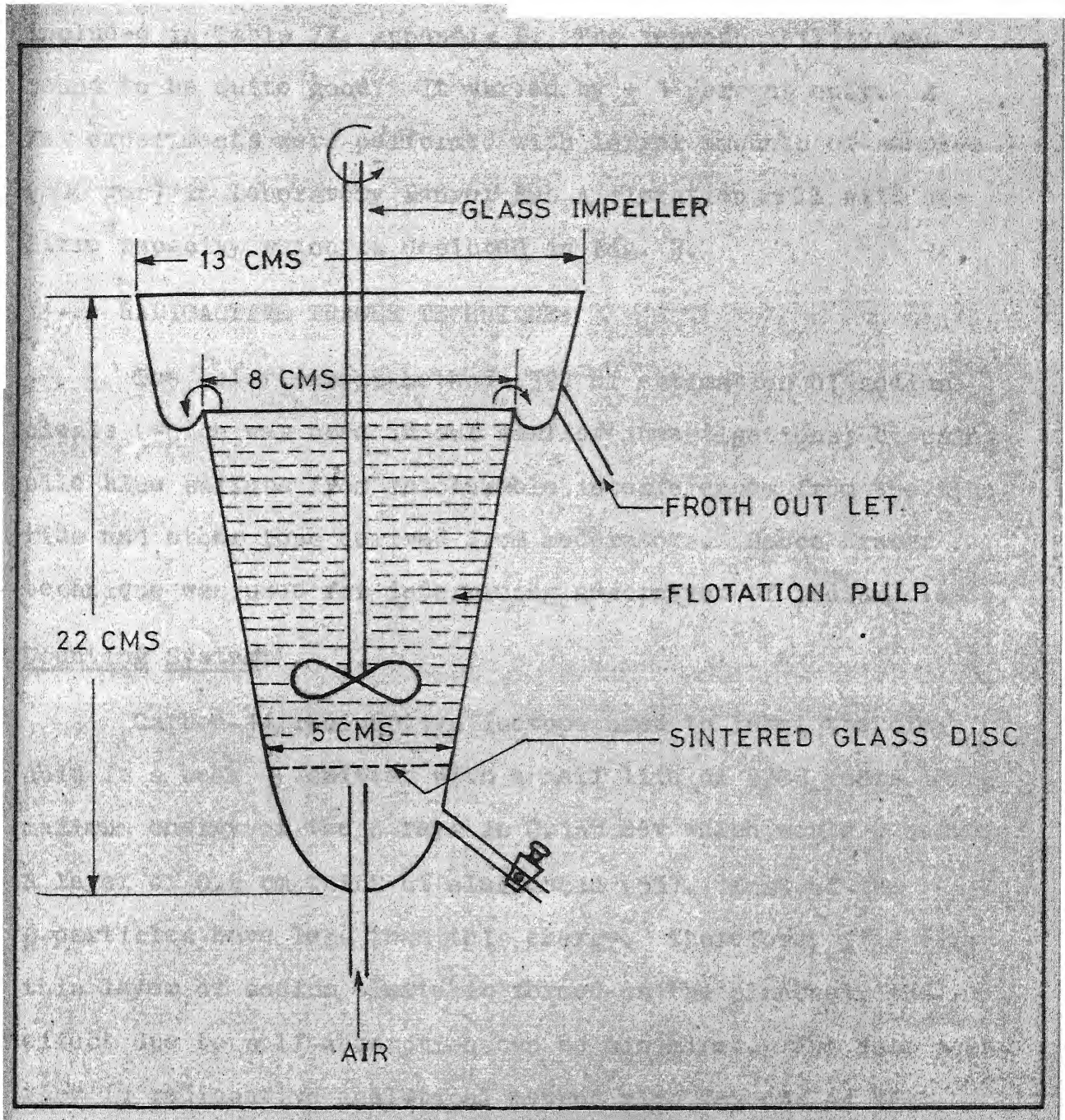

FIGURE 1 LABORATORY GLASS FLOTATION CELL

included in Table IX, Appendix D. The reproducibility was found to be quite good. It varied by ± 1 percent only. A few experiments were performed with larger amounts of samples (100 gms) in laboratory Denver Sub A flotation cell with one litre capacity which is depicted in Fig. 2.

II-2 RADIOACTIVE TRACER TECHNIQUE:

The colorimetric method (52) of estimation of sodium oleate (which was used in our earlier investigations) by using nile blue suffers from intolerable interferences from the fluoride and other ions derived from moderators. Hence tracer technique was used for determining adsorption of sodium oleate.

Counting System:

Carbon-14 radioactive isotope used to label the oleic acid is a weak β-emitter with a half life of 5700 years. The maximum energy of the β-rays is 0.155 mev which would penetrate a layer of 0.2 cm thick of oleic acid (53). Most of the β-particles have less than this energy. Therefore, if a very thin layer of sodium oleate is formed on the planchet, the effect due to self-absorption can be minimised. The best accuracy in radioactive analytical method also depends on high count rate of the experimental sample with respect to background, reproducible geometry and stable behaviour of the counting device. In the present determinations, the Geiger-Muller counting system with end window detector (type I-1030 supplied by Electronic Corporation of India, Hyderabad) has been used.

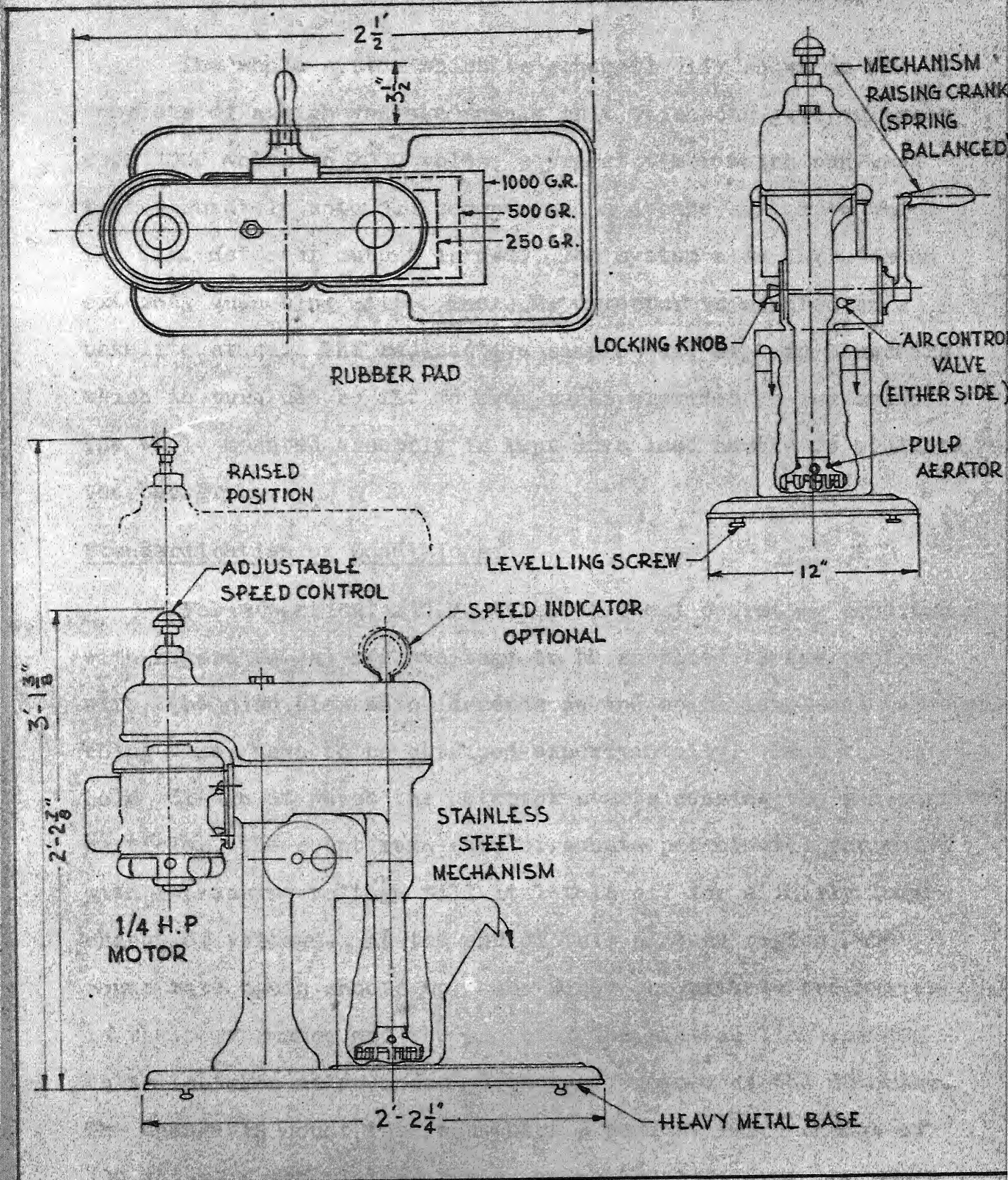

FIGURE 2 DENVER FLOTATION CELL

The whole system which is schematically shown in Fig.3, consists of a high voltage supply unit which can give voltages from 1000 volts to 2000 volts; a preset timer which can read time accurately upto 0.1 seconds and a decade scaler to which the G.M. detector output is fed. The system also includes an external quenching unit. The G.M. detector is mounted on a bakelite stand. The radioactive samples are kept in planchets which in turn can be fitted over racks provided in the stand. The whole mounted assembly is kept in a lead castle to minimise the background.

Standardisation of Conditions:

For a particular G.M. tube, the best operating conditions with regard to (a) high voltage to be supplied to the central wire, (b) disc bias which depends on the noise level and (c) quenching time, have to be obtained experimentally. From the threshold voltage at which the detector starts sensing the radioactive particles, the count rate (No. of counts per minute) increases with increasing voltage till it levels off for a fairly large change of voltage. At the end of this plateau region, the count rate again shoots up. The wider the plateau the better is the performance and the slope of the plateau line per 100 volts is taken as an index of the performance of the detector. The change in count rate was about 5 percent for a change of 100 volts in the plateau region as was specified by the manufacturers(Fig. 4).

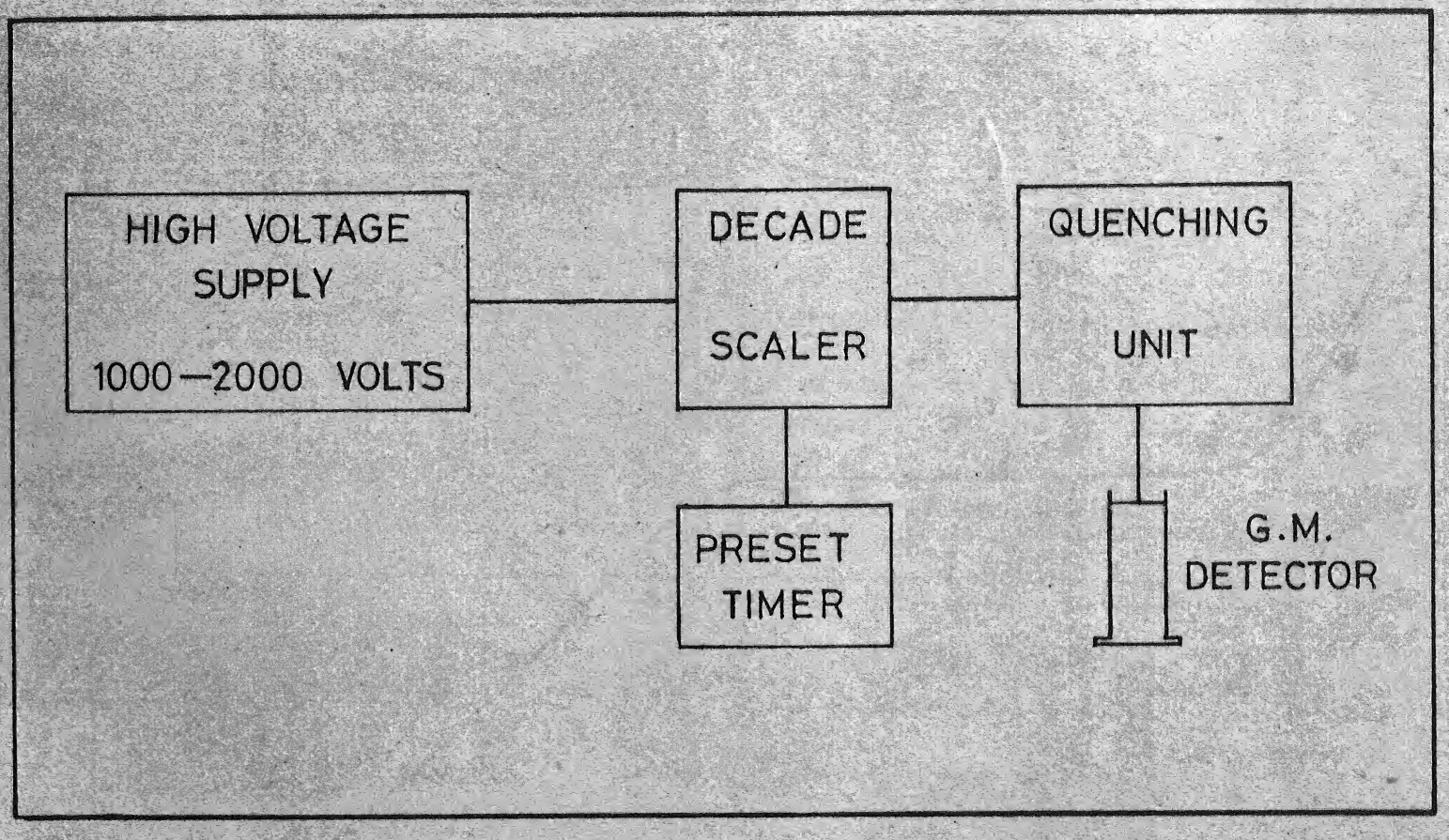

FIGURE No.3 SCHEMATIC DIAGRAM OF THE COUNTING SYSTEM

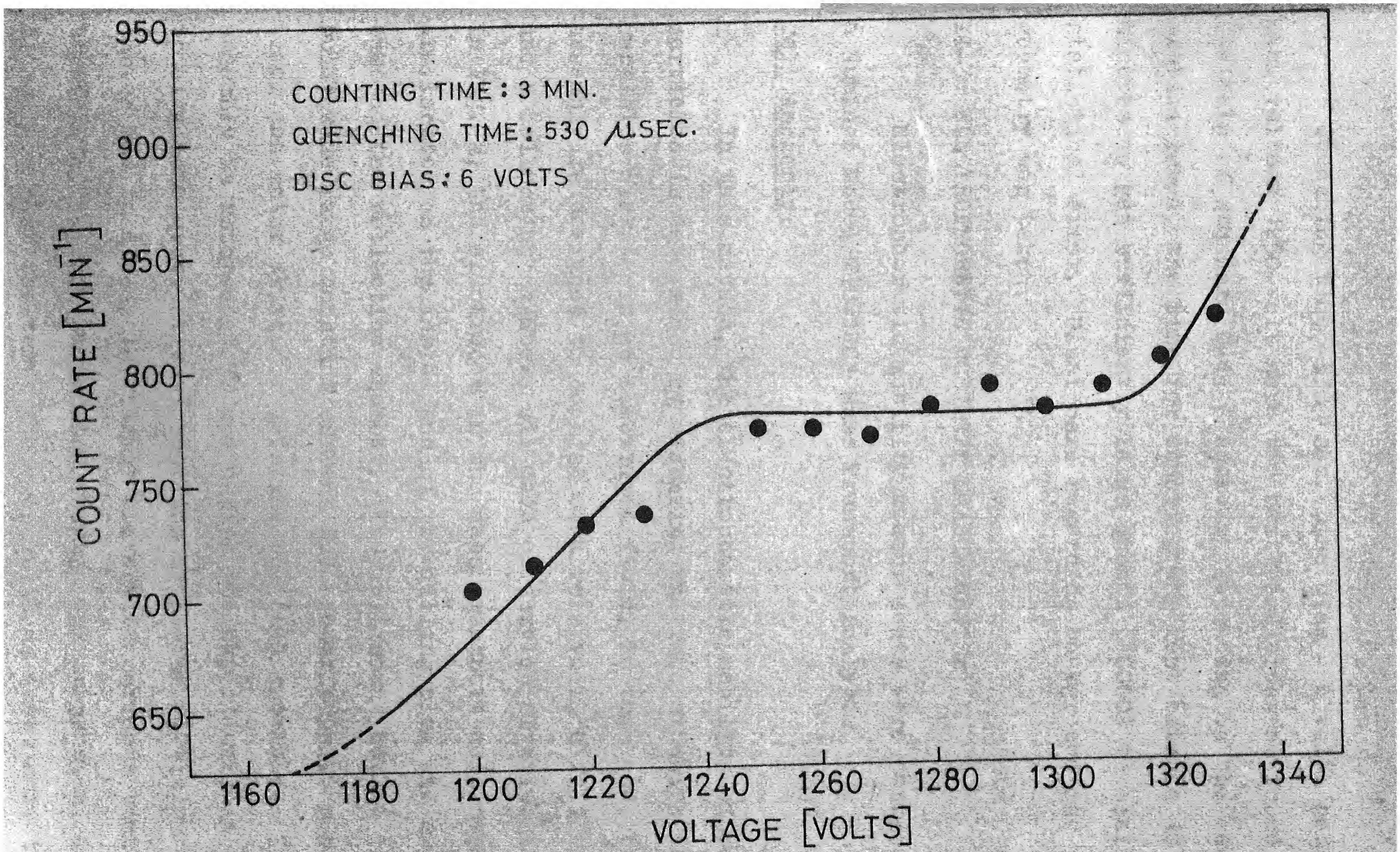

FIGURE 4 CHARACTERISTIC CURVE FOR THE G.M DETECTOR

Quenching time -530 μ sec. Disc bias - 6 volts and filament voltage 1250 volt were the best conditions as found with the help of standard C-14 β source. Depending on the concentration level, the time for counting was kept between 10 - 30 minutes to get sufficiently large counts (10000) to minimise statistical error. Usual care regarding background and fixed geometry was taken.

II-3: ELECTROPHORETIC MOBILITY MEASUREMENTS:

Electrophoretic mobility measurements were carried on a Numinco Model MIC-1201 Mass Transport Analyser.

Cell Assembly:

In this method, the electrophoretic mobility of solid particles is determined by measuring the rate at which the particles migrate in an electrical field. To this end, the whole assembly is designed to consist of a reservoir, a filling plug and a collection chamber, all made of acrylic plastic. As shown in Fig. 5, the electrodes in the mass transport cell assembly are located on the inside end of the filling plug and at the base of the collection chamber. The instrument has an in-built wide range constant current D.C. power supply, a preset timer and motor drive for rotating the cell assembly. The cell assembly is rotated at 30 rpm during the experiment, in order to eliminate gravitational settling of coarse particles as a factor and to dissipate thermal convection currents that may be created by the current passing through the suspension. Calculations show that the temperature increase is never more than $1^{o}C$

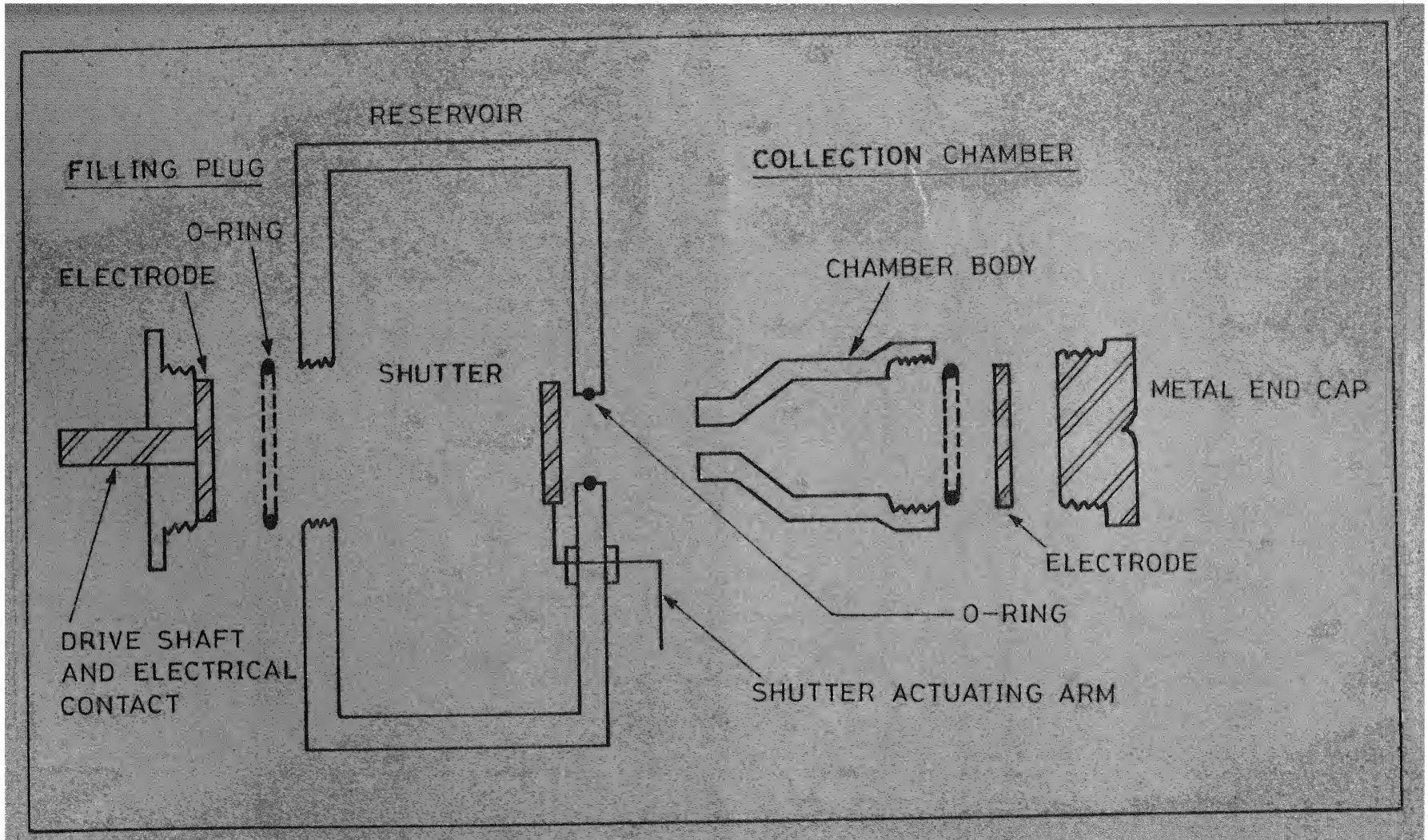

FIGURE 5 SCHEMATIC DIAGRAM OF THE MASS TRANSPORT CELL ASSEMBLY

Quantitative Relationship:

To relate the change in the mass of the contents of the collection chamber (See Fig. 5) to electrophoretic mobility, suitable mass balance equations have to be set up.

Let,

V - velocity of the particles in cm. $sec.^{-1}$

A - cross sectional area of chamber entry in cm^2

M - concentration of solids in $g\text{-}cm^{-3}$ of suspension.

Thus, the mass of the solids entering the chamber per second can be written as,

$$\frac{W_1}{t} = VAM \qquad (II.1)$$

As solids enter, they displace an equivalent volume of suspending liquid. Therefore, the mass of the liquid leaving the collection chamber per second can be written as,

$$\frac{W_2}{t} = VAM \ \delta_w/\delta_s \qquad (II.2)$$

where δ_s and δ_w are the densities of the solid and the suspending liquid respectively. Therefore, the net charge in the mass of the liquid is given by,

$$\Delta W = W_1 - W_2$$

so that,

$$V = \frac{\Delta W \ \delta_s}{tAM \ (\delta_s - \delta_w)} \qquad (II.3)$$

The velocity of the solid particles V, as given by Eqn. (II.3) is the result of two components: the electrophoretic

velocity V_e, of the particles in the chamber and the velocity in the opposite direction of the liquid coming out of the chamber V_w. Under conditions of steady state flow, it can be written that,

$$V = E V_e - V_w \qquad \text{(II.4)}$$

where E is the potential gradient in volts cm^{-1}, V_e is expressed in cm $sec.^{-1}$/volt cm^{-1} and V_w is in cm sec^{-1}.

The velocity of the liquid V_w, can be determined from the amount of liquid displaced and effective cross-sectional area of the cell entry. Thus,

$$V_w = \frac{V A M}{\delta_s A(1 - M/\delta_s)} \qquad \text{(II.5)}$$

Substituting Eqns. (II.5) and (II.3) in Eqn. (II.4), and setting $M/\delta_s = \emptyset$, the volume fraction of dispersed phrase, we get,

$$V_e = \frac{\Delta W}{tEA\ \emptyset(1-\emptyset)(\delta_s - \delta_w)} \qquad \text{(II.6)}$$

The potential gradient, E can not be reliably determined from the overall applied potential because of polarisation effects and because of the change in cell resistance caused by the deposition of solids on the electrode of sign opposite to that of the particles. However, by maintaining a constant current during the course of the experiment, the effective voltage gradient at the entrance to the chamber can be computed from the current i, the area A, specific conductance, λ .

Thus,

$$E = i/\lambda A \qquad \text{(II.7)}$$

Hence,

$$V_e = \frac{\Delta W \times \lambda}{ti\ \phi(1-\phi)(\delta_s-\delta_w)} \qquad \text{(II.8)}$$

Eqn. (II.8) gives us the relationship between the weight change in collection chamber and the electrophoretic mobility in terms of other measurable quantities, and is used for computing the electrophoretic mobility from the experimental data.

Calculation of Zeta Potential:

The zeta potential, which is defined as the electrical potential in the shearing plane between the fixed and flowing liquid, may be calculated from the Helmholtz-Smoluchowski equation

$$\zeta = \frac{4\ V_e\ \pi\ \eta}{D} \qquad \text{(II.9)}$$

where,

ζ - zeta potential

D - dielectric constant

η - viscosity in poise

If V_e is expressed in micron sec^{-1}/volts cm^{-1}, ζ in millivolts can be written for water at 25°C as,

$$\zeta = 13\ V_e \qquad \text{(II.10)}$$

The Helmholtz-Smoluchiwoski equation is strictly valid under the following assumptions and conditions (55).

i) The particles are non conducting and for these, radius of curvature at any point is large as compared to the extension of the double layer.

ii) The surrounding liquid is assumed to have an electrical conductance, dielectric constant and viscosity equal to that in the bulk phase.

iii) The distribution of charges in the ionic double layer is not affected by the applied field.

iv) No surface conductance effect is involved. The validity of the equation, however, does not depend on the shape of the particle.

II-4 INFRARED SPECTRA OF SURFACE SPECIES:

Though infrared spectroscopy has been quite popular amongst structural chemists because of its utility in elucidating molecular structures, its application to the surface chemical problems is quite recent.

This is so especially in case of adsorbed species on the solid surface from aqueous solutions. Special sample preparation is required so that sufficient amount of solute may be adsorbed and the surface species is suitably detected by infrared spectra. Secondly the collector molecules that may be adsorbed on solids in flotation systems are usually long chain molecules. Because of this, van der waal's forces between adsorbate molecules are considerable, and adsorption may not be

restricted to monolayer coverage only. It may not then be possible to distinguish (by infrared spectroscopy) the first layer adsorbed from the overlaying multilayers. Adsorption in such a case, in general, is less well characterised than adsorption of smaller gas molecules.

Moreover, because of the greater molecular size, the infrared spectra will be less complete. Important bands indicating the modes of adsorption may be masked by other less characteristic bands. Also, there is every possibility of the solvent molecules interacting with the surface along with the solute. Thus the intense solvent bands might mask bands of the adsorbed solute.

In spite of these difficulties, this technique has proved to be of great help in studying the flotation systems. The details of the various applications of infrared spectroscopy in the investigations of the surfaces have been covered in details in two recent monographs (56,57). It would be worthwhile to mention here the concept of group frequencies which has proved to be one of the most important qualitative contributions to infrared spectroscopy. According to this concept, one can assign a characteristic frequency to the stretching as well as bending modes of the group and it will mostly lie in a very narrow region in all compounds in which the group is present. Excellent confirmatory evidence is supplied by the works of Mecke (58), Van Vleck (59) and Herzberg (60) regarding the theoretical origins of the characteristic group frequencies.

Special Techniques for Surface Species:

The detection of surface effects requires that the solids have large surface areas and that the particles themselves be less than approximately one micron in diameter (61) to minimise scattering of rays. In addition, the solid sample must be suspended uniformly and reproducibly for quantitative work.

Several techniques have been used in the past to study solid specimens. e.g. Nujol mull technique, placing solid samples between sheets of mica or polyethylene etc. However, the most popular of these techniques is that used by Stimson and O'Donnell (62) in which solid samples are thoroughly mixed with finely ground KBr. Discs are then pressed out in a vacuum die. It has been demonstrated that this way of suspending the solid is more convenient and reproducible (63). The transmittancy is also quite good. For quantitative studies, precautions regarding the reproducibility of the pellet dimensions and uniform distribution have to be taken.

In the present investigations, the KBr pellet technique and Perkin-Elmer 521 spectrometer have been employed for recording the infrared spectra of solids.

CHAPTER III

ANALYTICAL TECHNIQUES

In the series of investigations, various estimations have been made of the oleate, fluoride and silicate concentrations. Whereas the oleate and fluoride were estimated as such abundance of $SiO_3^=$ species was estimated in terms of the total and silicon concentration. The methods of estimation of Ol^-, Si^{4+}, and F^- individually or in the presence of one another are described below.

III-1 ESTIMATION OF SILICON:

Silicon was determined by forming yellow silicomolybdenum complex and then estimating colorimetrically (64,65).

Standard Silicon Solution:

Weighed quantity of powdered SiO_2 was treated with $HF + H_2SO_4$ acid mixture in a platinum crucible and evaporated to dryness. The weight of the original sample minus the weight of the residue represents the true weight of silica. An accurately weighed powdered sample was transferred to a platinum dish. 10 ml of redistilled water and 1 gm. of KOH pellets were added and the whole mass was gently heated till complete dissolution occurs. Working quickly, the hot mass was poured into 350 ml. of water and the dish was washed out in the beaker to

transfer material completely. The volume was made upto 500 ml and the solution obtained was stored in plastic bottles for further estimation.

Colorimetric Procedure:

Fresh ammonium molybdate solution was prepared by dissolving 10 gms. of the solid in 250 ml. redistilled water. It was then used to develop yellow color by adding to the experimental silicon solutions at pH 1.55-1.60 obtained by adding 0.15 ml of 50:50 H_2SO_4.

The blank prepared consisted of all the reagents except silicon solution. A wide range of wavelengths has been suggested in the literature (66,67) for the colorimetric estimation. After testing the complete range between 360 m μ to 420 m μ, 400 m μ was found as the suitable wavelength. An excellent straight line relationship between absorbance and concentration as required by Beer's law was obtained as shown in Fig. 6. Since, it is required to know the concentrations in the presence of the oleate, the effect of oleate was also noted. It was found that the usual small amounts of oleate 3m moles/lit. do not affect the determinations.

III-2 COLORIMETRIC DETERMINATION OF FLUORIDE:

The red cerous chelate of Alizarin Fluorine blue ($C_{14}H_7O_4 \cdot CH_2 \cdot N(CH_2COOH)_2$, mol. wt: 385.34) changes to blue in the presence of fluoride and is used for fluorine determinations. Of the many colorimetric methods available, probably

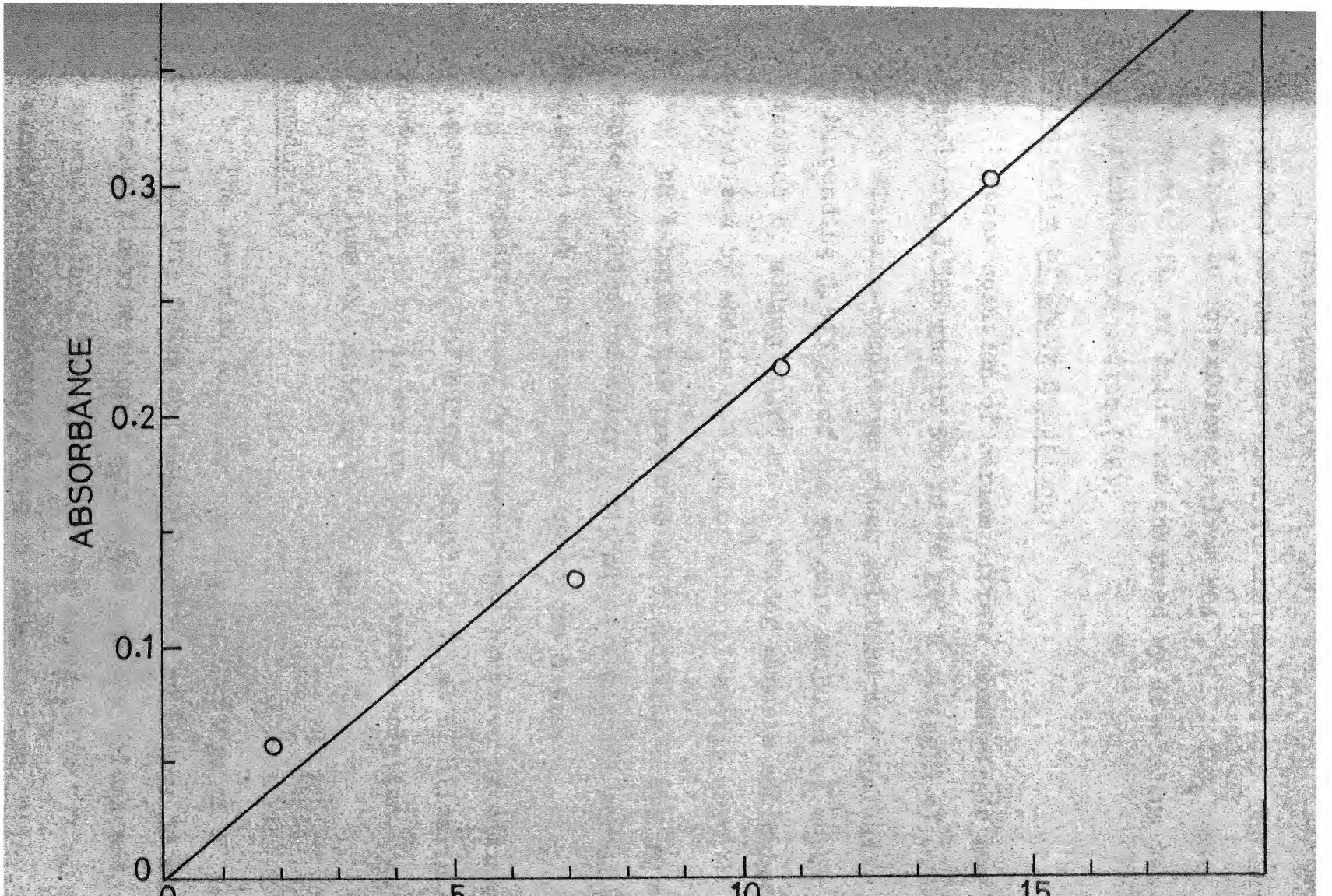

FIGURE 6 STANDARD CURVE FOR THE COLORIMETRIC ESTIMATION OF SILICON AS YELLOW MOLYBDATE

this method is the most specific and sensitive. The method is not subject to interferences from NO_3^-, Cl^-, ClO_4^- etc. Stability and sensitivity of color are enhanced by developing the color in acetone-water medium.(68).

Preparation of Stock Solutions:

Stock solution of cerium nitrate hexahydrate was made by dissolving 3.326 gms in 500 ml to get a strength of 0.0167 M.

Alizarin-complexone stock solution was similarly prepared by suspending 0.643 gm of the reagent in 50 ml of water. It was dissolved by adding 0.25 ml of strong ammonia and subsequently neutralised by adding 0.25 ml of glacial acetic acid.

pH 4 buffer was prepared by dissolving 6 gms of sodium acetate in 500 ml of water. 115 ml of a glacial acetic acid was added and the volume made up to one litre.

Composite fluoride reagent was prepared by mixing 330 ml of acetone, 68 ml of buffer solution, 10 ml of alizarin-complexon solution and 10 ml of cerium (ous) nitrate solution. After mixing the volume was made up to 500 ml.

Procedure:

The fluoride solution containing 1-25 μ gm of F^- was taken in a volumetric flask and neutralised if necessary 15 ml of the composite fluoride reagent was added and the volume made upto 50 ml with water. Transmittance was measured at 617 mμ after 20 minutes. The standard curve is shown in Figs. 7 (69,70). Small amounts of oleate do not interfere.

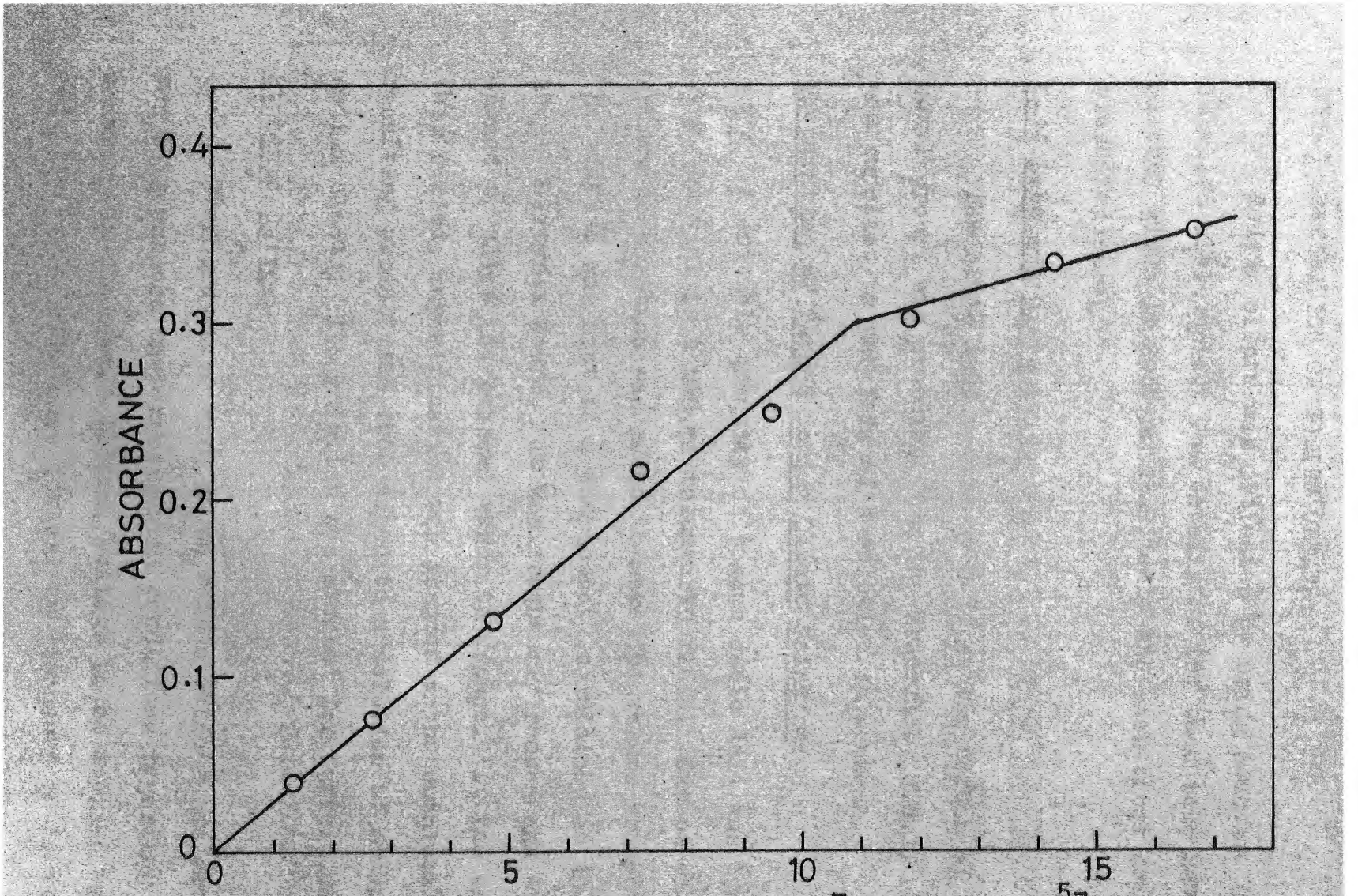

FIGURE 7 STANDARD CURVE FOR THE COLORIMETRIC ESTIMATION OF FLUORIDE WITH COMPLEXONE

III-3 ESTIMATION OF SODIUM OLEATE:

Sodium oleate was estimated by using β-active C-14 labelled oleic acid. The details of the technique have been already given in Section II-2, only the analytical details are presented here.

C-14 Labelled Oleic Acid:

The oleic acid tagged by C-14 at the carbon of the carboxyl group, was procured from the Tracerlab, U.S.A. The acid was supplied in the form of a solution in benzene.

Preparation of Tagged Sodium Oleate Solution:

A suitable quantity of tagged oleic acid was transferred from the vial to a 500 ml volumetric flask. Excess of sodium hydroxide solution was added to make the volume around 15 ml. The mixture was kept in a thermostat maintained at 40°C for about thirtysix hours. It was frequently shaken and the stopper opened to allow the benzene vapor to escape. At the end of this period, saponification was assumed to be complete. The resulting product was then added to a solution of ordinary sodium oleate. The solution was stocked for further use.

Standard Curve:

Standard curve with known concentrations was determined. For this purpose the experimental conditions regarding the geometry of the sample holder, voltage to be applied to filament etc. were fixed once for all as discussed in Section II-2.

The sample holder used was made out of perspex and was circular in geometry and about 1/8 inch deep. It could contain 2 ml. of the solution. Varying volumes of samples of tagged oleate solution (less than 2 ml.) were withdrawn from the stock solution and transferred to the planchet. To make the total volume 2 ml the balance was made up by adding ordinary sodium oleate solution of the same concentration to the planchet. The planchets were then kept in oven for about 10 hours at a temperature of 40°C. This time was found sufficient for water to evaporate. There was absolutely no loss of sodium oleate upto 60 hours as shown previously (53), The planchet was then directly transferred to the counting assembly. Total number of counts generally ranged between 8000-10000. Necessary background correction was made. The standard calibration curve thus determined is shown in Fig. 8. The standard calibration curves thus determined were used for estimation of solute in solutions of unknown concentration.

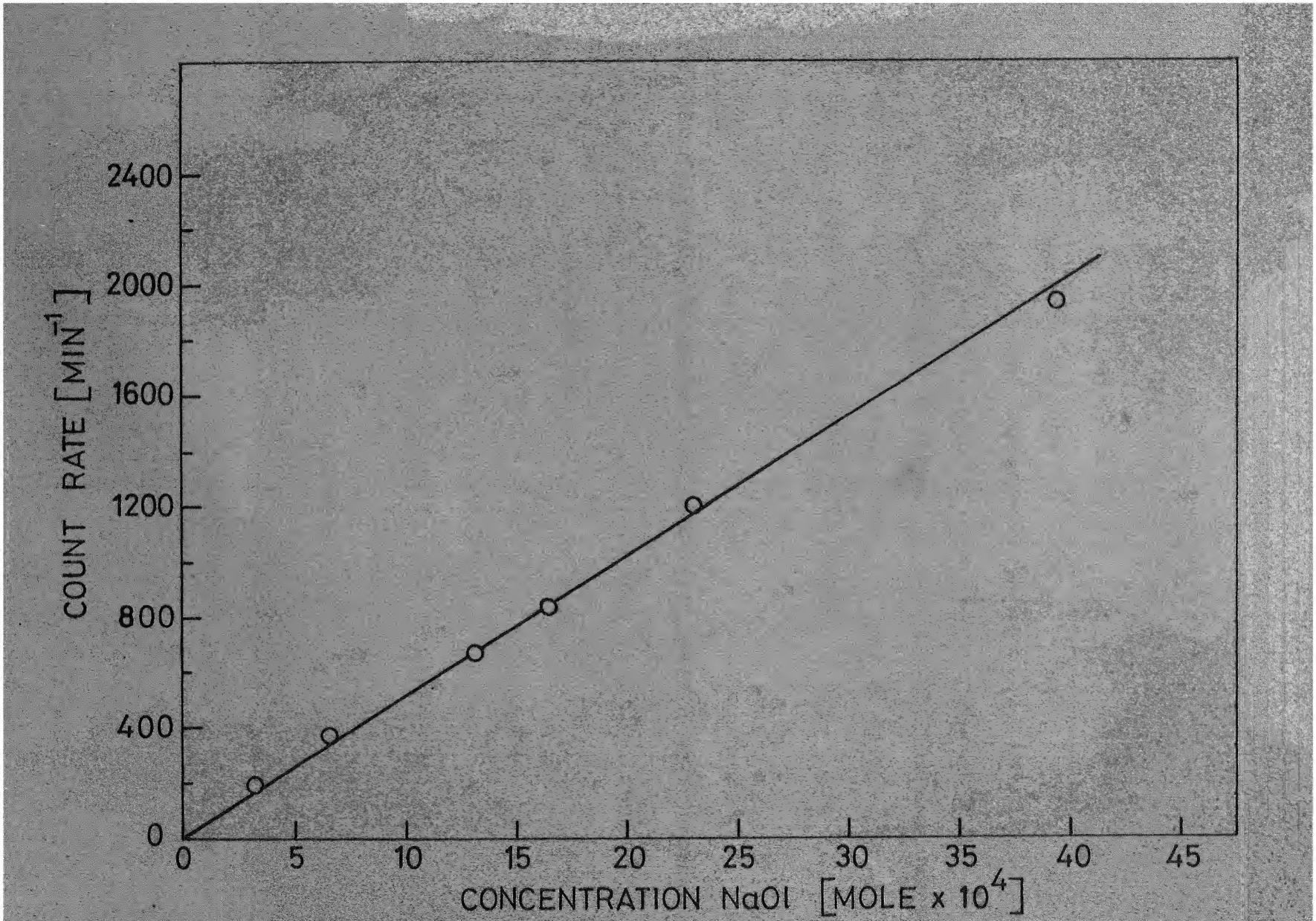

FIGURE 8 STANDARD CURVE FOR THE ESTIMATION OF SODIUM OLEATE BY C^{14} TRACER

CHAPTER IV

MATERIALS PREPARATION

In this chapter, detailed accounts of the chemicals and materials used are given.

IV-1 ZIRCON:

The zircon sample used in the present studies was procured from semielements Co. USA. It was of mineral origin and was claimed to be of 99 percent purity by the suppliers. X-ray fluorescence analysis of the sample showed no other impurity except hafnium (Appendix C). Microscopic examination of the coarse grains of around 100 mesh size showed nice transparent crystals.

Sample Preparation for Flotation Experiments:

The original sample which was supplied as coarse grains of about 100 mesh size, was thoroughly washed with water and then with dilute hydrochloric acid. This was followed by repeated washing. More than 85 percent of the material was in the size range -100 to +150 mesh. The sample was stored under distilled water.

Sample Preparation for Adsorption and Electro kinetic Studies:

The original sample was washed thoroughly and ground wet in alumina pebble mill for more than 30 hours. It was then suspended in 1.5 litres of water in a 2 litre beaker. The

fraction which settled in first 10 minutes was taken and the rest removed by decantation. The decanted material was further processed to prepare samples for electrophoretic mobility measurements while the sedimented fraction was treated with dilute hydrochloric acid and then washed repeatedly with redistilled water. The material was stored under redistilled water in plastic bottles for adsorption studies. A part of the sample was dried in oven at 150°C and was used for surface area measurements by the method using p-nitrophenol as described by C.H. Giles (71). The adsorption isotherm was determined and from the plateau, surface area was calculated. The surface area of the sample was found out to be 2.414 meter^2/gm as described in Appendix C.

For electrokinetic measurements, the finer fraction removed after 10 minutes settling as described above was further subjected to grinding for a considerable time (20 hours) and then again suspended in 1.5 litres of distilled water. The sample which remained suspended after one hour was removed as it contained colloidal matter. The process was repeated to remove all the colloidal matter so that supernatent liquid after settling remained clear.

IV-2 FLOTATION COLLECTOR, FROTHER AND MODERATORS:

Sodium oleate was used as a collector throughout the course of these investigations.

Oleic Acid:

The oleic acid was obtained from the Hormel Institute's fatty acid project at University of Minnesota, USA. Estimated purity was more than 99 percent as determined by gas-liquid and thin layer chromatography analysis. Iodine value was found out to be 89.9 and diene conjugation 0.03 percent.

Preparation of Sodium Oleate:

The procedure followed was similar to that of S.S. Kajiji (72). Equivalent amounts of oleic acid and analytical grade sodium hydroxide were transferred to a round bottom flask and 50 ml of dry absolute alcohol was added. (The ethyl alcohol used had been distilled, kept overnight over quicklime and re-distilled.) The whole mass was refluxed over a water bath for about an hour. Subsequently, excess alcohol was removed by evaporation and the syrupy mass was poured hot in acetone which had been distilled after keeping overnight with $CaCl_2$. Sodium oleate thus precipitated was filtered and washed with acetone. The dried powder was stored in a cool, dry place.

Dowfroth-250:

Dowfroth-250 was used as a frother in all the flotation experiments. This is a low viscosity liquid readily soluble in water and has a general formula $CH_3-(O-C_3H_6)_n-(OH)$. It is effective as a frother even at low concentrations.

Other Chemicals:

Chemicals used for analytical purposes were all of analytical grade.

Sodium silicate used was supplied by Riedel-de haen A.G. Germany. The SiO_2:Na_2O ratio was found out to be 1.0.

Sodium fluoride and sodium fluosilicate were also of analytical grade.

CHAPTER V

EXPERIMENTAL RESULTS

In the present investigation the following systems were studied.

1. Zircon-Water
2. Zircon-Sodium Oleate
3. Zircon-Sodium Oleate - NaF
4. Zircon-Sodium Oleate - Na_2SiO_3
5. Zircon-Sodium Oleate - Na_2SiF_6

The principal variables were pH and collector as well as moderator concentrations.

Electrokinetic measurements were done in case of zircon-water system in the presence of KCl. In case of zircon-sodium oleate system, flotation, adsorption, electrokinetic and infrared spectroscopic investigations were carried out. Finally in case of systems 3, 4 and 5 flotation, adsorption and electrokinetic experiments were performed.

This chapter contains the results of these investigations according to the type of measurement involved along with some preliminary discussion. The detailed discussions are to be found system wise in the subsequent chapters.

V-1 FLOTATION RECOVERY RESULTS:

Most of the flotation experiments were carried out in the all glass laboratory flotation cell. The details about the cell and the set up have been already described in Section II-1 (also see Appendix D, Table IX).

About 25 gms of the zircon sample prepared for the experiment were transferred to a 600 ml glass beaker and to it was added 350 ml of sodium oleate solution. The final pH was recorded after 4 1/2 minutes' conditioning of the pulp. Beckman research pH meter was used to measure pH values correct upto second place. The conditioned pulp was then transferred to the flotation cell and 5 ml of 5 percent (by volume) solution of Dowfroth-250 were added and the flotation was carried out by passing air from the compressor for about two minutes. The concentrates and tailings were collected in enamel trays, dried and weighed. Moderators wherever necessary were added with the collectors.

The results so obtained are tabulated in Appendix D. Fig. 9 and Table X shows the effect of sodium oleate concentration on the flotation recovery of zircon. It is seen that the recovery first increases rapidly then remains constant for a fairly large additions of sodium oleate and then around sodium oleate concentration 1.0×10^{-3} mole/lit it decreases.

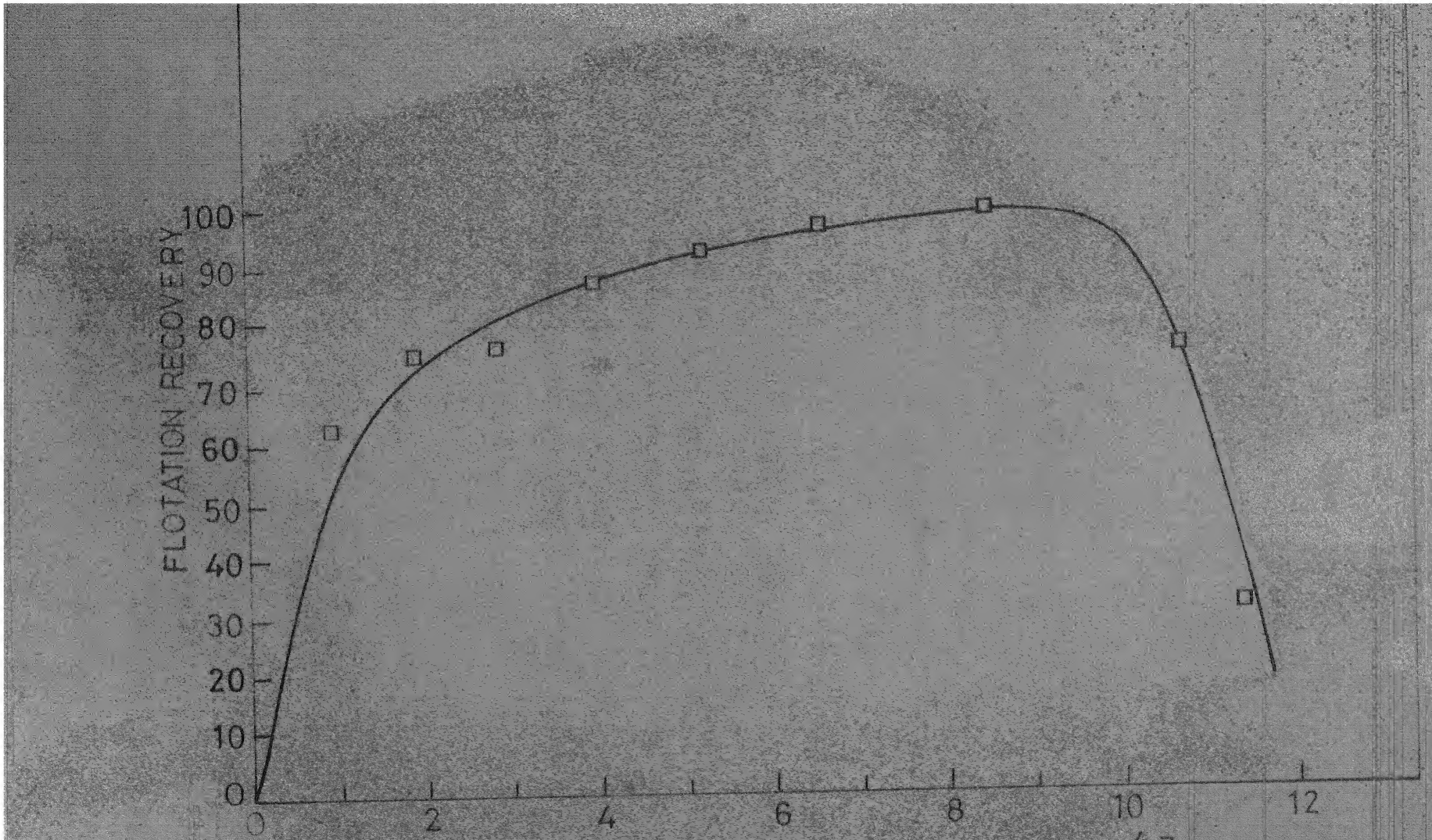

FIGURE 9 EFFECT OF SODIUM OLEATE ADDITION ON THE FLOTATION RECOVERY OF ZIRCON AT CONSTANT pH 9.0

The effect of pH on the flotation recovery is shown in Fig. 10 for the collector concentrations 9.327×10^{-5} mole/lit, 1.875×10^{-4} mole/lit, 3.948×10^{-4} mole/lit and 6.579×10^{-4} mole/lit. The data along with 'flotation activity' to be defined at a later stage (Chapter VII) is included in Table XI.

As the pH is increased from the acidic range the percent recovery increases steeply, attains maximum and again falls at higher pH values. The pH at which the recovery is just nil on the acidic side is about the same for all the sodium oleate concentrations studied. The maximum recovery is as expected a function of the collector concentration. In the alkaline range the 'upper critical pH' that is the pH at which the recovery is just zero is different for different collector concentrations.

The effect of sodium fluoride concentration at constant sodium oleate concentration of 4.934×10^{-4} mole/lit and constant pH of 9.7 ± 0.05 is shown in Fig. 11 and Table XII. It is seen therefrom, that the recovery first increases at lower concentrations of sodium fluoride then remains fairly constant even upto 8.5×10^{-3} mole/lit (350 mg/l) addition of NaF. Above this it seems to decrease. Thus it can be said that at lower concentration sodium fluoride acts as an activator and at higher concentrations a very weak depressor.

Effect of sodium silicate as moderator was studied for constant collector concentration and pH. Three different collector concentrations of 6.579×10^{-4} mole/lit, 3.948×10^{-4} mole/lit and 2.829×10^{-4} mole/lit at final pH 9.1 and 4.934×10^{-4} mole/lit

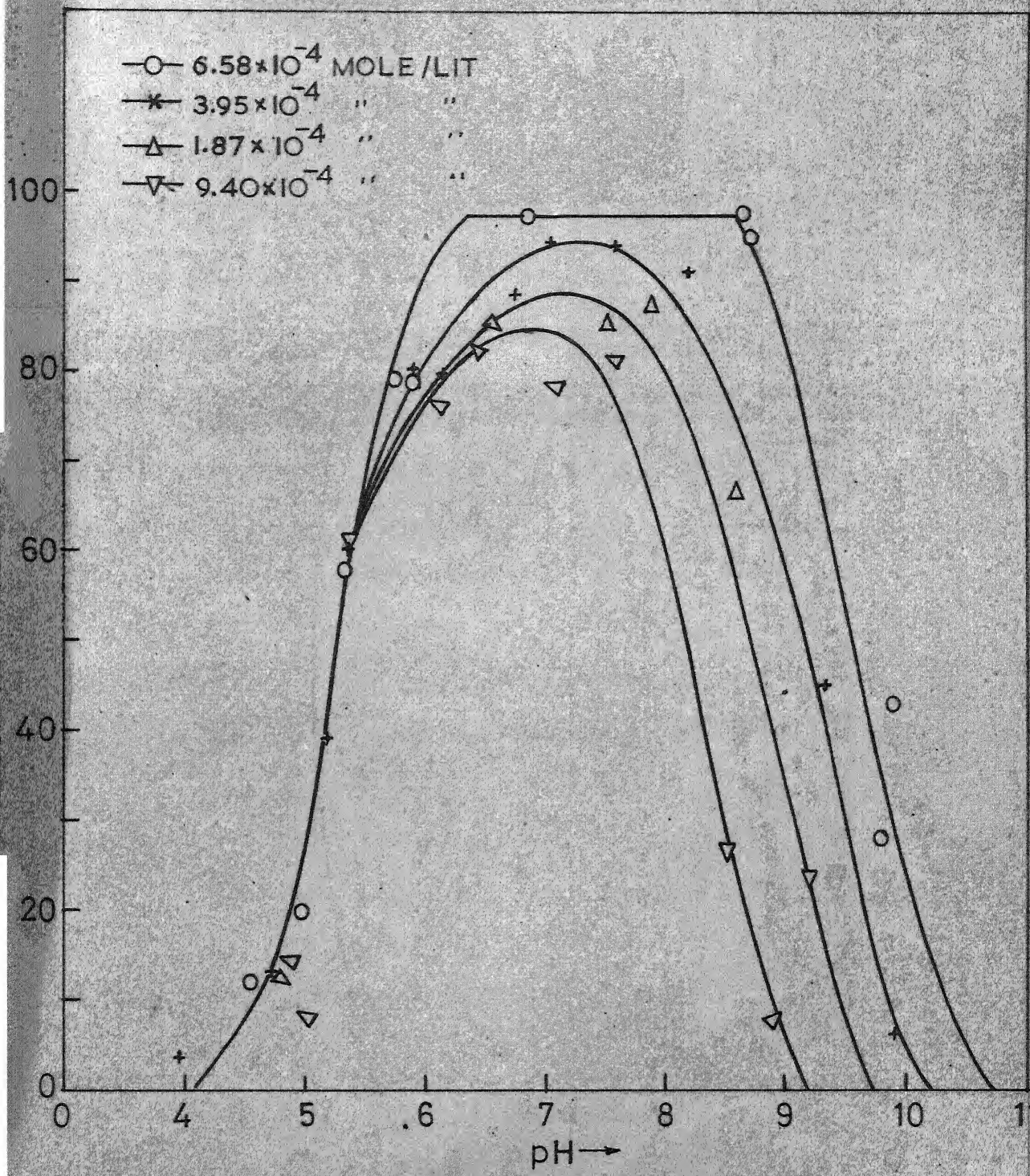

FIGURE 10 EFEECT OF pH ON FLOTATION RECOVERY OF ZIRCON AT VARIOUS SODIUM OLEATE CONCENTRATIONS

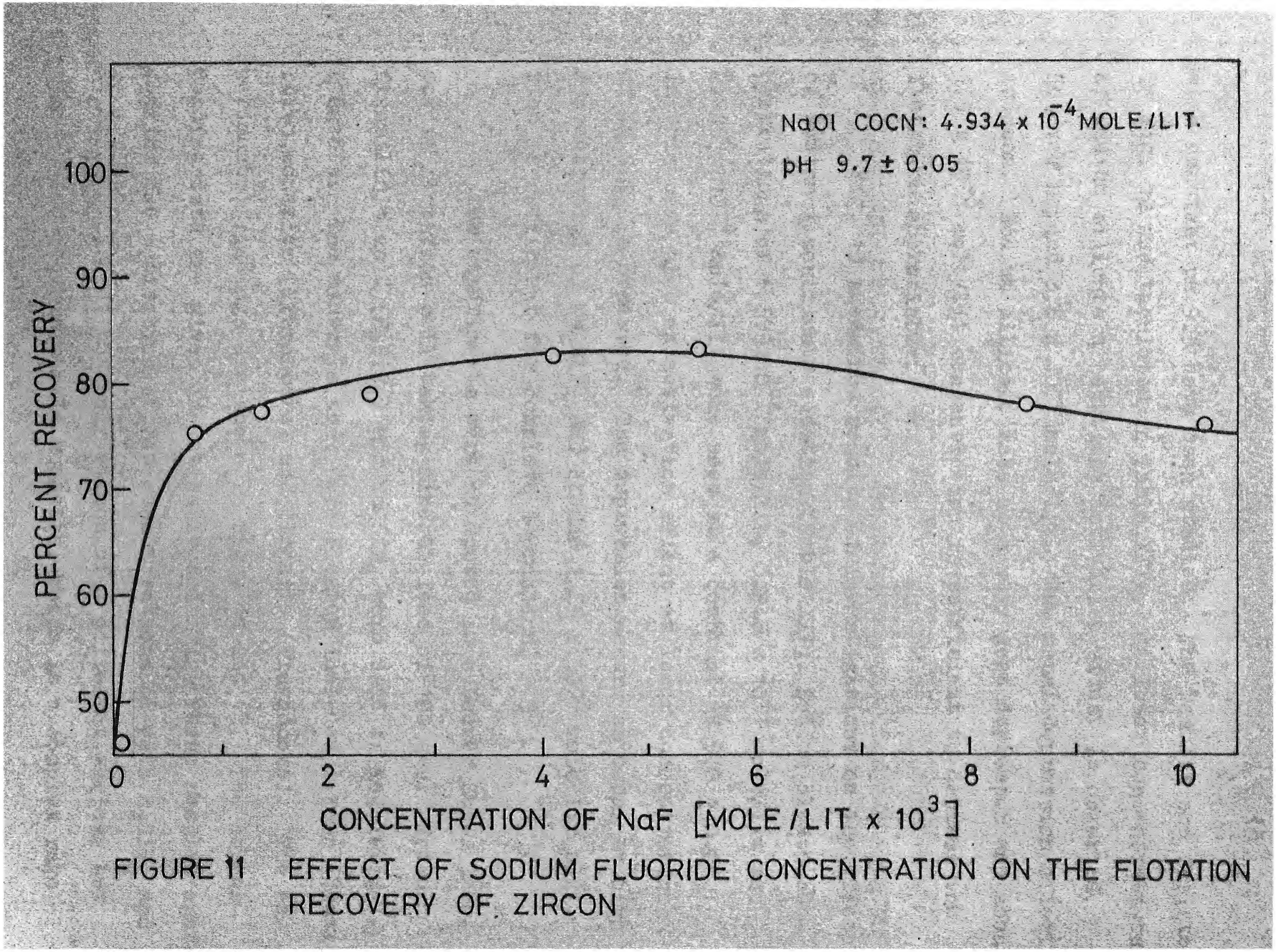

FIGURE 11 EFFECT OF SODIUM FLUORIDE CONCENTRATION ON THE FLOTATION RECOVERY OF ZIRCON

at a constant pH 9.5 have been studied. The results are depicted in Fig. 12 and tabulated in Table XIII. At lower concentrations of sodium silicate a distinct activation effect is observed. However beyond 3.5×10^{-4} mole/lit. the usual depression effect is seen. Sodium silicate acts as a very good depressor and about 1.5×10^{-3} mole/lit concentration is sufficient to depress the flotation appreciably.

Fig. 13 shows the results of investigations on the effect of sodium fluosilicate addition (Table XIV). Sodium oleate concentrations of 6.579×10^{-4} mole/lit, 3.948×10^{-4} mole/lit and 2.829×10^{-4} mole/lit were used at a constant pH 9.0 ± 0.05. In this case also an activation effect at lower concentrations of Na_2SiF_6 is observed. The depression occurs as usual at high concentration of Na_2SiF_6 and around 1.25×10^{-3} mole/lit addition is sufficient for complete depression.

A few experiments were conducted in a Denver Sub-A laboratory flotation cell taking mineral feed of 100 gms. Hydrofluosilicic acid (H_2SiF_6) and Na_2SiF_6 were used as moderating reagents. The minerals that were floated included zircon (Travancore), Monazite (Travancore) and Ilmenite (Travancore). The experimental findings are shown in Figs. 14 and 15. The corresponding data are given in Tables XV and XVI. These results again confirm the activation at low concentrations of both H_2SiF_6 and Na_2SiF_6 in case of not only zircon of a different variety but also of two other minerals monazite, which is a complex rare

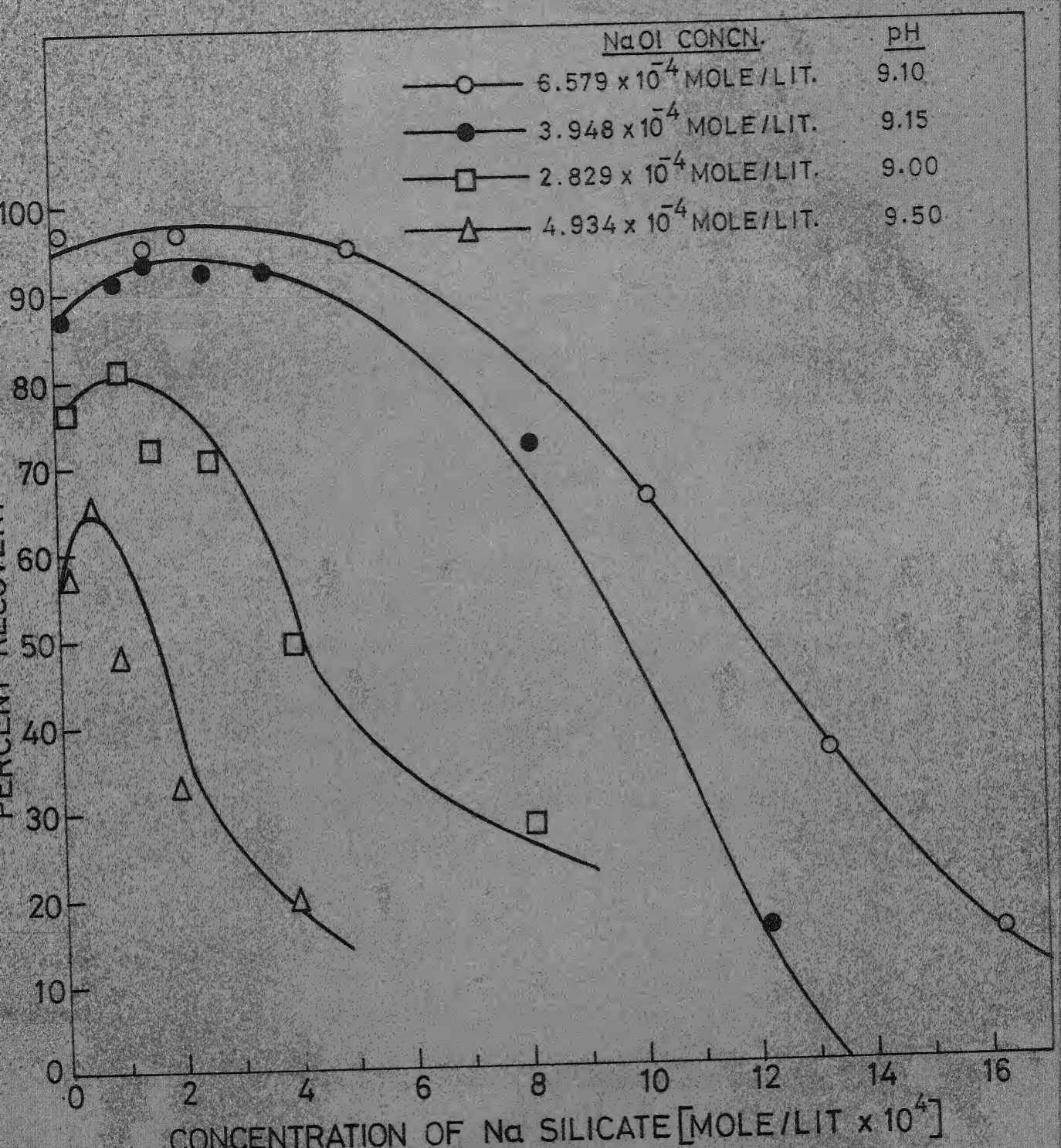

FIGURE 12 EFFECT OF SODIUM SILICATE CONCENTRATION ON THE FLOTATION RECOVERY OF ZIRCON

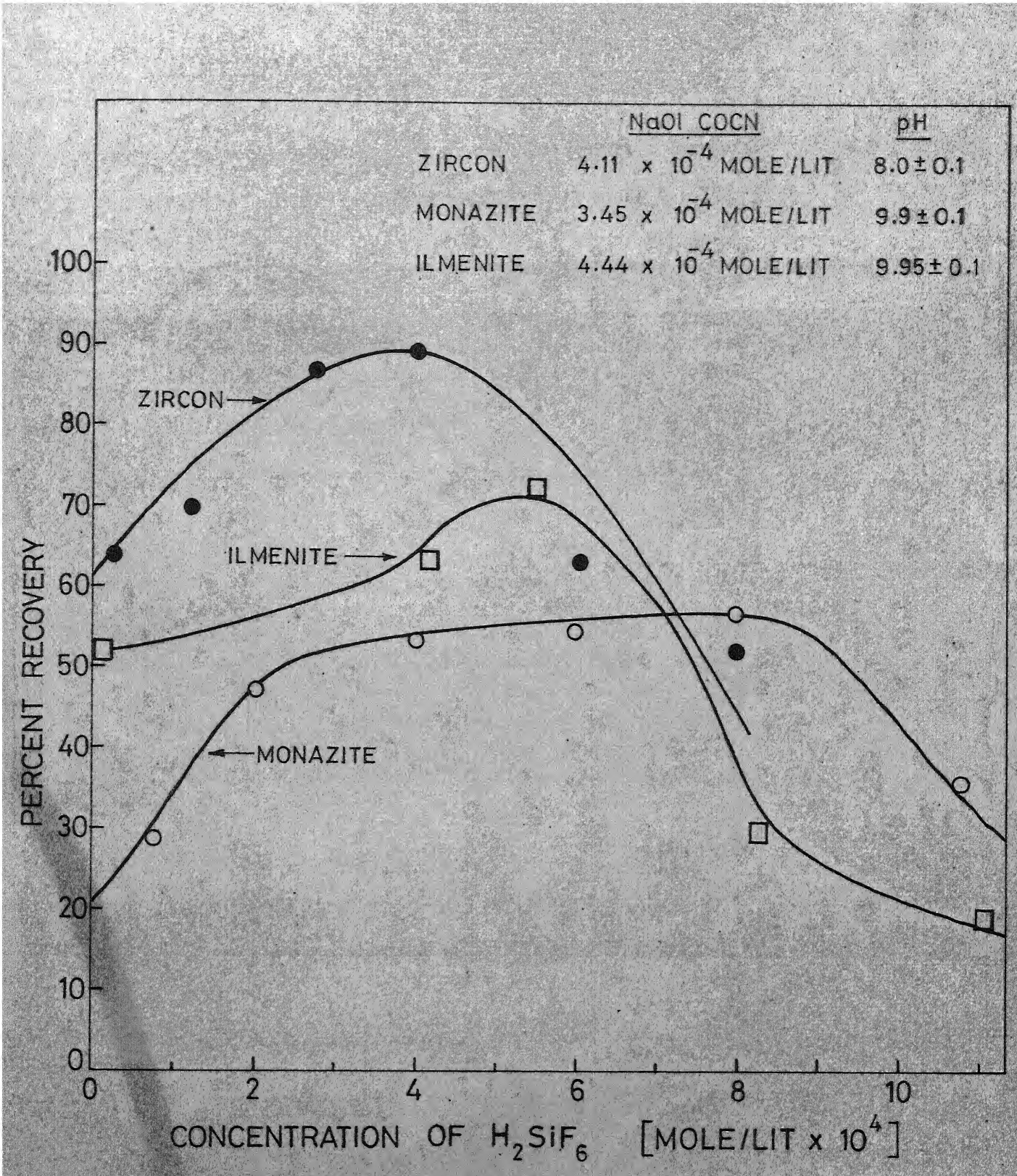

FIGURE 14 EFFECT OF FLUOSILICIC ACID CONCENTRATION ON THE FLOTATION OF SOME BEACH SAND MINERALS

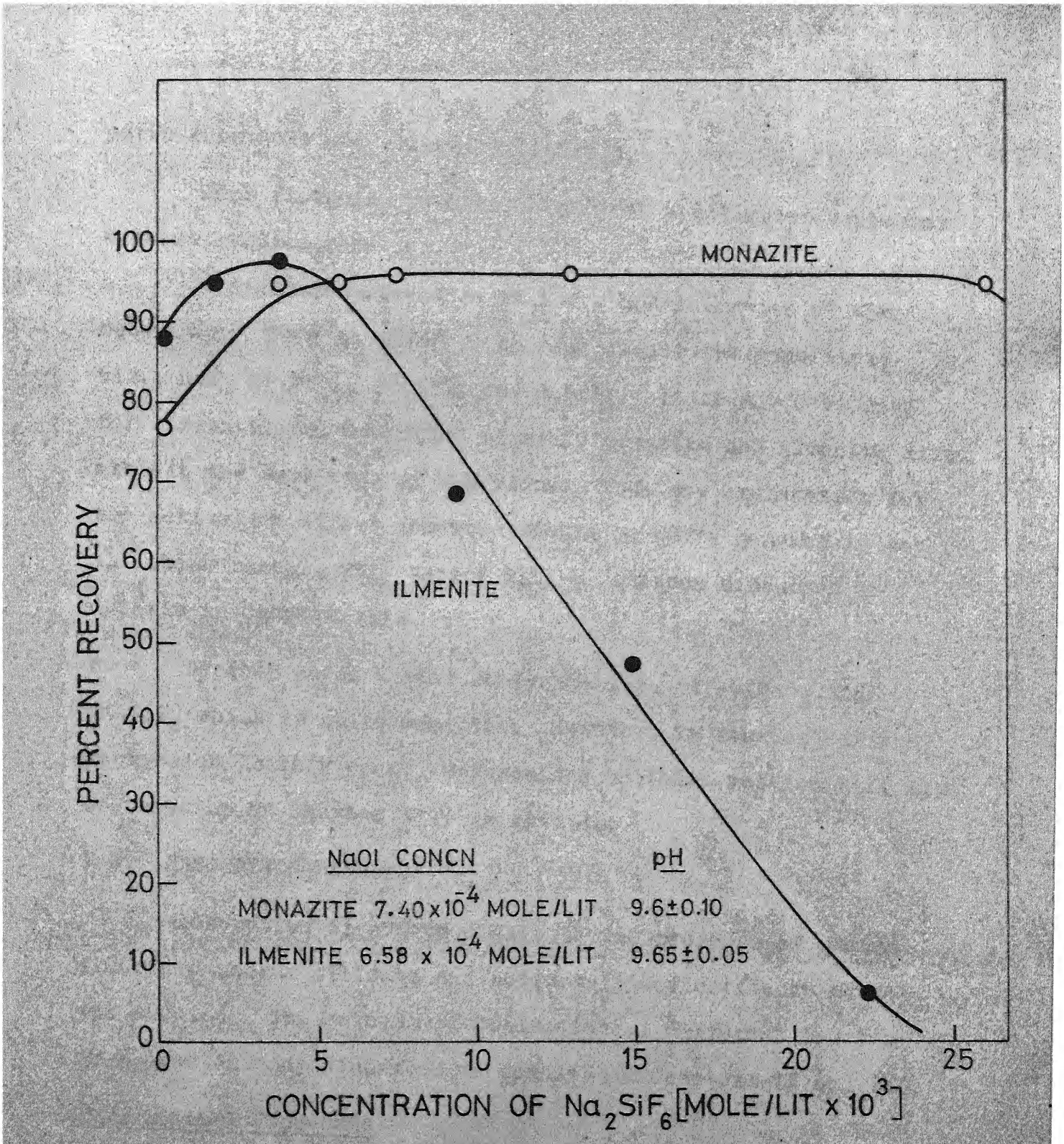

FIGURE 15 EFFECT OF SODIUM FLUOSILICATE ON THE FLOTATION RECOVERY OF SOME BEACH SAND MINERALS

earth phosphate and ilmenite ($FeTiO_3$).

Thus flotation results on mineral - collector-depressor systems studied show

a. a distinct activation at lower concentration of the moderator. This is observed in case of all the moderators viz., NaF, Na_2SiO_3, Na_2SiF_6 and H_2SiF_6. It is not exclusive for zircon alone. Two other minerals monazite and ilmenite also exhibit the same type of behaviour. Thus any explanation for the activation effect observed should be quite general to cover all these cases. This aspect will be further discussed in details in Chapter VIII.

b. Depression at higher concentrations of Na_2SiO_3 and Na_2SiF_6 which is quite expected. However, in case of NaF the depression is very poor. Discussions on these results will also be taken up in Chapter VIII in details.

V-2: ADSORPTION RESULTS:

Adsorption of sodium oleate in the presence of sodium fluoride, sodium silicate and sodium silicofluoride on zircon was studied. The methods of estimation of different species have been already described in details in Chapters II and III.

Experimental Procedure:

The sample prepared for adsorption experiments was weighed wet and about 3 gms transferred to bottles. Sodium oleate solution tagged with C-14 β-active tracer and moderator,

if any, were added in requisite quantities. Total volume was made up to 100 ml. The bottles were then tightly stoppered and shaken for about 30 minutes in a shaking machine. After that, these were transferred to a thermostat maintained at 30 ± 0.1°C by a transistor relay and Beckman regulator. The contents were allowed to equilibrate for about 5 hours. Final pH measurements were made after equilibration from the supernatent solution. A part of the supernatent solution was taken for determining the equilibrium concentration of different species while the solid mineral was dried and accurately weighed.

For sodium oleate estimation, a part of the supernatent solution was centrifuged for 5 minutes at 1500 RPM, to remove any suspended solids and 2 ml of the clear liquid was transferred to the planchets for counting. The planchets were then carefully shifted to an oven maintained at 40°C and the liquid evaporated for about 8 hours after which the counting was held immediately.

In the cases of fluoride and silicon estimations, respective colorimetric procedures described in Chapter III were followed. The results of these investigations are tabulated in Appendix E.

Zircon-Sodium Oleate System:

Adsorption isotherm of sodium oleate on zircon was determined at a constant initial pH of 9.0 and is depicted in Fig. 16 (Table XVII). It is seen that the adsorption first increases

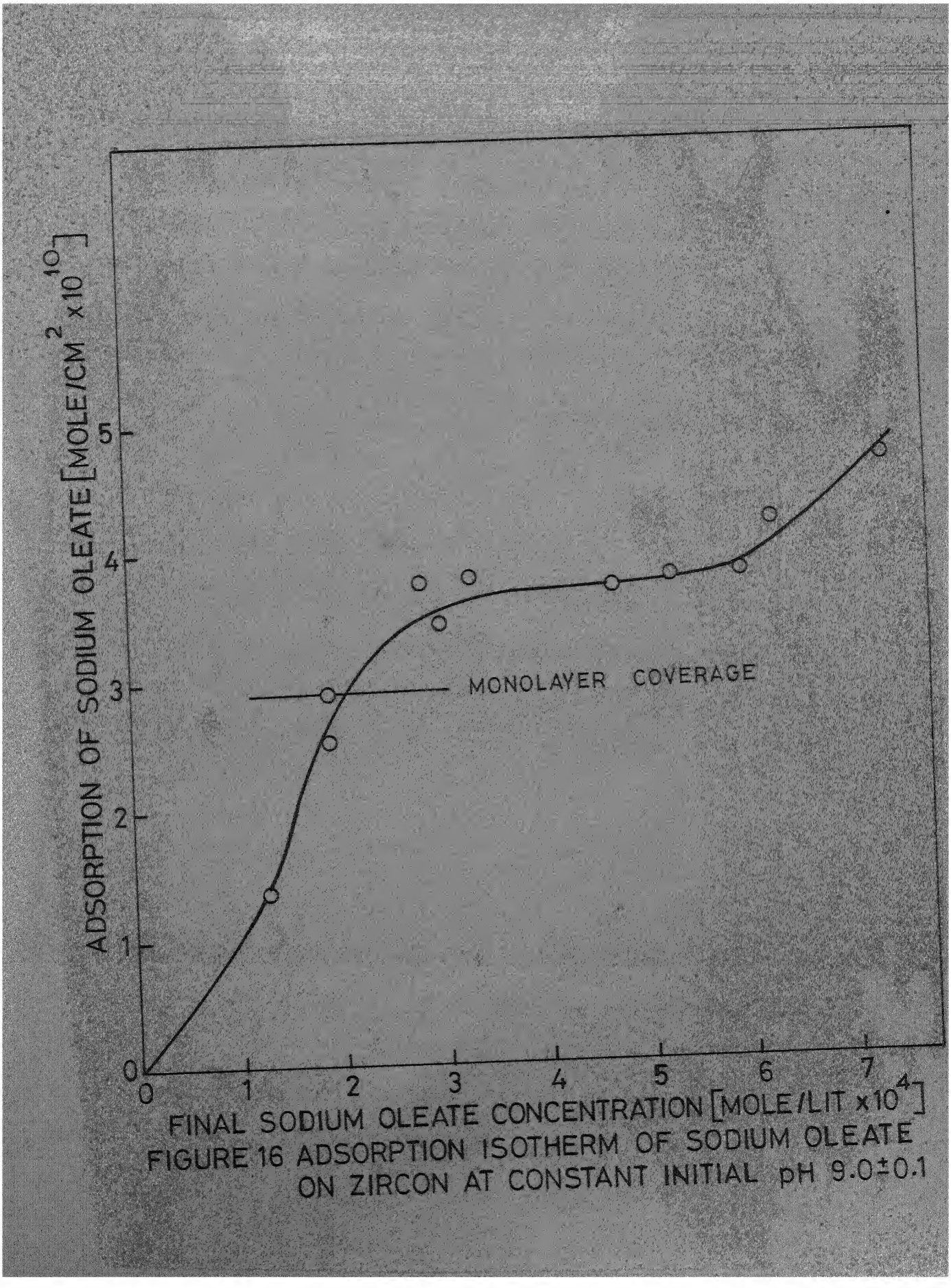

FIGURE 16 ADSORPTION ISOTHERM OF SODIUM OLEATE ON ZIRCON AT CONSTANT INITIAL pH 9.0±0.1

steeply, then shows a plateau region and at an initial concentration of 1.0×10^{-3} mole/lit the adsorption again shoots up. The monolayer coverage of Naoleate occurs at 2.913×10^{-10} mole/cm^2 adsorption as determined by taking cross sectional area of Naoleate as 57 $\mathring{A}^2$ (73). It is shown by a dotted line in the figure.

Next, the effect of pH on the adsorption of sodium oleate on zircon was investigated. Most of the investigations were made in the pH range of 9 to 10.5 since in this alkaline range the sodium oleate exists mostly in ionic form, and secondly, depression studies are fruitful in the higher alkaline range.

A word about pH adjustments would be worth-while. The pH adjustment was always done by analytical grade hydrochloric acid and sodium hydroxide solutions. The initial pH was kept constant in some experiments by adjusting the pH of the solution to a fixed value and then adding the solid mineral to it. Some experiments were also done at constant final pH which largely depended on the quantity of solid added. Therefore, to maintain the constancy of the final pH was rather a difficult job. No buffer was used to keep the pH constant as this would introduce the undesirable additional influence of buffer ions.

The effect of pH on the adsorption of sodium oleate was first studied at different constant sodium oleate concentrations of 2.302×10^{-4} mole/lit, 3.290×10^{-4} mole/lit, 4.934×10^{-4} mole/lit and 6.579×10^{-4} mole/lit.

The results are shown in Fig. 17 and later in Fig. 55 and tabulated in Tables XVIII, IX, XX and XXI.

In Fig. 17 the effect of pH at constant sodium oleate concentration 6.579×10^{-4} moles/lit is shown between pH 5.5 and 10.5. The behaviour exhibited is typical of all other concentrations of sodium oleate. Between pH 7 and 10.5 the curve resembles a bell-shape showing a maximum at around pH 8.35. In acidic region between pH 7 to 5.5 the adsorption again increases as the pH is decreased as shown by the dotted offshoot. It is clearly due to the progressive precipitation of the oleic acid from the sodium oleate solution. This will be more evident from the later discussion on the hydrolysis behaviour of the sodium oleate. The bell-shaped nature of the curve will also be explained later.

The effect of temperature on the adsorption of sodium oleate was also investigated. The temperature was varied at an interval of $5^{\circ}C$ between $25^{\circ}C$ to $40^{\circ}C$. Sodium oleate concentration was maintained constant at 3.289×10^{-4} mole/lit. Three initial pH's were chosen, one in the acidic range at 6.02 the second at 8.45 where adsorption is relatively expected to be high and the third pH was fixed in the higher alkaline region at pH 9.55. The experimental behaviour is plotted in Fig. 18 and tabulated in Table XXII. It is seen that at initial pH 6.02 the adsorption increased as the temperature rose from $25^{\circ}C$ to $30^{\circ}C$ and then decreased as the temperature is further increased

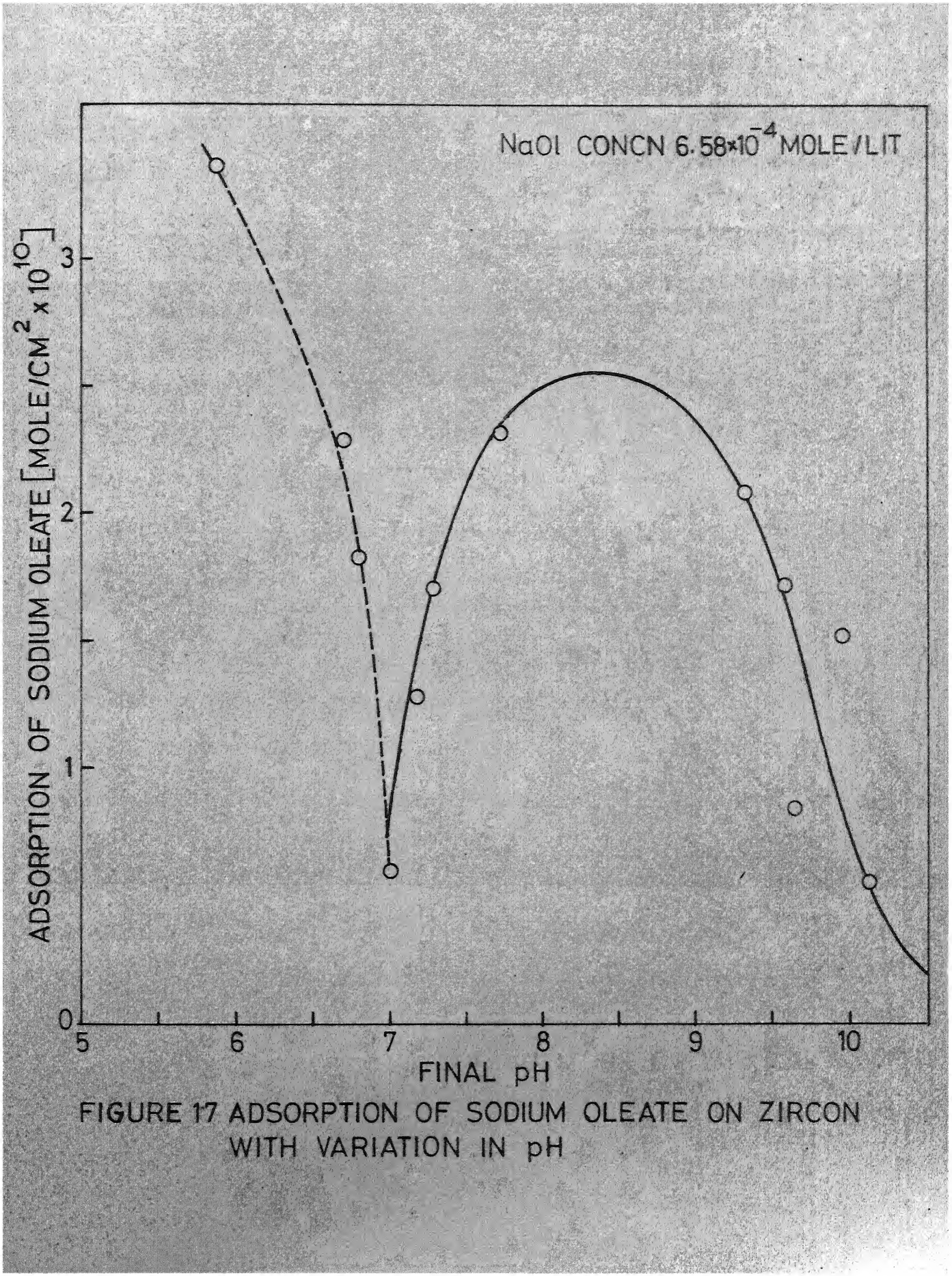

FIGURE 17 ADSORPTION OF SODIUM OLEATE ON ZIRCON WITH VARIATION IN pH

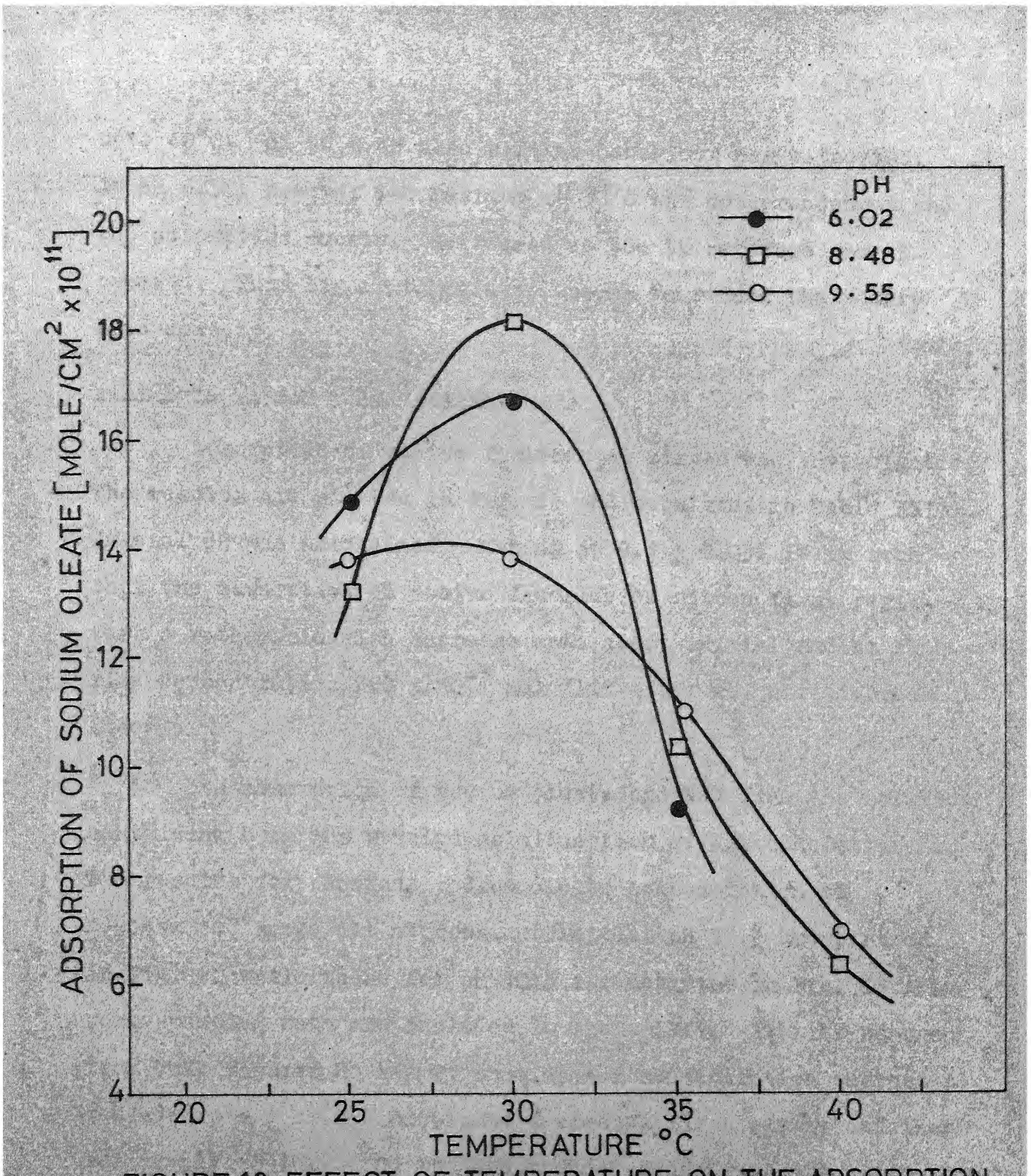

FIGURE 18 EFFECT OF TEMPERATURE ON THE ADSORPTION OF SODIUM OLEATE ON ZIRCON

upto 40°C. At pH 8.45 also similar behaviour was witnessed. At pH 9.55, however the maximum at 30°C was not pronounced and the adsorption smoothly decreased as the temperature was increased. Thus higher temperature seems to reduce the adsorption density.

Zircon-Na Oleate - NaF System:

Adsorption of sodium fluoride on zircon was investigated. The results are plotted in Fig. 19 and tabulated in Table XXIII. Initial pH was maintained constant at 9.1 ± 0.05. It is seen that the adsorption of sodium fluoride on zircon first registers a rather sluggish increase upto about initial sodium fluoride concentration 2.0×10^{-3} mole/lit after which it increases steeply.

The adsorption of sodium oleate and NaF from the solution containing both was studied as a function of NaF concentration. The results for constant sodium oleate concentration of 4.934×10^{-4} mole/lit at constant initial pH 10.3 are plotted in Fig. 20 while those for pH 10.5 are depicted in Fig. 21. The corresponding data are included in Table XXIV. It will be seen from both figures 20 and 21 that as NaF concentration increases the adsorption of sodium oleate decreases first slowly and then relatively rapidly. On the otherhand NaF adsorption density increases first gradually and then steeply. The nature of the adsorption pattern of NaF is the same as that found without sodium oleate (Fig. 19).

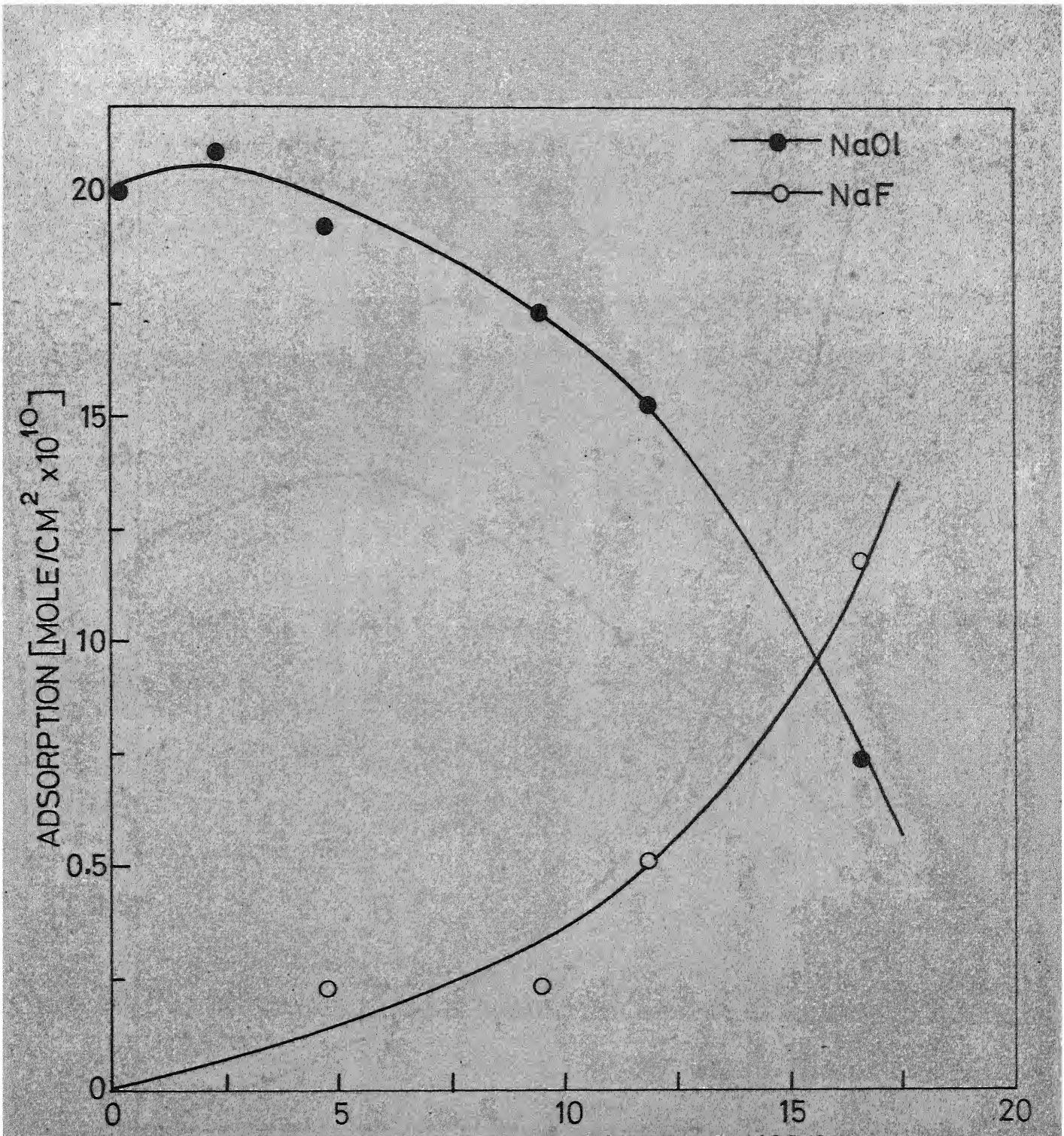

FIGURE 20 ADSORPTION OF SODIUM OLEATE AND SODIUM FLUORIDE ON ZIRCON AT CONSTANT INITIAL pH 10.3

CONCN OF SODIUM OLEATE 4.934×10^{-4} MOLE/LIT

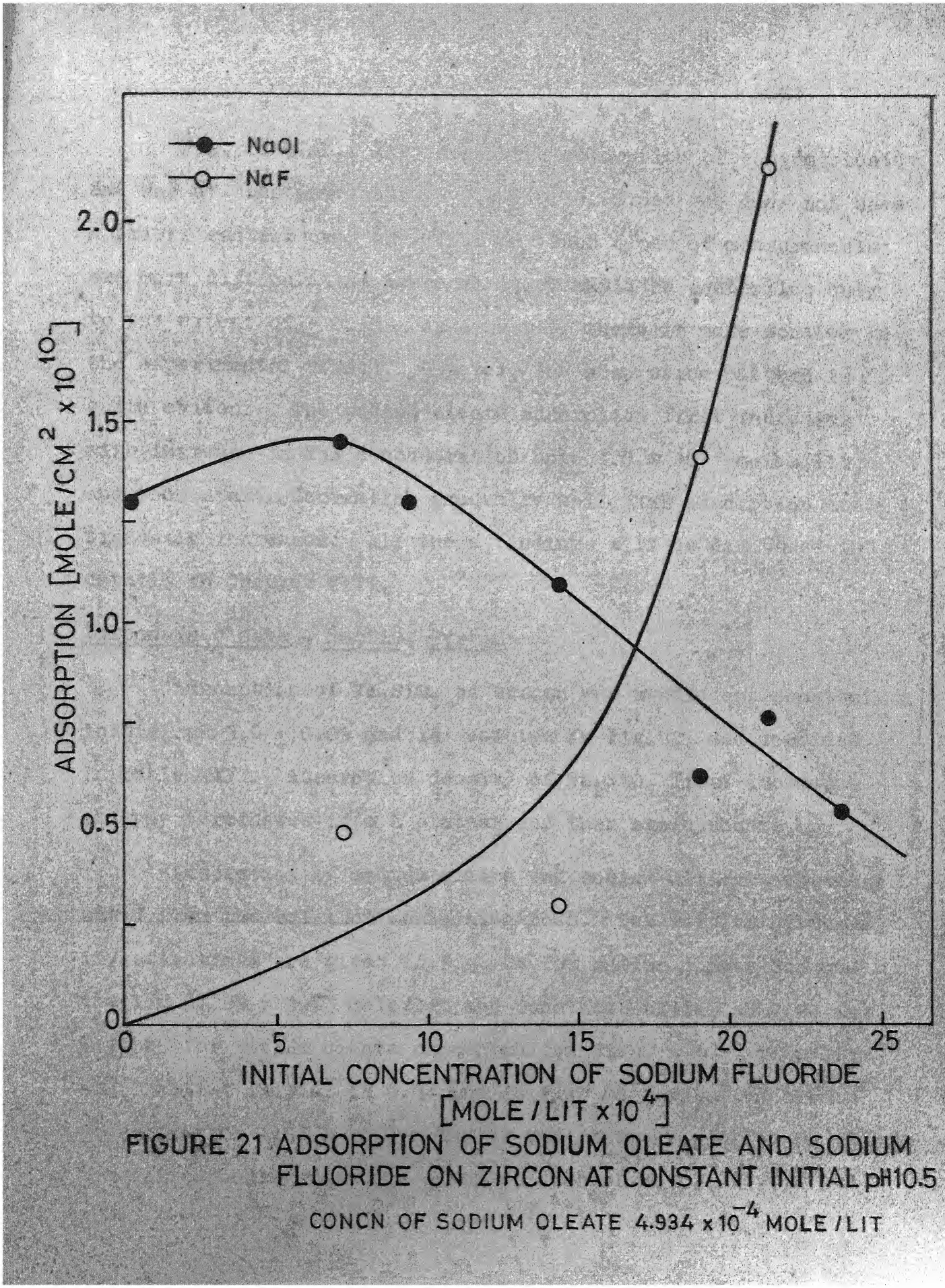

FIGURE 21 ADSORPTION OF SODIUM OLEATE AND SODIUM FLUORIDE ON ZIRCON AT CONSTANT INITIAL pH10.5

CONCN OF SODIUM OLEATE 4.934×10^{-4} MOLE / LIT

Fig. 22 (Table XXV) shows the adsorption of sodium oleate and NaF at constant final pH 9.7 ± 0.15. Since one does not have a priori control over the final pH such types of measurements are more difficult and hence final pH could be controlled only to the extent of ± 0.15. As a result, there is more scatter in the experimental points. However, the adsorption pattern is quite evident. The sodium oleate adsorption first increases with increase in NaF concentration upto 1.0×10^{-3} moles/lit. and then starts decreasing gradually while NaF adsorption continuously increases. All these findings will be discussed in details in Chapter VIII.

Zircon-Na Oleate - Na_2SiO_3 System:

Adsorption of Na_2SiO_3 on zircon was studied at constant initial pH 9.2 ± 0.05 and is depicted in Fig. 23 and recorded in Table XXVI. Adsorption density of Na_2SiO_3 first increases sharply terminates into a plateau and then again shoots up.

Adsorption of sodium oleate and sodium silicate was measured from the solution containing both. The results of these investigations are given in Fig. 24 for sodium oleate concentration 3.289×10^{-4} mole/lit and constant initial pH 9.0, in Fig. 25 for sodium oleate concentration 3.289×10^{-4} mole/lit. and constant initial pH 9.94 and in Fig. 26 for sodium oleate concentration 4.93×10^{-4} mole/lit and constant initial pH 10.0, The corresponding data are given in Tables XXVII, XXVIII and XXIX.

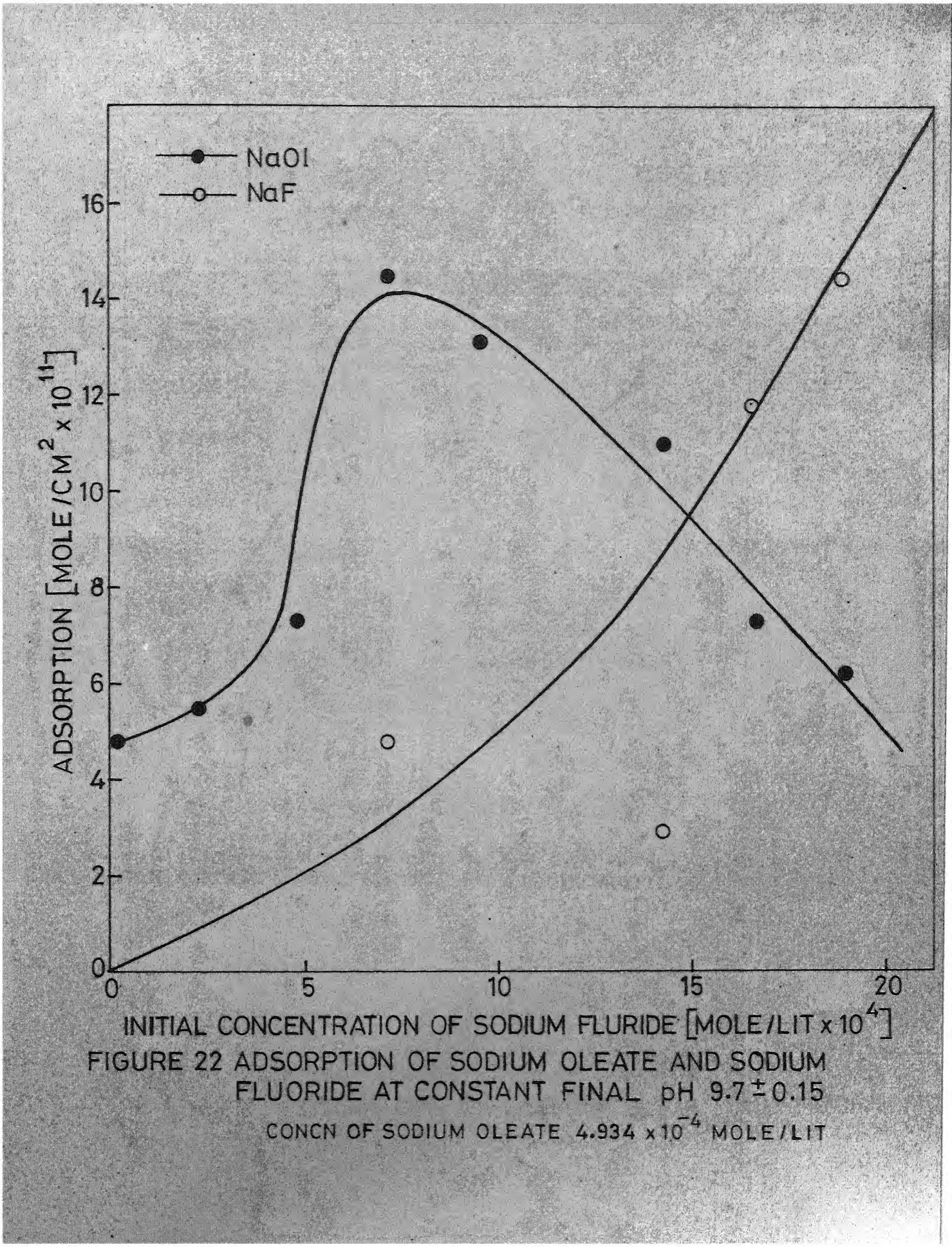

FIGURE 22 ADSORPTION OF SODIUM OLEATE AND SODIUM FLUORIDE AT CONSTANT FINAL pH 9.7 ± 0.15

CONCN OF SODIUM OLEATE 4.934 x 10^{-4} MOLE/LIT

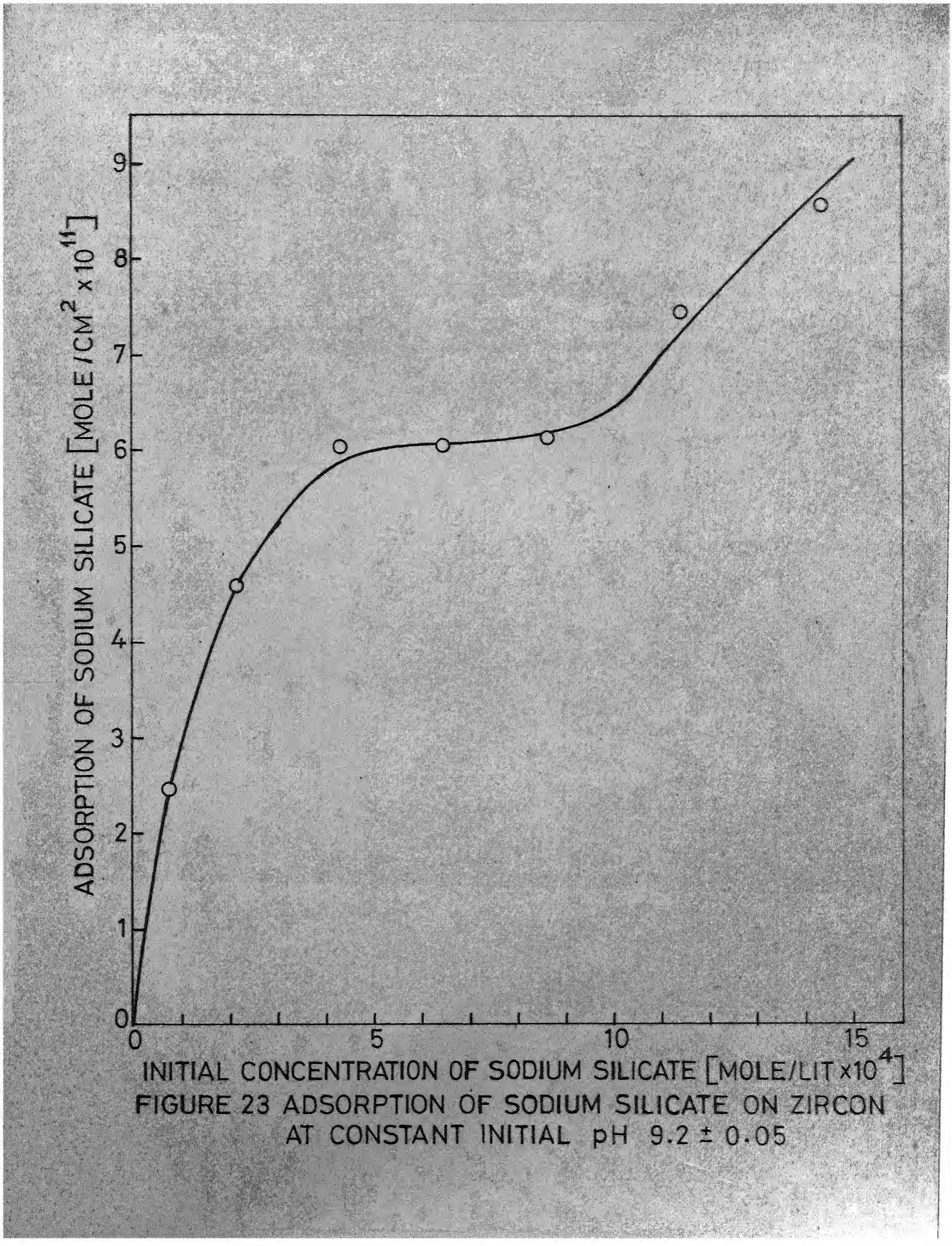

FIGURE 23 ADSORPTION OF SODIUM SILICATE ON ZIRCON AT CONSTANT INITIAL pH 9.2 ± 0.05

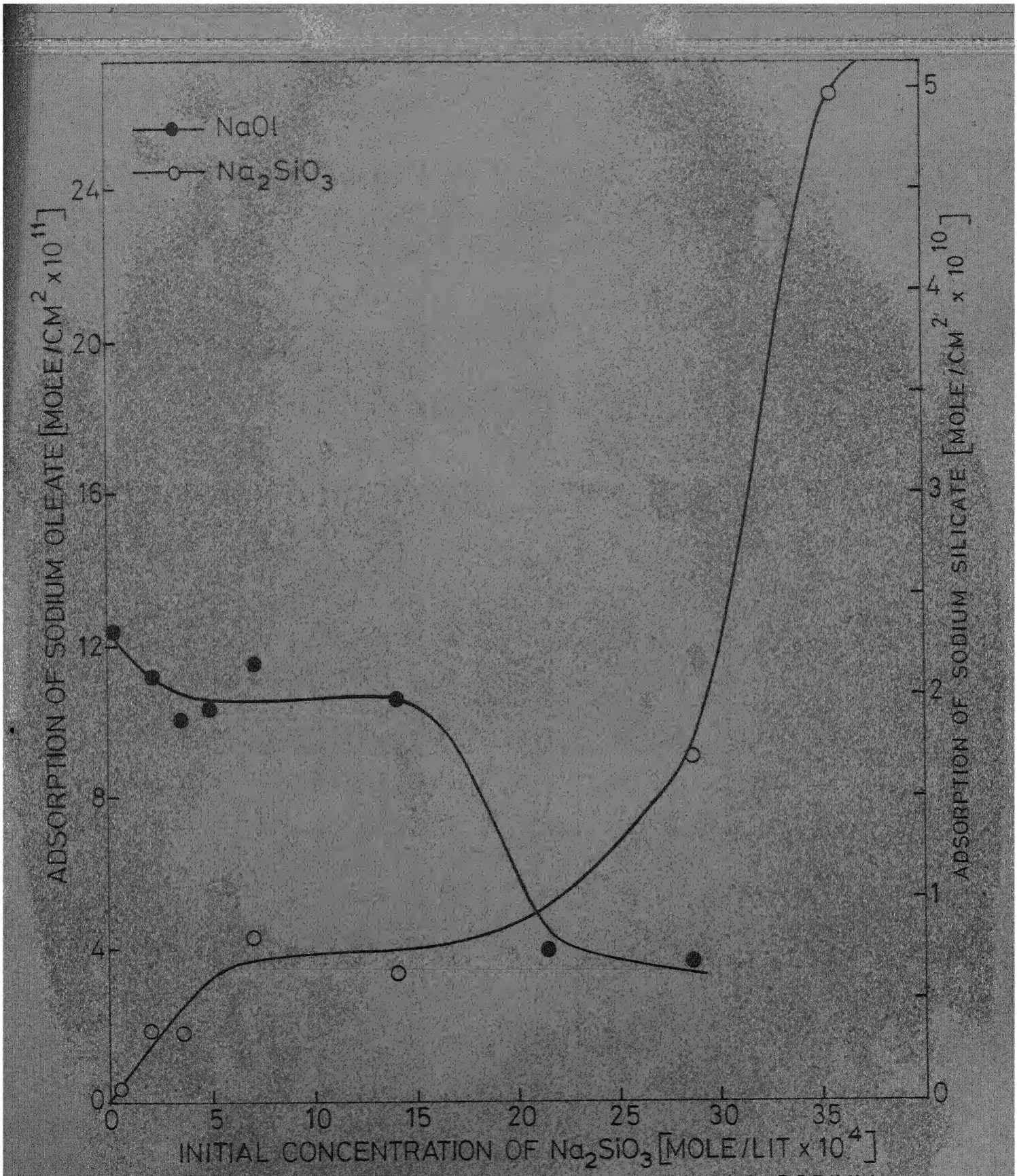

FIGURE 24 ADSORPTION OF SODIUM OLEATE AND SODIUM SILICATE ON ZIRCON AT CONSTANT INITIAL pH 9.0±0.5

CONCN AT SODIUM OLEATE 3.289×10^{-4} MOLE/LIT

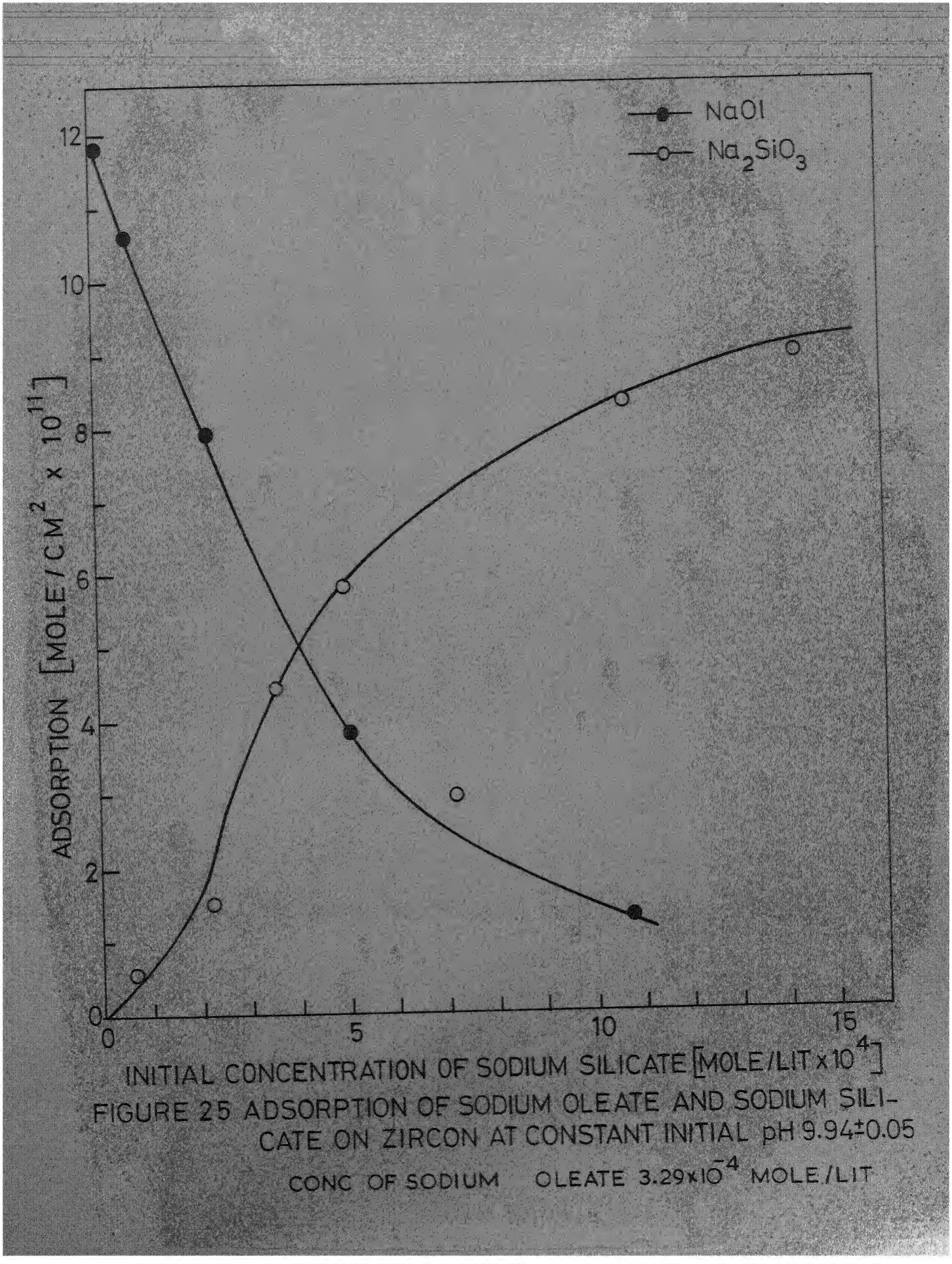

FIGURE 25 ADSORPTION OF SODIUM OLEATE AND SODIUM SILICATE ON ZIRCON AT CONSTANT INITIAL pH 9.94±0.05

CONC OF SODIUM OLEATE 3.29×10^{-4} MOLE/LIT

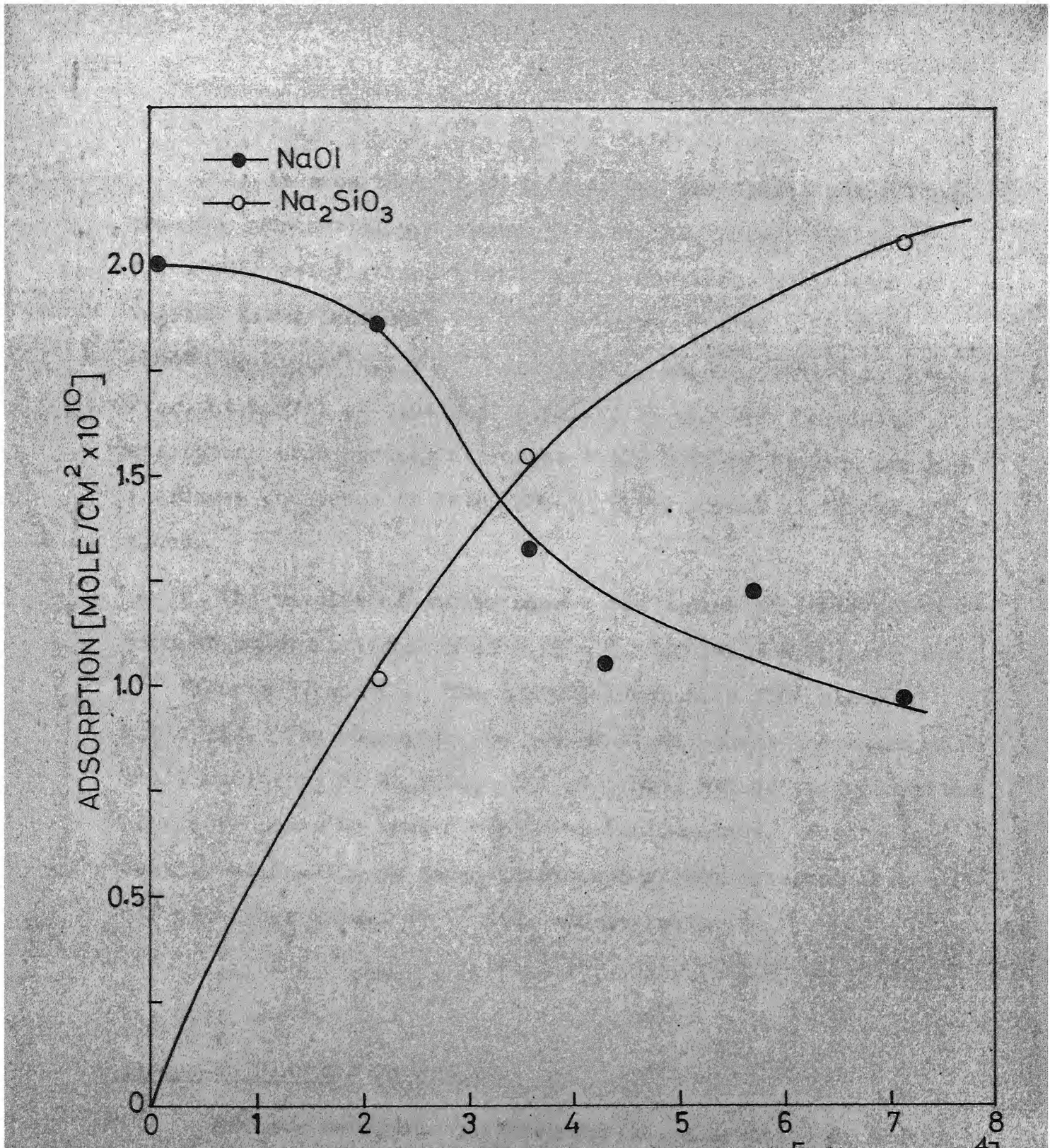

FIGURE 26 ADSORPTION OF SODIUM OLEATE AND SODIUM SILICATE AT CONSTANT INITIAL pH 10.0 ± 0.1

CONCN OF SODIUM OLEATE 4.93×10^{-4} MOLE/LIT

It is seen that at pH 9 (Fig. 24) the oleate adsorption remains substantially constant till Na_2SiO_3 concentration of 1.7×10^{-3} mole/lit and then abruptly decreases while that of Na_2SiO_3 first increases rapidly, remains constant and then shoots up around 1.7×10^{-3} mole/lit of Na_2SiO_3 addition. However, at higher pH 9.94 and 10 (Figs. 25 and 26) the oleate adsorption continuously decreases while that of Na_2SiO_3 briskly increases and tends to level off at higher amount of Na_2SiO_3 added.

The results of sodium oleate and sodium silicate adsorption at constant final pH of 9.45 ± 0.1 and 9.85 ± 0.1 are shown in Figures 27 and 28. The corresponding data find place in Table XXX. The adsorption of sodium oleate first increases at small additions of Na_2SiO_3. But at higher values the adsorption of oleate seems to remain substantially constant. Adsorption density of Na_2SiO_3 as usual continuously increases and levels off at higher values of Na_2SiO_3 concentration.

All these results will be discussed in details in Chapter VIII.

Zircon-Na Oleate - Na_2SiF_6 System:

Efforts were made to determine the adsorption of sodium oleate and sodium fluosilicate from the solution containing both. However, these efforts were met with only partial success due to difficulties in analysis. Thus, only adsorption of sodium

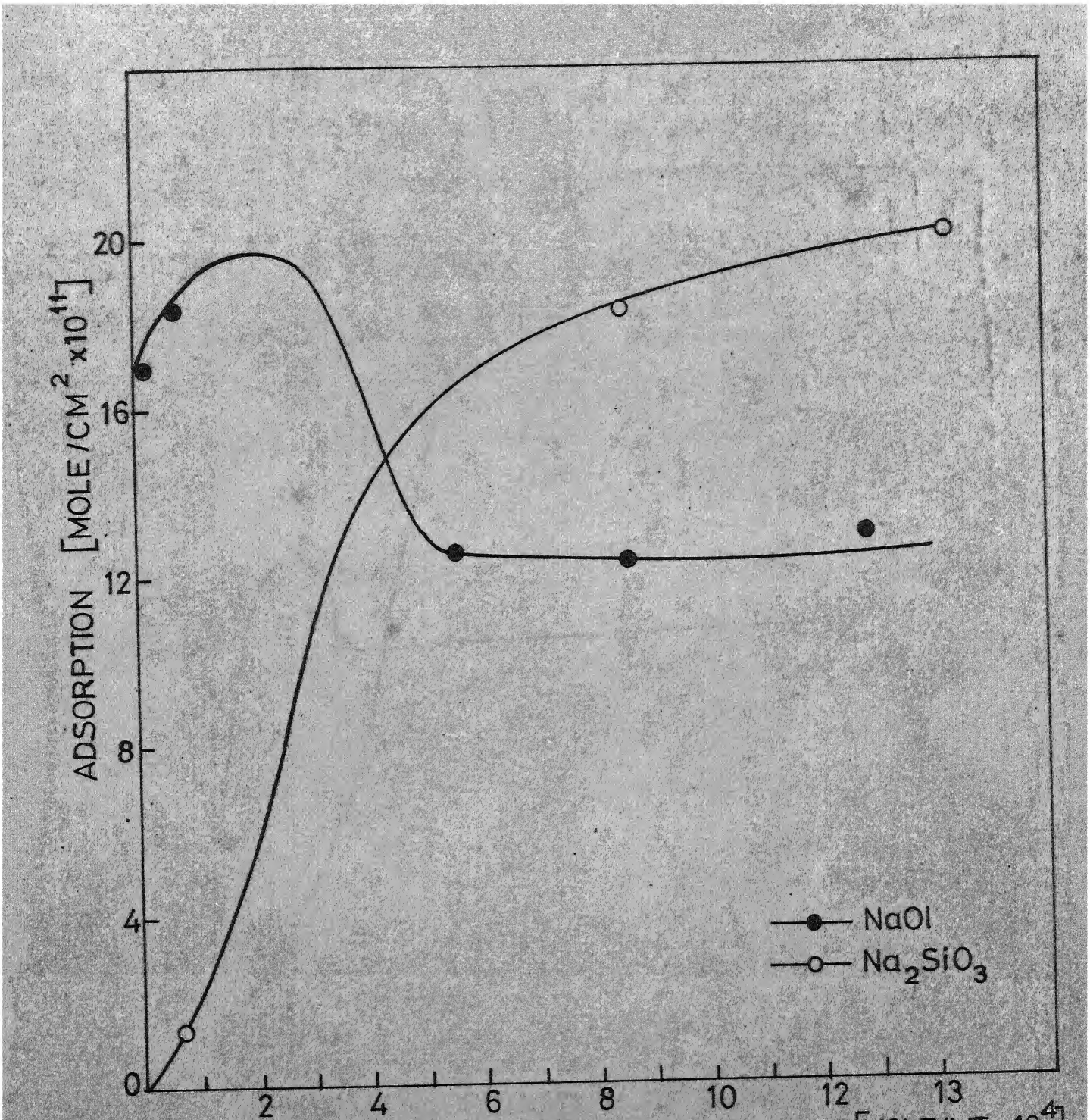

FIGURE 27 ADSORPTION OF SODIUM OLEATE AND SODIUM SILI-
-CATE ON ZIRCON AT CONSTANT FINAL pH 9.45±0.1

CONCN OF SODIUM OLEATE 4.93×10^{-4} MOLE/LIT

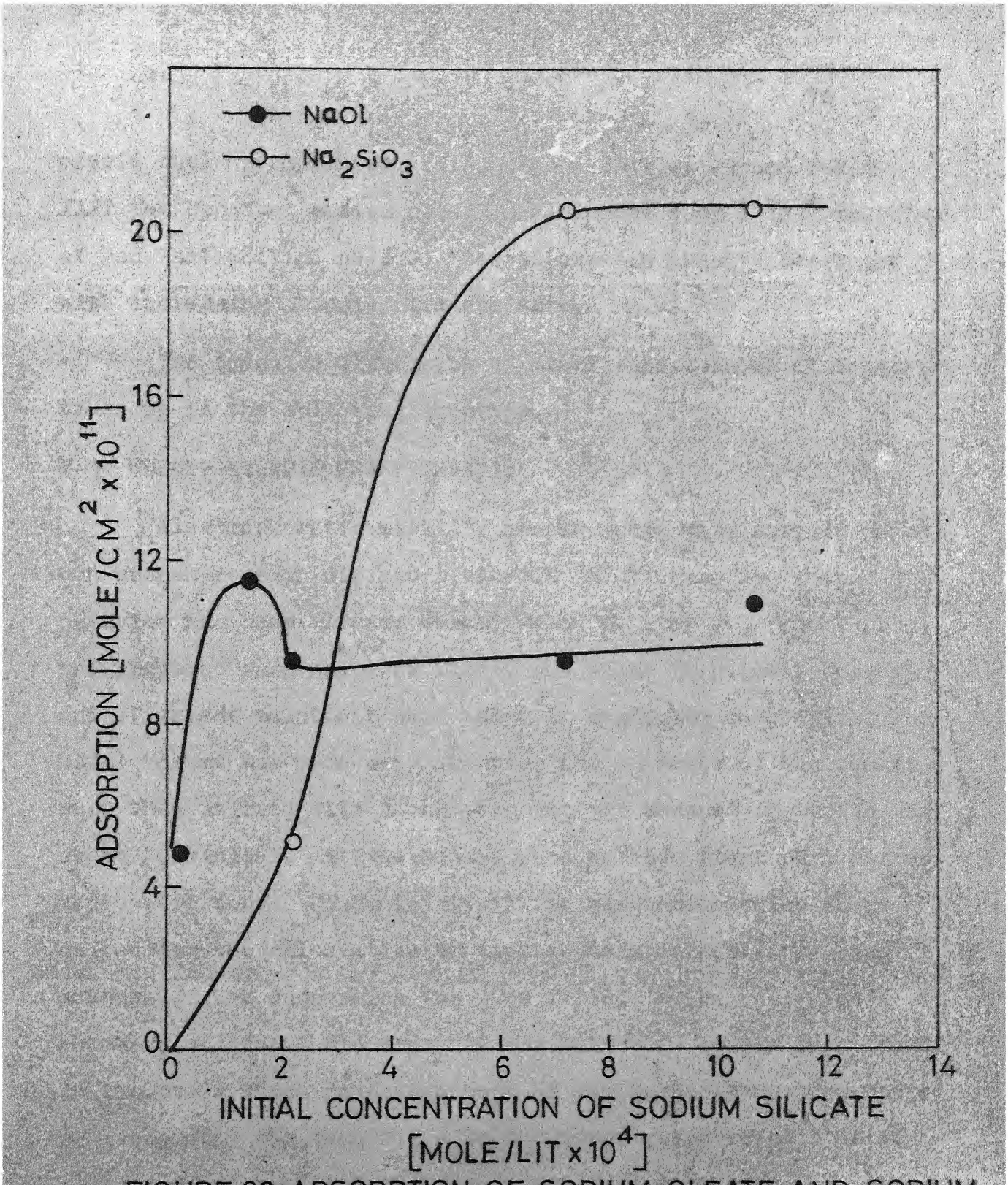

FIGURE 28 ADSORPTION OF SODIUM OLEATE AND SODIUM SILICATE ON ZIRCON AT CONSTANT FINAL pH 9.85 ± 0.1

CONCN OF SODIUM OLEATE 4.93 × 10^{-4} MOLE/LIT

oleate could be measured. It is shown in Fig. 29 and Table XXXI for constant sodium oleate addition of 4.93×10^{-4} mole/lit at constant initial pH 9.0. The adsorption density decreased with increasing fluosilicate addition.

The detailed discussion of these experimental findings is taken up in the following chapters.

V-3 ELECTROKINETIC MEASUREMENTS:

Electrophoretic mobility measurements were carried on zircon suspensions in different aqueous solutions. The sample preparation has been already described in Chapter IV. 25 ml of the prepared suspension of zircon was taken in plastic beakers and different solutions were added in requisite quantities. The total volume was made upto 125 ml. The contents of the beaker were then stirred with a magnetic stirrer encased in teflon for about 20 minutes. At the end of this period, final pH measurements were done. Conductivity of the suspension which is required for the calculation of electrophoretic mobility, was measured. The suspension was then filled in the collection chamber, and the whole assembly was weighed. It was then fixed in reservoir which contained rest of the suspension. The whole cell assembly was then fixed to the motor which rotated it at a speed of 30 rpm, and the zircon was kept in a state of suspension during the course of the experiment. Now, fixed current of 2-5 mA was applied and mass transport in the cell under the d.c. potential so applied, was allowed to take place for about

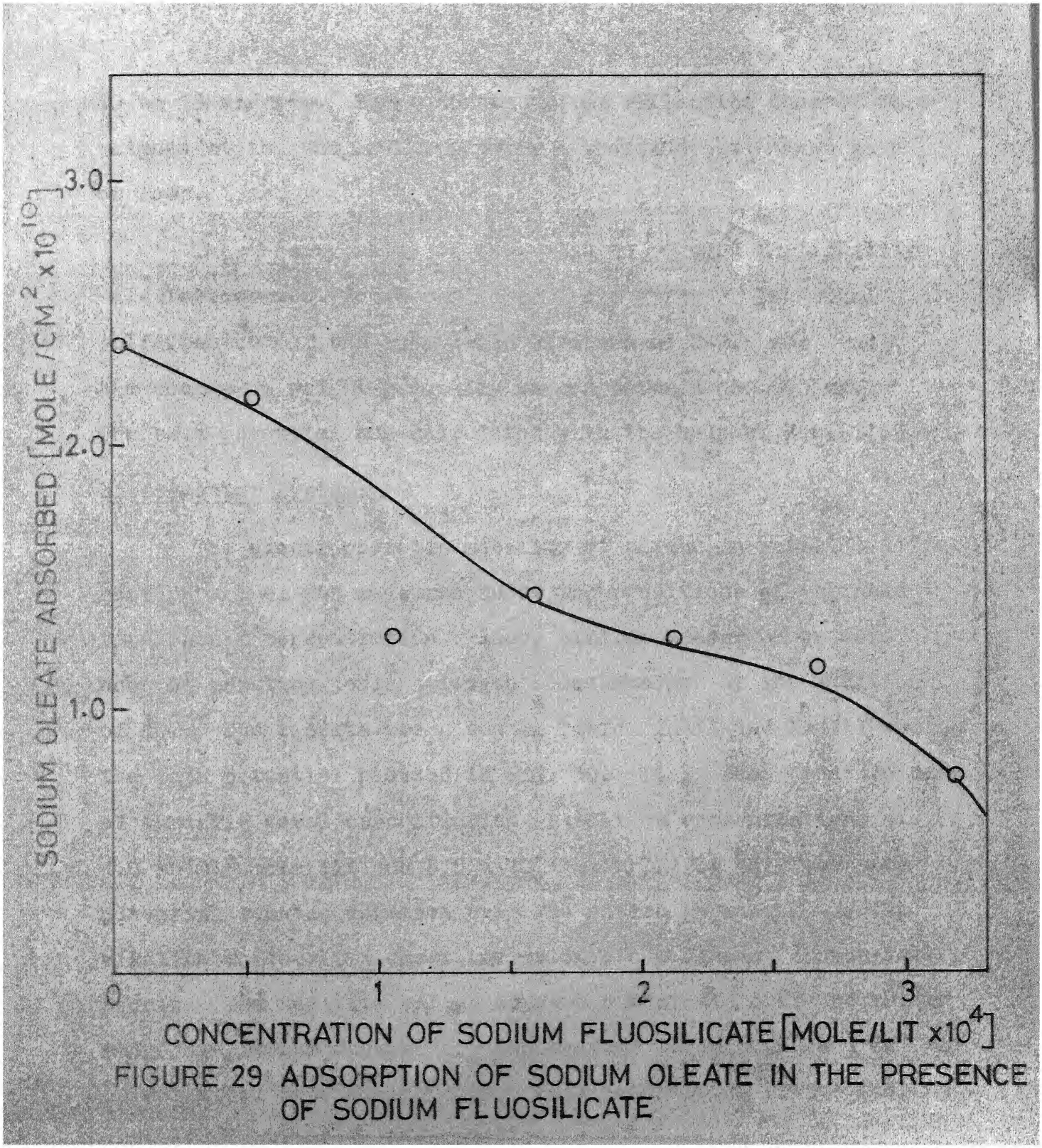

FIGURE 29 ADSORPTION OF SODIUM OLEATE IN THE PRESENCE OF SODIUM FLUOSILICATE

10 to 15 minutes. The contents of the collection chamber were weighed at the end of the experiment to find out weight gain or loss.

The density value of the solid to be used for mobility calculations was found out to be 4.456 gm/cm^3. The total solid content of the suspension were around 2-2.5 gms. and the change in weight generally ranged between 100-600 mg. The zeta potential was calculated with the help of Eqn.(II.9).

Zircon-Water System:

The electrophoretic mobility of zircon in water at different pH values was measured under the conditions of variable total ionic concentration. Also, similar measurements were done at constant ionic strength so maintained by the addition of KCl. The results are given in Tables XXXII and XXXIII and the zeta potential plotted in Fig. 30. It is seen that in case of variable total concentration as well as concentrations of 1.0×10^{-3} mole/lit and 5.0×10^{-3} mole/lit of KCl, the zeta potential remains negative over the entire pH range. In the alkaline range, it seems to merge into one line at appropriate points. The negative values of zeta potentials over the entire range are rather unusual for the systems in which H^+ and OH^- act as potential determining ions. This interesting result will be further discussed in Chapter VI.

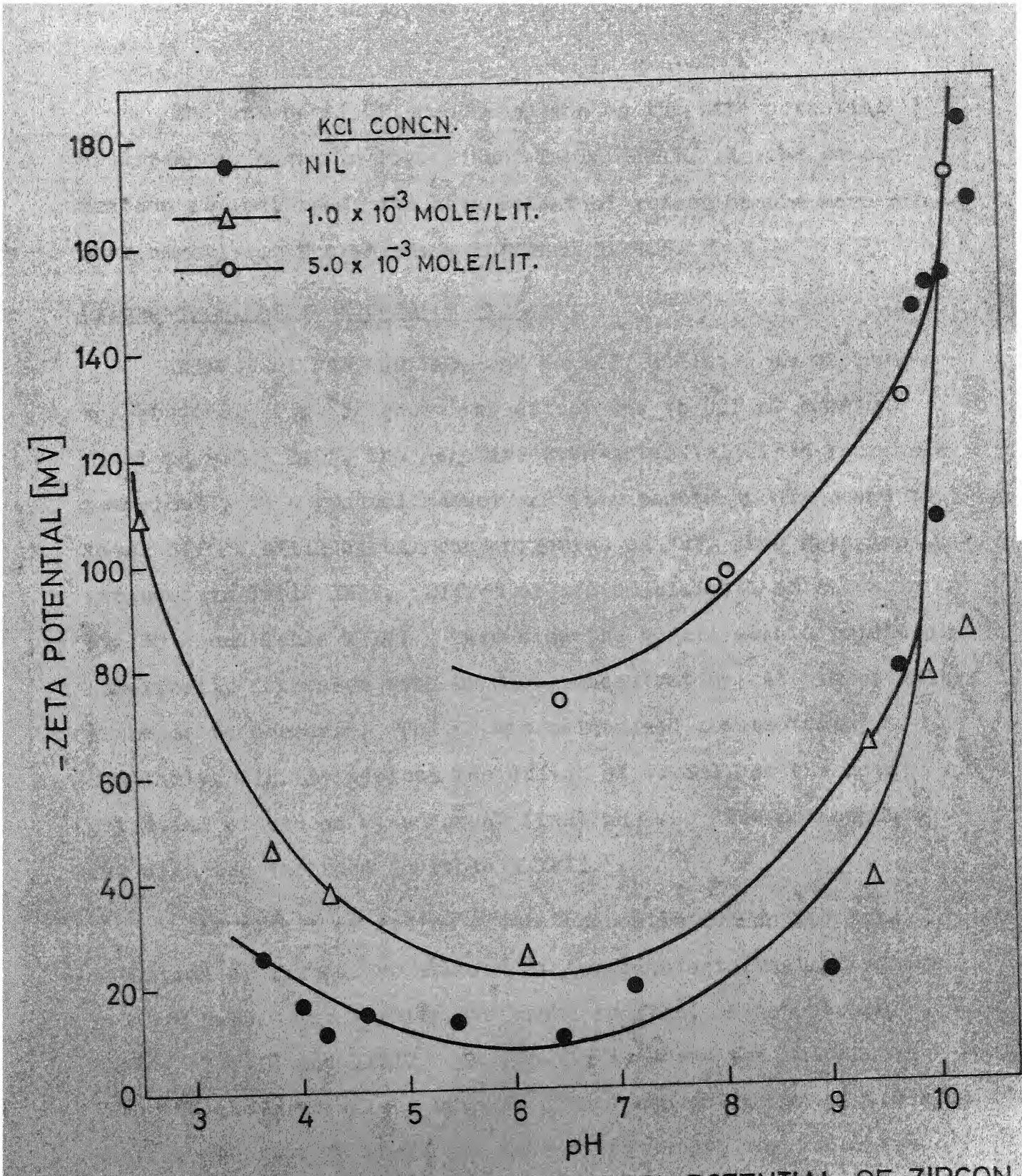

FIGURE 30 VARIATION OF THE ZETA POTENTIAL OF ZIRCON WITH pH AT DIFFERENT KCl CONCENTRATION

The effect of KCl concentration on the zeta potential of zircon is shown in Fig. 31 and Table XXXIV. As the concentration is increased, the zeta potential values become more and more negative. The pH was maintained at 6.5.

Zircon-Na Oleate - Moderator System:

Effect of NaF, Na_2SiO_3 and Na_2SiF_6 addition on zircon was studied. Fig. 32 shows the effect due to NaF at constant final pH 9.0 $\pm$ 0.05. The negative zeta-potential first increases numerically in a gradual manner and then shoots up. It seems to level off at still higher concentration of NaF. The data is included in Table XXXV. Effect of sodium silicate is shown in Fig.33 and Table XXXVI. Here also the negative zeta potential numerically increases with Na_2SiO_3 concentration. At higher values it seems to decrease. The pH was maintained constant at 9.0. Similarly, Fig. 34 depicts the effect of Na_2SiF_6 on the zeta potential of zircon at constant final pH 9.0. The corresponding data are included in Table XXXVII.

The effect of sodium oleate concentration on the zeta potential of zircon was studied at two constant final pH values 9.0 and 9.95. The results are shown in Figs. 35 and 36 and Tables XXXVIII and XXXIX. In Fig. 35 is shown the results at both the above pH values upto Na oleate concentration of 1.0×10^{-3} whereas the Fig. 36 shows the data at pH 9 upto the concentration 2.5×10^{-3} mole/lit. on a compressed scale. It is seen from Fig. 35 that the magnitude of negative zeta potential

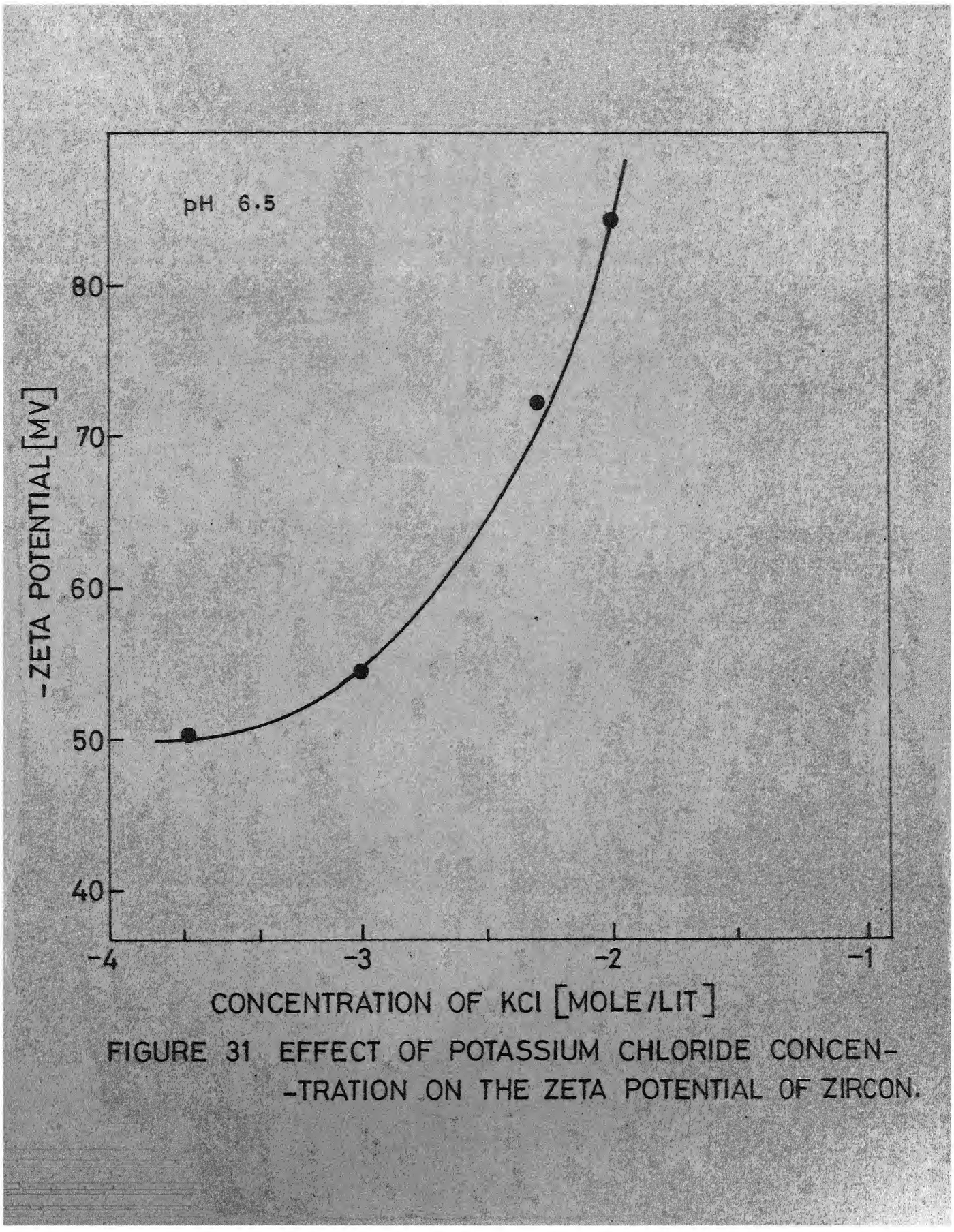

FIGURE 31 EFFECT OF POTASSIUM CHLORIDE CONCEN-
-TRATION ON THE ZETA POTENTIAL OF ZIRCON.

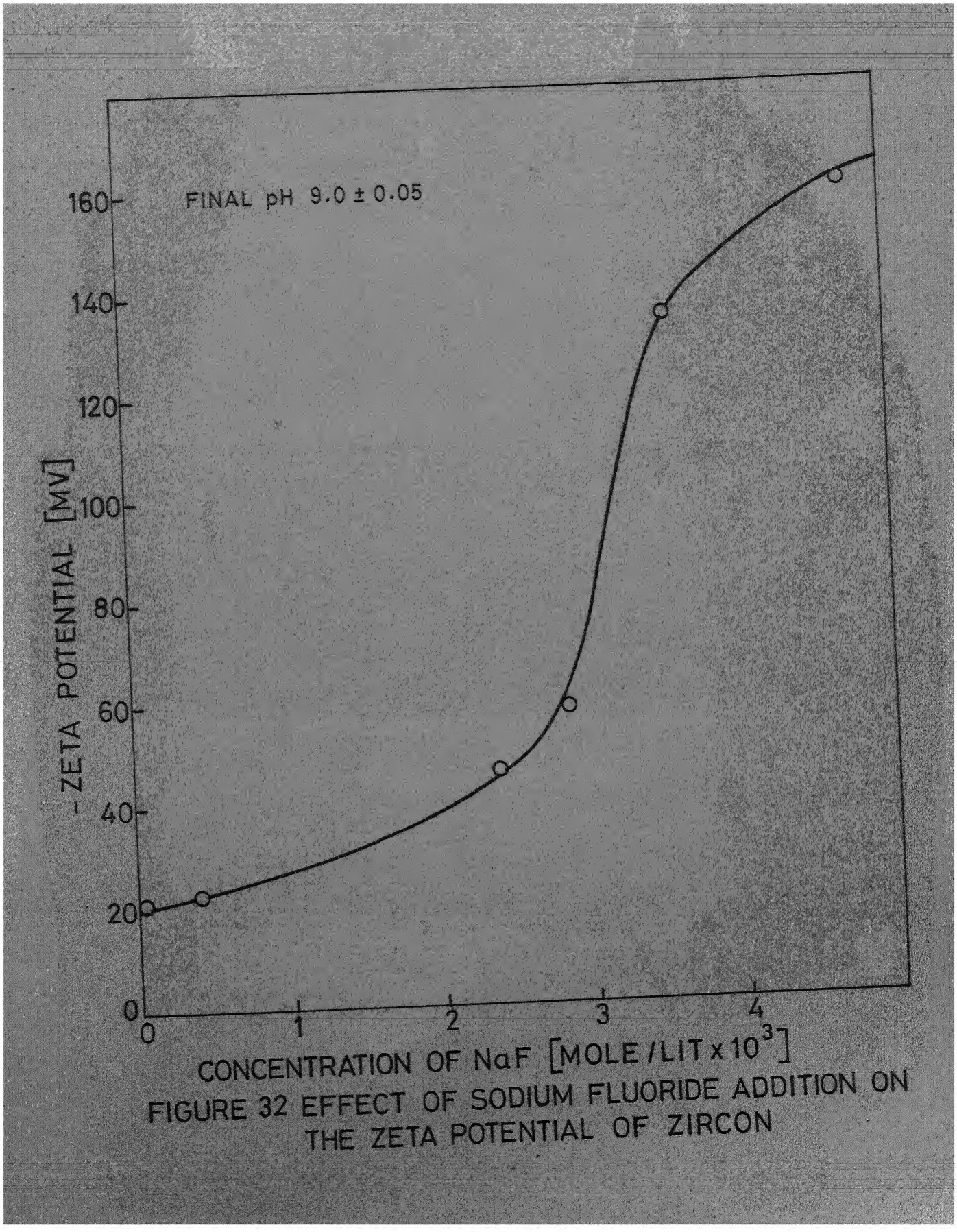

FIGURE 32 EFFECT OF SODIUM FLUORIDE ADDITION ON THE ZETA POTENTIAL OF ZIRCON

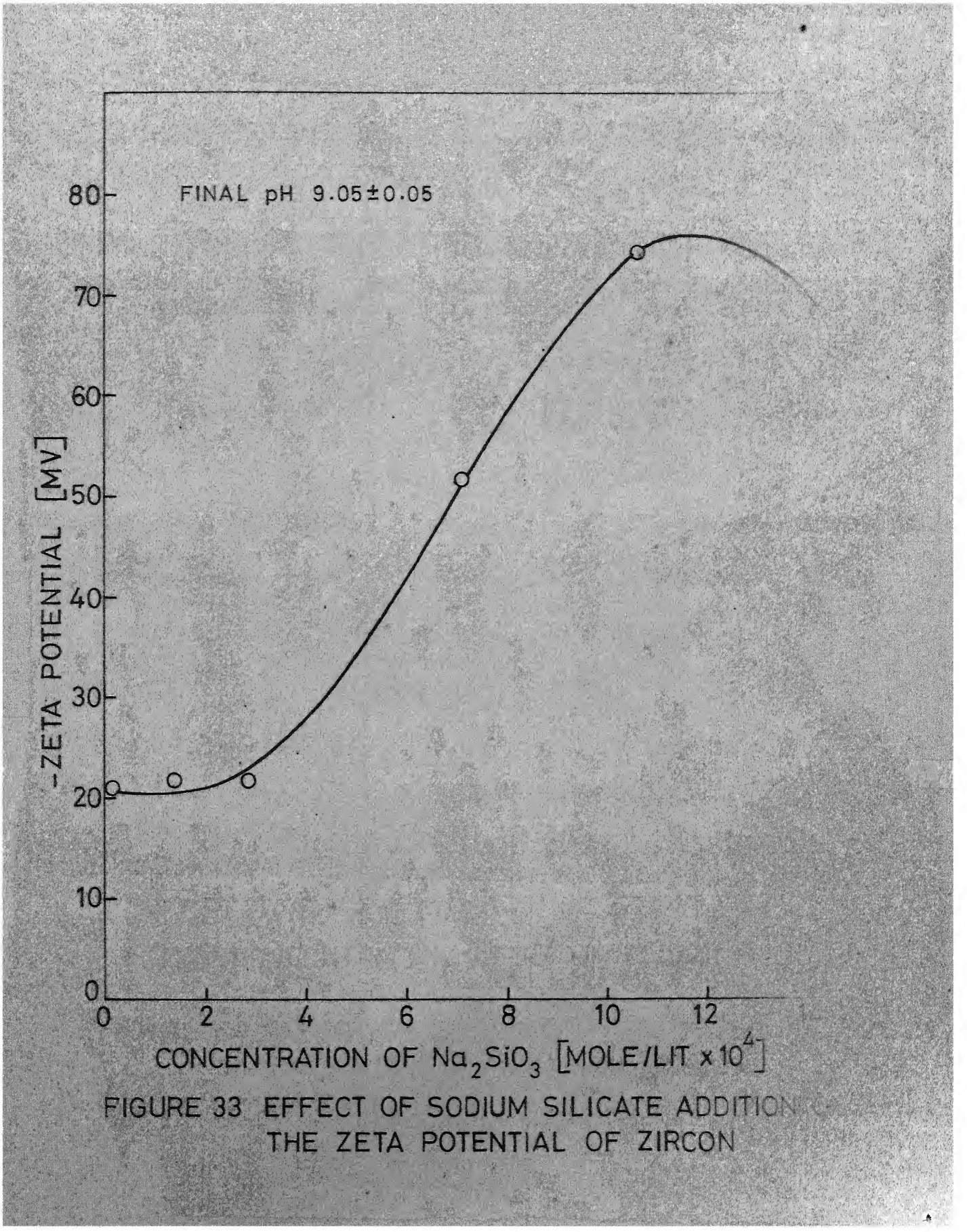

FIGURE 33 EFFECT OF SODIUM SILICATE ADDITION ON THE ZETA POTENTIAL OF ZIRCON

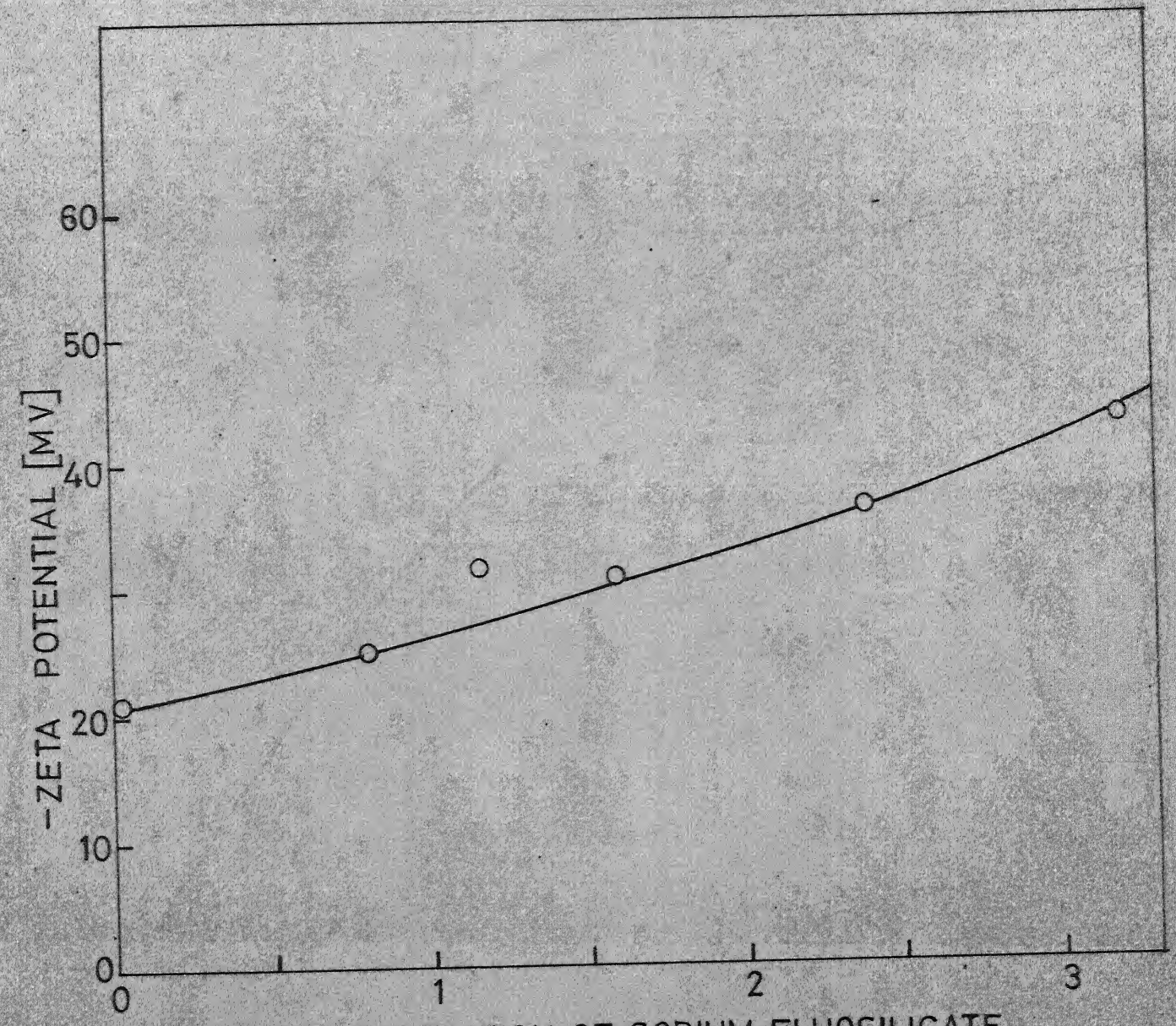

FIGURE 34 EFFECT OF SODIUM FLUOSILICATE ADDITION ON THE ZETA POTENTIAL OF ZIRCON

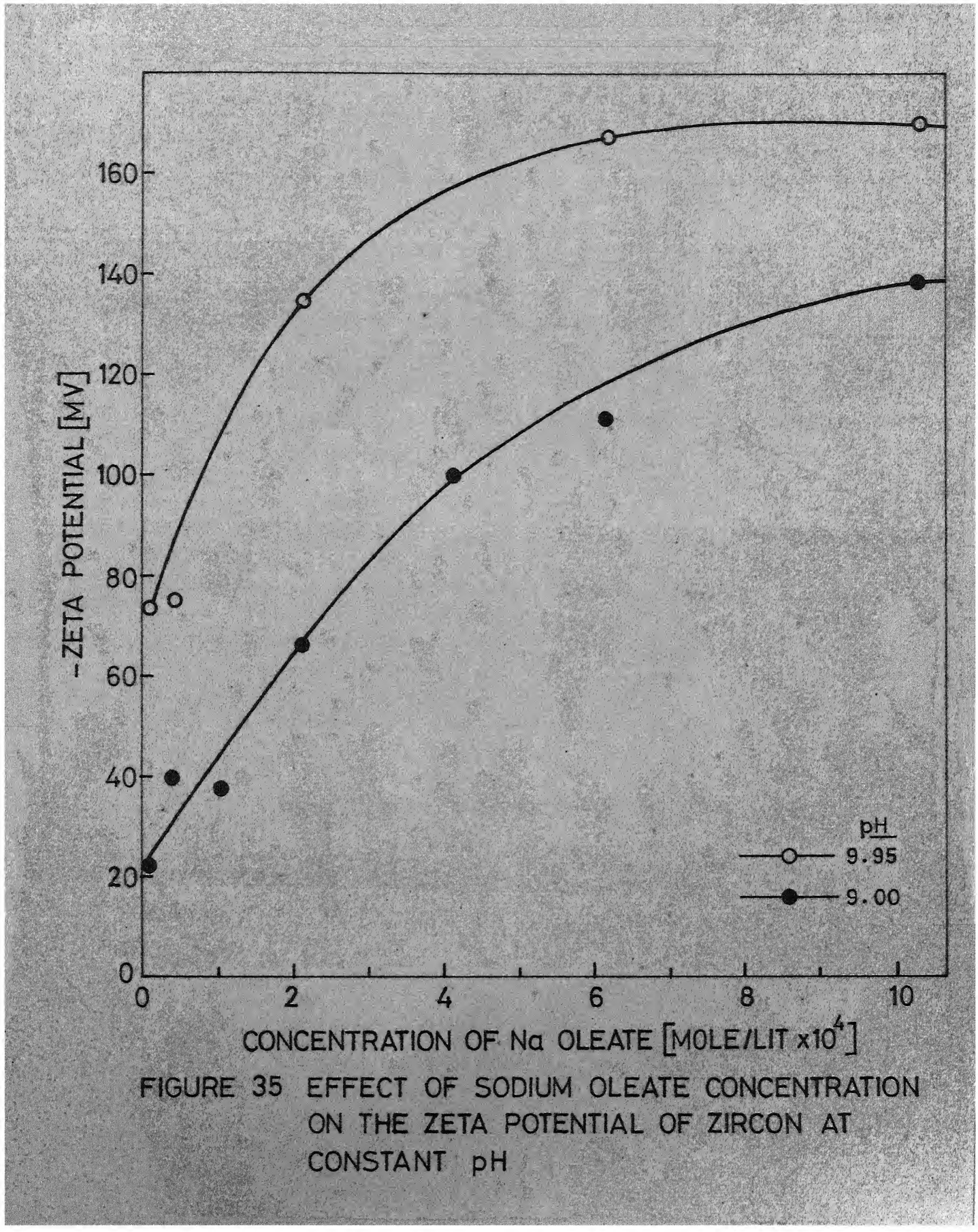

FIGURE 35 EFFECT OF SODIUM OLEATE CONCENTRATION ON THE ZETA POTENTIAL OF ZIRCON AT CONSTANT pH

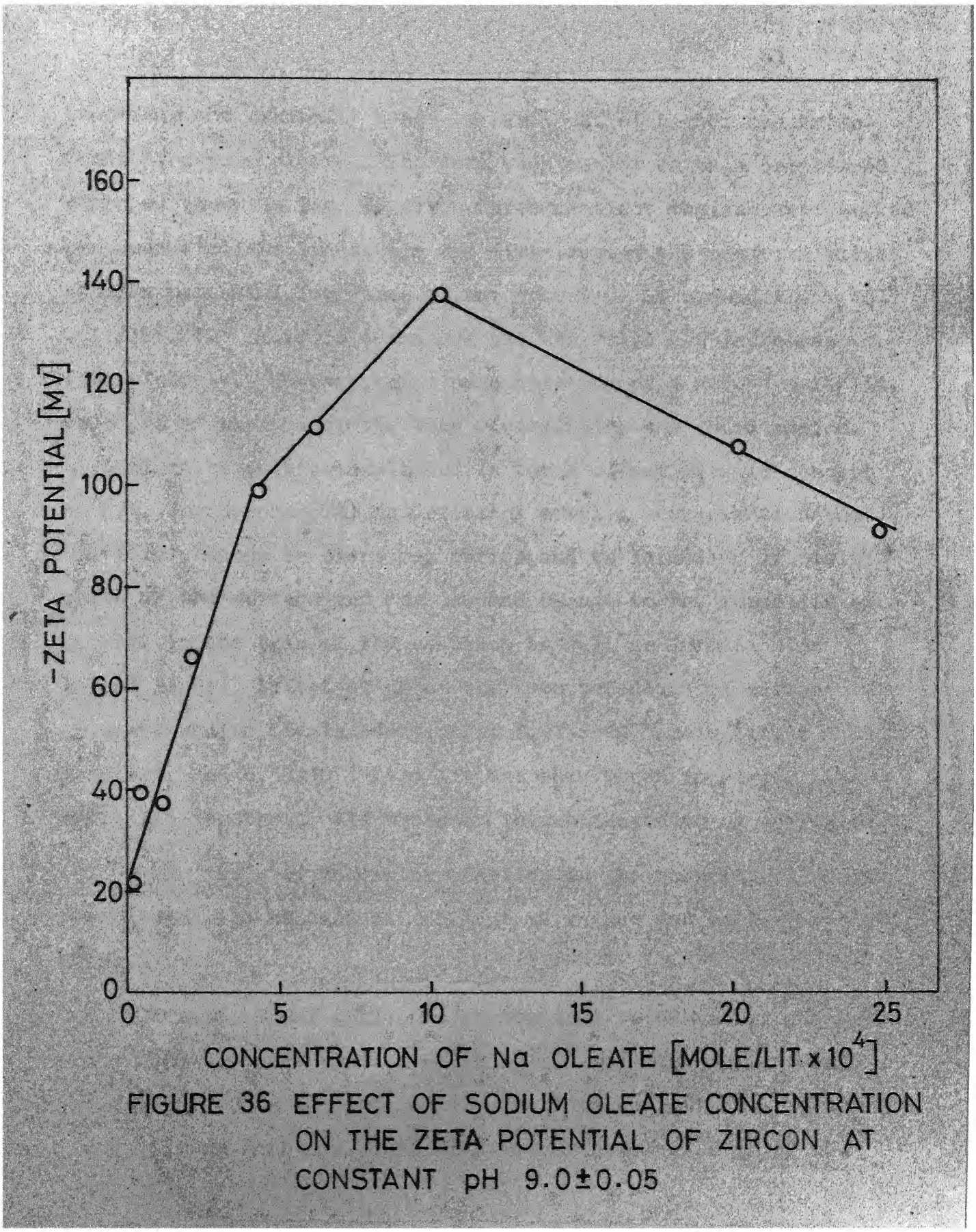

FIGURE 36 EFFECT OF SODIUM OLEATE CONCENTRATION ON THE ZETA POTENTIAL OF ZIRCON AT CONSTANT pH 9.0±0.05

increases and gradually tends to level off at higher concentrations of sodium oleate. The data when replotted on a compressed scale as shown in Fig. 36 gives three distinct regions represented by three straight lines. In the first region the negative value of zeta potential increases rather steeply. At around 4.0×10^{-4} mole/lit. the slope is decreased and the value now increases rather slowly. However, at a concentration of 1×10^{-3} mole/lit. there is a sharp decrease thus representing the third region. This might be perhaps explained in terms of hemimicelle concept of D.W. Fuerstenau (74) and critical micelle concentration (cmc). The first change in slope may correspond to formation of hemimicelle on the surface and the second change to the formation of micelle in the bulk of the solution as well as formation of second layer. Effect of pH on the zeta potential of zircon at constant sodium oleate addition of 1.97×10^{-4} mole/lit, 4.11×10^{-4} mole/lit. and 6.58×10^{-4} mole/lit has been shown in Fig.62 (and Table XL) in Chapter VII where it is considered to be appropriate.

The role of moderator addition in the presence of sodium oleate was also studied at constant pH values and collector additions.

Effect of NaF additions on the zeta potential at constant sodium oleate concentration 6.579×10^{-4} mole/lit and constant initial pH 9.0 as also at sodium oleate concentration 4.934×10^{-4} mole/lit. and constant final pH 9.70 are shown in Fig. 37 and Table XLI.

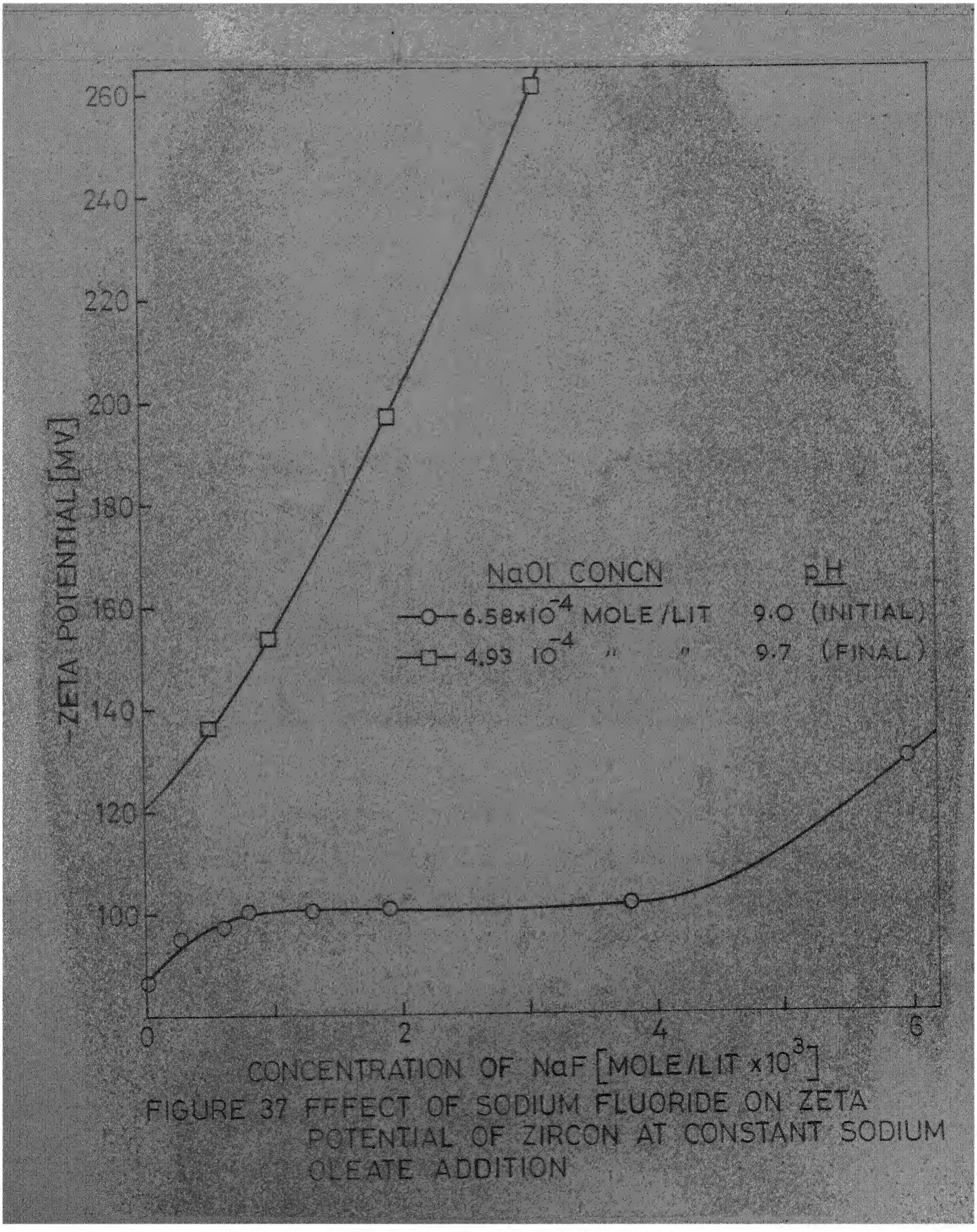

FIGURE 37 EFFECT OF SODIUM FLUORIDE ON ZETA POTENTIAL OF ZIRCON AT CONSTANT SODIUM OLEATE ADDITION

Similarly results with sodium silicate at sodium oleate concentration 6.58 x 10^{-4} mole/lit. and constant final pH 9.0 as well as at sodium oleate concentration 4.934 x 10^{-4} mole/lit. and constant final pH 9.5 are shown in Fig. 38 and tabulated in Table XLII.

Table XLIII and Fig. 39 contain the results of the investigations on Na_2SiF_6 as moderator. With sodium oleate concentration at 3.948 x 10^{-4} mole/lit at constant final pH 9.00 and sodium oleate concentration of 6.579 x 10^{-4} mole/lit. at constant final pH 9.06.

All these results will be discussed in Chapter VIII.

V-4: INFRARED SPECTRA:

Infrared spectroscopic investigations were carried out to know the nature of adsorbed species. Since the quantity of the adsorbed species if any, is always very small, a large surface area should be available. Therefore, the zircon sample for infrared studies was made very fine. The particle size was in submicron range. The spectra of the solid samples were recorded in KBr pellet. I.R. grade KBr was used for this purpose. It was heated at 110°C to remove any free moisture. 200 mg of this were then taken in an agate mortar and to it was added 1-2 mg of zircon with or without adsorbed collector. Thus the experimental solid in the KBr matrix was around one percent. The two were then intimately mixed and pressed into a vacuum die at 12000 lbs pressure for 5 minutes. at the end of which a transparent pellet

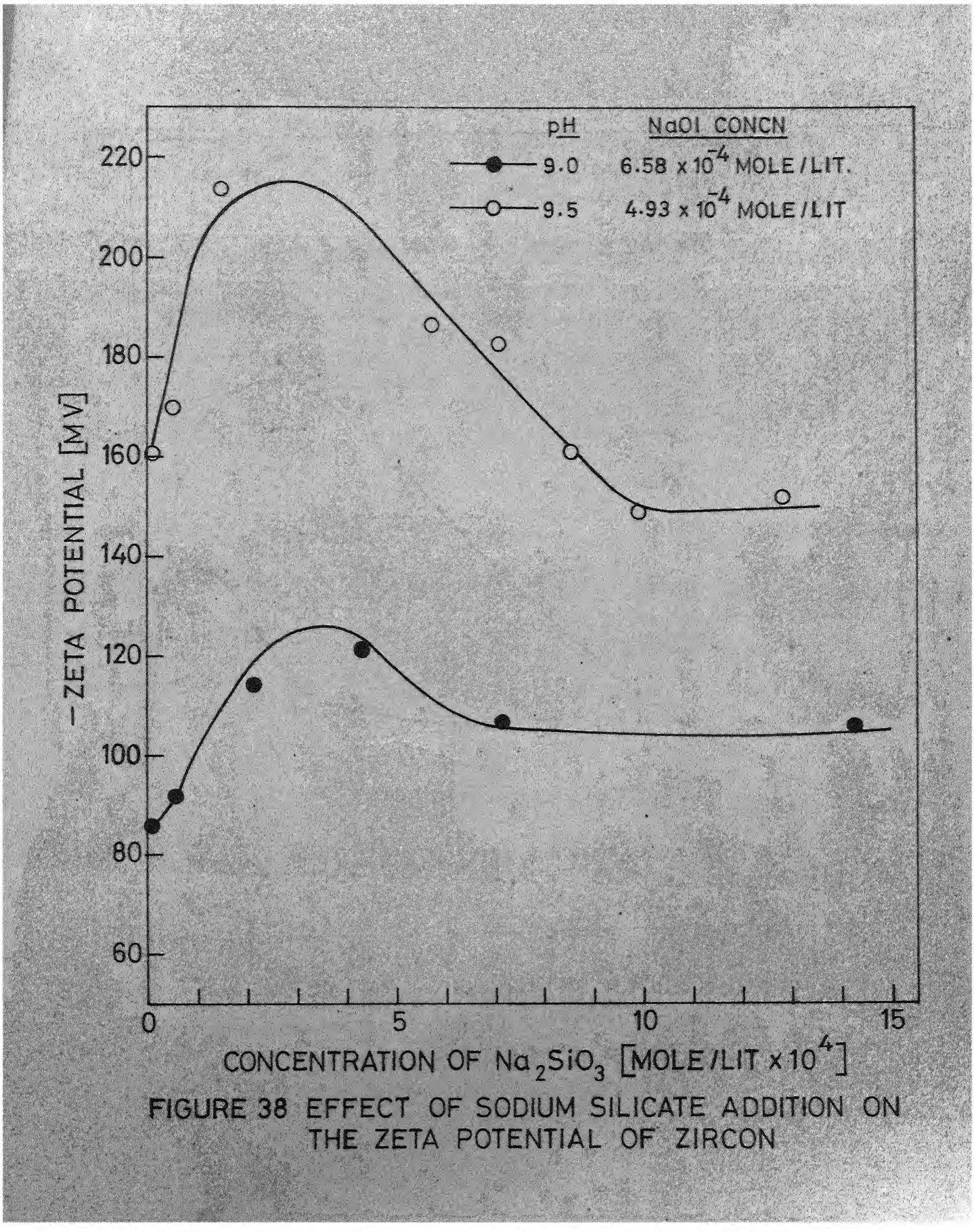

FIGURE 38 EFFECT OF SODIUM SILICATE ADDITION ON THE ZETA POTENTIAL OF ZIRCON

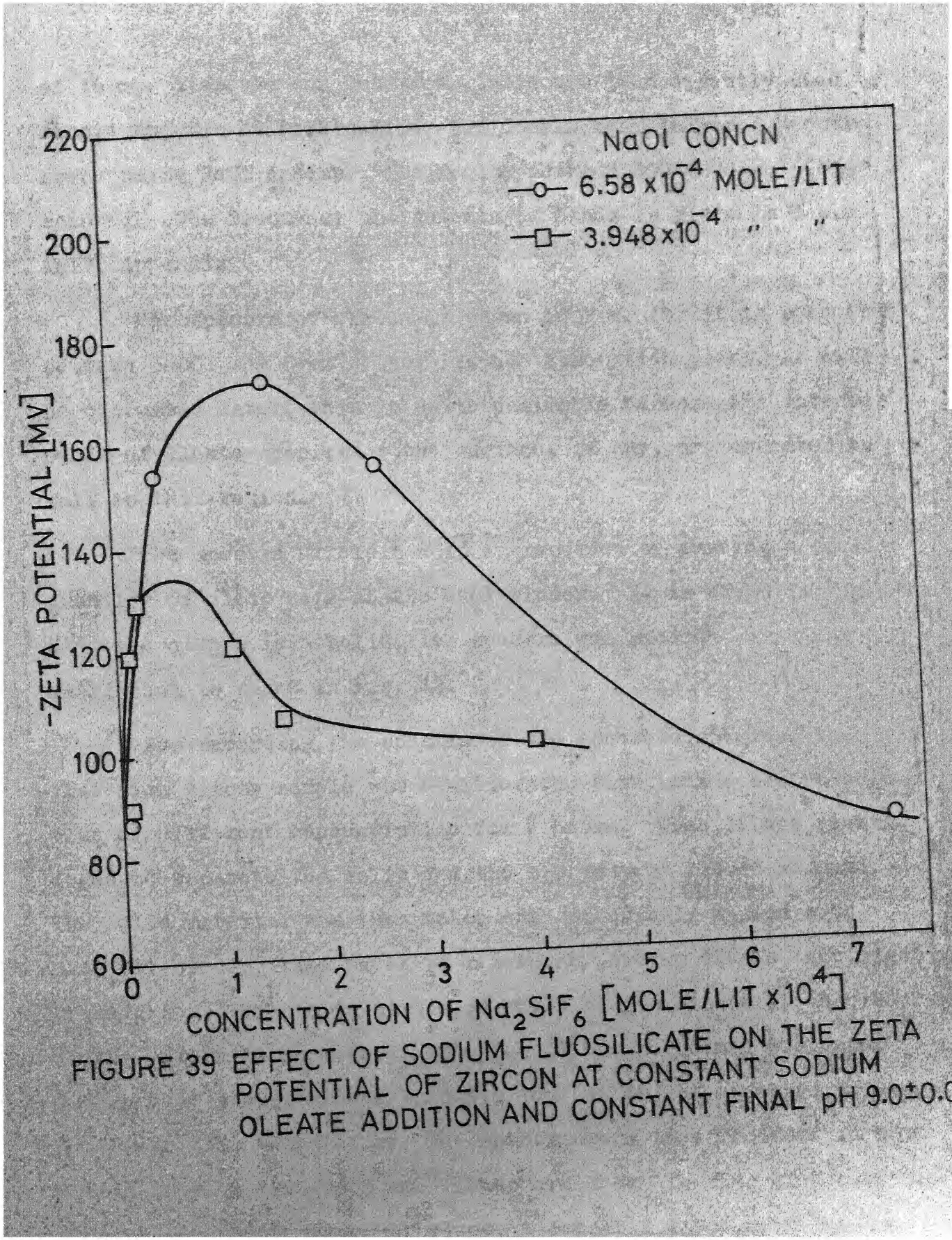

FIGURE 39 EFFECT OF SODIUM FLUOSILICATE ON THE ZETA POTENTIAL OF ZIRCON AT CONSTANT SODIUM OLEATE ADDITION AND CONSTANT FINAL pH 9.0±0.05

of 16 mm. diameter was obtained. This was then directly used to record spectra on Perkin-Elmer 521 double beam infrared spectroscope using NaCl optics. The region between 400-4000 cm^{-1} was scanned. The frequency assignments of bands is given in Table XLIV, Appendix G.

The spectra of zircon is shown in Fig. 40. It is seen that between 3000 - 1400 cm^{-1} there is no absorption peaks. As will be discussed later, this is quite desirable because the intense peaks of oleate species at the surface, if any, are expected to fall in this region.

The spectra of oleic acid is recorded by pasting a small quantity of oleic acid at the NaCl window. It is shown in Fig.41. Since Na oleate is a solid, its spectra was recorded in a KBr matrix and is shown in Fig. 42.

For recording the spectra of the adsorbed species, the fine size zircon sample was equilibrated with sodium oleate solution of different concentration for 2 hours. Then it was centrifuged to separate the solid and the supernatent liquid removed. The solid material was then taken out and quickly washed with 5-10 ml. of distilled water to remove any sodium oleate that might be sticking. The solid zircon on which sodium oleate is adsorbed is then dried in an oven at 80°C for 12 hours. Since the vapor pressure of sodium oleate is quite low it is not expected to evaporate at this temperature. The spectra were then recorded in KBr matrix between 1200-3500 cm^{-1}.These are shown in Fig. 43 for different sodium oleate concentrations. A detailed discussion follows in Chapter VII.

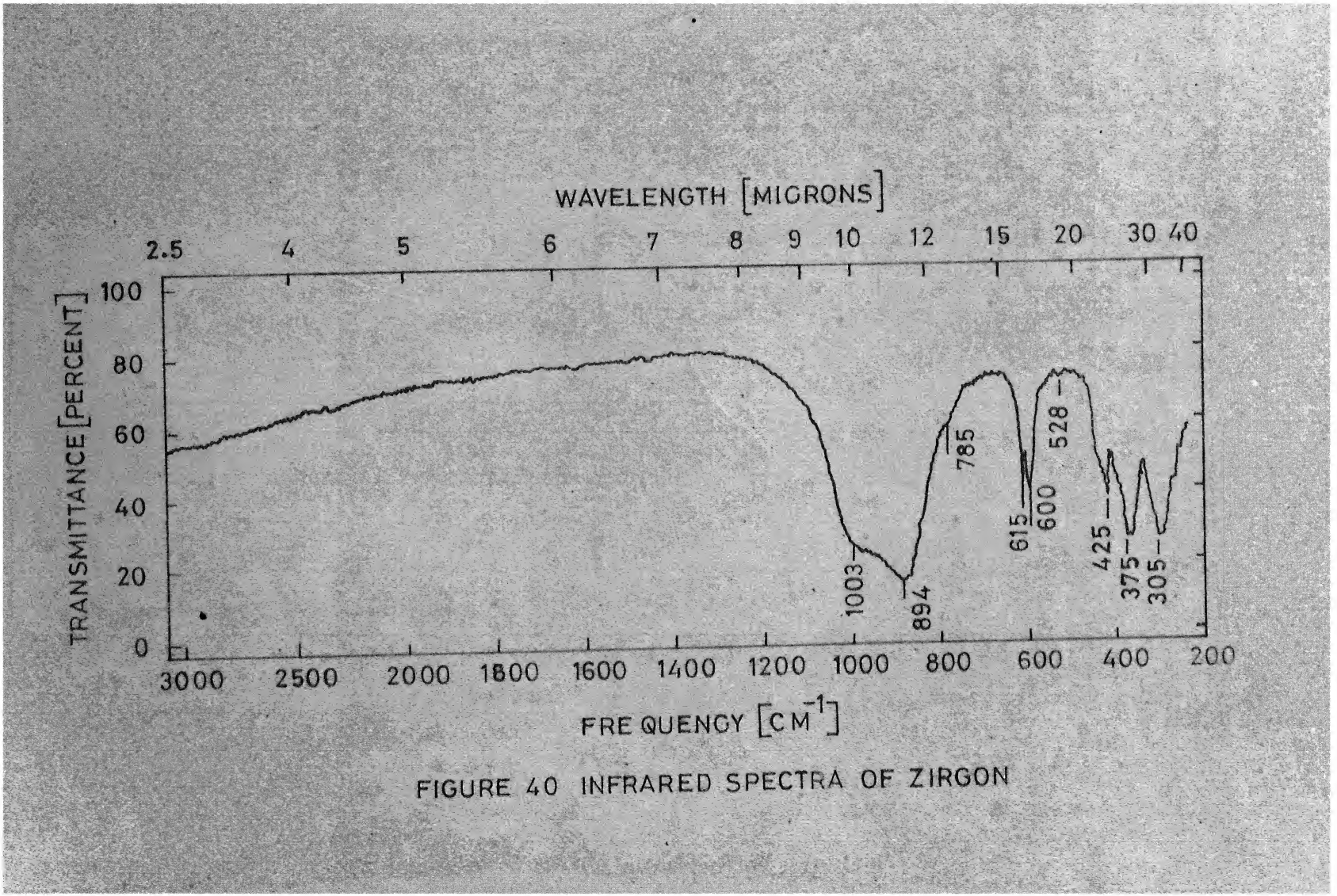

FIGURE 40 INFRARED SPECTRA OF ZIRGON

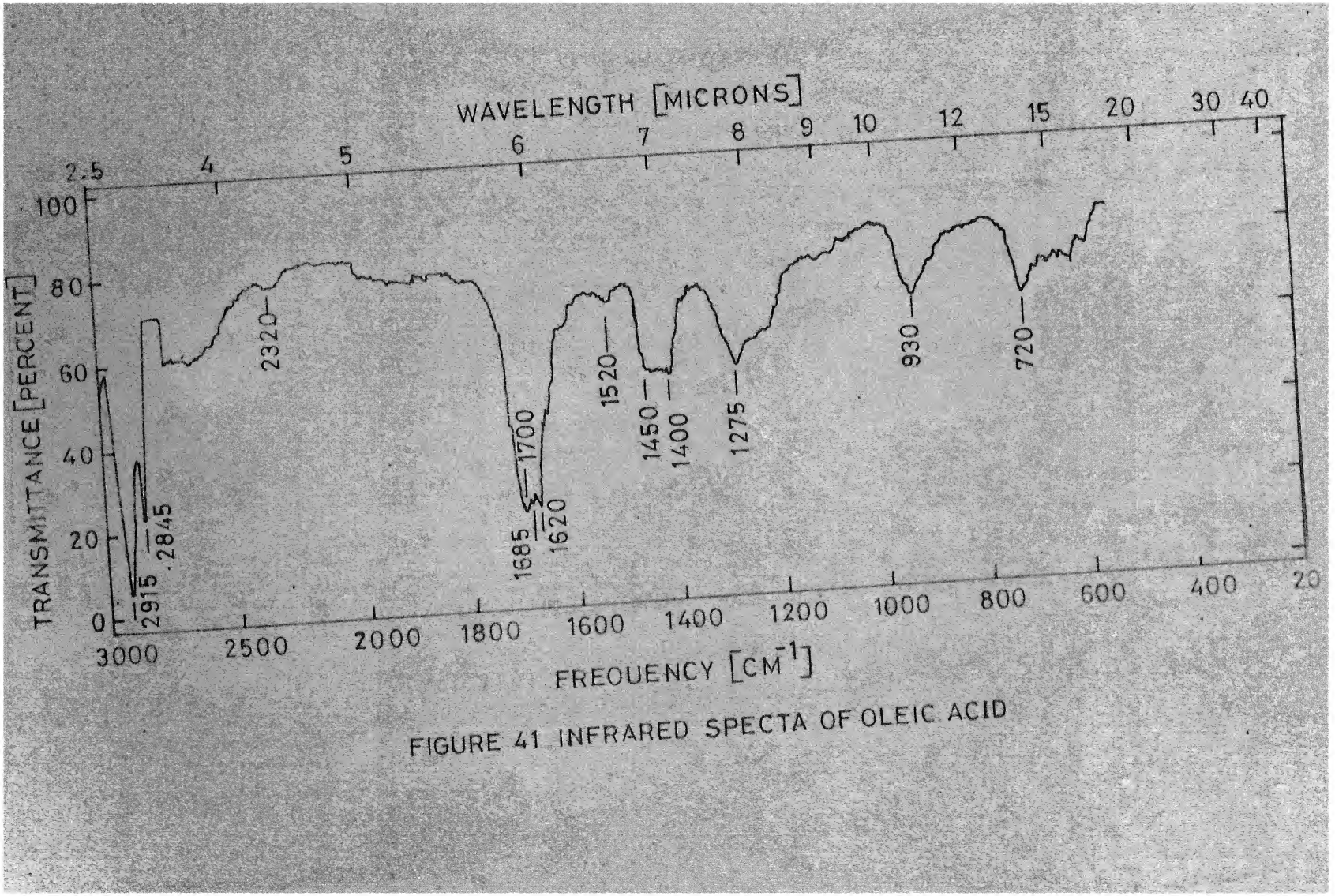

FIGURE 41 INFRARED SPECTA OF OLEIC ACID

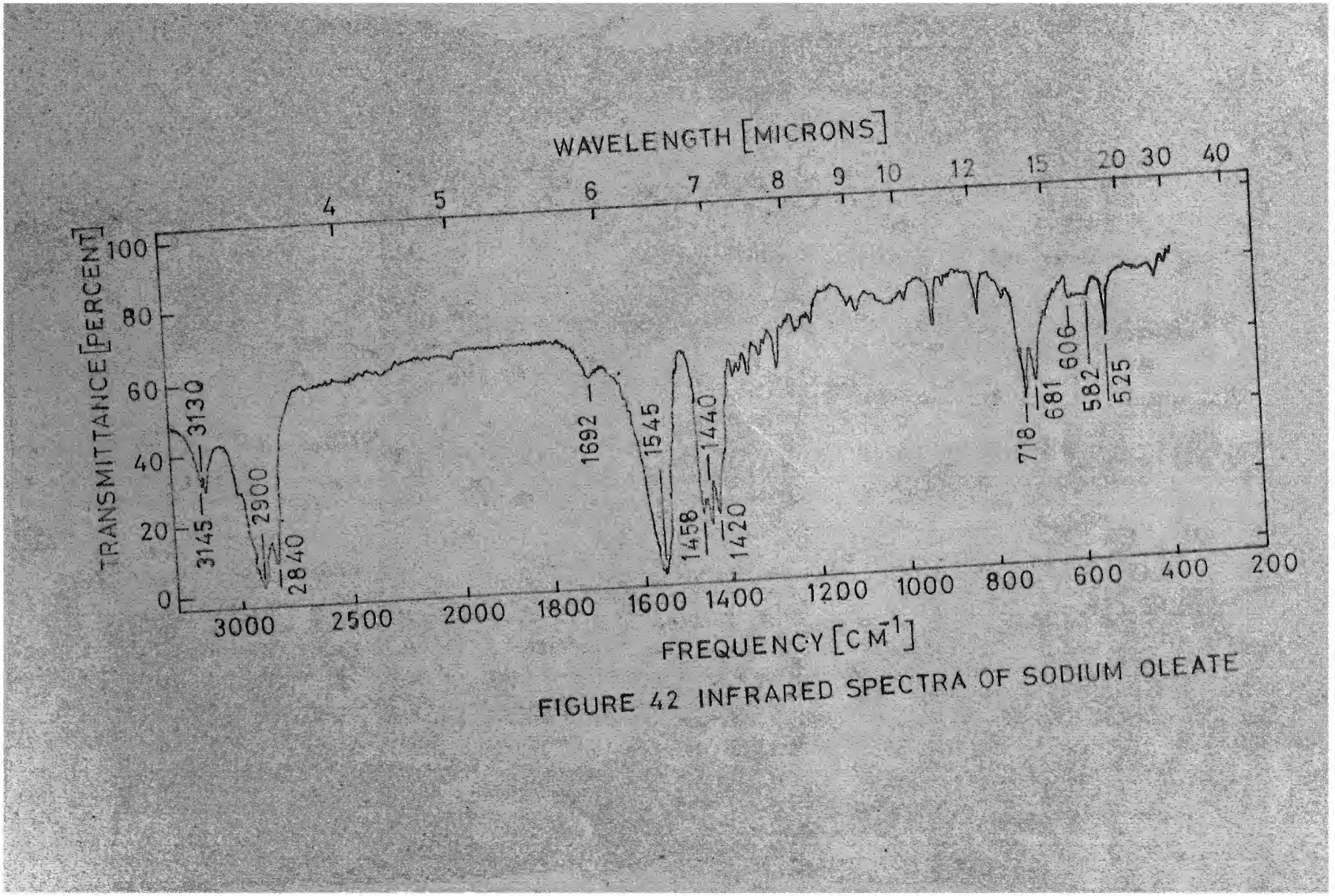

FIGURE 42 INFRARED SPECTRA OF SODIUM OLEATE

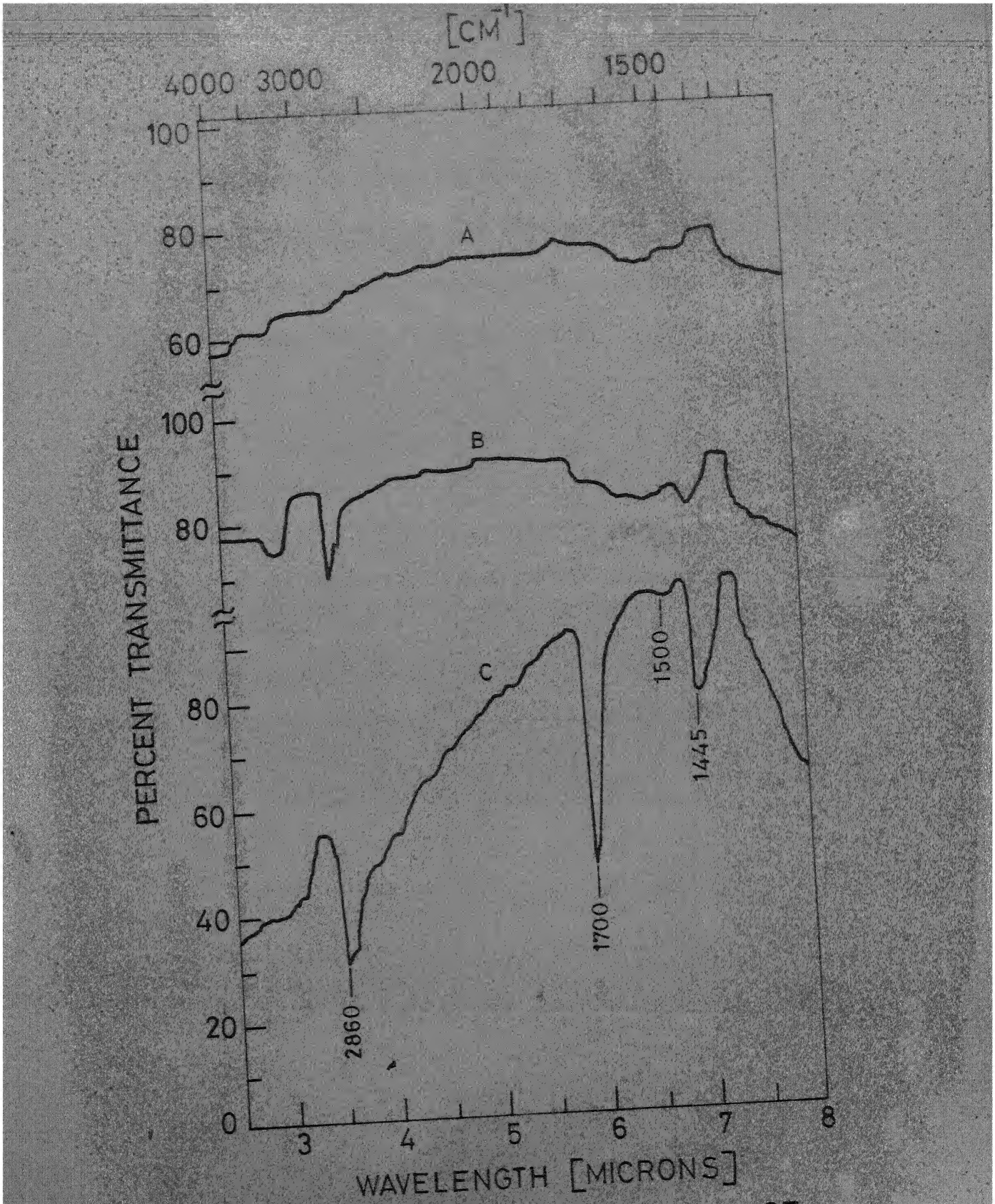

FIGURE 43 INFRARED SPECTRA OF SODIUM OLEATE ADSORBED ON ZIRCON

NaOl CONC.

A 1.096×10^{-3} MOLE/LIT.

B 1.316×10^{-3} MOLE/LIT.

C 1.862×10^{-3} MOLE/LIT.

CHAPTER VI

DISCUSSION OF RESULTS - I: ZIRCON-WATER SYSTEM

Prior to the discussions on the experimental data a brief reference about the electrical double layer would be worthwhile.

VI-1 THE ELECTRICAL DOUBLE LAYER:

The distribution of ions in the vicinity of the solid-liquid interface gives rise to what is generally known as the electrical double layer. It consists of two parts. One in immediate contact of the solid is called the fixed part of the double layer while the other which extends quite a bit in the liquid bulk phase is called the diffuse part of the double layer. The description of this double layer is generally given in terms of the models of Gouy and Chapman as well as that of Stern and Grahame (75). A schematic model of the double layer is given in Fig. 44.

According to Stern-Grahame model,

$$n_i = 2 r n_o e^{-W_i/kT} \qquad (VI.1)$$

where,

r - radius of the unhydrated ion

n_i - number of ions/cm^2 in the inner Helmholtz plane

n_o - number of ions/cm^3 in the bulk.

and W_i - work of adsorption of ions from the bulk to the inner Helmholtz plane.

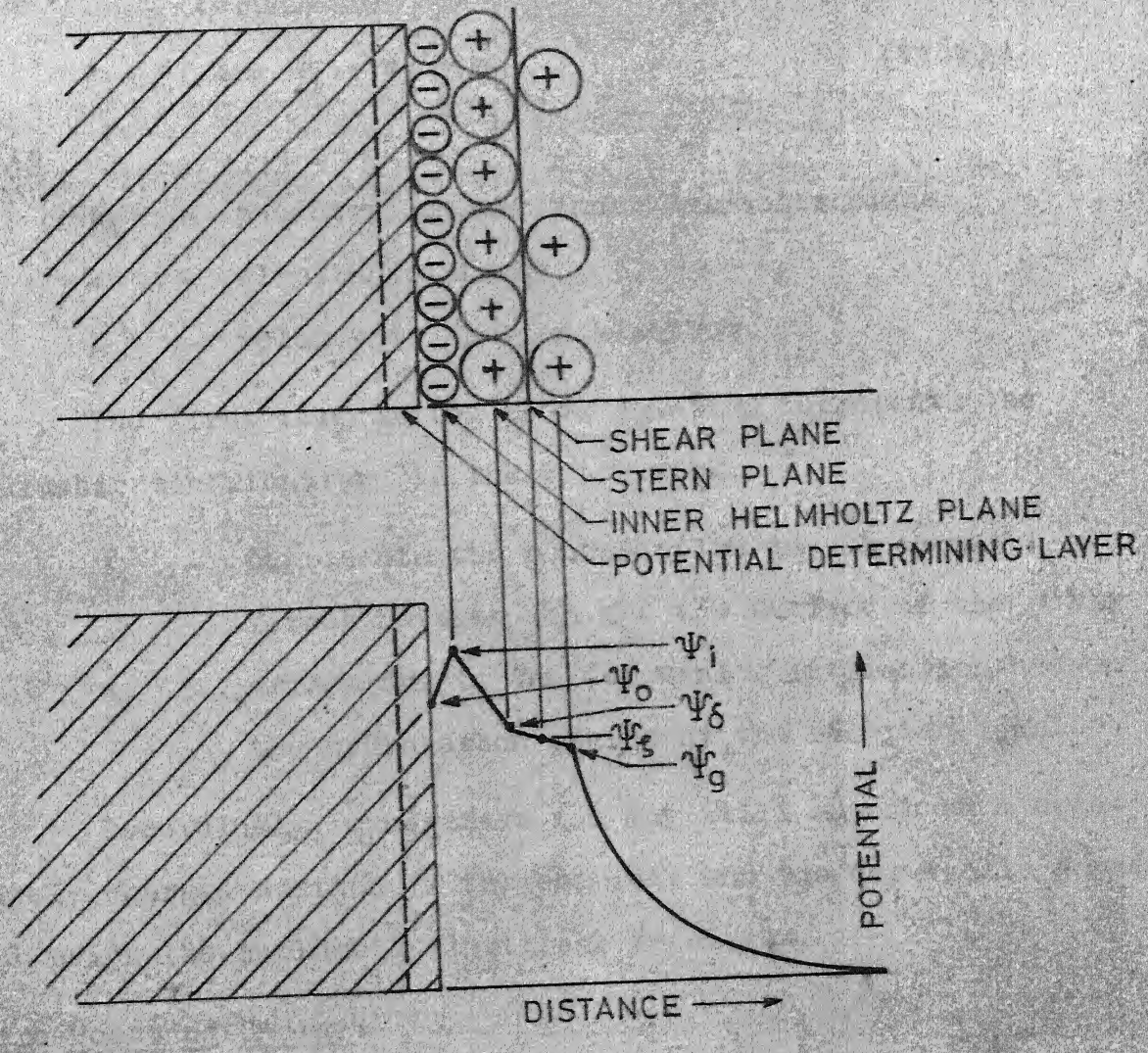

FIGURE 44 SCHEMATIC REPRESENTATION OF THE ELECTRICAL DOUBLE LAYER.

Splitting this work term into coulumbic and noncoulumbic terms we get,

$$W_i = Z e \psi_i + w_1 + w_2 \qquad \text{(VI.2)}$$

where

ψ_i - potential at the inner Helmholtz plane

e - electronic charge

Z - valency of the ion adsorbed

The first term in the above equation represents the coulumbic contribution to the total work.

w_1 - represents the contribution due to chemical forces between ion and the surface of the solid

w_2 - arises due to van der Waal's interaction between the hydrocarbon chains of the adsorbed ions.

Accordingly, a negative ion may still adsorb on a negatively charged surface if the chemical and van der waal's forces out weigh the coulumbic electrical repulsion.

Zero Point of Charge:

In case of most of the oxygen bearing minerals and solids, hydrogen and hydroxyl ions are potential determining. The overall reaction in such cases may be adequately represented by

$$\boxed{\text{Negative surface site}} + 2H^+ = \boxed{\text{Positive surface site}} \qquad \text{(VI.3)}$$

so that,

$$k^{o} = (a^{s}_{+} / a^{s}_{-})\, a^{-2}_{H^+} \qquad (VI.4)$$

where,

k^{o} - surface equilibrium constant

a^{s}_{+} and a^{s}_{-} - activity of the positive and negative surface sites respectively.

and a_{H^+} - activity of the protons in solution.

A particular activity $a^{o}_{H^+}$, yields a condition known as zero point of charge for which a^{s}_{+} / a^{s}_{-} is equal to unity. Zero point of charge is an important parameter characteristing the double layer of the system.

The value of the zero point of charge (zpc) for any substance is characterised by the mode of sample preparation, its history and the method of determination. This is why widely divergent values of zpc are reported for the same substance. It is, therefore, necessary to realise that the zpc is characteristic of the system under investigation rather than of the substance as such.

VI-2 STRUCTURAL AND AQUEOUS CHEMISTRY OF ZIRCON:

Towards understanding the surface properties of zircon, a knowledge of its crystal chemistry and its aqueous behaviour is very helpful.

Crystal Chemistry:

True zircon has a chemical composition corresponding to the formulae $ZrO_2 \cdot SiO_2$ or $ZrSiO_4$. Any one of these representations is a matter of preference. However, none of these is fairly adequate as the former conveys an unwarranted implication that the ZrO_2 and SiO_2 have independent compound status whereas the latter implies that the oxygen atoms are more especially associated with silicon than with zirconium.

Zircon is tetragonal and has the symmetry of space group $4D_i - 19$ (D_{4h}^{19}). The crystal structure of zircon has been investigated by several workers (76,77,78) and is shown in Fig. 45. The lattice parameters of zircon according to most recent measurements (78) are a = 6.616 Å and c = 6.015 Å. The unit cell consists of four molecules of $ZrSiO_4$ and the tetrahedron is somewhat distorted. The Zr–O bond length is reported to be 2.05 Å and Si–O 1.62 Å. Huckel (79) has stressed that the silica tetrahedra have no point of contact with each other and there is no SiO_4^{-4} orthosilicate anion.

Bluementhal (80) pictures zircon as consisting of series of chains of the structure shown in Fig. 46 (a). Each successive pair of oxygen atoms is arranged transverse to previous pair. The structure is bonded in three dimensions by coordinate covalencies acting between zirconium atom of one chain and oxygen atoms of a neighbouring chain. Thus the entire crystal is held together by valency forces.

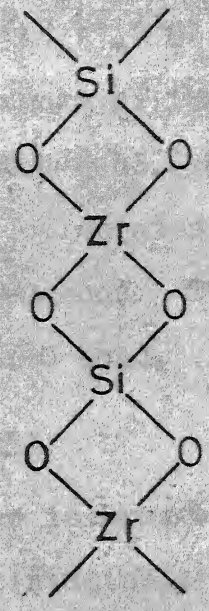

FIGURE 46(a) CHAIN DESCRIPTION OF ZIRCON STRUCTURE

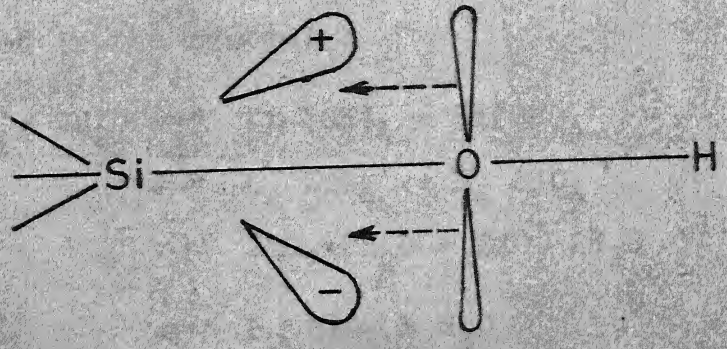

FIGURE 46(b) SURFACE SILANOL GROUP

The percentage ionic character P of the bond is given by the impirical relation due to Pauling (81).

$$P = 16\,|X_A - X_B| + 3.5\,|X_A - X_B|^2 \qquad \text{(VI.8)}$$

where X_A and X_B are the measure of the electronegativity of the atoms A and B forming the bond. The percentage ionic character on this basis is calculated to be 48.935 for Zr–O bond and 36.915 for the Si–O bond. Thus Zr–O bond has more ionic character than the Si–O bond.

Aqueous Chemistry of Zircon:

When powdered zircon is brought in contact with water at different pH values it invariably interacts with H^+ and OH^- ions to produce a number of complex species involving Zr and Si. These species may either remain at the surface are get dissolved in aqueous bulk phase.

The following reactions represent the major ionic equilibria involved in the system.

$$ZrSiO_4 + 4H_2O \rightleftharpoons Zr(OH)_4 + Si(OH)_4$$
$$\rightleftharpoons H_4ZrO_4 + H_4SiO_4$$
$$\rightleftharpoons ZrO_2\cdot 2H_2O + SiO_2\cdot 2H_2O \qquad \text{(VI.9)}$$

$$H_4SiO_4 \rightleftharpoons H_2SiO_3 + H_2O \qquad \text{(VI.10)}$$

$$H_2SiO_3 \rightleftharpoons HSiO_3^- + H^+ \qquad \text{(VI.11)}$$

$$HSiO_3^- \rightleftharpoons SiO_3^{=} + H^+ \qquad \text{(VI.12)}$$

$$H_4ZrO_4 \rightleftharpoons H_2ZrO_3 + H_2O \qquad \text{(VI.13)}$$

$$H_2ZrO_3 \rightleftharpoons HZrO_3^- + H^+ \qquad \text{(VI.14)}$$

$$HZrO_3^- + 3H^+ \rightleftharpoons ZrO^{++} + 2H_2O \qquad \text{(VI.15)}$$

$$ZrO^{++} + 2H^+ \rightleftharpoons Zr^{4+} + H_2O \qquad \text{(VI.16)}$$

The thermodynamic data e.g. ΔH^{o}_{f}, ΔS^{o}_{f}, ΔG^{o}_{f} where ΔH^{o}_{f} is the standard heat of formation, ΔS^{o}_{f} Standard entropy of formation and ΔG^{o}_{f} is the standard free energy of formation, are given in Appendix B (Table VI) for different ionic species. The free energy of formation of $ZrSiO_4$ has been calculated by indirect method and is included in Appendix B. The free energy change of different reactions along with the equilibrium constants have been also included in Appendix B (Table VII).

With the help of these data an attempt was made to calculate the pH-concentration relationships for various species. However, the values obtained were inconsistent and unrealistic. It may be due to unreliable data. Nevertheless, it may be mentioned here that $H_2 SiO_3$ is the predominant species upto pH 10. Between pH 10 to 12 $H SiO_3^-$ is the predominant species whereas above pH 12 $SiO_3^{=}$ is more abundant. Similarly, in case of zirconium species Zr^{4+} is found abundantly only below pH 1. ZrO^{++} is predominant upto pH 6.65 and $H ZrO_3^-$ is predominant above that pH. However, the actual concentrations of all these species would depend on the extent of reaction (VI.9). From Table VII (Appendix B), it will be seen that the equilibrium constant for the above reaction is 10^{-87} which means that the actual concentrations of the species would be negligible. Nevertheless, excessive grinding would largely determine the values of the actual concentrations of the species derived from zircon in aqueous bulk phase.

VI-3 ZIRCON-WATER SYSTEM: ELECTROKINETIC BEHAVIOUR:

The experimental results of the electrophoretic mobility measurements (wherein the effect of pH and ionic strength of the electrolyte (KCl) have been studied e.g. Figs. 30 and 31) reveal that:

i) In the alkaline range negative electrophoretic mobility (or negative zeta potential) is obtained. It increases numerically as the pH is increased.

ii) Between pH 5-8, the zeta potential-pH curves show a broad minima but zeta potential is still negative.

iii) In acidic pH below 5 the zeta potential is still negative and goes on increasing with decrease in pH.

iv) It was not possible to locate zpc with the present sample as there is no charge reversal.

v) With increasing total ionic concentration the mobility increased numerically and was more and more negative at all pH values studied.

vi) Curves for all the concentrations of KCl merge into one at some pH values indicating that the zeta potential is solely governed by OH^- ions at higher alkaline pH.

Discussion of Results:

The occurrence of negative zeta potential in the acidic range is rather unusual but by no means unprecedented for the oxide or silicate systems.

For example H.F. Holmes et. al. (82) observed during their studies on the electrokinetic properties of ThO_2 that the sample fired at lower temperatures upto 1000°C showed both + ve and - ve zeta potential in appropriate pH ranges, whereas the sample fired at 1600°C did not show + ve potential at all. This was also observed to be the case for sintered oxides by O'Connor (83) who ascribed the behaviour to the basic dissociation of surface hydroxyl group.

O'Connor and Buchanan (84) further investigated three samples of SnO_2. One of them showed only -ve potentials. The same authors reported that initial + ve electrokinetic potential of alumina could be changed to -ve by ignition above 1000°C and then back to positive by grinding. Street (85) found that while the powdered specimens of synthetic sapphire exhibited zpc, bulk specimens tested with radial flow method did not. Zukov, I.I. and Kryukov A.A. (86) also failed to locate zpc on their alumina sample.

T.W. Healy and V.R. Jellet (87) in their studies on ZnO reported only negative zeta potentials over the entire pH range studied. Their curves were similar to those in the present studies showing a minima. They interpreted this in terms of the adsorption of the hydroxy complexes on the surface.

Buchanan and Heymann (88) found that the intrinsic potential of both natural and synthetic samples of barium sulphate was always positive. These authors suggested that the positive

surface charge of $BaSO_4$ is due to preferential release of SO_4^{-2} ions from the crystal lattice.

D.J. O'Connor (89) studied the electrical surface properties of natural scheelite ($CaWO_4$) in aqueous medium. It showed a -ve zeta potential for entire pH range. This was attributed to the preferential release of Ca^{++} ions and preferential adsorption of WO_4^{-2} ions from the double layer. Similar behaviour was reported recently by M.C. Fuerstenau et. al.(90) for scheelite.

All the above examples establish beyond doubt the dependence of zeta potential on size, sample preparation, pH and electrolyte concentration. It is immediately realised that

i) apart from H^+ and OH^- ions there may be other potential determining ions e.g. Zr^{4+}, ZrO^{++}, SiO_3^{-2}, SiO_4^{-4}, Cl^- etc. in case of zircon.

ii) The oxide or silicate may be soluble in the form of different complexes and there may be preferential dissolution of some ions from the lattice. This means that the crystal structure, breakage characteristics and sample preparation are important in determining the surface characteristics.

It is, therefore, worth while to examine the present system in all these aspects.

Possible Breakage Characteristics of Zircon:

The crystal chemistry of zircon is already discussed in Section VI-2. As is clear from Fig. 45 each atom of Zr is surrounded by 8 oxygen atoms four of which are at a distance of 2.15 Å while the remaining four atoms are at a distance 2.29 Å. The silicon atom on the other hand is surrounded by the four oxygen atoms only to form a somewhat distorted tetrahedron.

When a solid is subjected to grinding it will break in such a manner that the weakest link in the whole crystal will be mostly broken. This is not to suggest that other bonds do not break at all but the probability will be much less. Therefore, the factors that would be responsible for the type of surface produced when ground are a) bond strength b) coordination number of the cations c) ionic character of the bond d) polarisability which would help the bonds distort without breaking and in wet grinding e) hydration energy of the ions which may subsequently pass into solution. The effect of solvent media on grinding is well known.

According to A.S. Joy et al. (29), non-frame work silicates would tend to break in such a way that the silicate or polysilicate groupings are preserved as far as possible. The breakage of zircon which is a non-frame work orthosilicate is expected to present surfaces in which cations (Zr^{4+}) would be exposed as high energy sites. These may subsequently get hydrolysed in contact with water.

Also Si–O bond is more covalent than Zr–O bond as surmised from their percent ionic character. Since, covalent bond is stronger, the Zr–O bond is expected to break in preference to Si–O bond. In terms of Pauling's (81) electrostatic bond strength also, Zr–O is more likely to break in preference to Si–O bond. Thirdly, SiO_4 tetrahedra is more polarisable and can resist breakage by considerable distortion. Therefore, assuming that only Zr–O bonds are broken, we have the following possibilities as regards the type of sites that will be exposed at the surface following Bluementhal's simple chain description of the zircon structure.

i) 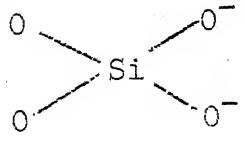

Corresponding Zr site is 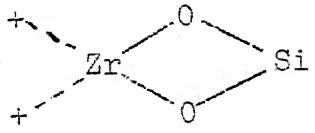

Herein two Zr–O bonds are broken.

ii) 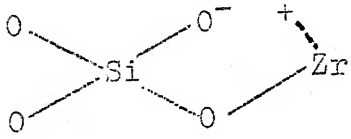

Here only one Zr–O bond is broken.

In addition Zr ions may pass into bulk phase after detaching from the surface. Thus, it will be seen from the above breakage scheme that exposed zircon surface carries uncompensated negative charges of value -1/2 while the uncompensated positive charges are + 1/2, + 1 and in some cases + 3/2. However, the preferential dissolution of zirconium ions into the aqueous bulk phase would leave on the zircon surface a net negative charge. This may happen under conditions of severe wet grinding.

In aqueous surroundings the above sites would be invariably hydrolysed as follows:

i) $\geqslant Si{-}O^- + H^+ \rightarrow \geqslant Si{-}OH$

ii) $Si(O^-)_2 + 2H^+ \rightarrow Si(OH)_2$

iii) $Zr^{+}_{+} + 2OH^- \rightarrow Zr(OH)_2$

iv) $\geqslant Zr \ldots + + OH^- \rightarrow \geqslant Zr - OH$

v) $Zr^{+4} + 4\ OH^- \rightarrow Zr(OH)_4$

Some more hydrolysis schemes of minor significance may also be written.

Chlorohydroxy Complexes of Zirconium:

Various chlorohydroxy complexes of zirconium have been reported. For example, Adolf and Pauli (91) have suggested complexes such as $Zr(OH)_4\ ZrO^{++}$, $Zr(OH)_4\ Cl_2^-$, ZrO^{++}, $Zr_2O_3^{++}$, $ZrOOH^+$, $ZrO_2Cl_2^=$ etc. under various conditions of pH and soluble Zr-Salt. In view of the divergent claims, it is difficult to know the nature of the actual species existing. However, it is evident that zirconium almost invariably remains as a hydrolysed species, probably $Zr(OH)_4$. Following Hildebrand (92), we assume the hydrolysed zirconium to be amphoteric in nature; so that both acidic and basic behaviour may be exhibited. Now Cl^- ions may attach themselves to hydrolysed zirconium on the surface either by

replacing OH^- ions or by loose adsorption or through coordinate covalencies by donating its one electron to the central zirconium ion.

About hydrolysed silicon sites also it may be safely assumed that it acts as a Bronsted acidic site. This is because of the π-bonding interaction between the unshared electrons on the oxygen atom and an empty d-orbital on the silicon atom. The resulting drift of electrons away from the oxygen results in the positive character of the hydrogen as shown in Fig. 46(b). Thus

Si—OH may dissociate to give negative sites as follows:

$$Si{-}OH \rightarrow Si{-}O^- + H^+.$$

Explanation of the Anomalous Behaviour of Zircon:

With the information given in the previous paragraphs it is now possible to give a reasonable explanation of the anomalous negative zeta potential of zircon in the acidic pH range:

a) The fact that the charge on the surface never comes down to zero or becomes positive, strongly suggests that Zr is preferentially removed from the solid surface in the form of cation or some complex into the aqueous phase by severe grinding and subsequent hydration. This leaves the surface negatively charged.

The presence of zirconium species in the aqueous grinding media has been qualitatively confirmed by Alizarin-red-S dye which developes rose red lake with zirconium salts.

b) In order to explain the negative charge in the acidic pH range the acidic site postulate may be proposed, as was done by O'Connor (84). Thus,

$$Si — OH \rightleftharpoons Si — O^- + H^+$$

With similar dissociation for Zr—OH site also we have negatively charged zircon surface.

However, the above scheme implies that as the hydrogen ion concentration is increased i.e. pH is decreased the number of negative Si—O^- sites would also decrease since the equilibrium would be shifted towards left. However, in case of zircon the negative value of zeta potential increases numerically with decrease in pH in acidic range. This together with the fact that the negative zeta potential increases numerically with KCl concentration strongly suggests that Cl^- ions get adsorbed on the surface to make it more and more negative.

It is, therefore, proposed that the following type of Cl^- ion adsorption at the silica sites takes place,

$$Si \xleftarrow{} \overset{-}{O} — \overset{+}{H} \ldots Cl.$$

This is possible because of the drift of electrons towards Si as depicted in Fig. 46(b), thus leaving H some what positive which then can act as an adsorption site for negative chloride ions.

Also negatively charged chlorohydroxy complexes of zirconium or some loosely bound adsorbed Cl^- aggregate with hydrated

zirconium sites would invariably contribute to the negative charge. The adsorbed Cl^- ions coming from the added KCl or HCl (which lowers pH) molecules would enhance the numerical value of negative zeta potential.

To summarise, preferential dissolution of Zr atoms from the surface and specific adsorption of Cl^- ions on a suitable site account for the observed electrokinetic behaviour of zircon.

General Discussion of the Anomalous Electrokinetic Behaviour in Oxygen Bearing Solids:

It has been seen that the anomalous pH vs. zeta potential curves of oxides and other oxygen bearing solids fall mainly into two categories as depicted ideally in Fig. 47(a) and (b).

The first type shows a gradual decrease in the numerical value of negative potential with decrease in pH without showing minima. Alumina, ThO_2 Sapphire, SnO_2 belong to these categories.

The second type, however, passes through a minima as the pH is decreased and then registers a stiff increase as the pH is further decreased. ZnO, Scheelite ($CaWO_4$) and zircon fall in this category.

It will be seen that the postulate of amphoteric nature of metal hydroxides at the surface showing both acidic and basic character in appropriate pH ranges is sufficient to account for the behaviour observed in former case. Whereas to explain the

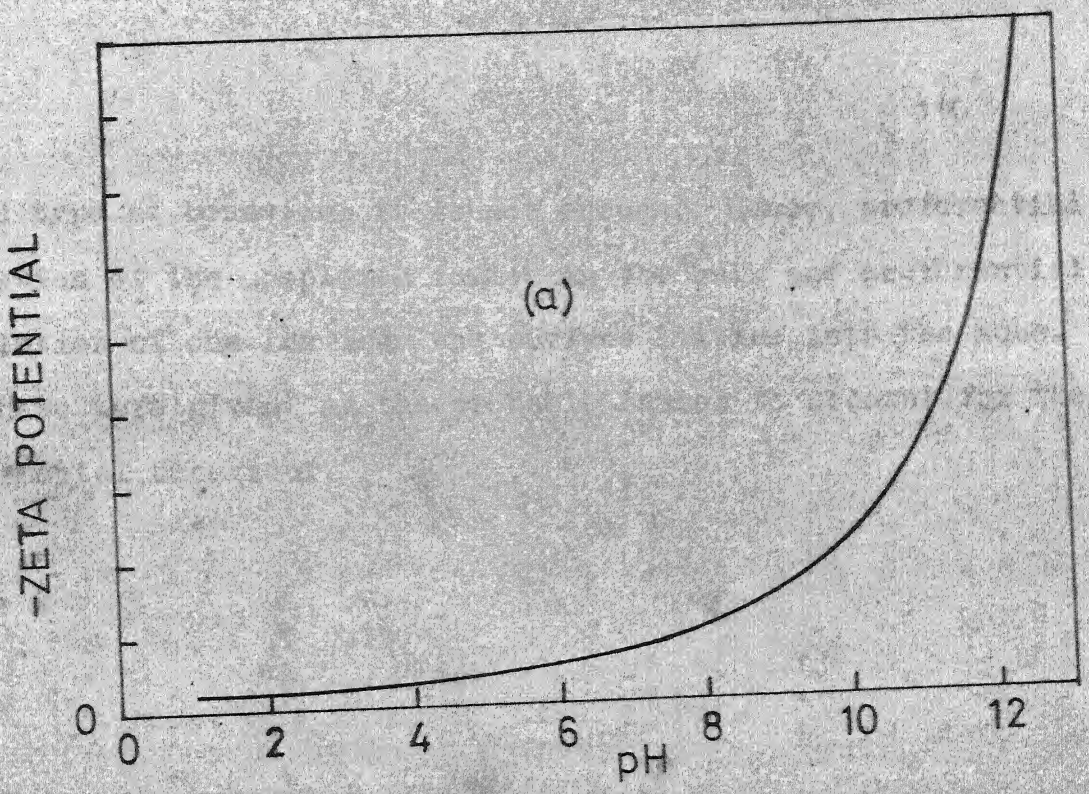

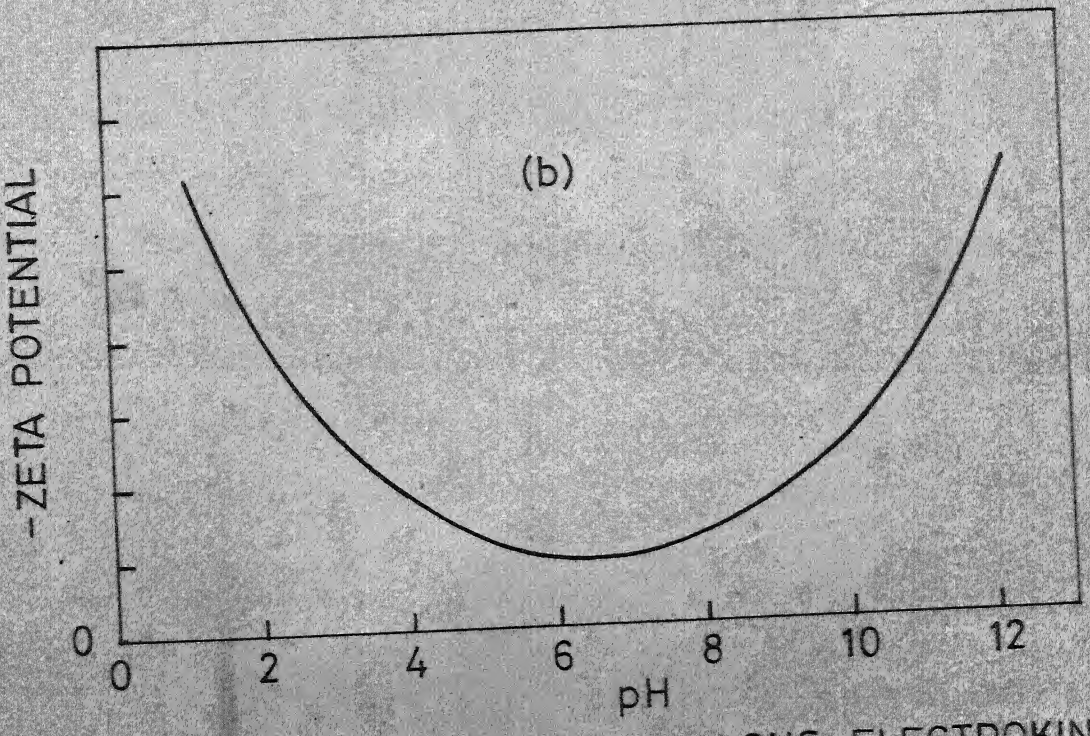

FIGURE 47 TYPICAL ANOMALOUS ELECTROKINETIC BEHAVIOUR OF SOME SOLIDS

second type of behaviour it is not enough. Hence, preferential adsorption of the complexes formed in the bulk and preferential dissolution of one ion from the surface lattice into the aqueous phase were given as the probable causes to account for the experimental behaviour.

CHAPTER VII

DISCUSSION OF RESULTS-II ZIRCON-SODIUM OLEATE SYSTEM

The results of experimental investigations on the flotation, adsorption, electrophoretic mobility measurements and infrared spectra have been already given in Chapter V. In this chapter, we take up the detailed discussion of the results on zircon-sodium oleate system.

VII-1 pH-DEPENDENCE OF FLOTATION RESPONSE:

The effect of pH on the flotation recovery of zircon for various constant collector concentrations has been shown already in Fig. 10.

In anionic collector-mineral system at constant collector concentration, such as zircon-sodium oleate, the variation of flotation recovery with pH, is in general represented by a bell-shaped curve with sharp maximum at lower concentrations and a flat plateau at relatively higher concentrations of the collector. This behaviour is evidently due to the varying conditions of the mineral surface with pH, and variation of relative amounts of the ionic species and non ionic species derived from the collector on the mineral surface.

For example, for oxygen bearing minerals such as oxides, silicates etc. the H^+ and OH^- ions are potential determining

along with others which may be derived from the mineral surface. The actual condition of the mineral surface is thus a function of pH. This aspect has been already discussed in case of zircon in Chapter VI.

The different collector species that may exist also depend very much on pH. In case of sodium oleate, this variation is discussed in section VII-2.

Thus the whole flotation system is quite complex and involves an interplay of the surface condition of the mineral and ionic condition of the aqueous bulk phase. Added to this are the mechanical factors. Hence, it is very difficult to attempt the quantitative explanation of the pH-percent recovery curves in analytical fashion. It is surprising that till todate no quantitative equations are given for the pH vs. percent recovery curves though they are invariably the first to be determined for any flotation system. As a first attempt we present an essentially semi-empirical model which is based on a similar model proposed by P.D. Cratin (93) to characterise pH dependence of interfacial tension of Asphaltenes, Resins and enzyme activity. Cratin observed that many interfacial properties have optimum magnitudes at intermediate pH and this is due to adverse effects exerted by the species which are predominant at extreme pH values. A similar phenomenon might exist in the flotation system.

Mathematical Formulation:

Let us first define a term 'Flotation Activity'. If R_o is the maximum percent recovery and R_i is the percent recovery at any other pH, then flotation activity is defined by the ratio R_i/R_o which is the percent recovery expressed as a fraction of the maximum recovery.

It is quite evident that

$$R_i/R_o = 1 \qquad \text{when } R_i = R_o$$

and (VII.1)

$$R_i/R_o = 0 \qquad \text{when } R_i = 0$$

Thus the value of flotation activity a_f would always lie between 0 and 1.

Physicochemical basis of the role of pH may be described with the help of the following schemes: one for the region before the maximum on acidic side and the other for the alkaline region beyond the maximum. Thus,

for acidic region we have,

$$HOl + OH^- \overset{I}{\rightleftharpoons} Ol^- + H_2O \qquad \text{(VII.2)}$$

$$\downarrow\uparrow \text{ II}$$

$$\frac{Ol^-}{[M]}$$

for which we may write,

$$\frac{[HOl]\,[OH^-]}{[Ol^-]_s} = K_b \qquad \text{(VII.3)}$$

where HOl represents oleic acid and M represents the mineral surface.

$[HOl]$, $[OH^-]$, $[Ol^-]_s$ represent concentrations of the respective species, the subscript s being used to denote the concentration at the surface.

Since the overall reaction (VII-2) involves adsorption process depicted by step II, the constant K_b is not a true equilibrium constant but it is some empirical constant and to this extent empiricism is involved in the present model. It will be seen that K_b may be a function of sodium oleate concentration added.

Similarly, for alkaline region the role of pH can be brought out with the help of the following ion exchange type reaction,

$$M\text{]} - OH + Ol^- \rightleftharpoons M\text{]} - Ol^- + OH^- \qquad \text{(VII.4)}$$

so that*,

$$K_c = \frac{[OH^-]\ [Ol^-]_s}{[Ol^-]_b\ [OH^-]_s} \qquad \text{(VII.5)}$$

Now since the surface is always thoroughly hydrolysed it is assumed that $[OH^-]_s$ is fairly large and can be taken as constant for particular oleate concentration. This together

---

* In the present model the equations VII.3 and VII.5 are anolagous to mass law equation. However, the analogy need not be carried any further and no thermodynamic significance be attached to the constants as was claimed originally by Cratin (93).

with the equation,

$$[H^+]\ [OH^-] \quad = \quad 10^{-14} \quad = \quad K_w$$

gives,

$$K_a = \frac{K_w}{K_c} = \frac{[Ol^-]_b\ [H^+]}{[Ol^-]_s} \qquad \text{(VII.6)}$$

Here again, K_a is not a true equilibrium constant and is invariably a function of the collector concentration added.

Now, the reaction represented by equation (VII.2) indicates that as the pH is increased the step I proceeds more and more towards right thus giving more of oleate ions as a result of hydrolysis. Since oleate ion is an active species which gets adsorbed on the mineral surface, the adsorption of oleate and hence flotation would also increase. Thus, we may say that for a constant collector addition more of oleate ions or less of HOl would be helpful in having more flotation. In other words, the amount of HOl present (or its fraction) can be taken as an index of the corresponding decrease in flotation activity.

Similarly reaction (VII.4) clearly brings out the competitive role of OH^- ions in the alkaline region.

We are now in a position to describe the flotation behaviour with variation in pH with the help of equations (VII.1), (VII.3) and (VII.6).

The flotation activity a_f increases with the adsorption of oleate ions on the mineral surface. Thus in acidic region as

shown in equation (VII.2) more of HOl would mean decrease in flotation. Hence decrease in flotation activity in acidic region may be assumed to be proportional to [HOl] . Similarly, in alkaline region, decrease in flotation activity is proportional to [OH^-] . Alternatively, by virtue of the exchange reaction we may say that the more the ionic oleate concentration in the aqueous bulk phase left after equilibration i.e. $[Ol^-]_b$ the less is the flotation activity. The last statement does not contradict the fact that the flotation recovery increases with increase in initial oleate concentration. It merely states that for the same collector addition, increased residual oleate concentration signifies less adsorption on the solid surface and hence less flotation recovery. In view of the exchange reaction (VII.4), the residual or bulk sodium oleate concentration is just a measure of the depression caused by the hydroxyl ions in reality.

But for these two factors namely the increasing [HOl] as pH is lowered in acidic range and OH^- ion depression as manifested by increased $[Ol^-]_b$ the flotation activity might have been ideally unity. Therefore, we may write,

$$R_i/R_o = a_f = 1 - \Sigma\, d_i f_i$$
$$= 1 - (d^c f^c + d^k f^k) \qquad \text{(VII.7)}$$

assuming that individual effects are additive.

In the above equation, d^c and d^k are the coefficients representing the capacity of the HOl and $Ol^-_{(bulk)}$ respectively

to affect the flotation activity and f^c and f^k are fractions of HOl and $Ol^-_{(bulk)}$ respectively. In equation (VII.7) fractions have been used instead of the actual concentrations because it is not possible to know the actual concentrations of the different species in a flotation experiment.

Now, we proceed to express the fractions as a function of proton concentration which is known from pH measurements.

By mass balance on oleate we have,

$$S = [HOl] + [Ol^-]_b + [Ol^-]_s \qquad \text{(VII.8)}$$

where S is the concentration of added sodium oleate. Thus,

$$f^c = [HOl] / S$$
$$\text{and} \quad f^k = [Ol^-]_b/S \qquad \text{(VII.9)}$$

By virtue of equations (VII.3) and (VII.6) we get,

$$S = \frac{K_b\,[Ol^-]_s}{[OH^-]} + \frac{K_a\,[Ol^-]_s}{[H^+]} + [Ol^-]_s \qquad \text{(VII.10)}$$

or

$$S = [Ol^-]_s\left[\frac{K_b\,[H^+]}{K_w} + \frac{K_a}{H^+} + 1\right] \qquad \text{(VII.11)}$$

Hence,

$$f^c = \frac{[HOl]}{[Ol^-]_s\left[\frac{K_b\,[H^+]}{K_w} + \frac{K_a}{[H^+]} + 1\right]}$$

or using equation (VII.3) and rearranging we get,

$$f^c = \frac{1}{1 + \frac{K_w}{K_b\,[H^+]} + \frac{K_a\,K_w}{K_b\,[H^+]^2}} \qquad \text{(VII.12)}$$

Similarly,

$$f^k = \frac{[OH^-]_b}{\left[[OH^-]_s \quad 1 + \frac{K_a}{[H^+]} + \frac{K_b [H^+]}{K_w} \right]}$$

or using equation (VII.6) we get,

$$f^k = \frac{1}{\left[1 + \frac{[H^+]}{K_a} + \frac{K_b [H^+]^2}{K_a K_w} \right]} \qquad \text{(VII.13)}$$

Thus we get f^c and f^k in terms of $[H^+]$, K_a and K_b. Substituting in equation (VII.7) we get,

$$R_i/R_o = a_f = 1 - \left[d^c \left(\frac{1}{1 + \frac{K_w}{K_b[H^+]} + \frac{K_a K_w}{K_b [H^+]^2}} \right) + d^k \left(\frac{1}{1 + \frac{[H^+]}{K_a} + \frac{K_b [H^+]^2}{K_a K_w}} \right) \right] \qquad \text{(VII.14)}$$

Equation (VII.14) is a working equation from which variation of R_i/R_o with pH can be computed provided K_a, K_b and d^c, d^k are known.

Values of the Constants K_a and K_b:

In analogy with the Gratin's (93) reasoning on amino acids and from our description of the flotation activity in terms of equations (VII.3) and (VII.6) it may be reasoned out that the inflection point at the left hand arm (Fig. 48) occurs when $[HOl] = [OH^-]_s$ so that

$$\text{pH of L.H.S inflection} = 14 - K_b \qquad \text{(VII.15)}$$

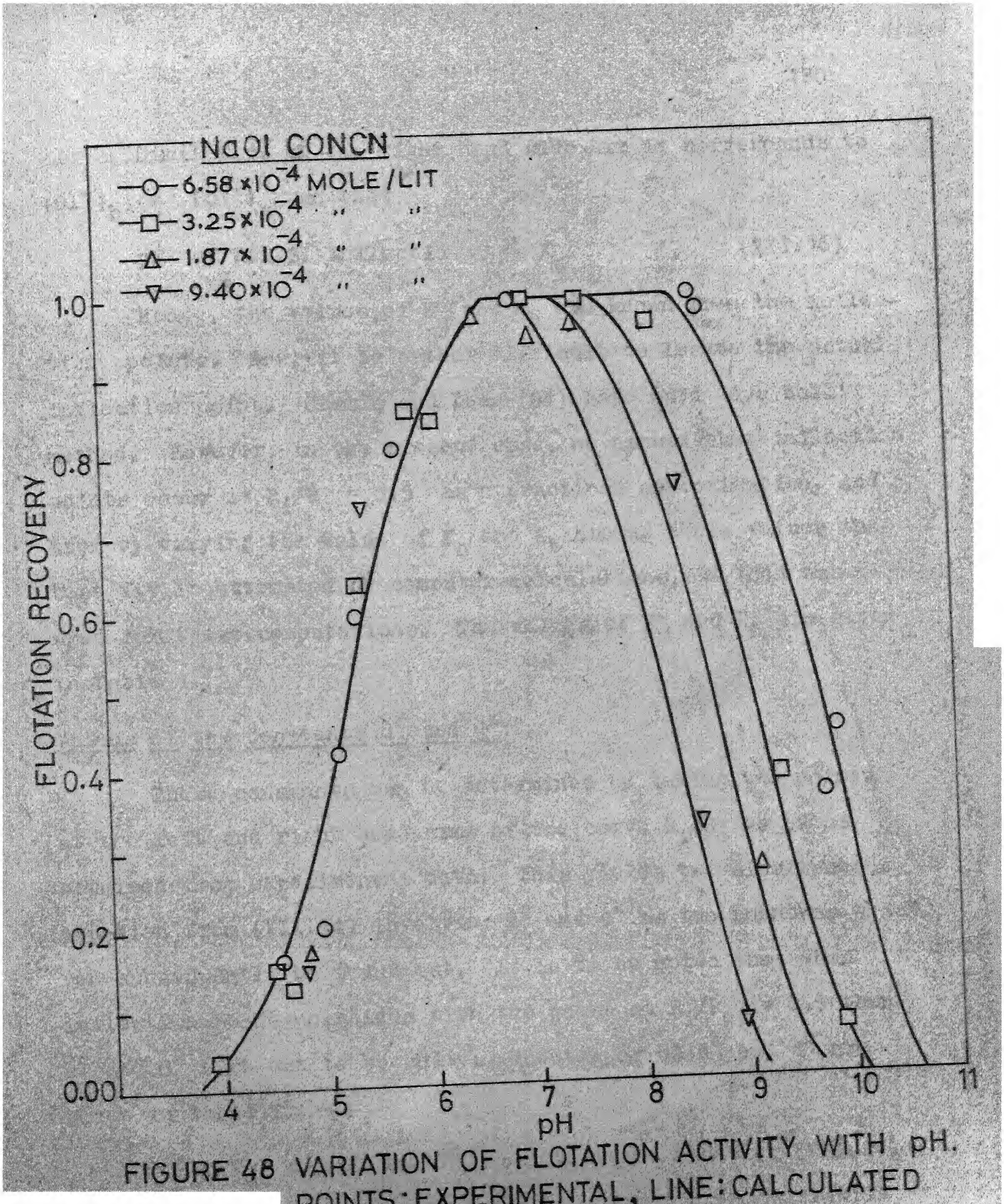

FIGURE 48 VARIATION OF FLOTATION ACTIVITY WITH pH. POINTS: EXPERIMENTAL, LINE: CALCULATED

Similarly, on the right hand side arm it corresponds to $[Ol^-]_b = [Ol^-]_s$ so that

pH of R.H.S. inflection $= K_a$ (VII.16)

Hence, the values of K_a and K_b are known from the inflection points. Now, it is rather difficult to locate the actual inflection point. Cratin and Dean (94) have used 'eye ball' method. However, in the present case, we assume that inflection points occur at $R_i/R_o = 0.5$ as a practical approximation. And then by varying the value of K_a and K_b around these values the best fit is attempted by computer calculations. IBM 7044 was used for these computations. The values of K_a and K_b are given in Table I.

Values of the Constants d^c and d^k:

These constants can be determined by taking two points at the left and right hand arms of the curve R_i/R_o vs pH as obtained from experimental data. This yields two simultaneous equation from (VII.14) involving d^c and d^k as two unknowns which can subsequently be found out. It is to be noted that when inflection point coincides with the point at $R_i/R_o = 0.5$ then d^c and d^k turn out to be unity. The values of d^c and d^k are given in Table I.

Once K_a, K_b, d^c and d^k are determined equation (VII.14) is fully known and can be utilised to compute R_i/R_o variation with pH.

Table I

Values of the Constants for Flotation Model

NaOl Concn.(S) mole/lit.	K_a	K_b	d^c	d^k
9.397×10^{-5}	4.35×10^{-9}	1.80×10^{-9}	1.00	1.15
1.875×10^{-4}	1.50×10^{-9}	1.80×10^{-9}	1.00	1.15
3.948×10^{-4}	6.25×10^{-10}	1.80×10^{-9}	1.00	1.15
6.579×10^{-4}	1.80×10^{-10}	1.80×10^{-9}	1.00	1.15

As is evident K_a, K_b, d^c, d^k are all empirical constants specific for a particular mineral-collector system and arise out of our incomplete knowledge of the mineral surface, adsorption pattern and its correlation with actual flotation recovery and mechanical factors. To this extent the present model is empirical.

The calculated curves alongwith experimental points are shown in Fig. 48. It is seen from the figure that agreement is quite good.

The variation of K_a with collector concentration is also plotted in Fig. 49. It is seen from the above figure that the functional relationship between K_a and S may be written as $K_a = K^o S^{-n}$ which is confirmed by an excellent straight line plot between log K_a and log S as seen from Fig. 49 (a).

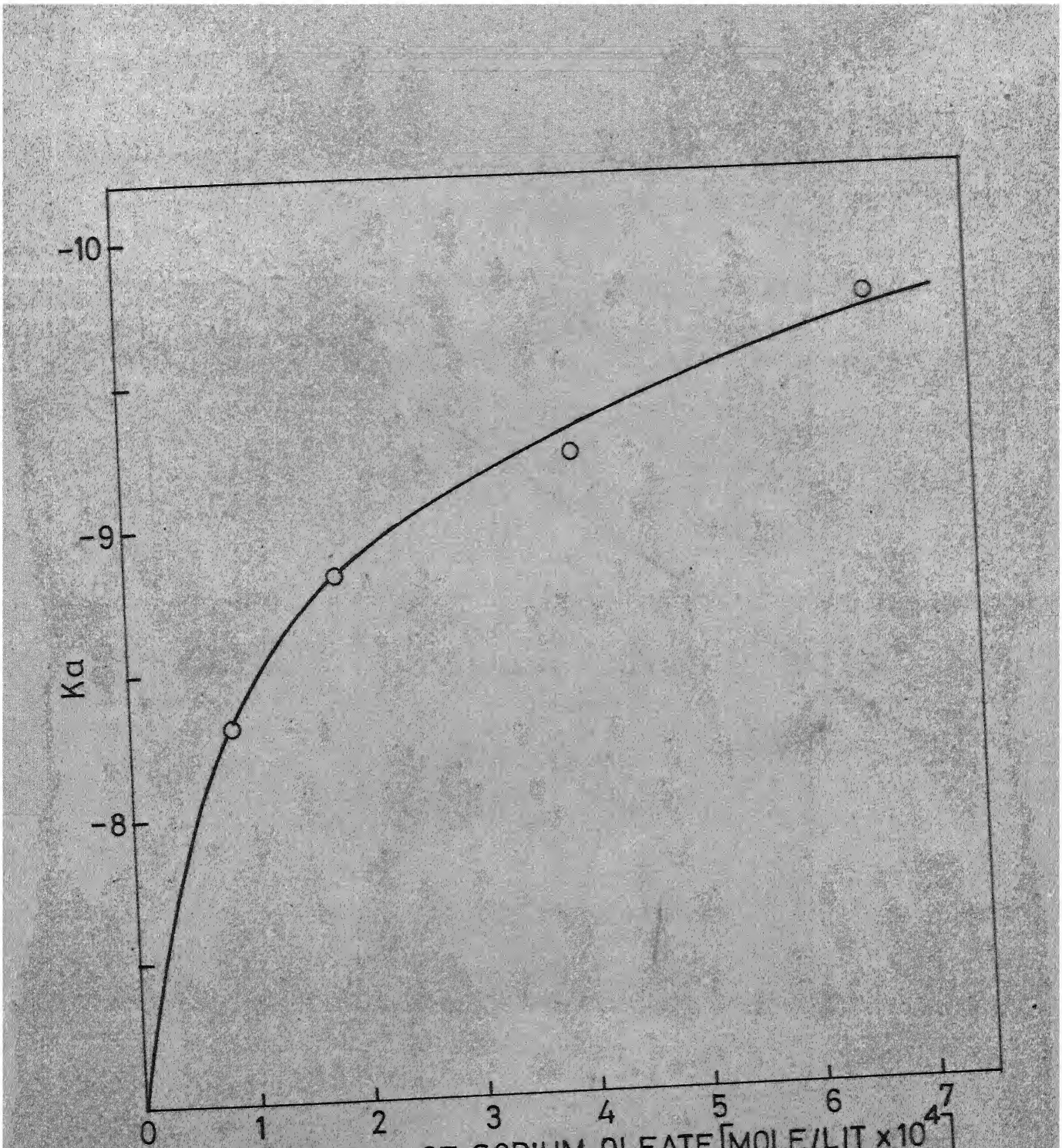

FIGURE 49 PLOT OF Ka AS A FUNCTION OF SODIUM OLEATE CONCENTRATION

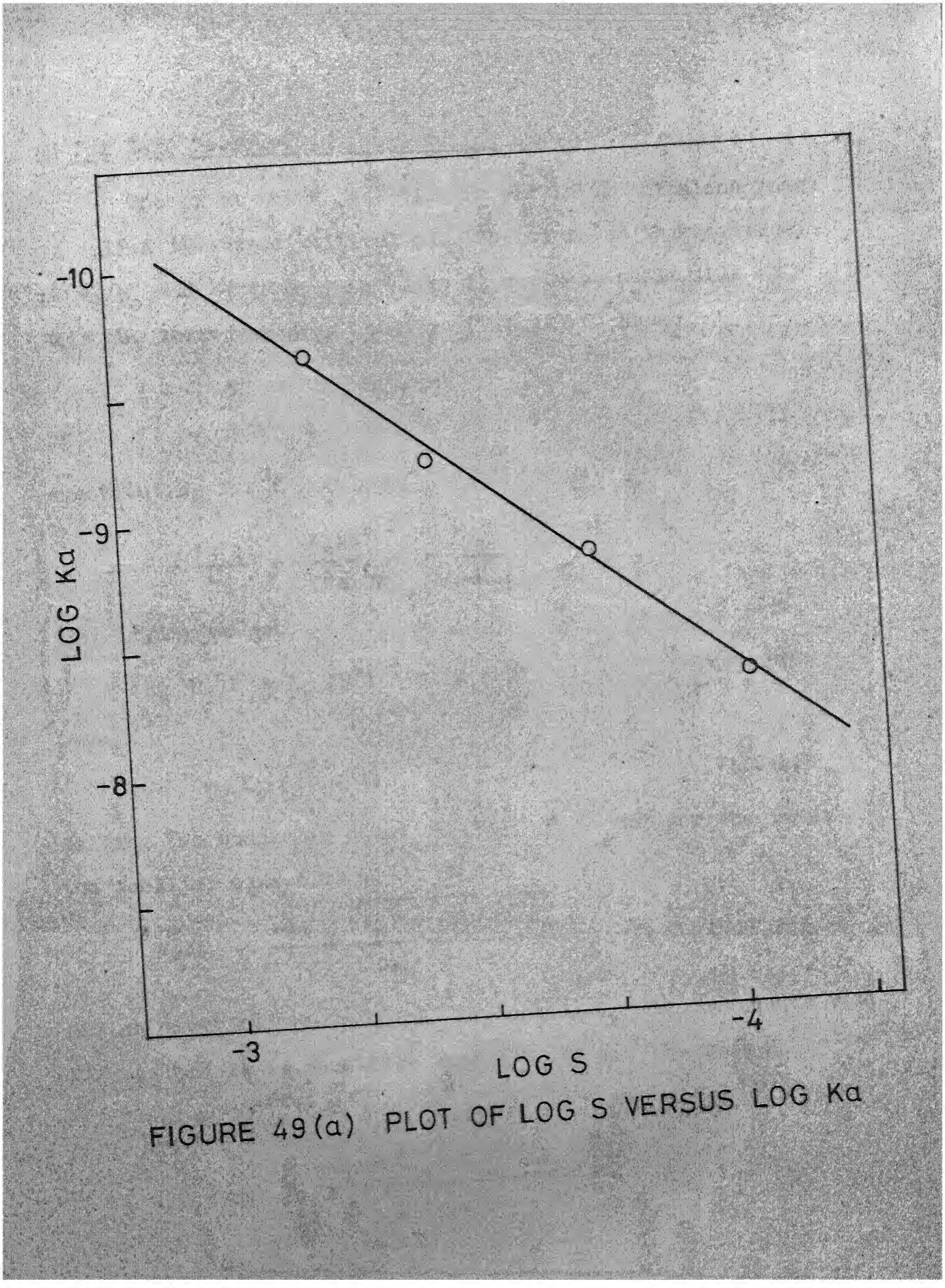

FIGURE 49(a) PLOT OF LOG S VERSUS LOG Ka

pH for Zero Recovery in the Alkaline Range:

The pH at which flotation is nil in the alkaline range is called the upper critical pH. Therefore at this critical pH $R_i/R_o = 0$ since $R_i = 0$. Also f^c would be negligible at this pH, therefore from equation (VII.14) we have

$$1 - d^k f^k = 0$$

or
$$f^k = 1/d^k \qquad \text{(VII.17)}$$

substituting for f^k, we get,

$$1 + \frac{[H^+]}{K_a} + \frac{K_b [H^+]^2}{K_a K_w} = \frac{1}{d^k}$$

Simplifying we get,

$$K_w [H^+] + K_b [H^+]^2 = K_a \cdot k' \qquad \text{(VII.18)}$$

where

$$k' = K_w (d^k - 1) \qquad \text{(VII.19)}$$

Solving the quadratic equation (VII.18) we get for the roots the familiar expression.

$$\text{Root} = \frac{-K_w \pm \sqrt{K_w^2 + 4K_b k' K_a}}{2K_b} \qquad \text{(VII.20)}$$

Taking positive sign only and neglecting K_w^2 in the square root sign (since it is much less than $4 K_b k' K_a$. Whereas $K_w^2 = 10^{-28}$ $4K_b k' K_a = 10^{-22}$) we get

$$[H^+]_{UCP} = \frac{-K_w + K_b^{1/2} k'^{1/2} K_a^{1/2}}{K_b} \qquad \text{(VII.21)}$$

Again $K_a^{1/2} K_b^{1/2} >> K_w$ hence neglecting K_w we get

$$[H^+]_{UCP} = \frac{K_a^{1/2} K'^{1/2}}{K_b^{1/2}} \qquad \text{(VII.22)}$$

Now, it is evident from the previous discussion that K_a/K_b is a function of collector concentration. It has been also shown that K_b is fairly constant for all collector concentrations whereas K_a varies as shown in Fig. 49. (Also see Table I). Therefore, the functional relationship can be simply expressed as (see Fig. 49(a)).

$$K_b/K_a = k'' S^n \qquad \text{(VII.23)}$$

From Fig. 49(a) the value of n is found out to be 1.46. Substituting in equation (VII.22) we get,

$$[H^+]_{UCP} = K_p / S^{n'} \qquad \text{(VII.24)}$$

where $K_p = (k'/k'')^{1/2}$ and $n' = n/2 = 1.46/2 = 0.73$.

From equation (VII.24) a plot of pH versus log S will have a slope 0.73. This slope would be compared with the actually found slope in section (VII.6). Now recalling that,

$$[H^+] = K_w / [OH^-]$$

We get from equation (VII.24)

$$S^{n'}/[OH^-] = K_p/K_w$$

or $$S/[OH^-]^{1/n'} = \text{constant} \qquad \text{(VII.25)}$$

Equation (VII.25) resembles the Barsky's law equation. Further discussion of the critical contact phenomenon would be taken up in Section VII-6.

In the following sections we discuss the physico-chemical aspects of the present system.

VII-2 AQUEOUS BEHAVIOUR OF SODIUM OLEATE:

In the previous section a mathematical model designed to quantitatively characterise the flotation dependence on pH was described. It is essentially semiempirical in nature. In the sections following, the physico-chemical aspects of the pH dependence of flotation, quantitative relationship between pH and the adsorption magnitude (Γ_{Ol}), correlation of flotation with adsorption and zeta potential and critical contact phenomena will be discussed. To begin with, the relevent properties of sodium oleate in aqueous solutions are being discussed in the present section.

Sodium oleate is an alkali salt of oleic acid which is a fatty acid having a formula $C_8H_{17}CH = CH\ (CH_2)_7\ COOH$. Thus oleic acid has a hydrocarbon chain having seventeen carbon atoms with a double bond between carbon atoms 9 and 10. When dissolved in water, sodium oleate hydrolyses according to the following equation,

$$\begin{array}{ccccc} Ol^-_a + Na^+ + H_2O & \underset{I}{\overset{k_h}{\rightleftharpoons}} & HOl_a + Na^+ + OH^- & & \\ \text{III} \searrow\!\!\nwarrow \text{II} & & & & \\ (Ol^-_m,\ HOl_m) & & & & \end{array} \qquad \text{(VII.26)}$$

where Ol^- represents oleate ions and the subscripts a and m stand respectively for aqueous phase and the micelle.

The micelles are formed only beyond a certain critical concentration called 'critical micelle concentration'. (c.m.c). The value of c.m.c. for sodium oleate has been determined by conductivity measurements. The plot of (λ) conductance versus (c) concentration gives two straight lines with different slopes. The point of intersection represents the c.m.c (Fig. 50). The value is found out to be 2.02×10^{-3} moles/lit. The ionic condition of sodium oleate is thus different below and above c.m.c and two distinct cases have to be realised. 1) for sodium oleate concentration below c.m.c and 2) for concentrations above c.m.c.

Oleate Ion Concentrations at Different pH Values:

In flotation the concentrations of sodium oleate used is always below c.m.c and hence only the first case will be considered. In such a situation steps II and III in reaction VII.26 do not come into picture. Thus for the hydrolysis reaction VII.26 (I) we have,

$$\frac{[HOl][OH^-]}{[Ol^-]} = K_h \qquad \text{(VII.27)}$$

where square brackets represent concentrations of the respective species and K_h is the hydrolysis constant.

From mass balance on sodium oleate we have,

$$S = [HOl] + [Ol^-] \qquad \text{(VII.28)}$$

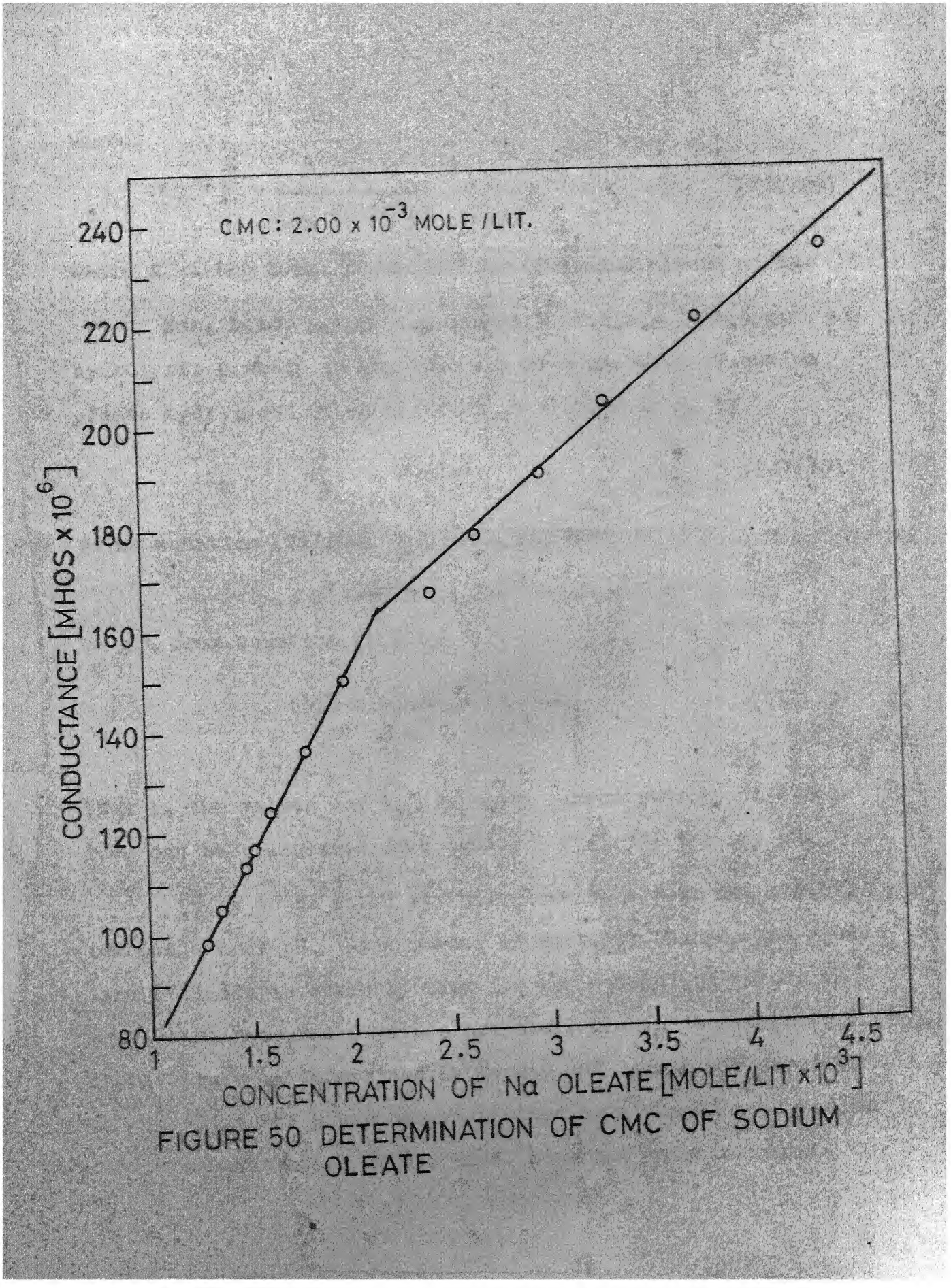

FIGURE 50 DETERMINATION OF CMC OF SODIUM OLEATE

Hence,

$$[Ol^-] = \frac{S.[OH^-]}{(K_h + [OH^-])} \qquad \text{(VII.29)}$$

where S - the total concentration of sodium oleate added.

Now, below c.m.c i.e., when S << c.m.c the degree of hydrolysis β which is the fraction of a gm. mole of sodium oleate hydrolysed at equilibrium is related to K_h by

$$K_h = \frac{\beta^2 . S}{1 - \beta} \qquad \text{(VII.30)}$$

Using equation (VII.30) and recalling that,

$$[H^+][OH^-] = 10^{-14}$$

We get from equation (VII.29)

$$[Ol^-] = \frac{S.10^{(pH-14)}}{\frac{\beta^2.S}{1-\beta} + 10^{(pH-14)}} \qquad \text{(VII.31)}$$

Thus if the values of K_h are known concentrations of oleate ions can be calculated from equation (VII.31) for any pH.

It is to be noted at this place that β is not strictly independent of pH. As a matter of fact, it changes and equation (VII.30) is strictly true for the natural pH values in which case measured β values are available in the literature (95). These values as determined by Powney and Jordan are depicted in Fig. 51. The β values are plotted as a function of sodium oleate concentration at different constant temperatures.

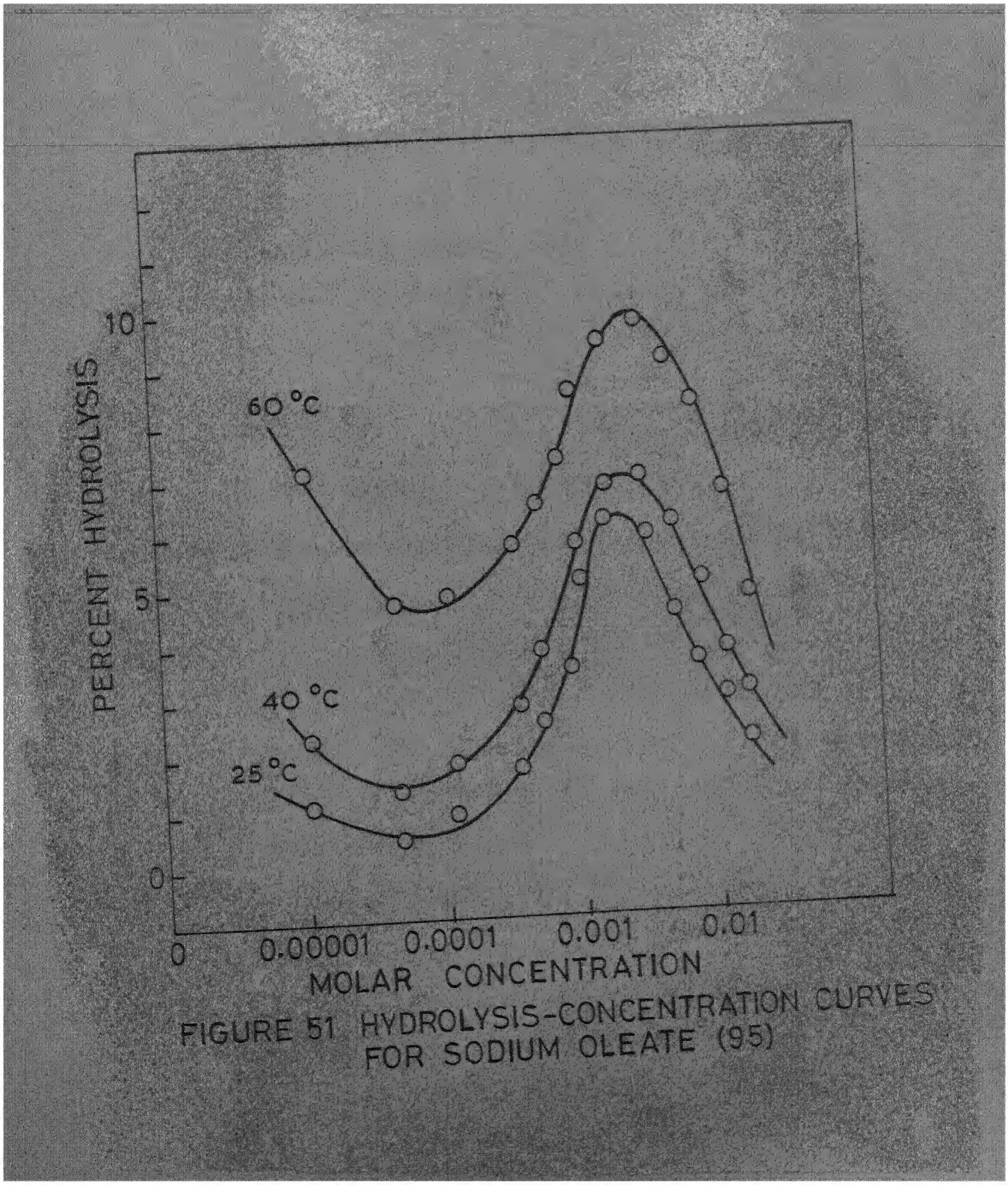

FIGURE 51 HYDROLYSIS-CONCENTRATION CURVES FOR SODIUM OLEATE (95)

However, irrespective of any changes in β the value of K_h at any temperature is assumed to remain substantially constant over a pH range.

The values of $[Ol^-]$ for different pH values can thus be calculated. A typical variation of $[Ol^-]$ with pH for the added sodium oleate concentration of 2.303×10^{-4} mole/litre is shown in Fig. 52. Oleate concentration increases as the pH increases and after pH 8.5 - 9 remains constant. This has an important bearing on the nature of the adsorption pattern and flotation of zircon with sodium oleate.

VII-3 pH DEPENDENCE OF ADSORPTION OF SODIUM OLEATE ON ZIRCON:

The experimental variation of adsorption density of oleate when pH is a variable has been already depicted in Fig.17 for constant sodium oleate concentration of 6.579×10^{-4} mole/lit. Similar results for sodium oleate concentrations 4.93×10^{-4} mole/lit. 3.29×10^{-4} mole/lit and 2.30×10^{-4} mole/lit. are being given in Fig. 55, where these have been compared with the calculated results.

Before discussing the mathematical model to calculate adsorption density as a function of pH it is worth while to consider the physicochemical aspects leading to the observed behaviour. The curve depicting the pH variation of adsorption density of sodium oleate on zircon, resembles somewhat a bell shape. If it is postulated that sodium oleate is adsorbed on the zircon surface primarily in the form of ionic (oleate)

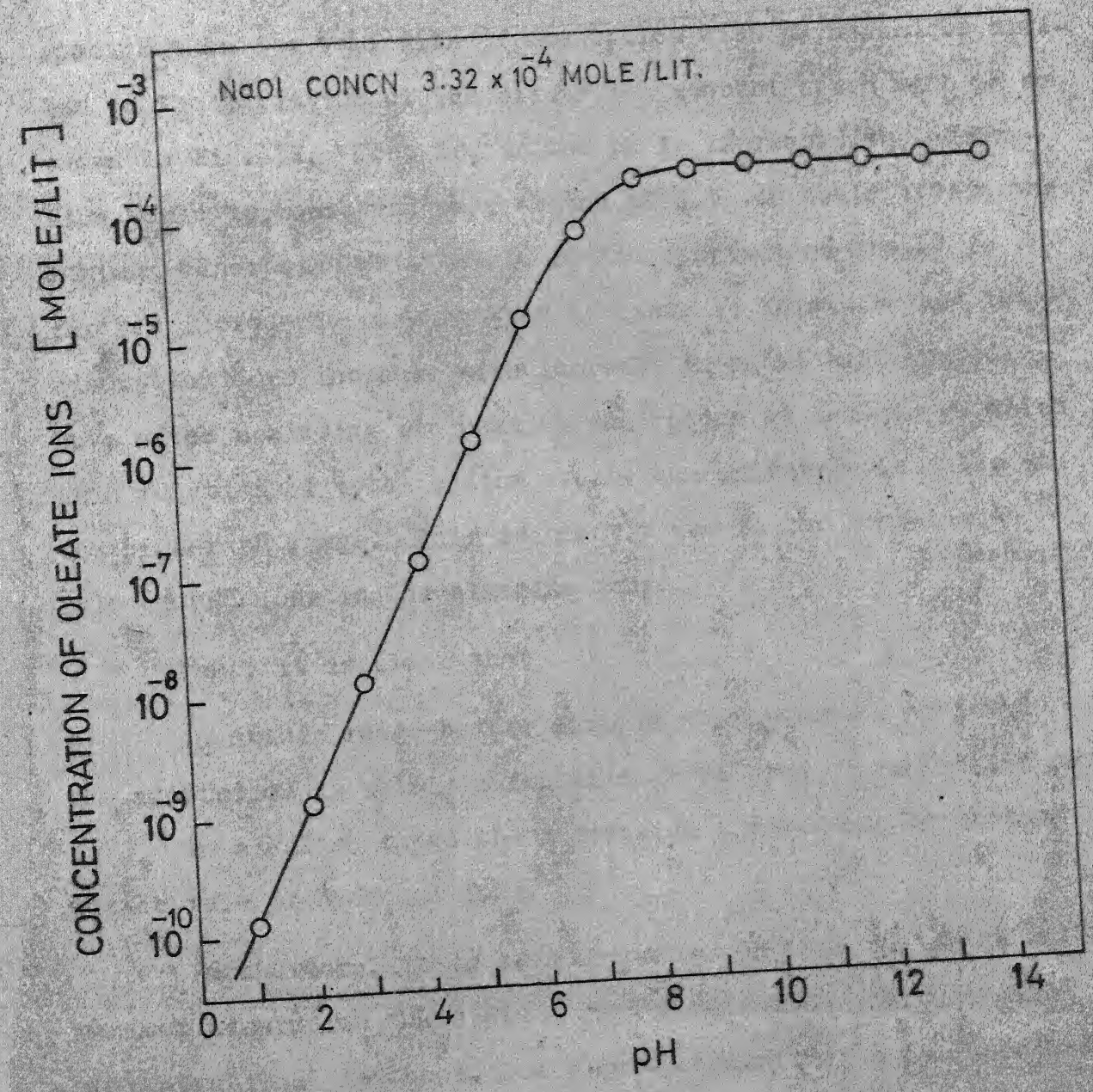

FIGURE 52 TYPICAL CURVE SHOWING VARIATION OF OLEATE ION CONCENTRATION WITH pH AT CONSTANT SODIUM OLEATE CONCENTRATION

species then the variation of adsorption with pH should be similar to the variation of the oleate ion concentration with pH as shown in Fig. 52. That is, as the pH is increased the adsorption would increase and then around pH 8.5 - 9 would attain the maximum adsorption which would remain constant as the pH is further increased. As a matter of fact, in acidic region the adsorption does increase with increase in pH as anticipated. But, after achieving the maximum adsorption at certain pH which is a function of total sodium oleate concentration it falls in the higher pH range. This is clearly due to the competitive role of OH^- ions in the alkaline range.

Thus, it is clear that

i) in acidic range before maximum adsorption is achieved the adsorption is solely a function of Ol^- ion concentration and

ii) in alkaline range the adsorption depends on the antagonistic role of hydroxyl ions.

Furthermore, it is seen from Fig. 55 that the pH at which maximum adsorption takes place is a function of sodium oleate concentration. As the sodium oleate concentration is increased the pH for maximum adsorption shifts to higher pH values. This is quite expected as the competitive role of OH^- ions would be felt at higher pH values for higher sodium oleate additions.

In acidic region, the curves for all concentrations seem to merge into one at some stage as seen from Fig. 55, within a short pH range.

However, the agreement between the experimental values and the calculated values was rather poor. This is probably due to the assumption of fruendlich type adsorption for both Ol^- and OH^- ions. The experimental results given in Figs. 16 and 62 however show that the adsorption isotherms for oleate and hydroxyl ions are S-type and may be assumed to be Langmuirian except for very low concentrations.

Therefore, in the present model, Langmuir type adsorption equation is assumed to hold good for Ol^- ion adsorption (In Section VII-5 it will be shown that beyond a sodium oleate concentration of 1.5×10^{-4} mole/lit Langmuir's equation is applicable (also see Fig. 53)). The role of OH^- ions is brought out in the form of a simple exchange reaction given by equation (VII.34).

The physicochemical basis of the role of pH may thus be described with the help of the following scheme as was done while reporting mathematical model for pH dependence of flotation activity (e.g. Section VII-1).

$$HOl + OH^- \overset{I}{\rightleftharpoons} Ol^- + H_2O \qquad \text{(VII.33)}$$

$$\Big\| \text{ II}$$

$$Ol^-$$

$$[M]$$

and for alkaline region,

$$M] - OH + Ol^- \rightleftharpoons M] - Ol^- + OH^- \qquad \text{(VII.34)}$$

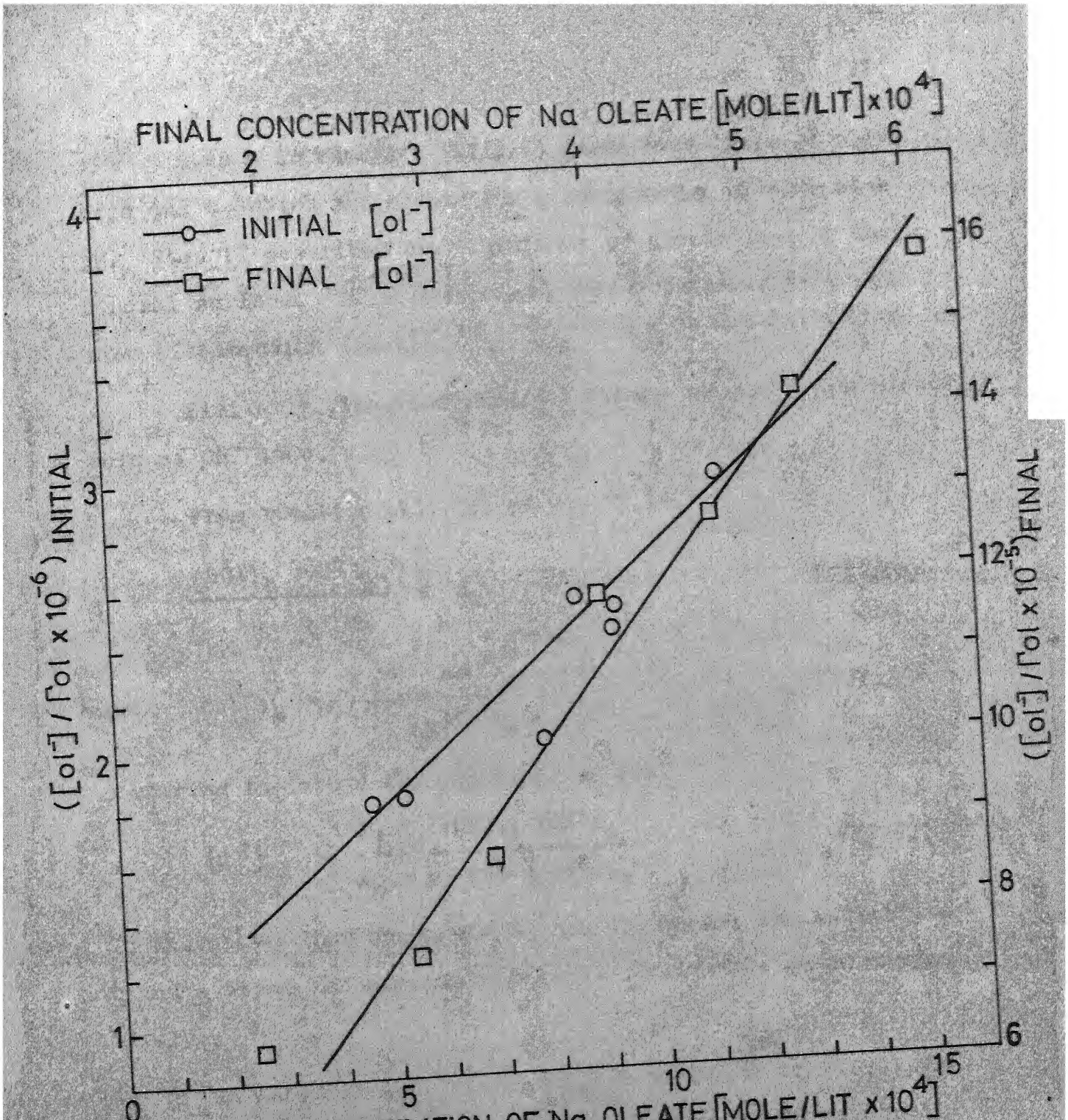

FIGURE 53 LANGMUIR PLOTS FOR ZIRCON-Na OLEATE FOR BOTH INITIAL AND FINAL CONCENTRATION OF THE OLEATE

Step I in reaction (VII.33) gives hydrolysis of oleic acid due to which the oleate ion concentration changes with pH. Step II describes the adsorption of oleate ions on the mineral surface. It is assumed to follow Langmuir type equation (See Section VII-5).

Similarly, reaction (VII.34) brings out the antagonistic role of OH^- ions.

From reaction (VII.33) we may write,

$$\frac{[HOl]_b \, [OH^-]_b}{[Ol^-]_b} = K_h \qquad \text{(VII.35)}$$

and $$[Ol^-]_s = \frac{k_1 . k_2 \, [Ol^-]_b}{1 + k_2 [Ol^-]_b} \qquad \text{(VII.36)}$$

combining the above two equations we get,

$$[Ol^-]_s = \frac{k_1 . k_2 \, [HOl]_b \, [OH^-]_b}{K_h + k_2 \, [HOl]_b [OH^-]_b} \qquad \text{(VII.37)}$$

In the above equation k_1 and k_2 are constants. The subscripts b and s stand for aqueous bulk phase and surface phase respectively.

In Langmuir type equation such as VII.36 or VII.37 the concentration terms usually correspond to terminal or equilibrium concentration values e.g. $[Ol^-]_b$, $[HOl]_b$ after equilibration with the mineral surface. However, it is highly desirable to get a relationship in terms of initially added collector concentration (S). This is achieved as follows. It is observed

from Fig. 53 that a fairly good Langmuir type plot is obtained even when initial oleate concentration, $[Ol^-]$ is taken as the parameter . Therefore, in equation VII.37 the $[HOl]_b$ term corresponding to terminal concentration after equilibration with the mineral adsorbent may be replaced by corresponding initial values in which case we are entitled to use equation VII.28 which relates [HOl] with S. It should be noted that the constants k_1 and k_2 would be the dependent on the values of S (95).

From equations (VII.28) and (VII.29) we may write,

$$[HOl] = S \left[1 - \frac{K_w / [H^+]}{K_h + K_w / [H^+]} \right] \qquad \text{(VII.38)}$$

which relates [HOl] with S the initial sodium oleate concentration added. Therefore,

$$\frac{1}{[HOl]\,[OH]_b} = \frac{K_h\,[H^+] + K_w}{S\,K_h\,K_w} \qquad \text{(VII.39)}$$

Thus, equation (VII.37) may be rewritten as,

$$\frac{1}{[Ol^-]_s} = k_3 \left(\frac{K_h\,[H^+] + K_w}{S\,K_h\,K_w} \right) + k_4 \qquad \text{(VII.40)}$$

where,

$$k_3 = \frac{K_h}{k_1\,k_2}$$

and $$k_4 = \frac{1}{k_1}$$

Since, k_1 and k_2 are functions of the sodium oleate concentration

(S) the values of k_3 and k_4 would also be different for different values of sodium oleate concentrations.

Thus, a straight line plot of $1/[Ol^-]_s$ against $\left(\frac{K_h[H^+]+K_w}{S\ K_h\ K_w}\right)$ would testify the applicability of the above equation (VII.40) for acidic region. Also, the constants k_3 and k_4 can be known there from. Such plots are shown in Fig. 54(a) which shows that straight line relationship is fairly obeyed.

Similarly, for alkaline region by virtue of the reaction (VII.34) we may write,

$$k_c = \frac{[Ol^-]_b\,[H^+]}{[Ol^-]_s} \qquad \text{(VII.41)}$$

Now in alkaline range sodium oleate is present completely in ionic form. Therefore, the mass balance on oleate ions would yield,

$$S = [Ol^-]_b + f\,[Ol^-]_s \qquad \text{(VII.42)}$$

The factor f has been included to take care of the different units in which $[Ol^-]_b$ and $[Ol^-]_s$ are expressed. Substituting from equation (VII.42) in equation (VII.41) and rearranging we get,

$$[Ol]_s = \frac{S[H^+]}{k_c + f[H^+]} \qquad \text{(VII.43)}$$

From the above equation it will be seen that a plot of $1/[Ol]_s$ versus $[H^+]^{-1}$ would be a straight line. This has been varified in Fig. 54(b) where fairly good straight line plots are seen to be emerging. The values of k_c and f are subsequently known

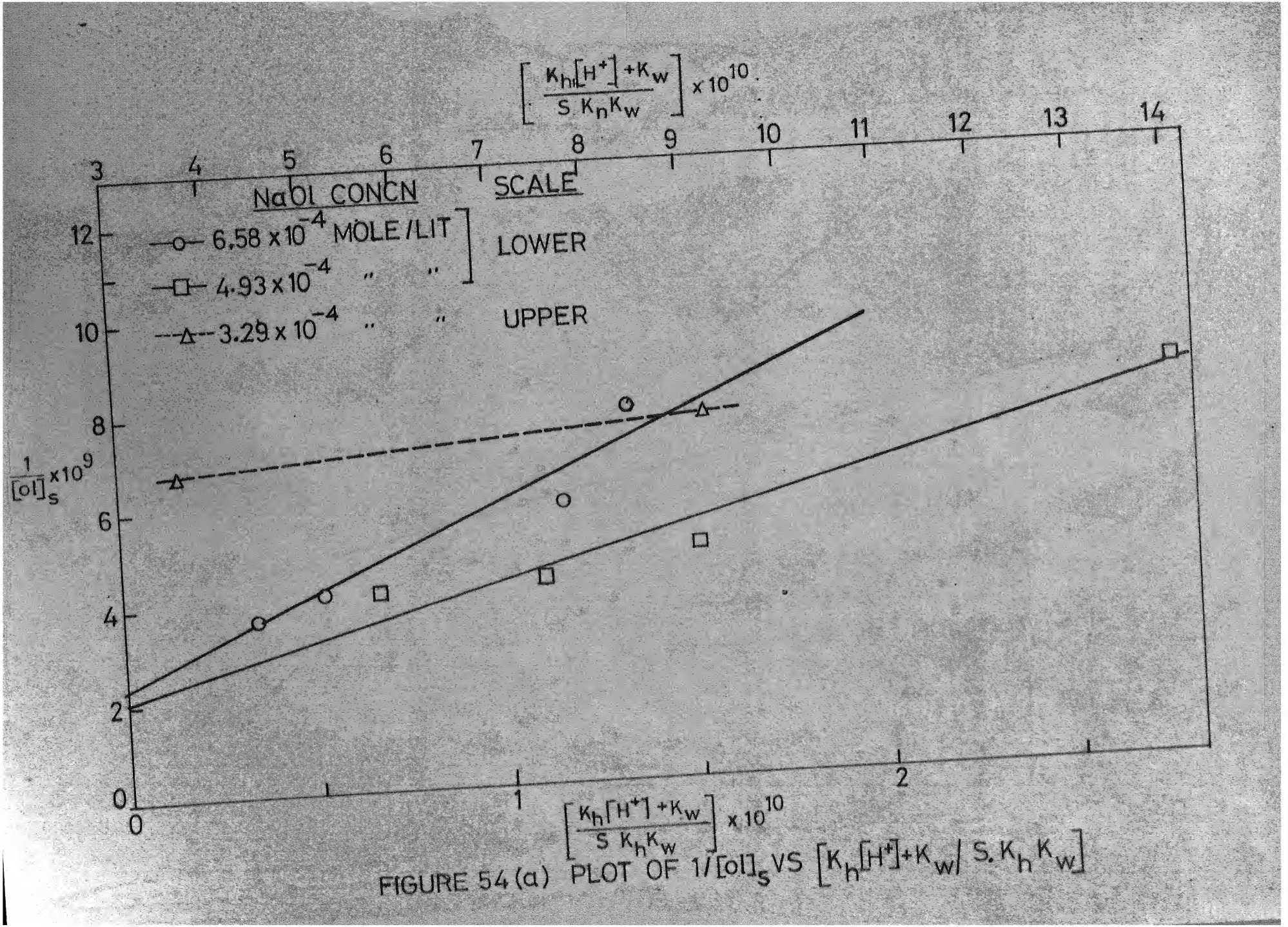

FIGURE 54 (a) PLOT OF $1/[ol]_s$ VS $[K_h[H^+]+K_w / S.K_h K_w]$

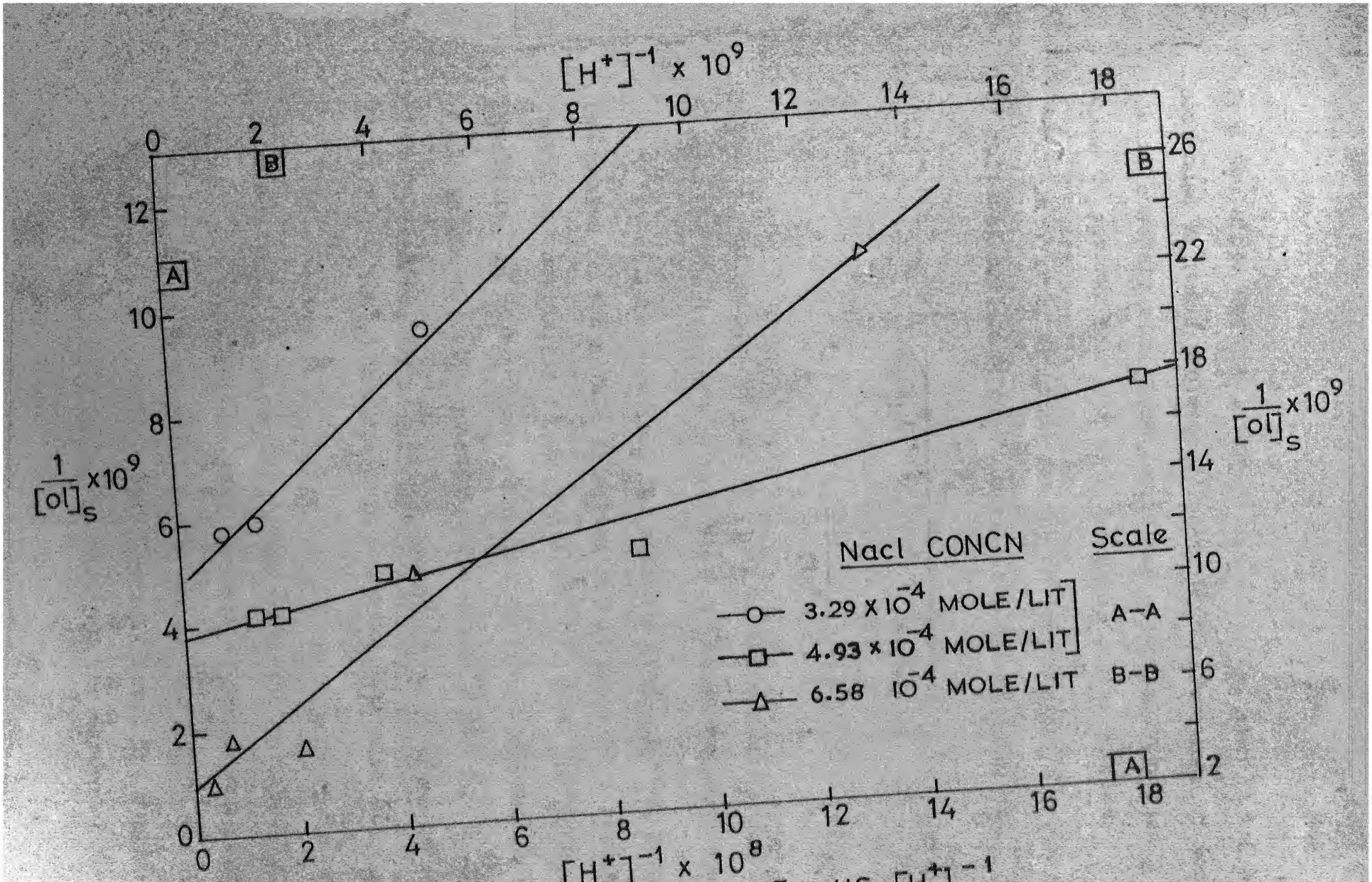

FIGURE 54 (b) PLOT OF $1/[ol]_s$ VS $[H^+]^{-1}$

from the slope and the intercept respectively. Also in the present case k_c and f are considered to be the functions of sodium oleate concentration S and determined separately for each S value to get the best fit with the experimental results.

An overall equation for the entire pH range is obtained by suitably combining equation (VII.40) and (VII.43) as,

$$\Gamma_{Ol} = [Ol^-]_s = \left[\left(\frac{S\, K_h\, K_w}{k_3\, K_h [H^+] + K_w + S\, K_h\, K_w\, k_4} \right) - \left(\Gamma_m - \left(\frac{S[H^+]}{k_c + f[H^+]} \right) \right)\right] \qquad \text{(VII.44)}$$

where Γ_m is a constant almost equal to the maximum possible adsorption density but can be varied to obtain a better fit.

It will be seen from the equation (VII.44) that before the maxima on the acidic side, the second bracketted term would contribute negligibly to the value of Γ_{Ol} since $S[H^+]/(k_c + f\,H^+) \simeq \Gamma_m$. Similarly, in higher alkaline range, the first bracketted term would assume almost a constant value nearly equal to Γ_m and would thus cancel the term Γ_m in the second bracket. Thus the term $S[H^+]/(k_c + f[H^+])$ would mostly determine the value of Γ_{Ol}.

The values of k_3, k_4, k_h, k_c, f and Γ_m for individual concentrations of sodium oleate are tabulated in Table II. The values of K_h are obtained from the data of Powney and Jordan (95) as described in Section VII-2. The values correspond to a constant temperature of 25°C. The computed curves are compared with the experimental data points in Fig. 55. The agreement is seen to be quite good.

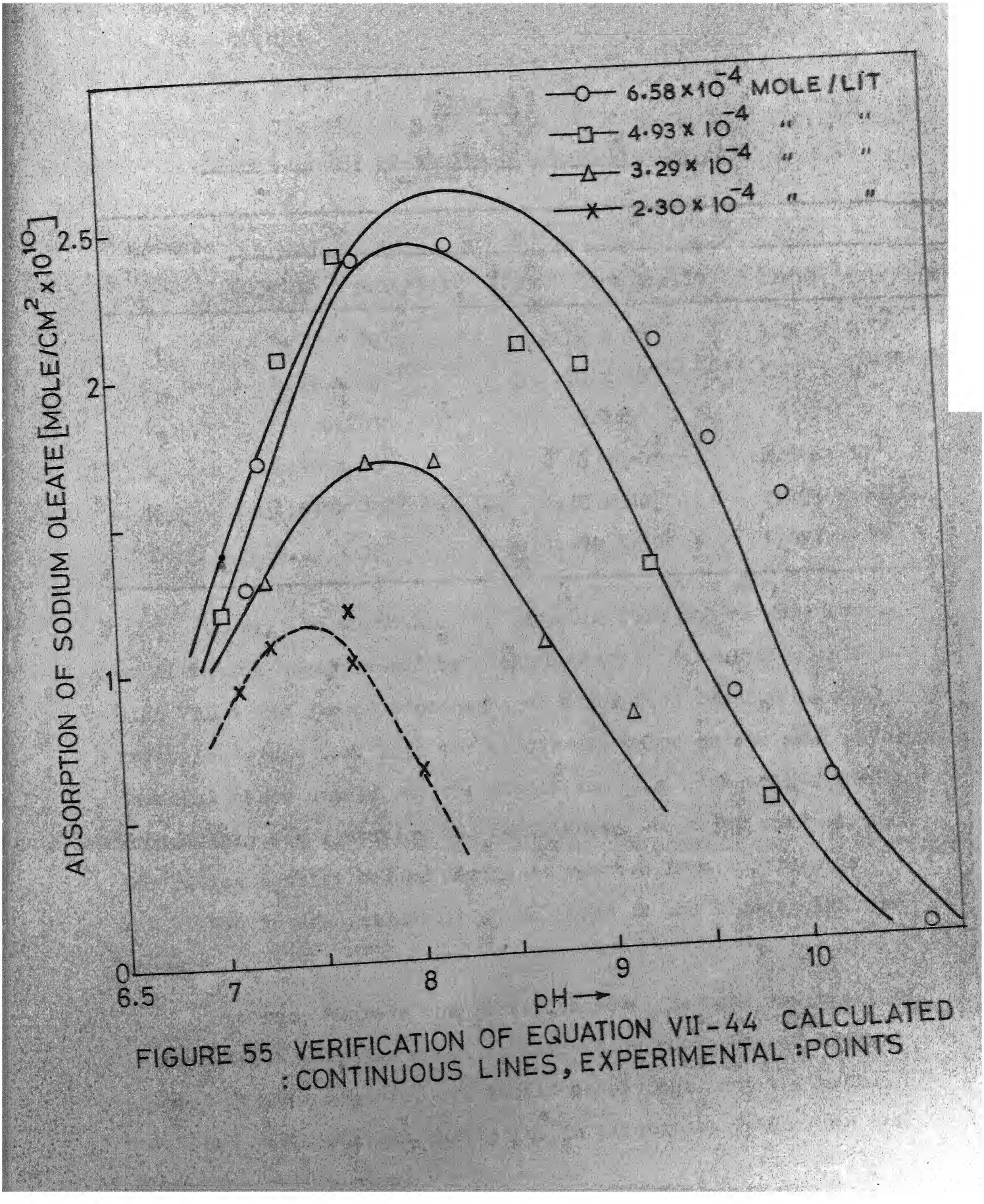

FIGURE 55 VERIFICATION OF EQUATION VII-44 CALCULATED : CONTINUOUS LINES, EXPERIMENTAL : POINTS

Table II

Values of the Constants in Adsorption Model

Constants	S		
	6.58×10^{-4} mole/lit.	4.93×10^{-4} mole/lit.	3.29×10^{-4} mole/lit.
K_h	5.10×10^{-7}	2.79×10^{-7}	1.30×10^{-7}
Γ_m	2.74×10^{-10}	2.60×10^{-10}	1.85×10^{-10}
k_3	0.2616	0.2187	0.1211
k_4	2.90×10^{9}	2.40×10^{9}	2.546×10^{9}
k_c	4.670×10^{-4}	1.10×10^{-3}	2.795×10^{-3}
f	2.37×10^{6}	1.870×10^{6}	1.677×10^{6}

It will be worthwhile to compare here the pH dependence of flotation as expressed by a mathematical formulation in Section VII-1 and the pH dependence of adsorption density as characterised just now. Both the models are based on the same physicochemical basis namely, a) the oleate ion is the active species responsible for flotation and contributes to major part of the adsorption density before maxima is reached from acidic side and b) the antagonistic role of OH^- ions in the higher alkaline range.

However, whereas the flotation model is more empirical in nature, the adsorption model is derived on the basis of known physicochemical aspects. It should be obvious that the model developed for flotation curves is, in principle, applicable to adsorption curves also.

VII-4 EFFECT OF TEMPERATURE ON ADSORPTION:

The effect of temperature on the adsorption of sodium oleate on zircon was studied and the results for initial concentration of 3.29×10^{-4} mole/lit of Na oleate at three different initial pH values 6.02, 8.48, 9.55 have been given in Fig. 18. It is seen that the adsorption increases upto temperature $30^{\circ}C$ and then decreases as it is raised to $40^{\circ}C$. The maxima in case of pH 9.55 is less pronounced.

The effect of temperature on the adsorption process may be due to (96):

1) change in the attractive forces between the solutes and the solid surface,
2) and adjacent adsorbed solute molecules,
3) change in the solubility of solute in the solvent.
4) change in the ionic condition of the solute with temperature.

An increase in adsorption of oleate from $25^{\circ}C$ - $30^{\circ}C$ can be attributed to the increase in the $[Ol^{-}]$ with rise in temperature as seen from the hydrolysis curves given in Fig. 51.

But, as the temperature is further increased, this increase is more than offset by the weakening of the attractive forces between the solute molecules and between the solute and the solid.

The aforesaid is further substantiated by the fact that the maxima is more pronounced at pH 8.48 than at 6.02 or 9.55. At pH 6.02, the Ol^- concentration is less than at pH 8.48, thus giving more initial increase at pH 8.48. At pH 9.55 however, the competition offered by the hydroxyl ions negates this effect and the maxima is not very sharp.

At higher temperature, the weakening of the attractive forces and increased solubility are the sole governing factors at all the pH values. The behaviour with regard to temperature indicates that the adsorption is probably due to van der waal's interaction between hydrocarbon chains which being rather weak in nature are easily affected by temperature. This will be further corroborated in the following sections.

The effect of temperature on the soap flotation of minerals is well known. G.V. Subramanya (37) has studied the temperature effect on the flotation of zircon with sodium oleate-stearate mixed collectors between 65°C and 90°C.

VII-5 ADSORPTION, ZETA POTENTIAL AND FLOTATION:

In this section, parallel adsorption, zeta-potential and flotation recovery results will be discussed and the mutual correlation among these will be brought out.

Adsorption Isotherm:

First of all, the adsorption isotherm for sodium oleate (Fig. 16) will be discussed. As will be seen from the figure the adsorption density (Γ_{Ol}) increases gradually in the initial

stages, then it shoots up rapidly to reach the plateau region. At the end of the plateau the adsorption density again increases. The concentration at which this rise after plateau region is observed lies around 1.00×10^{-3} moles/lit of the initial added concentration. This is nearer the cmc of sodium oleate. The mono layer coverage occurs at Γ_{01} value of 2.90×10^{-10} mole/cm^2 which is some what below the actual plateau region observed.

The adsorption isotherm (Fig. 16) according to Giles classification (95a) is of S-type. In the initial part of the isotherm there is a slight concavity towards the abscissa and the slope increases rapidly. This is obviously due to increased rate of change of site availability with increase in the solute adsorbed that is, the more the solute there is already adsorbed the easier it is for the additional amounts to become fixed. According to Giles (95a) this implies a side-by-side association between adsorbed molecules; helping to hold them to the surface. Such a situation is further facilitated if the solute molecule is a) monofunctional, b) has moderate intermolecular attraction and c) meets strong competition for surface sites from solvent molecules or other adsorbing species. Thus, the S-type of adsorption isotherm in the present case indicates the possibility of adsorption due to vander waal's attraction between the hydrocarbon chains. This view will be further substantiated at a later stage.

The latter part of the isotherm resembles a L-type isotherm and for this region Langmuir's adsorption equation is applicable (See Fig. 53). It would be worthwhile to mention here that F.W. Getzen and T.M. Ward (28) used langmuirian type equations for characterising pH dependence of oleic acid on graphite. This fact has been already made use of in developing the mathematical model to characterise pH dependence of adsorption density.

Zeta Potential:

The zeta potential under similar conditions of pH (e.g. pH = 9 and 10) and varying sodium oleate concentrations have been already depicted in Fig. 35. It is seen that the zeta potential varies almost similarly. The negative value first increases rapidly and then slowly, before it falls at around initial concentration 1.00×10^{-3} mole/lit of sodium oleate. Similar behaviour is observed at pH 9 as well as at pH 10. When plotted on a compressed scale (Fig. 36), the curve shows three distinct straight line regions with varying slopes. The initial straight line portion probably indicates associative adsorption while the change of slope may indicate the onset of hemimecelle formation on the solid surface. For second change of slope indicates the formation of micelle in the aqueous bulk and formation of the second layer on the mineral surface. The formation of hemimecelle would effectively decrease the negative charge, thereby, decreasing the slope. Whereas, the

formation of micelle in solution and second layer adsorption of the micelle packed with gegenions on the surface would decrease the effective negative charge to a very large extent. As a result the zeta potential decreases numerically.

Correlation of Adsorption and Zeta Potential with Flotation:

The correlation between the two solid-liquid interfacial parameters e.g. the adsorption density and zeta potential with flotation is brought out by plotting the three in Fig. 56. pH is kept constant at 9.0 $\pm$ 0.05 in all the cases while sodium oleate concentration is varied. It is observed that the flotation recovery increases more abruptly in the initial stages as compared to adsorption density or zeta potential. All the three parameters show a plateau region upto initial concentration of 1.00×10^{-3} mole/lit. of sodium oleate after which the adsorption density shoots up while flotation and zeta potential decrease abruptly. This point is very near the cmc which varies around the value 2.0×10^{-3} mole/lit depending on the pH of the solution. It is indicative of the fact that there is a rearrangement of ionic collector species in the bulk as well as at the surface. The formation of micelle and second layer adsorption may take place thus shooting up adsorption but decreasing the flotation recovery and zeta potential.

In view of the fact that the particle size of the experimental samples used in the above mentioned three sets of investigations differ markedly the above correlation obtained is remarkable.

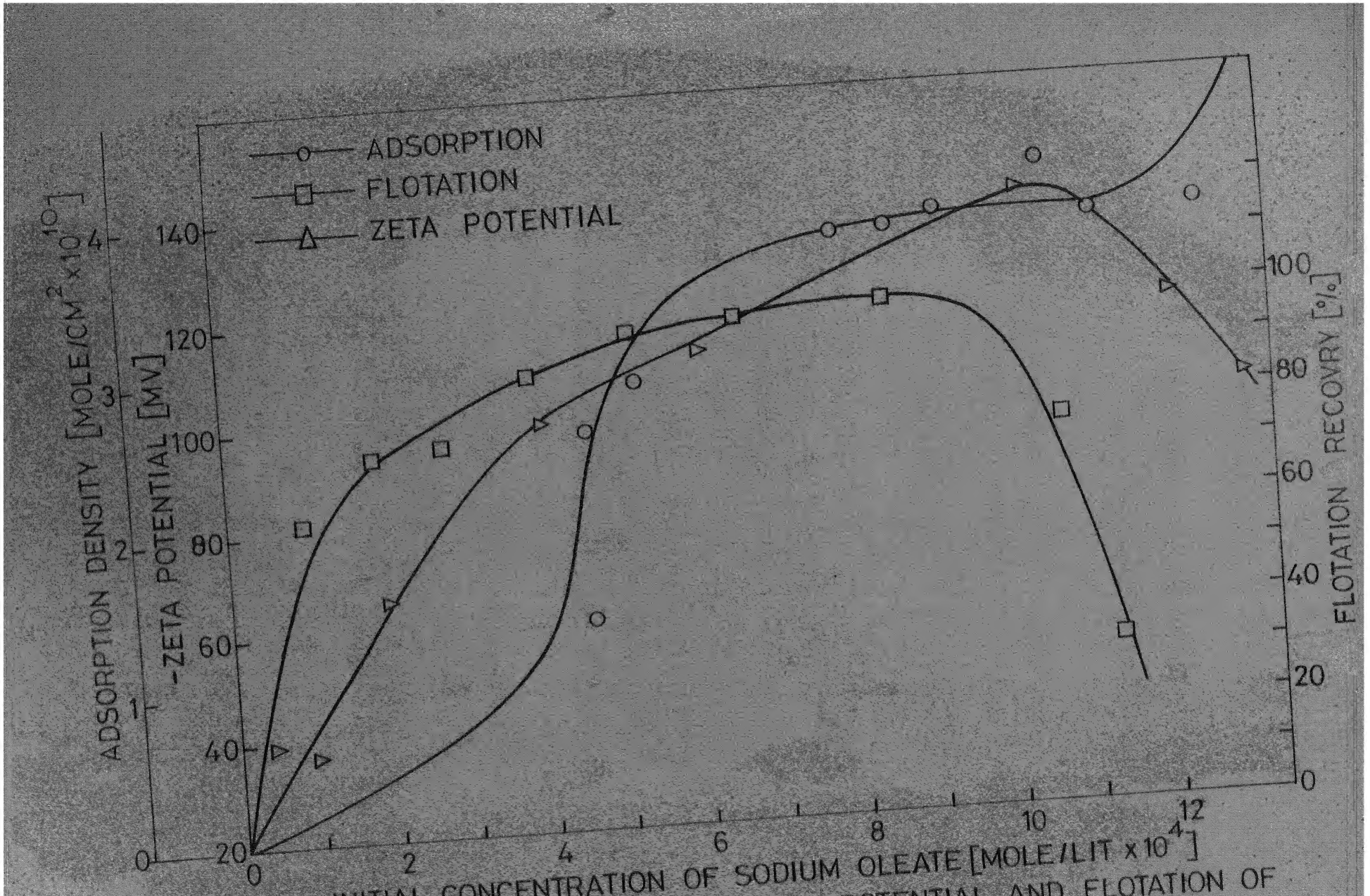

FIGURE 56 COMPARISON OF ADSORPTION, ZETA POTENTIAL AND FLOTATION OF ZIRCON AT pH 9 AND VARYING AMOUNTS OF SODIUM OLEATE

To bring out the above overall correlation more vividly, the flotation recovery and zeta potential are plotted against adsorption density (see Fig. 57). Though no single straight line correlation is obtained over the entire range of collector concentrations, excellent straight line relations for limited ranges are obtained. The entire range is adequately covered by two straight lines in both zeta potential vs. Γ_{01} and Flotation Recovery vs. Γ_{01} plots. The change in slope in both the cases is clearly due to the tendency on the part of flotation and zeta potential to increase more abruptly as compared to adsorption density in the initial stages and the difference in particle size. However, the very fact that excellent straight lines are obtained is indicative of mutual correlation among these parameters. The correlation coefficient in case of zeta potential vs. Γ_{01} curve for Ist portion is 0.981 and the equation obeyed is $\zeta = 21.05 + 1 \times 10^{12} \Gamma_{01}$. In this equation ζ is expressed in mv while Γ_{01} is in mole/cm^2. For IInd portion the correlation coefficient is 0.965 the equation iis $\zeta = 86.0 + 8.35 \times 10^{10} \Gamma_{01}$.

Similarly, for flotation recovery curves the equation for the 1st part is:Flotation Recovery = $1.98 \times 10^{12} \Gamma_{01}$ with correlation coefficient 0.942, and for IInd part the equation is:Flotation Recovery = $78 + 5.6 \times 10^{10} \Gamma_{01}$ with correlation coefficient 0.989.

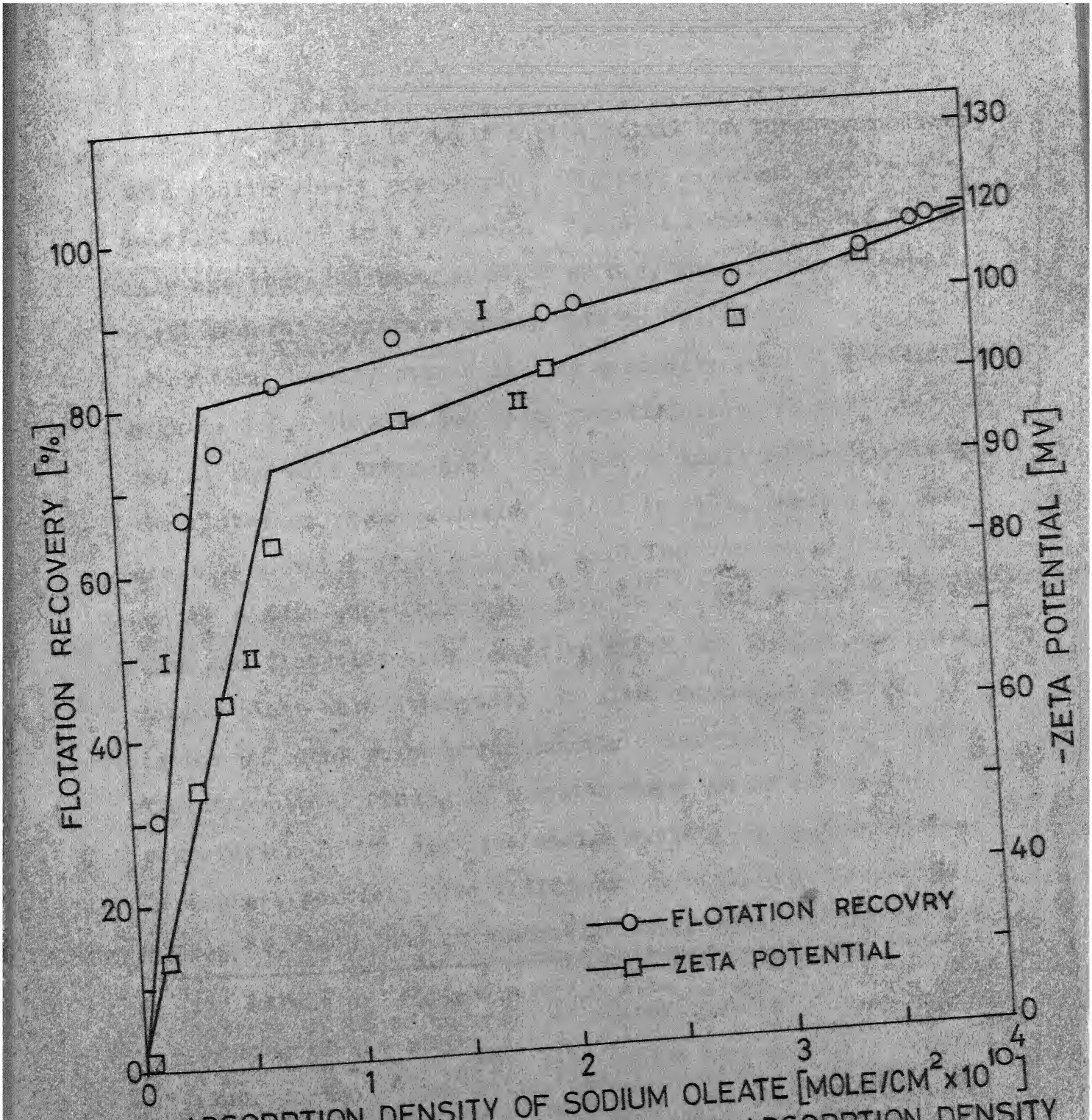

FIGURE 57 CORRELATION DIAGRAM FOR ADSORPTION DENSITY WITH FLOTATION RECOVERY AND ZETA POTENTIAL OF ZIRCON-SODIUM OLEATE SYSTEM AT CONSTANT INITIAL pH 9.0

The Fig. 58 is again a plot of all the three parameters when sodium oleate concentration is kept constant at 6.58×10^{-4} mole/lit and pH is a variable. The data between pH 8.5 to 10.5 only are compared because below pH 8.5, whereas the flotation still records maximum recovery upto pH 5.0, the adsorption density starts falling gradually even at a pH as high as 7.0. This is due to a) the difference in particle size and b) the well known fact that even at small surface coverage, the flotation is appreciable. Added to this, there is a progressive precipitation of oleic acid from the aqueous medium in the acidic pH. Therefore, even though the trends in adsorption and flotation with variation in pH are similar, no correlation plots were attempted. In alkaline medium however, it is the OH^- ions which predominantly determines the Γ_{Ol} and flotation both. Thus, in a system where pH is a variable, the correlation in the alkaline medium would be more meaningful. Of course, particle size difference is still a factor which should be taken into consideration while interpreting the results.*

* The effect of finer particle size on the adsorption magnitude would be to appreciably change the final pH and concentration of the sodium oleate solution. For example, for particle size +100, +150 mesh (which was used in flotation experiments), the difference in initial pH and final pH after conditioning would be hardly 0.15 whereas the corresponding figure for the adsorption experiments where particle size is much finer would be around 0.5 pH units. Similarly the difference in initial and final concentrations in flotation experiments would be 1×10^{-7} mole/l, assuming 50 percent monolayer coverage. The corresponding difference in adsorption experiments would be around 10^{-4} mole/lit.

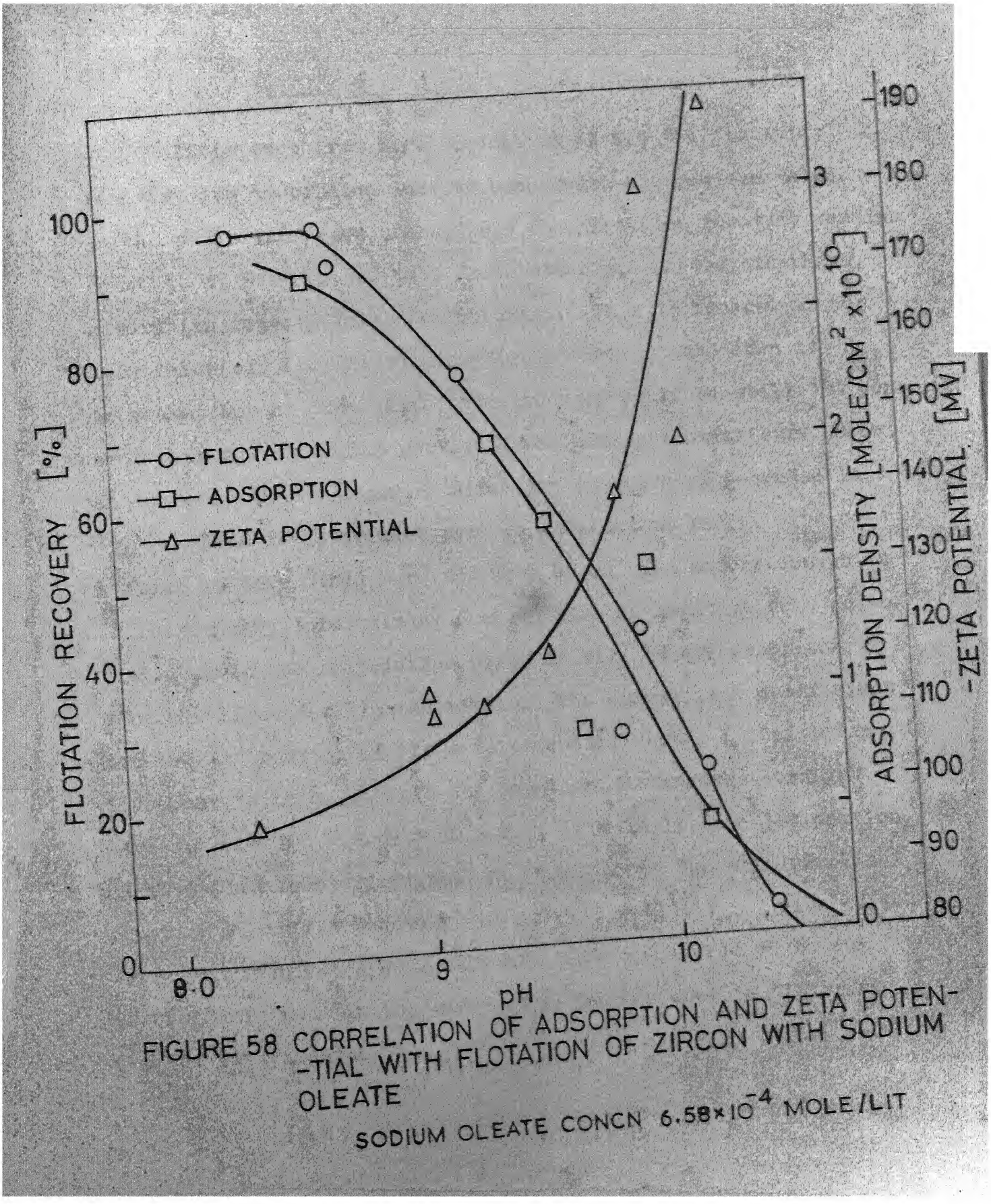

FIGURE 58 CORRELATION OF ADSORPTION AND ZETA POTEN-
-TIAL WITH FLOTATION OF ZIRCON WITH SODIUM
OLEATE

SODIUM OLEATE CONCN 6.58×10^{-4} MOLE/LIT

It is seen from Fig. 58 that at pH 8.5 the flotation recovery and adsorption density both reach the maximum value. As the pH is increased upto pH 8.9 the flotation recovery remains constant at maximum and then falls steeply. On the otherhand, adsorption density falls continuously. This is because at certain value of Γ_{Ol} the recovery is 100 percent and even if Γ_{Ol} increases beyond that value, the recovery would be still 100 percent thus giving a flat portion. The zeta potential curve shows an increase in the negative direction in spite of decrease in Γ_{Ol} . Thus it is evident that in alkaline pH range, zeta potential is determined more and more by OH^- ion adsorption which increases many folds giving a steep rise in negative zeta potential. Again the correlation plots in Fig. 59 are excellent straight lines for limited ranges.. The correlation coefficient for the 1st portion of the zeta potential versus Γ_{Ol} plot was found out to be 0.986 with the equation fitting the straight line as $\zeta = 108 - 2.95 \times 10^{11} \Gamma_{Ol}$, Similarly, the 1st portion of flotation recovery versus Γ_{Ol} plot obeys the straight line equation Flotation Recovery $= 0.7 + 3 \times 10^{11} \Gamma_{Ol}$ with correlation coefficient 0.998. The break is considered to be due to the difference in the sizes of particles used in different sets of experiments.

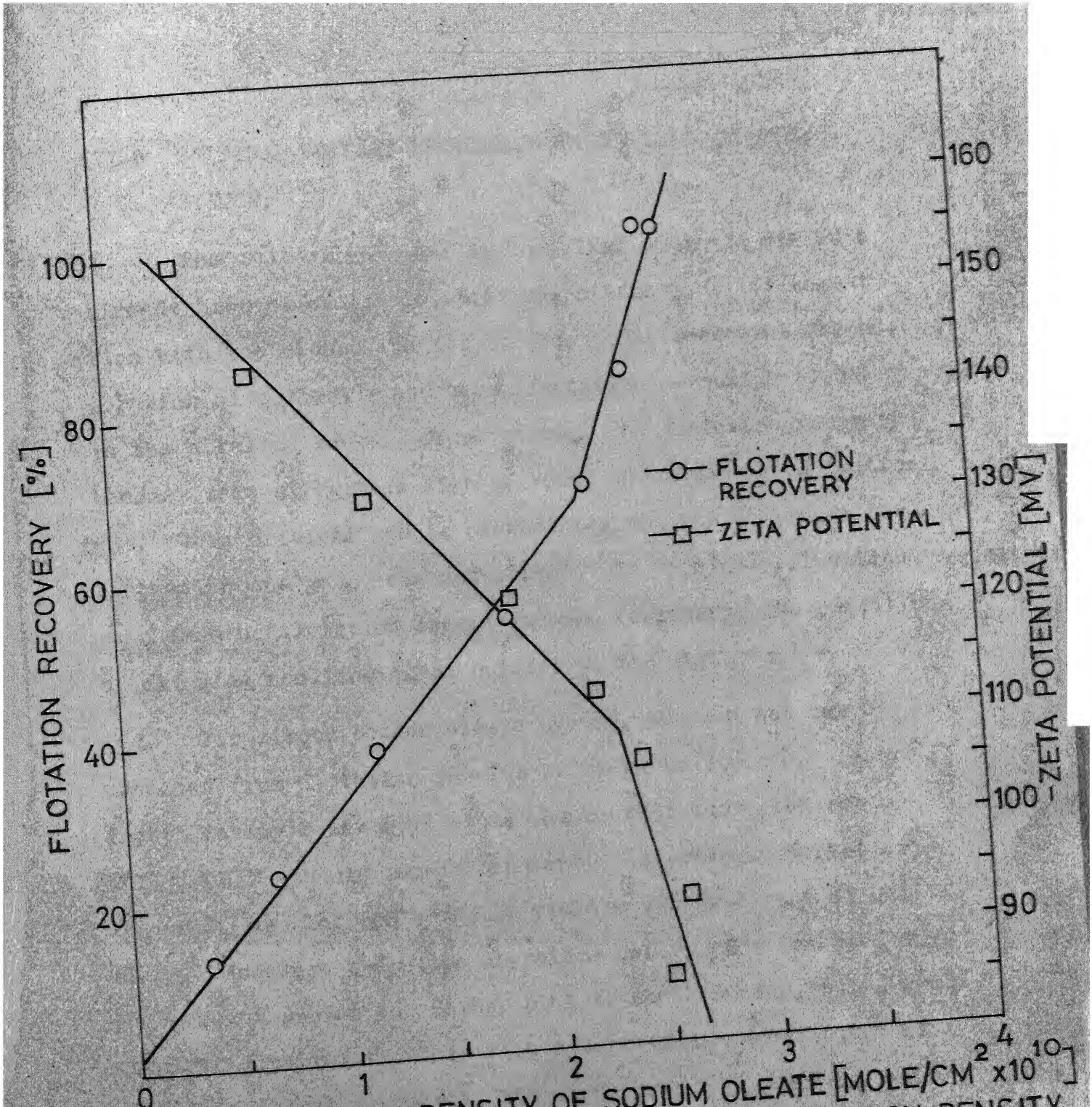

FIGURE 59 CORRELATION DIAGRAM FOR ADSORPTION DENSITY WITH FLOTATION RECOVERY AND ZETA POTENTIAL OF ZIRCON-SODIUM OLEATE SYSTEM AT CONSTANT OLEATE CONCENTRATION 6.58×10^{-4} MOLE/LIT

VII-6 CRITICAL CONTACT PHENOMENON IN ZIRCON - Na OLEATE SYSTEM:

The role of OH^- ions in the alkaline range has been already brought out in the previous discussion. Its competition with the oleate ion for surface sites decreases the adsorption of collector and hence flotation of sodium oleate in the alkaline range. Consequently, the flotation recovery becomes zero at certain high pH value known as 'upper critical pH'. When critical pH is plotted against the collector concentration one gets 'contact curve'. It separates flotation zone from no flotation zone. It also represents the condition of clinging/nonclinging of bubbles to the surfaces.

For zircon-sodium oleate system, the contact curve obtained from flotation results is shown in Fig. 60. According to Barsky's law (97) along the contact curve the ratio $[Ol^-]/[OH^-]$ should remain constant. Accordingly a plot of $\log [Ol^-]$ vs $\log [OH^-]$ should yield a straight line of unit slope. However, the slope is seldom unity. For example, for the present system the Barsky plot is shown in Fig. 61. A good straight line relationship with a correlation coefficient of 0.97 is obtained. However, the slope is 0.675 which is less than unity. It is worthwhile to compare this value of the slope with the value obtained with the help of the flotation model given in Section VII-1 wherein the slope is obtained from the relationship between K_a and S. The value of the slope so obtained

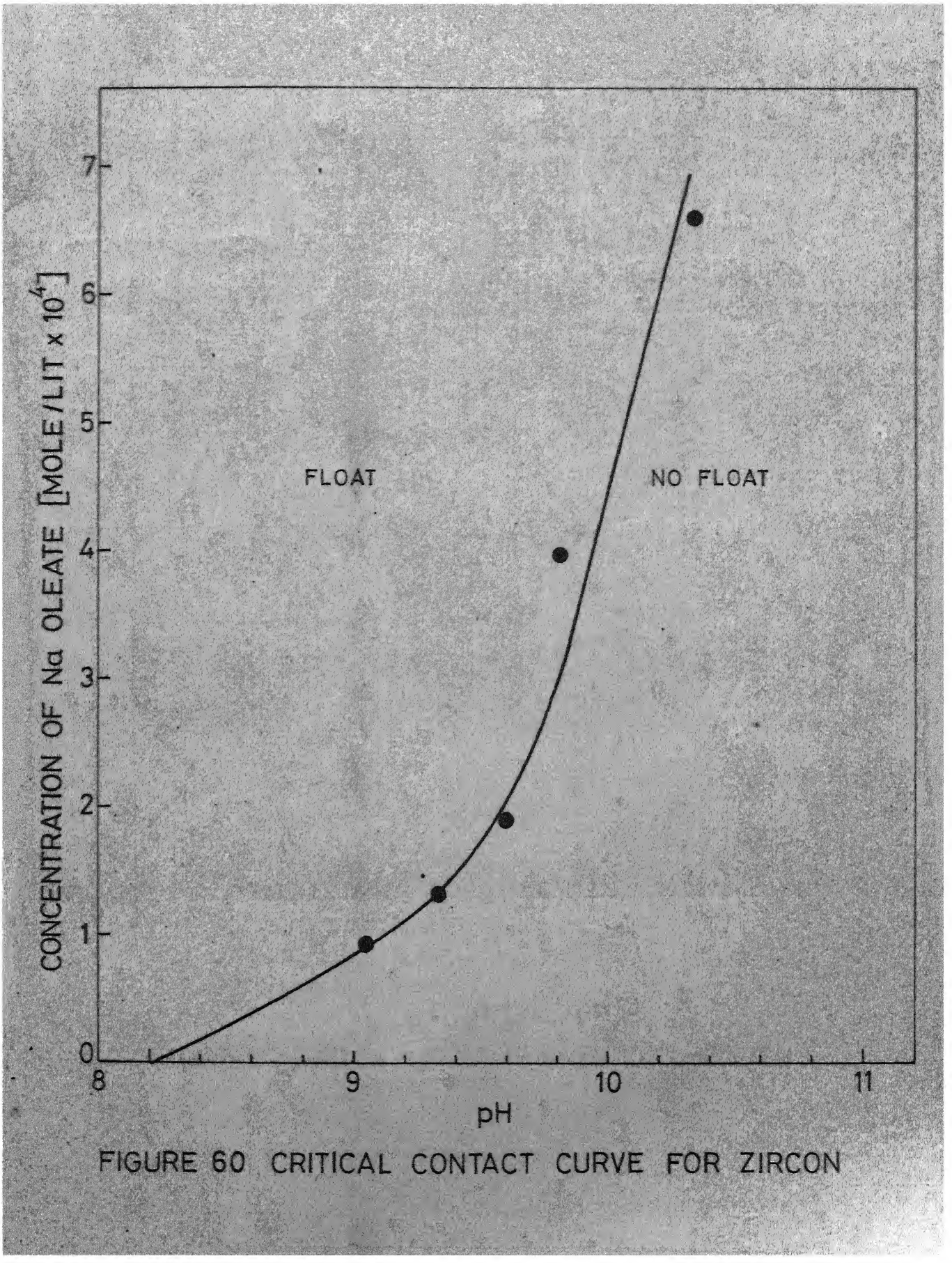

FIGURE 60 CRITICAL CONTACT CURVE FOR ZIRCON

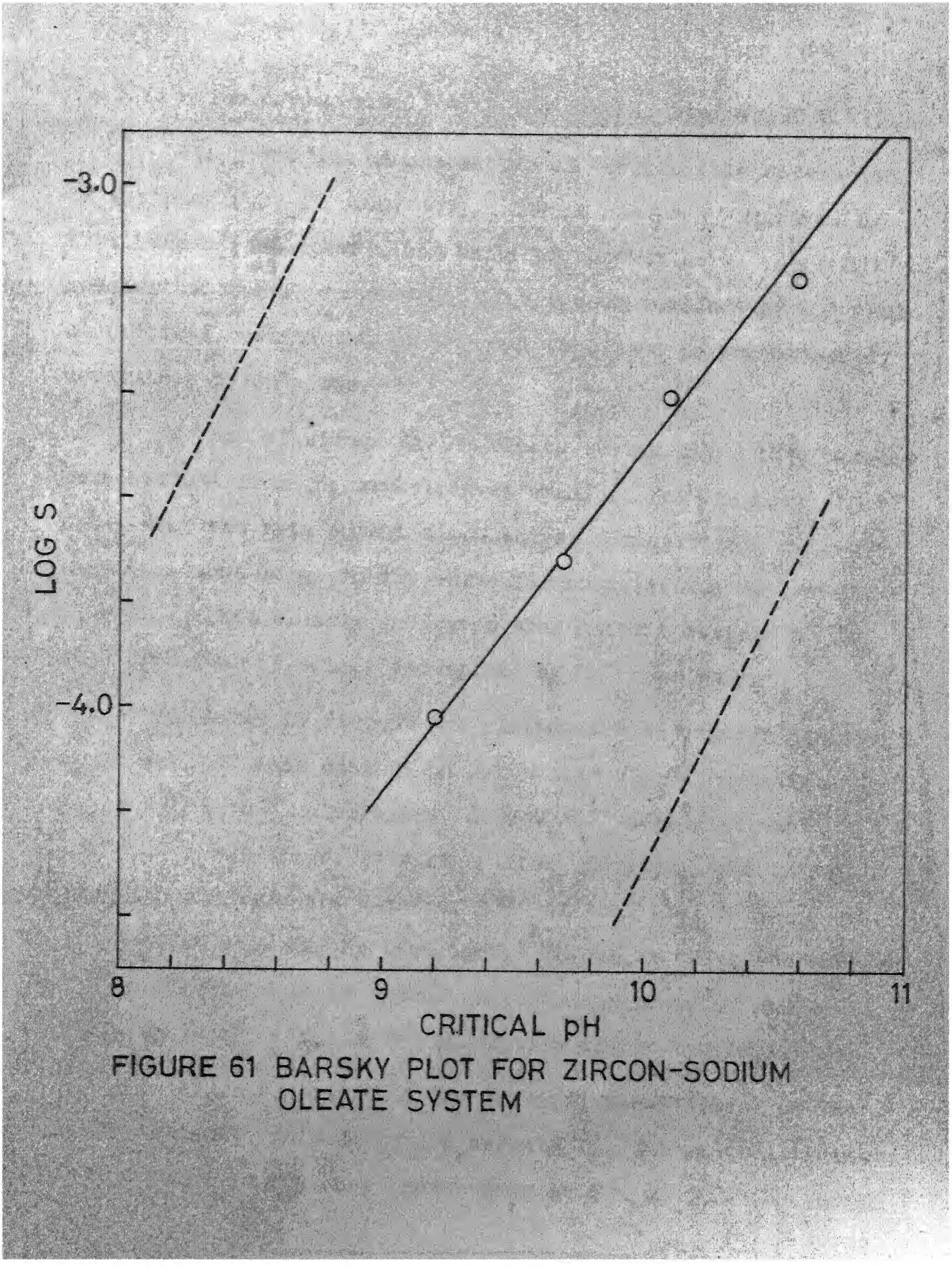

FIGURE 61 BARSKY PLOT FOR ZIRCON-SODIUM OLEATE SYSTEM

is 0.73 which compares well with the experimental value 0.675.

This point has been a matter of considerable discussion in the past (98, 99, 100, 101). And it has been suggested by A.M. Gaudin ([99]) that along critical contact curve $[Ol]/[OH]^m$ remains constant. In general, it has been realised by now that at critical contact the interfacial condition is predominantly determined by OH^- ions.

In case of zircon-sodium oleate system also, this becomes more evident from the experimental studies. For example, Fig.62 shows that the zeta potential-pH curves for different collector concentrations merge in the curve for no collector at certain pH value. This clearly indicates that after a certain pH the zeta potential is solely determined by OH^- ions only.

Similarly in Fig. 63 are plotted the adsorption density values for OH^- ions against pH for sodium oleate concentrations 6.58×10^{-4} moles/litre, 3.29×10^{-4} moles/lit. and 2.30×10^{-4} moles/lit. It will be seen therefrom that the adsorption isotherms are S-shape. All of them seem to merge in one straight line at the upper end. The pH at which the curves merge represent a point beyond which the presence of sodium oleate no longer affects the adsorption of the hydroxyl ions.

In order to bring out the critical significance of the ratio [Ol]/[OH] the adsorption density Γ_{Ol} is plotted against log [Ol]/[OH] in Fig. 64. Here again we notice that the curves

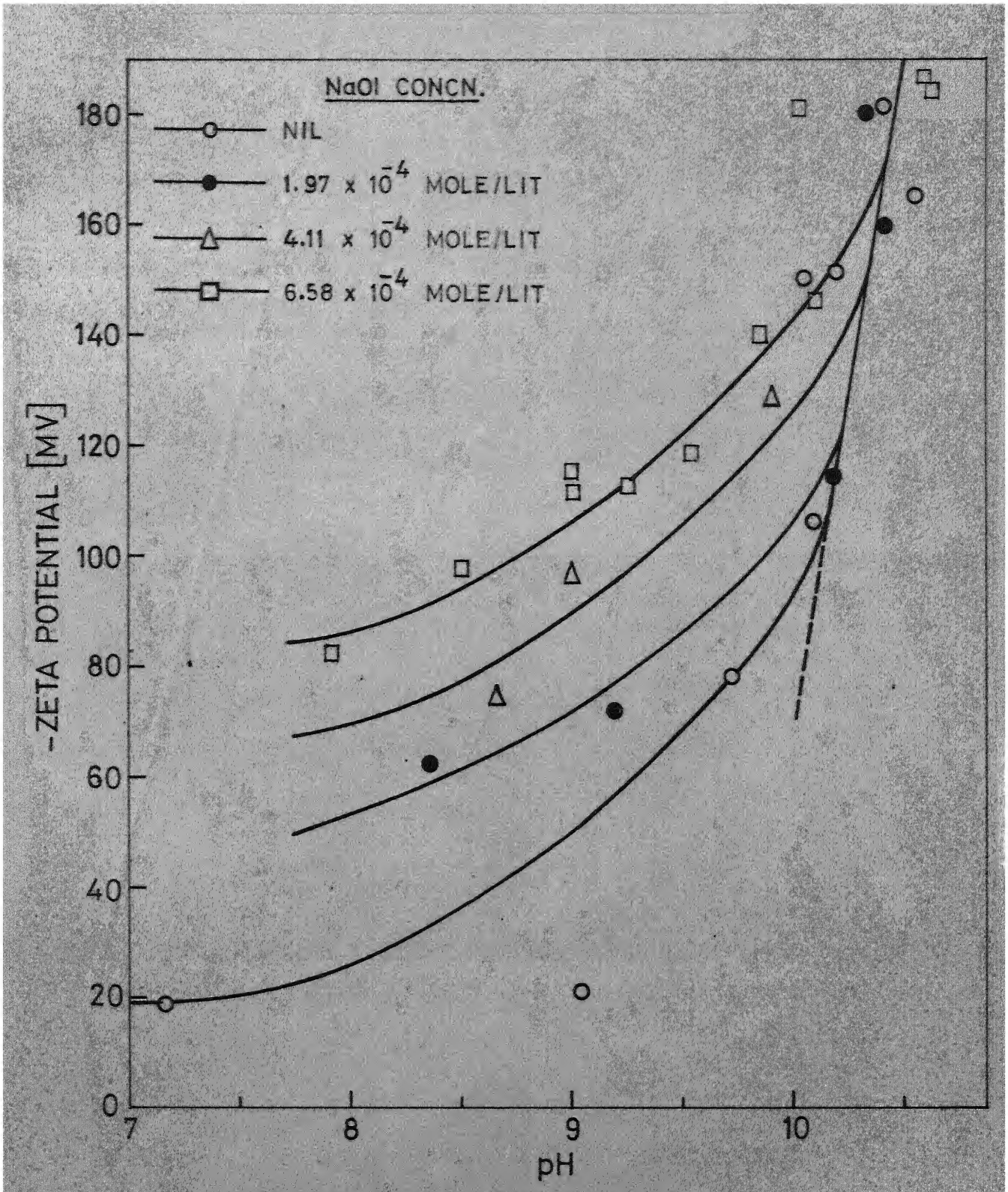

FIGURE 62 EFFECT OF pH ON THE ZETA POTENTIAL OF ZIRCON AT VARIOUS SODIUM OLEATE CONCENTRATIONS

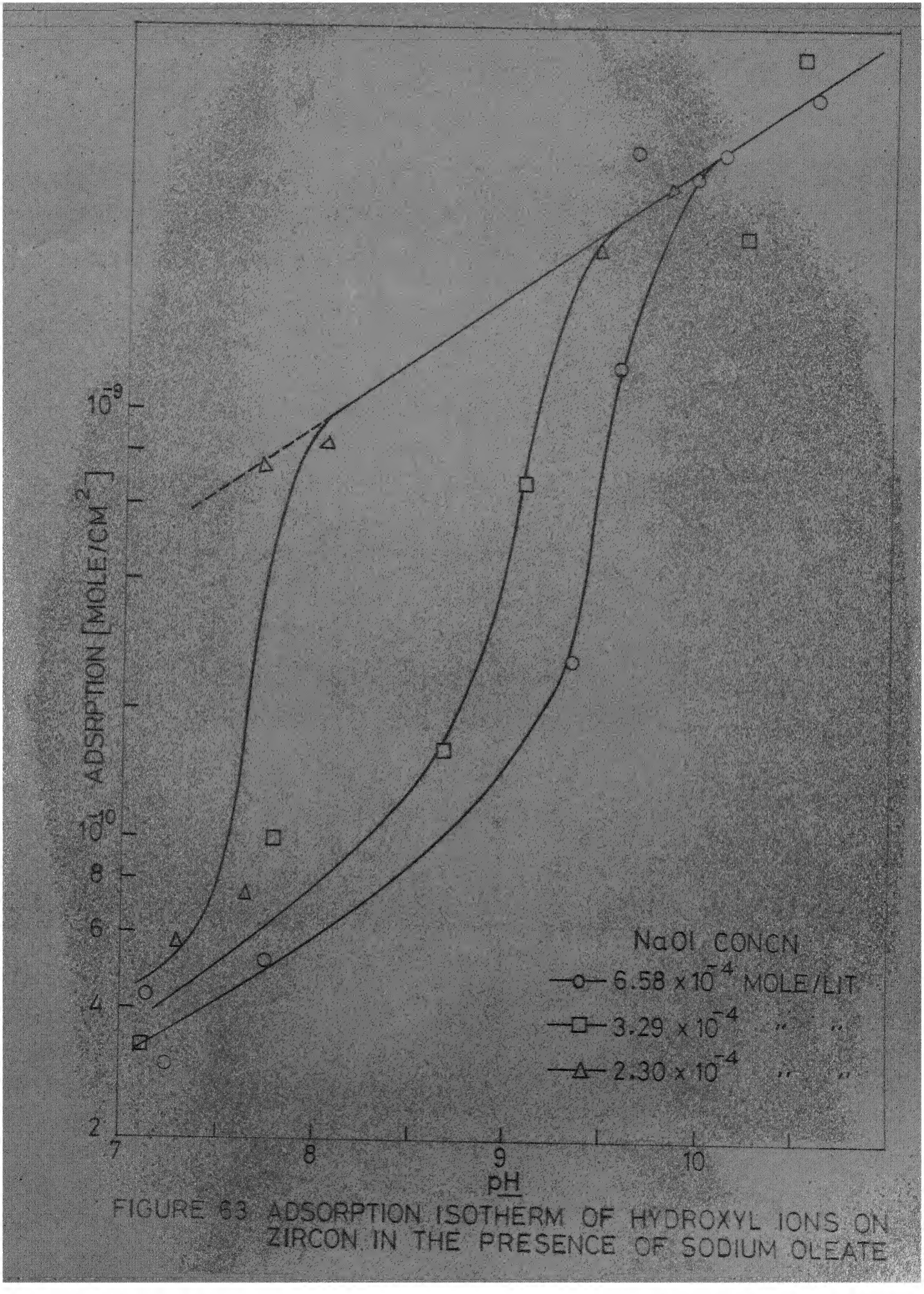

FIGURE 63 ADSORPTION ISOTHERM OF HYDROXYL IONS ON ZIRCON IN THE PRESENCE OF SODIUM OLEATE

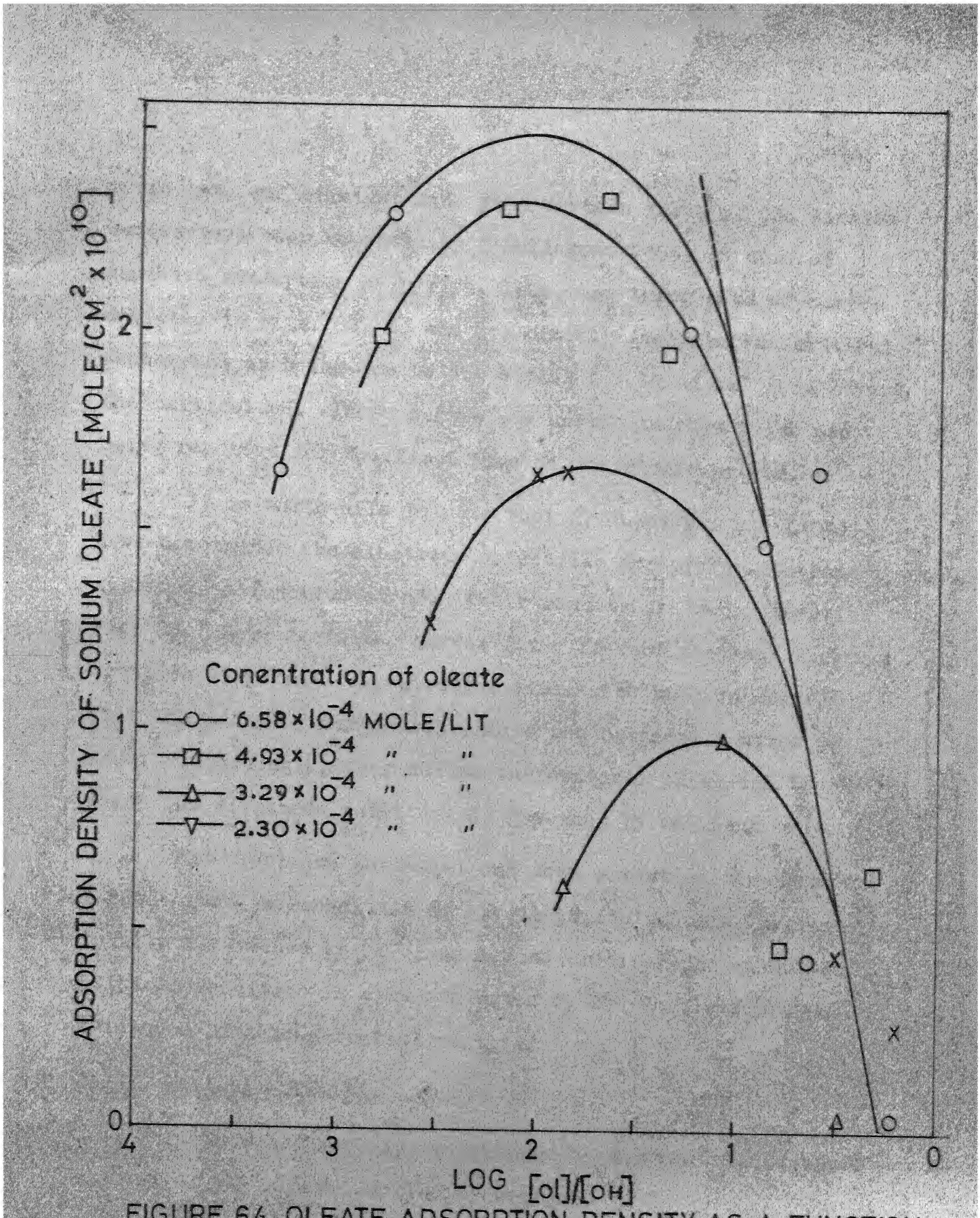

FIGURE 64 OLEATE ADSORPTION DENSITY AS A FUNCTION OF LOG [ol]/[oH]

merge into one straight line at a certain value of pH. Similar curves have been reported by O'Mellegren (103) in case of xanthate adsorption on pyrite. Thus, the three sets of curves depicted in Figs. 62, 63 and 64, clearly indicate the critical phenomenon as being due to the dominant role of OH^- ions beyond the critical pH. These curves are unique in that these are being reported for the first time on one single system.

It is worthwhile to note that S. Mukai et. al. (104), have determined the electrode potentials for pyrite-xanthate system as a function of pH. Their results are reproduced in Fig. 65. Here again the curves for different xanthate concentrations merge into one straight line. The authors suggest that the point of merger represents the critical contact pH also. Accordingly, they define the critical pH as one beyond which the electrode potential is governed by OH^- ions only.

The electrode potential and zeta potential measurements suggest that the condition of the electrical double layer is totally determined by OH^- ions beyond critical pH. Also the critical condition is also exhibited by the double layer as evidenced by zeta-potential results.

VII-7 INFRARED SPECTRA:

In this section, it is proposed to discuss the infrared spectra of the mineral-collector systems.

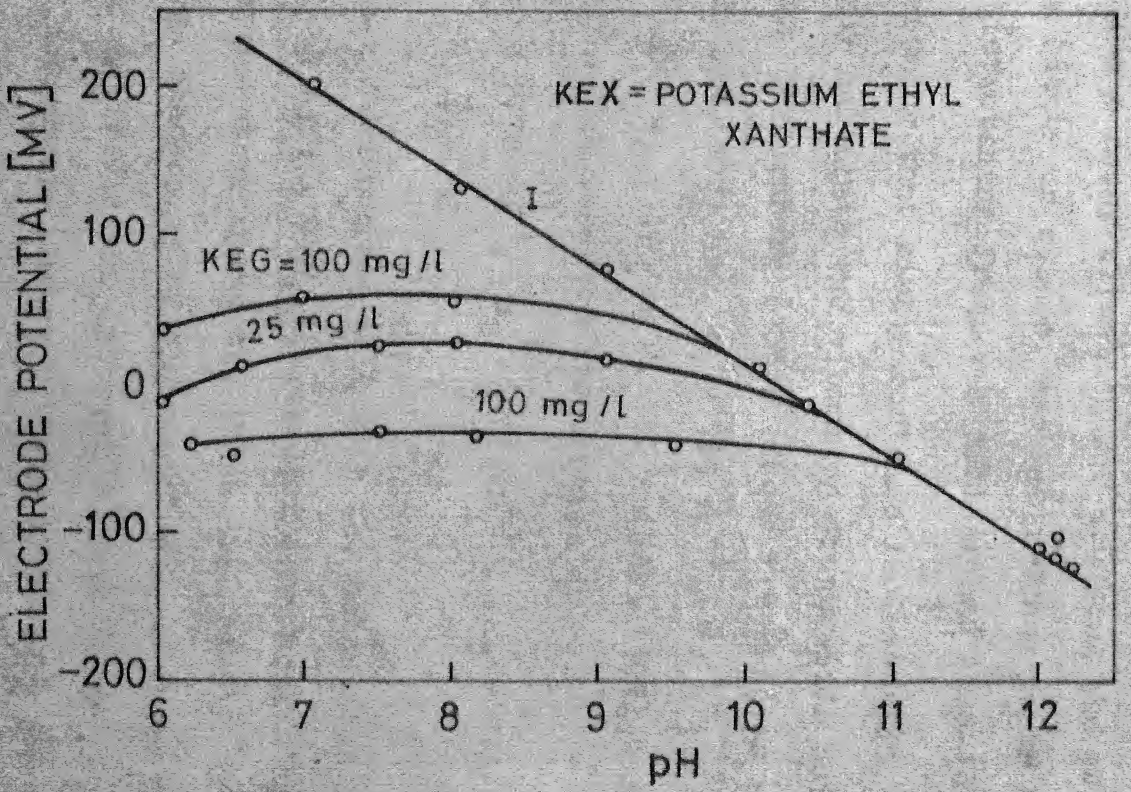

FIGURE 65 RELATION BETWEEN ELECTRODE POTENTIAL OF PYRITE AND pH AT VARIOUS CONCENTRATIONS OF POTASSIUM ETHYL XANTHATE (S. Mukai et al)

Infrared Spectra of Zircon:

The spectra for zircon has already been shown in Fig.40. It is seen that there is absolutely no peak between 3000 and 1200 cm^{-1}. All peaks appear below 1000 cm^{-1} only. This is particularly a happy situation for studying the adsorption of sodium oleate on zircon, because intense peaks due to carbonyl antistretching frequency fall around 1500-1700 cm^{-1}.

Assuming that zircon contains isolated SiO_4^{-4} tetrahedra one may calculate the vibration frequencies using the formulae given by Herzberg (105). These frequencies as calculated by B.D. Saxena (106) are $\omega_1 = 729\ cm^{-1}$, $\omega_2 = 473\ cm^{-1}$, $\omega_3 = 1031\ cm^{-1}$ and $\omega_4 = 493\ cm^{-1}$. F. Matossi (107) has reported the corresponding observed frequencies at

$\omega_1 = 770\ cm^{-1}$, $\omega_2 = 473\ cm^{-1}$, $\omega_3 = 944\ cm^{-1}$ and $\omega_4 = 493\ cm^{-1}$.

These values agree well with the calculated ones. The frequency ω_3 of the SiO_4 tetrahedron is a motion of silicon against oxygen atoms along the three axes (105). This involves rather large changes of dipole moment and so these modes will be strongly active in the infrared region. Also ω_3 is triply degenerate frequency. However, this degeneracy can disappear due to lower cell symmetry. For zircon (cell symmetry (D_{4h})) only two frequencies are expected (106) and these were observed at 1003 and 833 cm^{-1} respectively.

In the spectra reported in the present work, intense peaks at 1003, 894, 785, 615, 600, 425, 375 and 305 cm^{-1} were observed. Out of these, the ones at 1003, 894, 785, 375 match very well with the ones observed by Matossi (107) and Saxena(106). According to Saxena, the distinguishing features of the silicates containing isolated SiO_4 tetrahedron are the two strong bands at 1000 cm^{-1} and the other close to 893 cm^{-1}. These are evident in the present spectra. The frequencies at 615, 600, 425 and 305 cm^{-1} are also observed predominantly in the spectra given. However, these have not been reported by the previous workers. Probably, the samples used by these workers were much coarse and hence caused large scale scattering. This might have resulted in the weakening of peaks. This is evident from the very small peaks obtained in their work. It is not surprising, therefore, that except the very intense peaks, others with medium or low intensity were obscured. In the present case, however, the particle size is extremely small (less than 1 micron) and hence scattering effects are minimised. Probably, because of this the additional peaks appear as stated. However, the frequency assignment of these peaks has not been done as it does not pertain to the main theme of the present investigations.

Infrared Spectra of Oleic Acid and Sodium Oleate:

The spectra of oleic acid and sodium oleate solid have been already shown in Figs. 41 and 42. The bands at 3130-45 cm^{-1} in sodium oleate have been assigned to the stretching vibration

of C=C-H carbon hydrogen bonds. Intense bands at 2915 and 2845 cm^{-1} in oleic acid and 2900 and 2840 cm^{-1} in sodium oleate are due to CH_3 and CH_2 vibrations. The very intense band at 1700 cm^{-1} in oleic acid has been attributed to dimer formation in oleic acid and is assigned to C=O stretching in COOH. This is a distinguishing band for oleic acid. It is not observed in sodium oleate. Instead we have a strong band at 1545 cm^{-1} which is due to antisymmetrical stretching vibrations of COO^- group. This frequency is a distinguishing feature of sodium oleate and is not found in oleic acid. Assignments of other frequencies has also been done (108,109). These are reported in Table XLIV in Appendix G.

Infrared Spectra of Adsorbed Species:

Fig. 44 shows the i.r spectra of sodium oleate adsorbed on zircon. It shows that there is no trace of any surface compound being formed between sodium oleate and zircon, since no new absorption peaks are appearing. Also at lower concentrations of sodium oleate there is no evidence of any oleate species present at the surface. But if sodium oleate concentration is increased much higher (1.316×10^{-3} mole/lit.) characteristic band at 1700 and 2900 cm^{-1} appear. They grow in intensity as the sodium oleate concentration is further increased to 1.84×10^{-3} mole/lit. The band at 1700 is characteristic of C=O stretching frequency in COOH and is considered to arise due to formation of dimers of the type,

due to formation of dimers of the type,

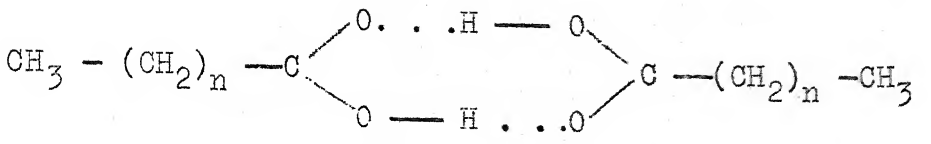

It is thus evident that at higher concentrations of sodium oleate there is a dimer formation at the surface of zircon.

This then is an evidence of the contention made earlier that sodium oleate is not chemisorbed on the zircon surface.

Carbonyl Stretching Frequency of Metal Oleates:

It is seen that there is a direct relationship between the ionic radius of cations forming the metal oleates and their carbonyl stretching frequency. This is shown in Fig. 66. The data for the frequency values are taken from the literature and tabulated in Table V Appendix A. Also, since this does not pertain to the present system it is discussed in details in Appendix A. Suffice it to mention here that the straight line relationship is useful to the extent that one can find out the unknown carbonyl stretching frequency of any other metal oleates once the radius of the cation is known.

VII-8 GENERAL REMARKS ON ZIRCON SODIUM OLEATE SYSTEM:

In this section, it is intended to consolidate the findings on sodium oleate system and draw some general conclusions on that basis.

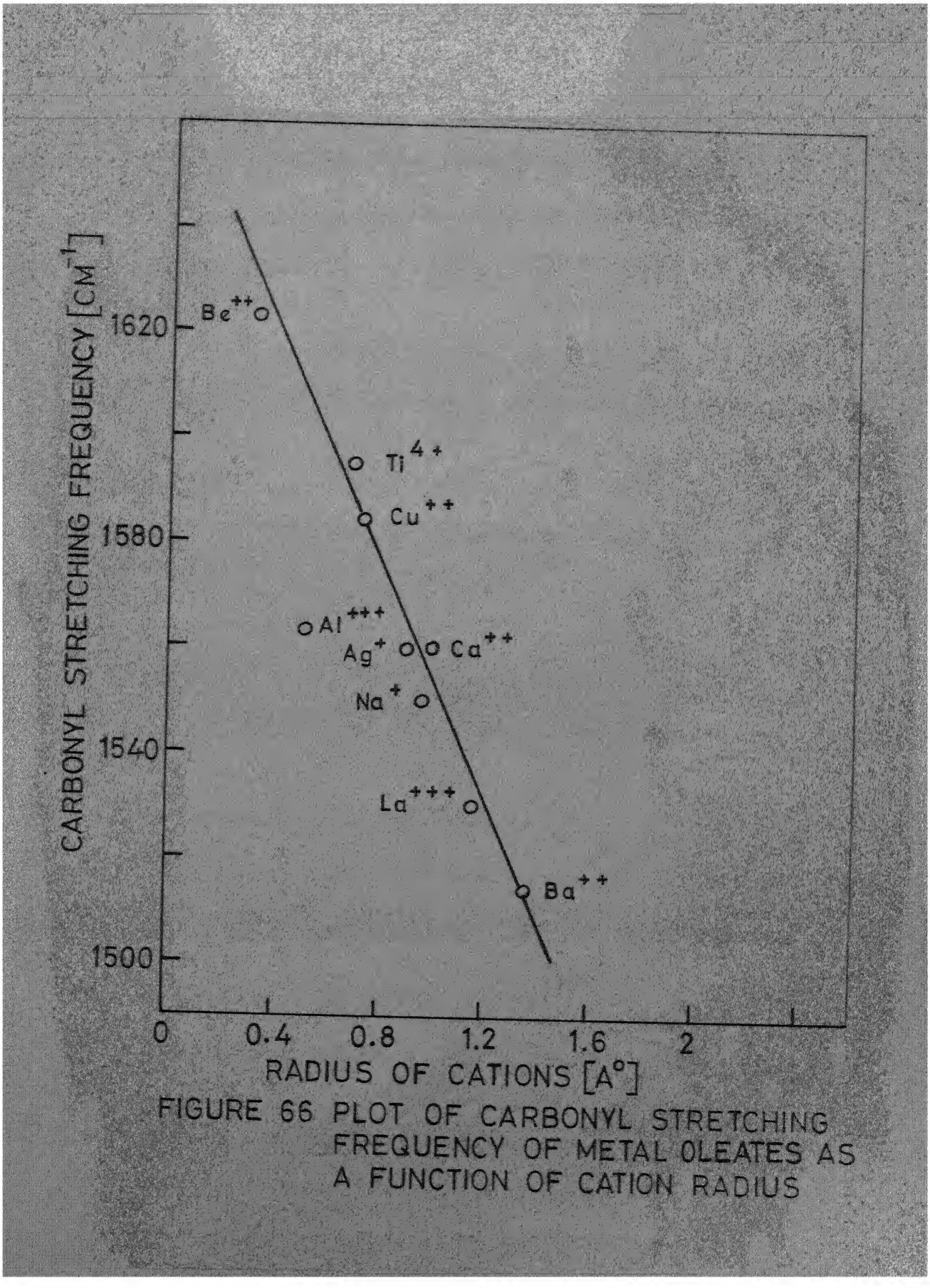

FIGURE 66 PLOT OF CARBONYL STRETCHING FREQUENCY OF METAL OLEATES AS A FUNCTION OF CATION RADIUS

It is aptly proven that sodium oleate is adsorbed on zircon in ionic form. This is evident from the fact that as the oleate ion concentration increases due to pH, adsorption density also increases till OH^- ions begin to play an antagonistic role.

It is seen that oleate ion is negatively charged as also the surface of the zircon in water. Thus, if adsorption were to be due to coulumbic attraction it would be quite negligible. However, it is found to be substantial. Thus coulumbic interaction does not play a major role in causing adsorption of oleate on to the surface of zircon.

Also it is seen from the temperature effect that adsorption is most likely to be physical in nature. I.R. evidence also shows the absence of any chemical species formed on the surface.

Now, according to equation (VI-2) the adsorption of negative species on a negative surface may occur only when the chemical affinity of collector species for surface sites is much higher or there is lateral interaction between the hydrocarbon chains of the van der waal's type so that coulumbic repulsion is overcome. Since i.r. evidence rules out the possibility of any specific chemical compound formation, it is clear that van der waal's interaction between hydrocarbon chains of oleate is mainly responsible for adsorption. The S-type

CHAPTER VIII

DISCUSSION OF RESULTS-III - ZIRCON-SODIUM OLEATE-MODERATOR SYSTEMS

Selective flotation of nonmetallic minerals such as zircon with fatty acid soaps is rather difficult due to the presence of other minerals which also respond favourably to these collectors. Therefore, moderators are always invariably used. Amongst those commonly used for beach sand minerals are the sodium silicate (Na_2SiO_3), sodium fluosilicate (Na_2SiF_6) etc. Due to the inherent affinity of silicon for F^- ions, sodium fluoride or HF have also at times been tried. In the present investigation, Na_2SiO_3, Na_2SiF_6 and NaF have been chosen as moderators and their effects on the soap flotation of zircon have been studied with the help of adsorption and zeta potential measurements.

As a first approach to the problem, it is perhaps worthwhile to go into the aqueous behaviour of these salts.

VIII-1 AQUEOUS BEHAVIOUR OF MODERATORS:

When dissolved in water the inorganic salt dissociates and hydrolyses to yield different ionic species the concentrations of which may vary with pH.

Sodium Fluoride:

When dissolved in water, the sodium fluoride being a moderately strong electrolyte dissociates completely into Na^+ and F^- ions. The fluoride ion in turn may interact with water to yield HF, HF_2^- etc. Hydrofluoric acid is a relatively weak acid with a dissociation constant of about 3.53×10^{-4} at 25^oC (110). The reason for the weak acidic character of HF lies in the very small size of the fluoride ions. At pH values less than pKa value 3.45, the molecular concentration of HF increases rapidly. Since in the present investigations all the measurements reported are in alkaline pH range, F^- ion should be the predominant species. The change in pH due to addition of NaF to sodium oleate solution of 4.93×10^{-4} mole/lit is shown in Fig. 67. It is seen that the pH decreases continuously with increasing NaF addition.

Sodium Silicate:

In addition to its role in promoting selectivity in flotation, sodium silicate is known to be a good flocculating agent. Literature contains many references to several sodium silicates e.g. Na_2SiO_3, $Na_2Si_2O_5$, Na_4SiO_4 etc. The properties of sodium silicates of different varieties depend on the ratio r/p in $pNa_2O.rSiO_2$ where p and r are number of Na_2O and SiO_2 molecules in the silicate. The ratio is known as the 'modulus' of sodium silicate.

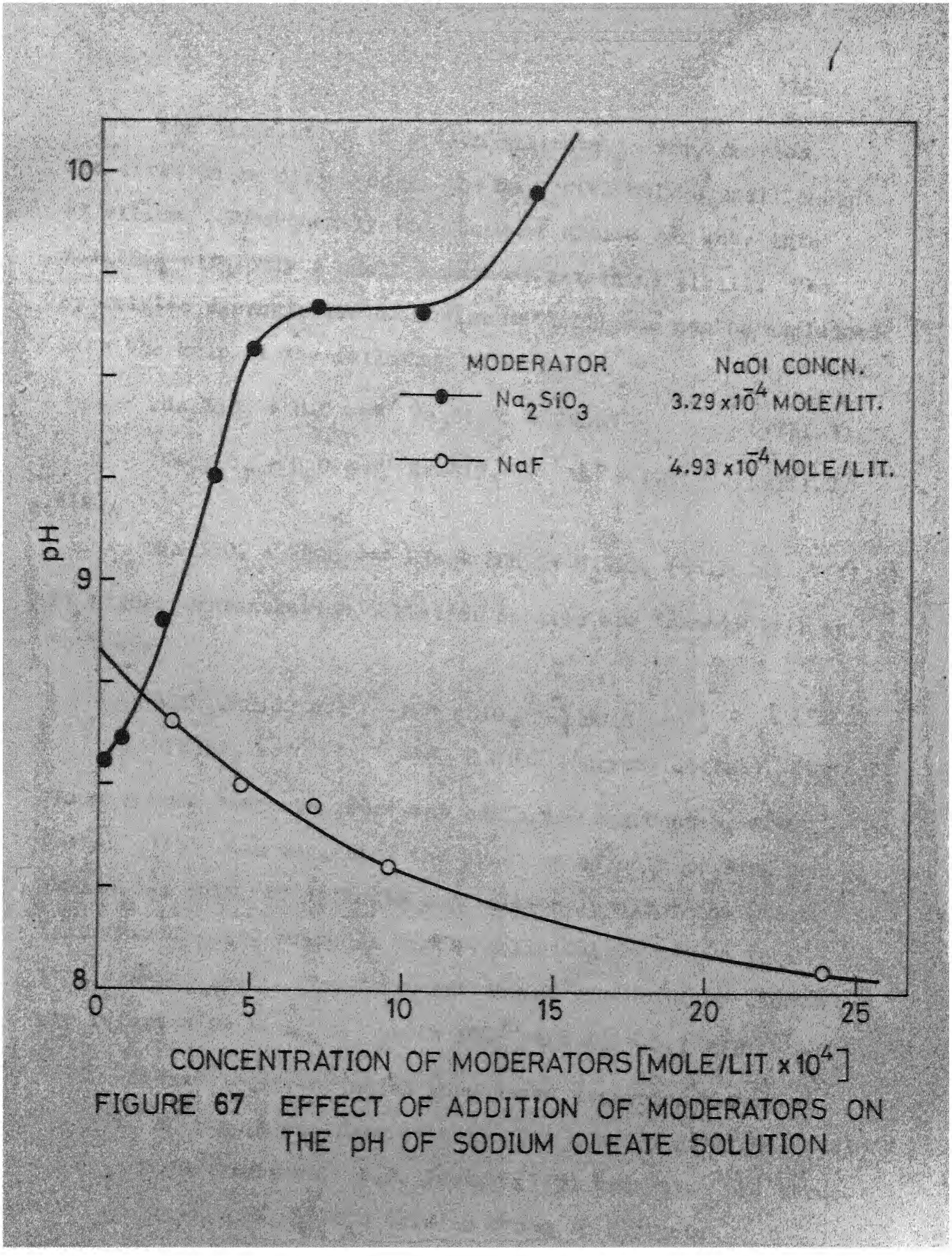

FIGURE 67 EFFECT OF ADDITION OF MODERATORS ON THE pH OF SODIUM OLEATE SOLUTION

The dissolution of sodium silicate is very complex. The first to be dissolved is the Na_2O with only a small amount of silica. Subsequently the residual silica gel goes into solution with only a small amount of remaining alkali. The hydrolytic dissociation of sodium metasilicate can be explained with the help of the following reactions:

$$2Na_2SiO_3 + H_2O \rightleftharpoons Na_2Si_2O_5 + 2NaOH \qquad \text{(VIII.1)}$$

$$Na_2SiO_3 + H_2O \rightleftharpoons NaHSiO_3 + Na^+ + OH^- \qquad \text{(VIII.2)}$$

Also,

$$Na_2SiO_3 + 2HOH \rightleftharpoons 2Na + 2OH^- + H_2SiO_3 \text{ (colloid)} \qquad \text{(VIII.3)}$$

At higher concentration colloidal species are formed (111) as follows:

$$(mSiO_3.nSiO_2\ aq)^{m''} \rightleftharpoons mSiO_3^{''} + [nSiO_2\ aq] \qquad \text{(VIII.4)}$$

$$(nSiO_2\ aq) \rightleftharpoons H_2SiO_3 \text{ (crystalloidal)} \qquad \text{(VIII.5)}$$

where square brackets represent colloidal aggregates. R.W. Harman (112) has suggested the presence of only Na_2SiO_3 and $NaHSiO_3$ as salts of definite composition in dilute solution. This means H_2SiO_3 which is partly colloidal in nature is a true dibasic acid. The first and second dissociation constants are reported to be $K_1 = 4.2 \times 10^{-10}$ and $K_2 = 5.1 \times 10^{-17}$.

Silicic acid, of which some seven varieties have been claimed, exists in the form of colloidal micelle at higher Na_2SiO_3 concentrations. N.P. Peskov (113) has given the structure of micelle of silicic acid as shown in Fig. 68.

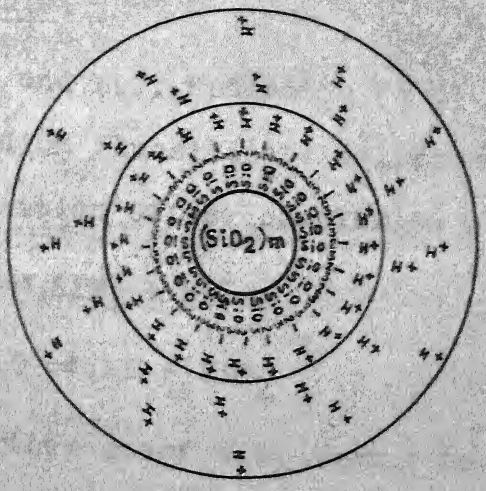

GENERAL FORMULA

$$\left\{(SiO_2)_m, yH_2SiO_3, xSiO_3^{2-}\right\} 2xH^+$$

FIGURE 68 STRUCTURE OF A MICELLE OF SILICIC ACID

The variation of pH due to addition of Na_2SiO_3 to sodium oleate solution is shown in Fig. 67. It is seen that the pH increases first steeply and then remains constant for higher additions of Na_2SiO_3. This is quite understandable in the light of the hydrolysis reactions (VIII.1), (VIII.2) and (VIII.3).

Sodium Fluosilicate:

A.G. Rees and L.J. Hudleston (114) investigated the equilibria in sodium fluosilicate solutions and suggested that the decomposition of the complexion proceeds as follows:

$$SiF_6^{-2} \rightleftharpoons SiF_4 + 2F^- \qquad \text{(VIII.6)}$$

and $$SiF_4 + 2H_2O \rightleftharpoons 4HF + SiO_2 \qquad \text{(VIII.7)}$$

Also SiO_2 may further react with water to give

$$SiO_2 + H_2O \rightleftharpoons H_2SiO_3 \text{ (Colloidal)} \qquad \text{(VIII.8)}$$

Alternatively we may write,

$$SiF_6^{2-} + 2H_2O \rightleftharpoons SiO_2 + 4H^+ + 6F^- \qquad \text{(VIII.9)}$$

I.G. Ryss (115) has given the equilibrium constants of the reactions (VIII.6), (VIII.7) and (VIII.9) as 6.5×10^{-7}, 1.04×10^{-8} and 5.4×10^{-27} respectively. N.T. Crosby (116) has shown that at 20°C the fluosilicate ion is 36 percent dissociated at a concentration of 0.0015 M.

Furthermore SiF_4 formed in aqueous solution may react with HF formed to give H_2SiF_6 as follows:

$$SiF_4 + 2HF \rightleftharpoons H_2SiF_6 \qquad \text{(VIII.10)}$$

Formation of SiF_5^- is also suggested (117),

$$SiF_6^{2-} + H^+ \rightleftharpoons SiF_5^- + HF \qquad \text{(VIII.11)}$$

Thomsen (118) suggests that in excess of silica the acid present is $H_2SiF_6.SiF_4$. Hexafluosilicic acid is a strong acid, slightly stronger than even sulphuric acid, and its structure can be represented by (119),

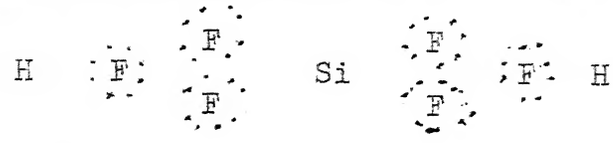

Rees and Hudleston (114) and Cooke and Minski (120) give the equilibrium constant of reaction (VIII.10) as 1.3×10^{-6}. It is a function of fluosilicate concentration and decreases with increase in fluosilicate concentration. It is thus obvious that in aqueous solution fluosilicate reacts to give HF, H_2SiF_6, and H_2SiO_3 which are all acids. Therefore with increasing fluosilicate concentration pH should decrease rapidly. This is shown in Fig. 69, which describes the sodium oleate-sodium fluosilicate system.

VIII-2 ROLE OF SODIUM FLUORIDE AS A MODERATOR:

Having discussed the aqueous chemistry of the moderators employed in the present investigations, we proceed on to the discussion of the effect of moderators on flotation, adsorption and zeta potential of zircon.

The adsorption isotherm for NaF without any sodium oleate addition has been given in Fig. 19. Corresponding zeta potential

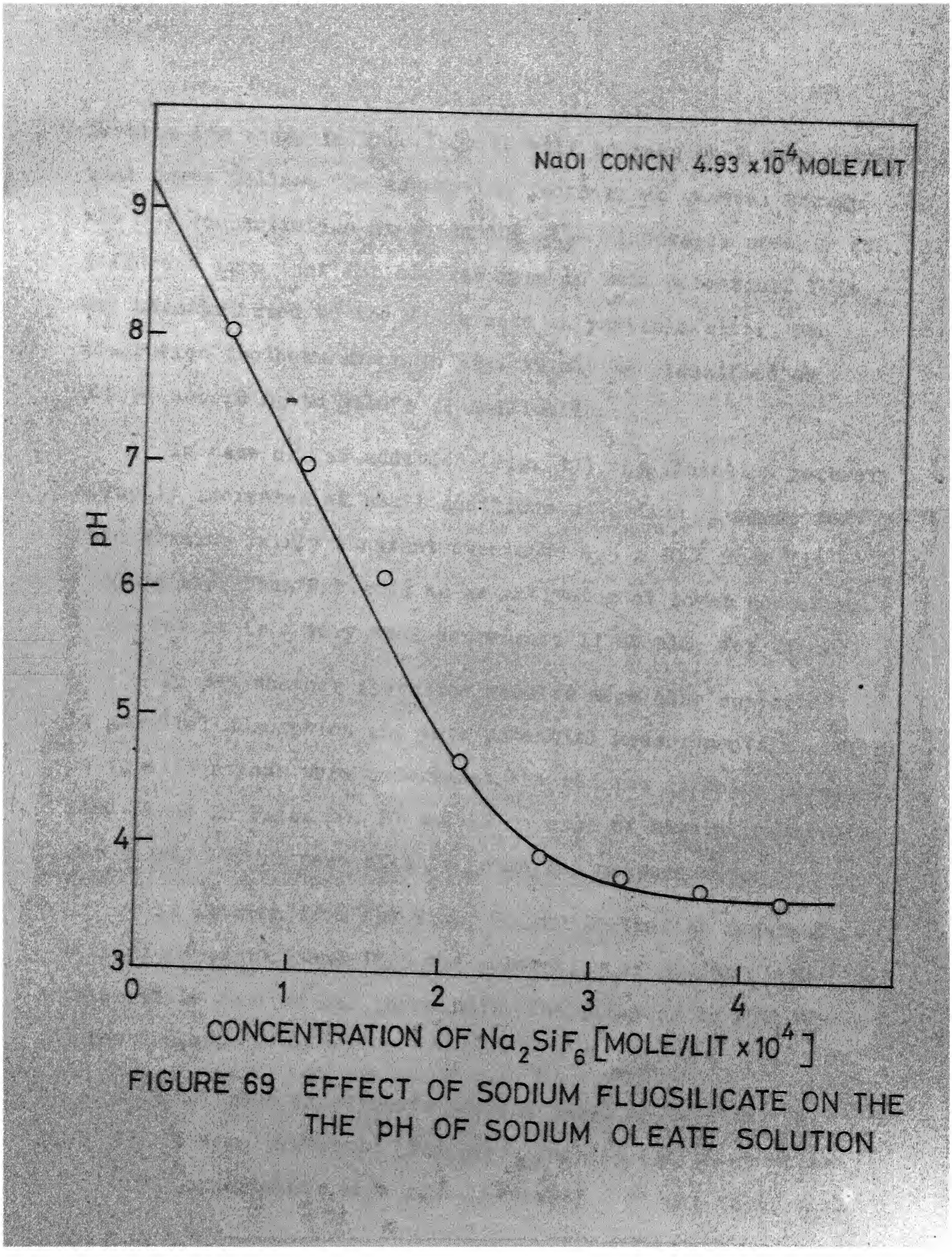

FIGURE 69 EFFECT OF SODIUM FLUOSILICATE ON THE THE pH OF SODIUM OLEATE SOLUTION

results are shown in Fig. 32. It will be seen that zeta potential curve follows the adsorption isotherm in general though the NaF concentration at which the Γ_{F^-} increases steeply is different from that for similar rise in zeta potential. This may be attributed to the difference in particle size. The adsorption isotherm shown in Fig. 19 may be classified as S-type according to Gile's classification.

In case of NaF addition (Fig. 11) the flotation recovery abruptly increases at small additions of sodium fluoride and then remains fairly constant even upto 8.5×10^{-3} mole/lit (350 mg/l). Thus NaF acts as an activator at lower concentrations but it is a very weak depressor, if at all, for zircon.

To see whether flotation results were also supported by parallel adsorption and zeta potential measurements a series of investigations were undertaken the results of which already find place in Figs. 20, 21 and 22 in case of adsorption studies and in Fig. 37 in case of zeta potential measurements.

It is seen from the Figs. 20 and 21 that at constant initial pH of 10.3 and 10.5 the adsorption of sodium oleate falls while that of NaF increased. The final pH in both the cases varied.

Also, some experiments keeping final pH constant at 9.7 ± 0.15 were performed (Fig.22). This is the pH at which flotation experiments were also performed. It was found that

sodium oleate adsorption first increases and then falls at higher concentrations of sodium fluoride. Thus, the initial activation can be attributed to the increased oleate adsorption. However, the depression expected at higher NaF additions is not distinctly visible even at higher concentrations of sodium fluoride.

Zeta potential experiments conducted at final pH 9.7 and initial pH 9.0 (Fig. 37) show that at final pH 9.7 the negative zeta potential increases briskly. The results at initial pH 9 show that the negative zeta potential first increases numerically then remains substantially constant for comparatively large additions of NaF and then seems to take off at still larger additions of NaF.

This is quite understandable in terms of the adsorption behaviour already reported (Fig. 22). At final pH 9.7 and with smaller additions of NaF, both Γ_{NaF} and Γ_{Ol^-} increase thus increasing the negative zeta potential numerically. After certain concentration of the NaF, though the adsorption of sodium oleate decreases, that of NaF rises steeply more than compensating for the decrease due to less sodium oleate adsorption.

Similarly, at initial pH 9, the zeta potential variation with NaF addition is explicable from the adsorption pattern reported in Figs. 20 and 21 for initial pH values 10.3 and 10.5 respectively. Though there is a difference between the pH

for the adsorption and zeta potential measurements the trend is expected to be the same as both lie in the alkaline range. It is observed from the adsorption curves that as the NaF concentration is increased Γ_{Ol} seems to slightly increase initially before it gradually falls while $_{NaF}$ first gradually increases and then steeply. It will be shortly shown that over a range of NaF concentration ($\Gamma_{Ol-} + \Gamma_{F-}$) remains constant. Now the negative zeta potential in Fig. 37 for pH 9, first increases somewhat and then remains constant upto certain concentration of NaF. This initial increase is due to the adsorption of NaF and slight initial increase in Γ_{Ol}. The constant portion arises due to constancy of ($\Gamma_{Ol-} + \Gamma_{F-}$) and the final steep rise at higher additions of NaF is due to steep rise in Γ_{F-} as compared to the decrease in Γ_{Ol-} value.

It is also to be noted that the type of adsorption pattern for sodium fluoride remains the same even in the presence of sodium oleate.

To know the mechanism of NaF action in decreasing the scdium oleate adsorption on zircon the sum ($\Gamma_{Ol-} + \Gamma_{F-}$) was calculated for various sodium fluoride concentrations as shown below in Table III and plotted in Fig. 70.

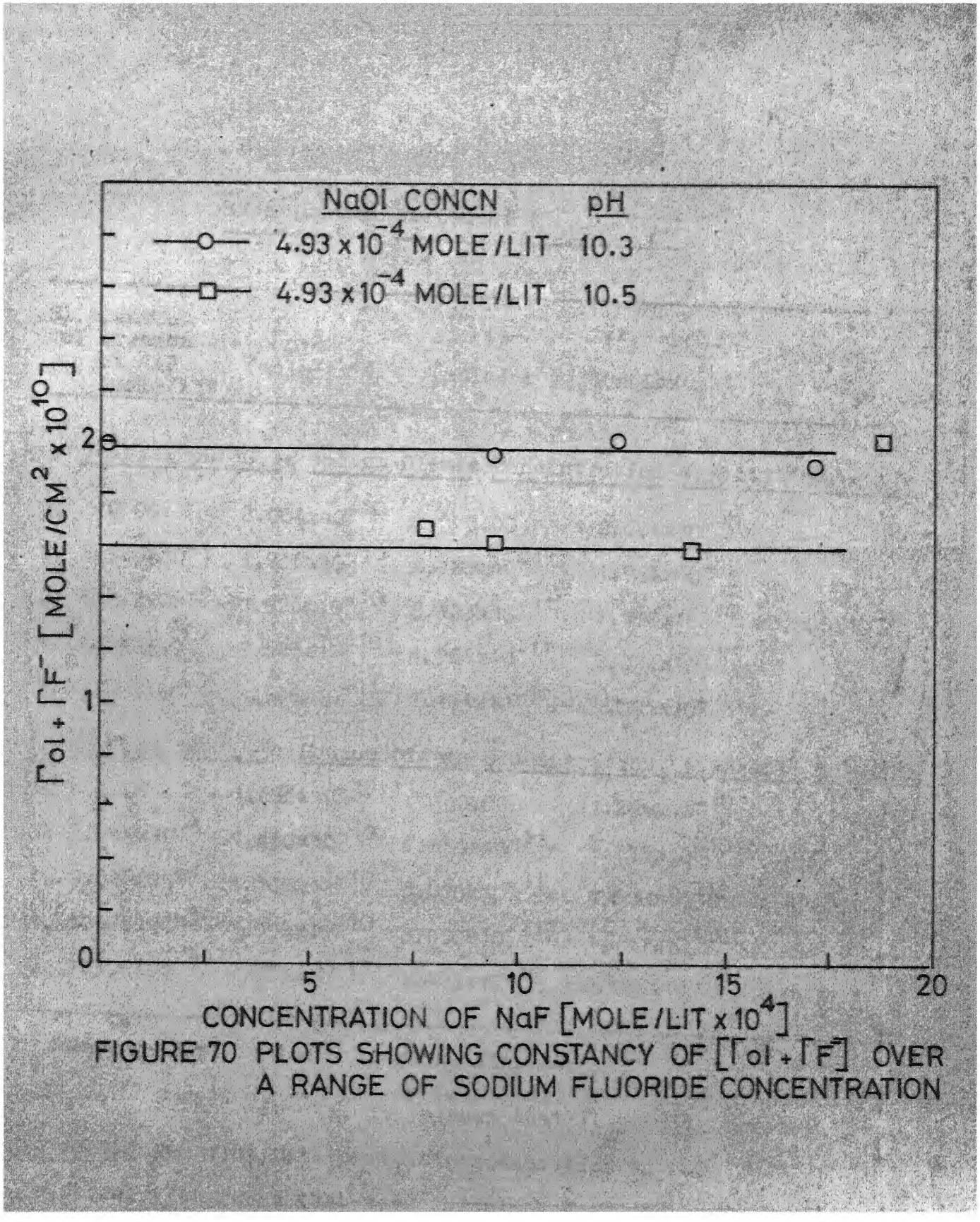

FIGURE 70 PLOTS SHOWING CONSTANCY OF [$\Gamma_{OI} + \Gamma_{F^-}$] OVER A RANGE OF SODIUM FLUORIDE CONCENTRATION

Table III

Experimental Values of $(\Gamma_{Ol^-} + \Gamma_{F^-})$

Sl. No.	Concentration of NaF (mole/lit)	Γ_{Ol} (mole/cm^2)	Γ_{F^-} (mole/cm^2)	$\Gamma_{Ol} + \Gamma_{F^-}$ (mole/cm^2)	Average $\Gamma_{Ol} + \Gamma_{F^-}$
	Initial pH 10.3: Sodium Oleate Concentration 4.93×10^{-4} mole/lit				
1.	0.00	2.004×10^{-10}	0.00	2.004×10^{-10}	
2.	9.526×10^{-4}	1.736×10^{-10}	2.185×10^{-11}	1.954×10^{-10}	
3.	4.762×10^{-4}	1.926×10^{-10}	2.123×10^{-11}	2.138×10^{-10}	2.005×10^{-10}
4.	1.191×10^{-3}	1.525×10^{-10}	4.986×10^{-11}	2.024×10^{-10}	
5.	1.666×10^{-3}	7.308×10^{-11}	1.174×10^{-10}	1.905×10^{-10}	
	Initial pH 10.5: Sodium Oleate Concentration. 4.93×10^{-4} mole/lit				
6.	0.00	1.296×10^{-10}	0.00	1.296×10^{-10}	
7.	7.145×10^{-4}	1.450×10^{-10}	2.250×10^{-11}*	1.675×10^{-10}	
8.	9.526×10^{-4}	1.308×10^{-10}	3.000×10^{-11}*	1.608×10^{-10}	1.628×10^{-10}
9.	1.429×10^{-3}	1.096×10^{-10}	5.050×10^{-11}*	1.601×10^{-10}	
10.	1.905×10^{-3}	6.223×10^{-11}	1.423×10^{-10}	2.045×10^{-10}	

* These values are taken from the Fig. 21.

From Table III, it is seen that $\Gamma_{Ol^-} + \Gamma_{F^-}$ remains fairly constant upto certain concentration of NaF. This strongly suggests that upto certain NaF addition, both oleate

ion and fluoride ions compete for the common surface sites and an ion exchange type mechanism can be suggested as follows:

$$M] - Ol^- + F^- \rightleftharpoons M] - F^- + Ol^-.$$

At higher concentrations, however, the F^- ions seek additional surface sites.

The initial activation is common to all the moderators and discussed in a separate section.

VIII-3 ACTION OF SODIUM SILICATE AS A MODERATOR:

It is seen from the flotation experiments (Fig. 12) that at lower concentrations of Na_2SiO_3 distinct activation effect is observed, while at higher concentration usual depression takes place. Na_2SiO_3 seems to be a very good depressor for zircon.

To study the modulating action, adsorption of sodium silicate was studied. The isotherm given in Fig. 23, shows that adsorption first briskly increases then seems to remain constant for a while till it again takes off at higher Na_2SiO_3 additions. According to Giles classification the isotherm is of L-type.

The corresponding zeta potential (Fig. 33) however does not closely follow the adsorption pattern. It first increases and at around 1.2×10^{-3} mole/lit. of Na_2SiO_3 seems to decrease.

The adsorption of sodium silicate and sodium oleate from the solution containing both is shown in Figs. 24 to 26. At pH around initial pH 9, though sodium silicate adsorption continuously increases with sodium silicate addition then remains constant before increasing steeply, the sodium oleate concentration at first sluggishly decreases and then falls rather steeply. However at higher pH around 9.9 - 10.00 the decrease in sodium oleate adsorption is rather steep.

If the final pH is kept constant and adsorption values obtained then we get the behaviour as depicted in Figs. 27 and 28. It will be seen that the oleate adsorption first increases with small additions of Na_2SiO_3 then decreases and almost remains constant, whereas the $\Gamma_{Na_2SiO_3}$ first increases rapidly and then tends to level off. Corresponding zeta potential measurements also indicate an initial rise in the numerical value of zeta potential before it comes down and remains constant (Fig. 38). The initial rise in flotation activity may thus be attributed to increased adsorption of Na oleate at small additions of Na_2SiO_3.

This correlation is more vividly brought out in Fig.71 where the flotation recovery, zeta potential and adsorption density of sodium oleate on zircon are plotted as a function of Na_2SiO_3 concentration. In view of the different particle sizes involved in each type of measurement the correlation is remarkable. This again proves that the two phase solid-liquid interfacial parameters are closely correlative.

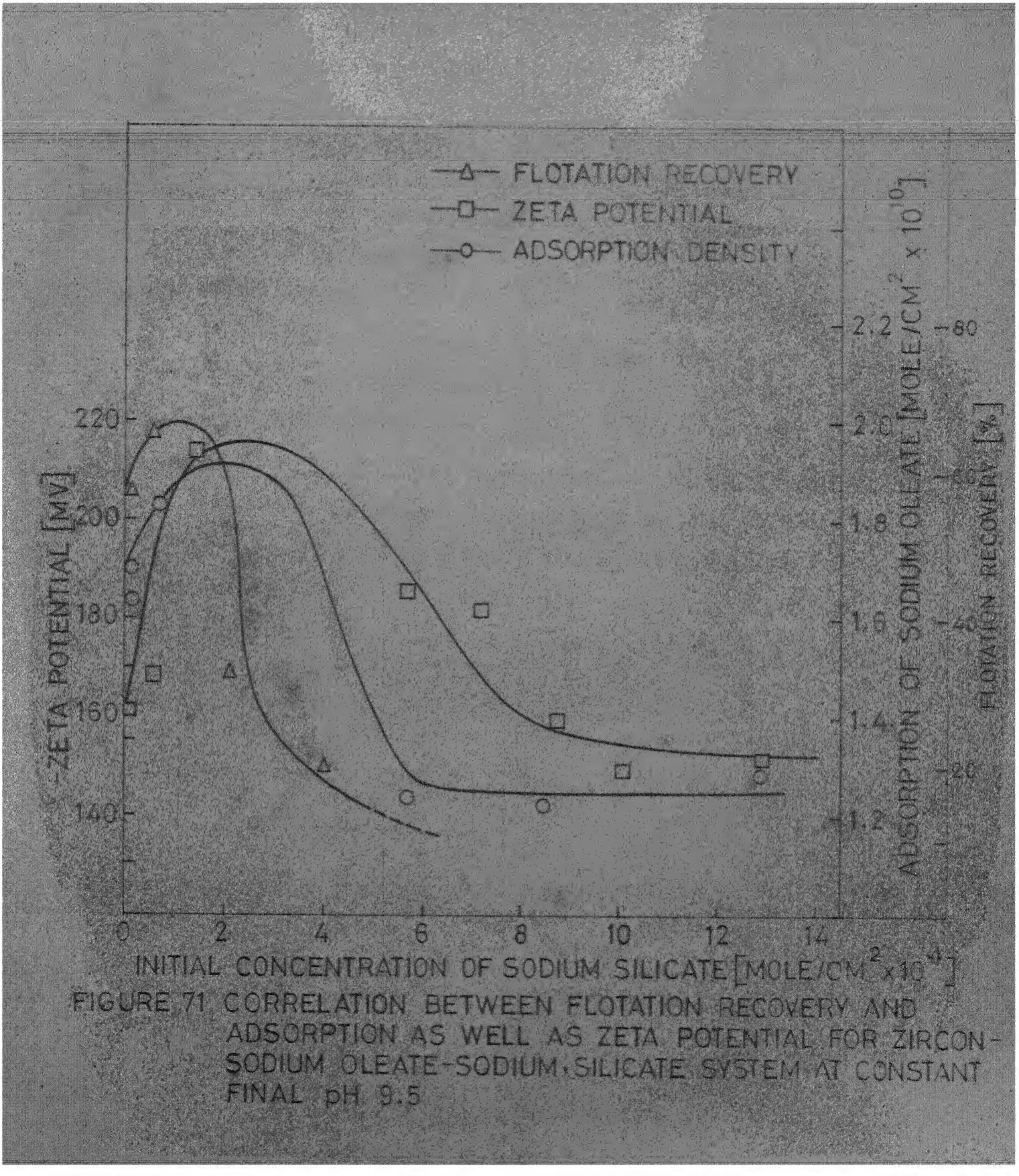

FIGURE 71 CORRELATION BETWEEN FLOTATION RECOVERY AND ADSORPTION AS WELL AS ZETA POTENTIAL FOR ZIRCON-SODIUM OLEATE-SODIUM SILICATE SYSTEM AT CONSTANT FINAL pH 9.5

In Fig.71(a), the zeta potential, and the sum ($\Gamma_{Ol}+\Gamma_{Na_2SiO_3}$) are plotted to emphasise the fact that the zeta potential curves follow the Γ_{Ol} curve and not the (Γ_{Ol} + $\Gamma_{Na_2SiO_3}$) curve. This clearly indicates that there is negligible contribution of the ionic species derived from Na_2SiO_3 hydrolysis to the numerical magnitude of the negative zeta potential. This strongly suggests that neutral H_2SiO_3 is the species that is adsorbed predominantly. At lower concentrations, H_2SiO_3 is expected to be present in separate molecular form. Thus at lower concentrations of Na_2SiO_3 such as the one studied, there would not be any substantial contributions due to Na_2SiO_3. The adsorption of $SiO_3^=$ and $HSiO_3^-$ species, if any, is expected to be marginal.

This can also be seen from the relative abundances of the species H_2SiO_3, $HSiO_3^-$ and $SiO_3^=$ in the pH range 9-10.

From the equations

$$H_2SiO_3 \rightleftharpoons HSiO_3^- + H^=$$

and $$HSiO_3^- \rightleftharpoons SiO_3^= + H^+$$

We have the corresponding equilibrium relationships as

$$\frac{[HSiO_3^-]\,[H^+]}{[H_2SiO_3]} = 10^{-10} \qquad \text{(VIII.12)}$$

$$\frac{[SiO_3^=]\,[H^+]}{[HSiO_3^-]} = 10^{-12} \qquad \text{(VIII.13)}$$

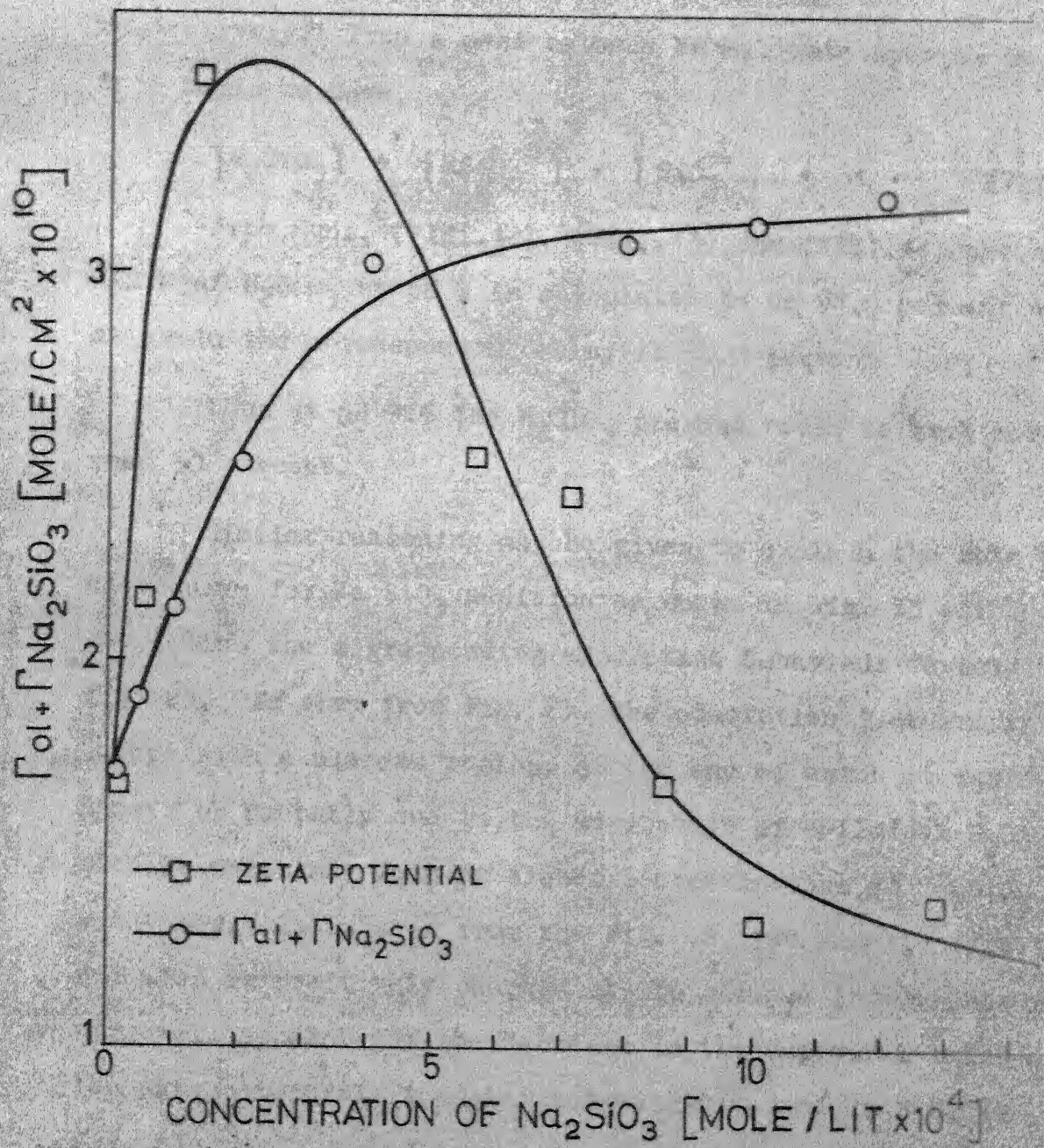

FIGURE 71(a) COMRARISON OF ZETA POTENTIAL BEHAVIOUR AND $\Gamma_{ol} + \Gamma_{Na_2SiO_3}$ VARIATION AS A FUNCTION OF SILICATE CONCENTRATION AT FINAL pH 9.5

NaOl CONC 4.93×10^{-4} MOLE /LIT

respectively. From a mass balance on silicate species on one mole basis we have,

$$[H_2SiO_3] + [HSiO_3^-] + [SiO_3^{=}] = 1 \qquad \text{(VIII.14)}$$

From Eqns. (VIII.12), (VIII.13) and (VIII.14) the abundance of H_2SiO_3 at pH 9 is calculated to be 91.0 percent while at pH 10 the corresponding value is 50.0 percent.

Thus at pH 9.5 the H_2SiO_3 present would be much more than 50 percent.

Similar reasoning may be given to explain the zeta potential curve for Na_2SiO_3 addition as shown in Fig. 33 which does not follow the corresponding adsorption behaviour depicted in Fig. 23. As seen from Fig. 23, the adsorption isotherm is of L-type with a plateau region, at the end of which it again shoots up probably due to the adsorption of colloidal H_2SiO_3 micelle which may form at higher concentrations of Na_2SiO_3 solutions. As is seen from the Fig. 68, the micelle of silicic acid is positively charged at its surface (126). This may very well account for the decrease in the numerical value of the zeta potential at higher concentrations of Na_2SiO_3 in Fig. 33.

In case of Na_2SiO_3, again, the mechanism of depression seems to be based on the competition of oleate and H_2SiO_3 for the common surface sites. Therefore, the sum $(\Gamma_{Ol} + \Gamma_{Na_2SiO_3})$ should remain constant over a range (See Table IV) of Na_2SiO_3

addition. This has been found out to be the case as shown below and depicted in Fig. 72.

Table IV

Experimental Values of ($\Gamma_{Ol^-} + \Gamma_{Na_2SiO_3}$)

Sl. No.	Concentration of Na_2SiO_3 (mole/lit)	Γ_{Ol^-} (mole/cm^2)	$\Gamma_{Na_2SiO_3}$ (mole/cm^2)	$\Gamma_{Ol^-} + \Gamma_{Na_2SiO_3}$ (mole/cm^2)	Average value ($\Gamma_{Ol^-} + \Gamma_{Na_2SiO_3}$)
Initial pH 10: NaOl Concentration: 4.93×10^{-4} mole/lit.					
1.	0.00	2.004×10^{-10}	0.00	2.004×10^{-10}	
2.	2.142×10^{-10}	1.857×10^{-10}	1.013×10^{-10}	2.870×10^{-10}	
3.	3.572×10^{-4}	1.339×10^{-10}	1.554×10^{-10}	2.893×10^{-10}	2.876×10^{-10}
4.	4.285×10^{-4}	1.050×10^{-10}	1.700×10^{-10}*	2.750×10^{-10}	
5.	5.714×10^{-4}	1.242×10^{-10}	1.750×10^{-10}*	2.992×10^{-10}	
6.	7.142×10^{-4}	9.632×10^{-11}	2.052×10^{-10}	3.015×10^{-10}	
Initial pH 9: NaOl Concentration: 3.29×10^{-4} mole/lit.					
7.	0.00	1.192×10^{-10}	0.00	1.249×10^{-10}	
8.	7.142×10^{-5}	8.966×10^{-11}	3.806×10^{-11}	1.277×10^{-10}	
9.	2.142×10^{-4}	1.113×10^{-10}	3.442×10^{-11}	1.456×10^{-10}	1.319×10^{-10}
10.	3.572×10^{-4}	1.009×10^{-10}	3.403×10^{-11}	1.349×10^{-10}	
11.	4.999×10^{-4}	1.034×10^{-10}	2.246×10^{-11}	1.259×10^{-10}	
12.	7.142×10^{-4}	1.155×10^{-10}	8.078×10^{-11}	1.963×10^{-10}	

contd...

Contd...

Sl. No.	Na_2SiO_3 Concentration	Ol Initial pH 9.95	Na_2SiO_3 NaOl Concentration	Ol + Na_2SiO_3 3.289×10^{-4} mole/lit
13.	0.00	1.192×10^{-10}	0.00	1.192×10^{-10}
14.	7.142×10^{-5}	1.058×10^{-11}	5.234×10^{-12}	1.11×10^{-10}
15.	2.142×10^{-4}	7.925×10^{-11}	1.521×10^{-11}	9.446×10^{-11}
16.	3.572×10^{-4}	1.093×10^{-10}	4.088×10^{-11}	1.502×10^{-10}
17.	4.999×10^{-4}	3.844×10^{-11}	5.776×10^{-11}	9.620×10^{-11}
18.	1.071×10^{-3}	9.387×10^{-12}	8.322×10^{-11}	9.361×10^{-11}

Activation phenomenon would be discussed in the Section VIII-5.

VIII-4 MODULATING ACTION OF SODIUM FLUOSILICATE:

Sodium fluosilicate as also hydrofluosilicate acid (H_2SiF_6) act as good depressors for zircon flotation with sodium oleate as the collector. According to I.N. Plaksin's work (42-46) Na_2SiF_6 is an effective regulator for the selective flotation of the titano-zirconium sand by the aerated emulsion of the oleic acid. Whereas the titanium mineral is not affected due to soluble complexes formed, the zircon gets efficiently depressed since complexes formed with zirconium are insoluble. The present investigations with Na_2SiF_6 show an initial activation with small additions (Fig. 13). This type

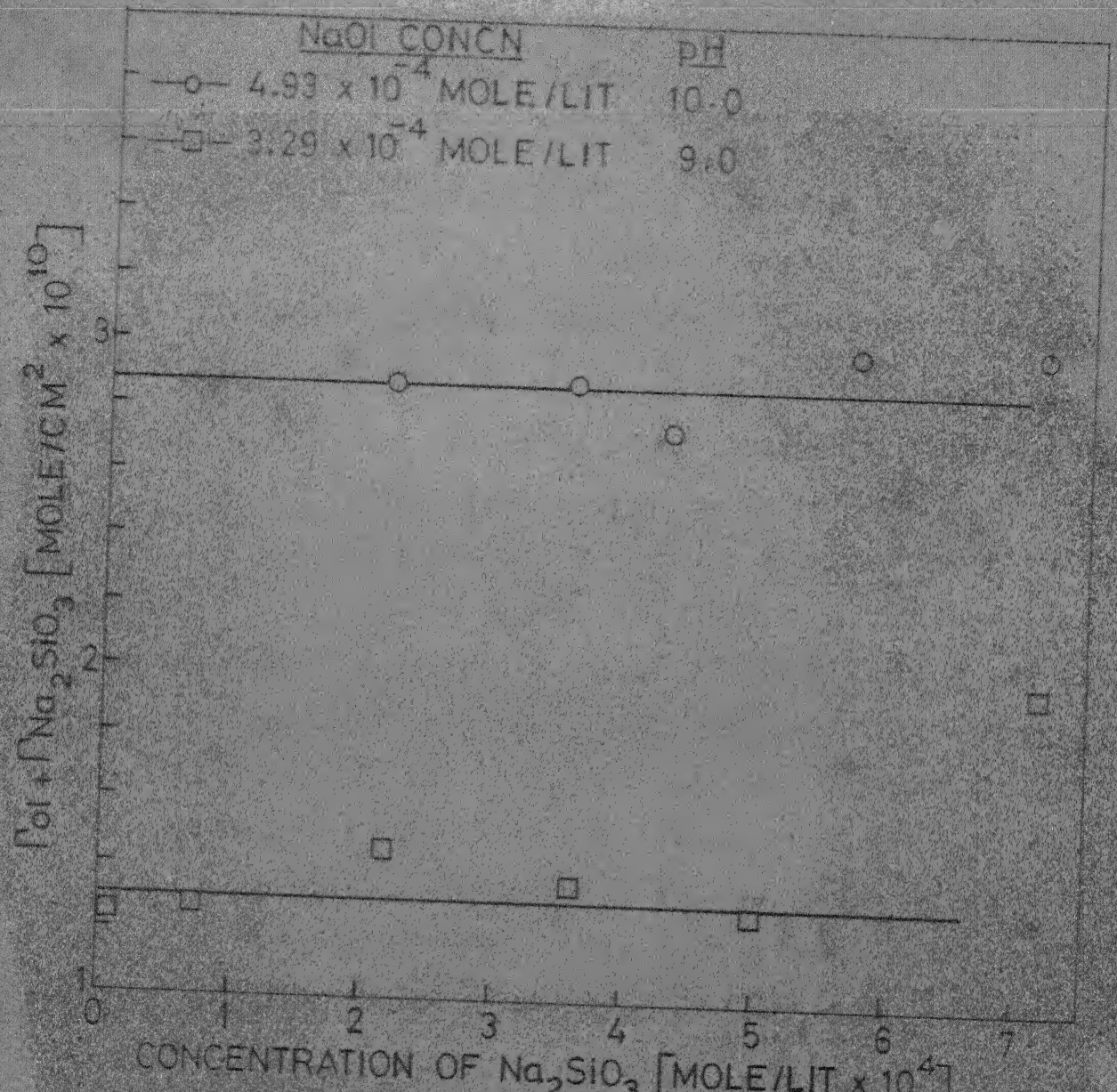

FIGURE 72 PLOTS SHOWING CONSTANCY OF $(\Gamma_{OI}+\Gamma_{Na_2SiO_3})$ OVER A RANGE OF Na_2SiO_3 CONCENTRATION

of initial activation is not only peculiar to zircon but other oxygen bearing minerals such as ilmenite ($FeTiO_3$) and monazite ($Ce\ Dy\ (PO_4)_3$) minerals also as seen from Figs. 14 and 15.

Zeta potential measurements with Na_2SiF_6 and Na oleate at constant final pH values also show that there is an initial increase in numerical value of negative zeta potential followed by almost constant values at higher Na_2SiF_6 additions (Fig.39).

Sodium oleate adsorption on zircon in presence of varying amounts of Na_2SiF_6 in solution and constant initial pH 9.0 were determined (vide Fig. 29). The adsorption data for fluosilicate on the mineral were not very reproducible due to the difficulty in estimating silicon and fluorine in the solution in presence of each other. The main difficulty lies in efficiently separating the Si and F^- before individually estimating them. From Fig. 29, it is observed that Γ_{01} rapidly decreases with increasing Na_2SiF_6 additions. It is proposed* that Na_2SiF_6 gives rise to H_2SiO_3 and F^- ions according to reactions VIII.6 and VIII.10. At 20°, for the Na_2SiF_6 concentration $SiF_6^=$ is reported (116) to be dissociated to the extent of 87 percent according to the equations VIII.6, VIII.7, and VIII.8.

---

* Though no value of $\Gamma_{Si^{4+}}$ and Γ_{F^-} are being reported because of the lack of sufficient reproducibility, a few qualitative observations support the above contention about H_2SiO_3 being the active depressing species. For example, it was observed that after adsorption, the supernatent liquid contained different proportions of Si^{4+} and F^- concentrations depending on the Na_2SiF_6 added. It was observed that as the Na_2SiF_6 concentration increased the ratio $[F^-]/[Si^{4+}]$ also increased in the supernatent liquid. This suggests that $SiF_6^=$ is not the sole species adsorbing. As is proposed, it is highly likely that it dissociates to give F^- and H_2SiO_3 and the latter then adsorbs in preference to F^- ions on the surface thus increasing the above ratio in the supernatent liquid.

Thus, H_2SiO_3 preferentially gets adsorbed on zircon as compared to fluoride and causes depression. Thus, it may be postulated that mechanism of depression mainly rests on formation and preferential adsorption of H_2SiO_3, since F^- even if adsorbed, has been found to be a poor depressor according to our investigations with NaF.

VIII-5 ACTIVATION OF FLOTATION AT SMALL ADDITIONS OF MODERATORS:

It has been stated in the previous sections that small additions of moderators activate flotation.This has been further confirmed by the parallel adsorption and zeta potential measurements which show increased sodium oleate adsorption.

Following aspects regarding this should be carefully noted.

1) Activation is caused by the moderators NaF, Na_2SiF_6 and Na_2SiO_3 and is not peculiar of any one of them.

2) Not only zircon but ilmenite and monazite also exhibit this behaviour.

3) There is a parallel increase in the adsorption density of Na oleate. However, this is evident only when the final pH is kept constant.

4) Zeta potential also shows more negative values in the activation range.

Besides, it will be worthwhile to note some other examples available in the literature.

Work done by M.A. Eigels (121) and Mokrousov (122) showed that sodium silicate in small quantity activates the flotation recovery of fluorite.

I.N. Shorsher (123) observed the activation by sodium silicate in case of carbonate minerals cerussite, malachite etc. The collector used was isoamyl xanthate. Similarly Beloglazov et.al. (124) noticed it in case of apatite flotation by oleic acid using Na_2SiO_3 as modifier. A.E. Zakharov et. al. (125) have studied the reaction of sodium sulfide on pyrochlore, zircon and monazite. They found that Na_2S addition upto 25 mg/l activates flotation while larger doses drastically decrease it.

Thus it is clear that the activation observed is quite a general phenomenon with oxygen bearing minerals. It has been generally observed with NaF, Na_2SiF_6, Na_2SiO_3, Na_2S used as modifiers, and xanthate as well as fatty acid used as collectors. Thus any explanation of the phenomenon should be general in nature.

Activating action of Na_2SiO_3 has been variously explained as being due to (126),

i) Improvement in the froth,

ii) Peptisation of the fine slimes,

iii) Change in the pH of the medium,

iv) Na_2SiO_3 removes 'unavoidable ions' responsible for combining with collectors into less active form. None of these explanations seem to be convincing.

Froth stability alone cannot explain enhanced flotation which distinctly involves increased oleate adsorption in the solid-liquid interface. Besides, single bubble flotation experiments (126) in which froth stability is not crucial have also shown activation effect.

Peptisation of fine slimes also appears to be untenable as the exclusive mechanism. In adsorption and electrokinetic measurements, it does not come into the picture. Secondly, the flotation samples of zircon, monazite and ilmenite contained absolutely no fines and yet showed activation. Thirdly, except Na_2SiO_3, no other moderator is known to be a peptising reagent.

Change in pH may definitely change recovery. Hence experiments were performed by keeping final pH constant. If instead initial pH is kept constant, then final pH varies and equilibrium condition does not remain constant as regards pH. Probably this is the reason why at initial constant pH values, the increased adsorption of oleate is not observed. The fact that it is observed only when final pH is kept constant rules out the pH charge as a factor underlying the phenomenon.

The fourth explanation viz., moderator combining with ions which otherwise react with collector to form less active forms also seems to be unlikely in the light of the fact that all the moderators varying in chemical nature may not be expected to behave similarly.

It is obvious that the increased flotation activity is due to increased oleate adsorption. Now, the question is, as to what enhances adsorption at lower additions of the moderator. According to Stern-Grahame treatment of the double layer (Section VI-1) the adsorption density n_i is a function of the concentration of the species i, its radius, and adsorption potential as given by the equation VI.1 which is reproduced here.

$$n_i = 2 r_i n_o \exp(- W_\delta/RT) \qquad (VI.1)$$

where,

$$W_\delta = ZF\Psi_\delta + w_1 + w_2$$

The work of adsorption W_δ comprises of three terms. The first is due to the coulumbic attraction. The second is due to the chemical affinity between solute and the solid surface, and the third is due to the van der waal's interaction between collector molecules.

It has been already shown in Chapter VII that sodium oleate adsorption on zircon is due to van der waals interaction between the hydrocarbon chains. Now, the zircon surface is negatively charged, and therefore, electrostatic interaction

term is most favourable for positively charged ions like Na^+ ions in the systems under study. On the other hand, it is unfavorable for negatively charged ions like F^-, Ol^-, $SiO_3^=$ and $SiF_6^=$ if present. However, it does not matter for oleate adsorbing through van der waal's interaction which is sufficient to over come electrostatic repulsion term. The presence of sodium ions in between the oleate ions decreases the repulsion between their similarly charged ionic heads. This induces greater adsorption of oleate ions on the mineral surface and enhanced flotation recovery.

At higher concentrations of the moderators however the appropriate depressor anionic species manage to adsorb more and more, and thus depression is observed. This is evident from actual adsorption values.

To summarise, (1) the presence of Na^+ ions at the surface causing reduction in the repulsive interaction of ionic heads of the oleate chains and (2) van der waal's type adsorption of the oleate chains augment the flotation recovery. The results indicate the need of measuring adsorption of Na^+ ions on minerals to check the above postulate regarding activation by the sodium salt modifiers. This is a fit subject for future experimentation.

CHAPTER IX

CONCLUSIONS

In this last chapter, the conclusions emerging out of the present investigations will be summarised.

It is observed that in case of the electrokinetic behaviour of zircon in aqueous solutions of KCl, zeta potential of zircon remains negative in alkaline as well as acidic pH range. Thus it is not possible to locate the zero point of charge (zpc). The unusual behaviour observed in the acidic pH range where zeta potential would be normally expected to be positive, has been explained on the basis of the preferential dissolution of Zr^{4+} ions from the surface into the solution and specific adsorption of Cl^- ions as well as some negatively charged hydroxychlorocomplexes.

At higher pH values the zeta potential curves for different KCl concentrations merge into the line obtained without any KCl addition at appropriate points. Thus, in higher alkaline range, OH^- ions are the sole potential determining species.

The adsorption isotherm of sodium oleate on zircon was classified as S-type according to Gile's scheme.

It has been concluded on the basis of the nature of the adsorption isotherm for sodium oleate, effect of temperature on adsorption and the infrared evidences that the adsorption is

mainly due to the van der waal's attractive forces between the hydrocarbon chains of the collector.and physical in nature.

The active adsorbing species is the oleate ion. The magnitude of Γ_{Ol^-} is solely dependent on the ionic oleate concentration $[Ol^-]$ which is a function of pH in the lower pH range. The magnitude of this concentration is governed by the hydrolytic dissociation of the sodium oleate at any pH in this range.

In alkaline range, hydroxyl ions act as competitors to oleate ions and thus affect the magnitude of Γ_{Ol^-} predominantly.

A quantitative relationship characterising the pH dependence of Γ_{Ol} has been proposed as,

$$\Gamma_{Ol} = [Ol^-]_s = \left(\frac{S K_h K_w}{k_3(K_h[H^+] + K_w) + S K_h K_w k_4} \right) - \left(\Gamma_m - \frac{S [H^+]}{K_c + f [H^+]} \right)$$

It has been shown that Γ_{Ol} values calculated from the above equation agree well with the experimentally determined values.

Similarly, on the basis of a semi-empirical treatment an equation to quantitatively describe the pH-dependence of flotation activity is found out to be,

$$R_i/R_o = a_f = 1 - \left[d^c \left(\frac{1}{1 + \frac{K_w}{K_b[H^+]} + \frac{K_a K_w}{K_b [H^+]^2}} \right) + d^k \left(\frac{1}{1 + \frac{[H^+]}{K_a} + \frac{K_b [H^+]^2}{K_a K_w}} \right) \right]$$

It has been shown that from the above equation, the Barsky[5]'s law, which characterises the critical contact phenomena, can be derived. The Barsky slope thus calculated was found out to be 0.73 which agrees quite well with the experimentally determined slope of 0.675.

The correlation between the flotation recovery and adsorption as well as zeta potential in the zircon-sodium oleate system was brought out with the help of superposition of the curves showing their variation with sodium oleate concentration and pH on one single diagram. It is observed from these diagrams that the two phase solid-liquid interfacial parameters e.g. zeta potential and adsorption density are in general correlative with flotation. This is quite expected in view of the fact that Γ_{Ol^-} governs both zeta potential and flotation recovery if pH is kept constant. However, in each type of measurement the particle size was different and hence exact correlation is some what obscured. This is evidenced by the absence of single straight line relationship when correlation diagrams between flotation recovery and Γ_{Ol} as well as zeta potential and Γ_{Ol} were plotted. In spite of the difference in particle size, the straight line correlations over limited ranges are remarkable. Similarly, correlations are obtained when pH is a variable.

It has been shown that under the critical contact situation, Γ_{OH^-} and zeta potential curves for different sodium oleate

concentrations merge into one curve. Also Γ_{Cl^-} versus log $[Cl^-]/[OH^-]$ plot brings out the critical significance of the $[Cl^-]/[OH^-]$ ratio. It has been suggested on the basis of these experimental findings that at critical contact, the hydroxyl ion concentration singularly determines the zeta potential, the electrode potential as also the magnitude of Γ_{OH^-}.

In case of zircon-sodium oleate-moderator system at small additions of NaF, Na_2SiO_3 and Na_2SiF_6 a distinct activation effect is observed. This has been further confirmed by increased adsorption in the activation range of sodium oleate and increased numerical value of the negative zeta potential. This activation effect has been critically examined in the light of the explanations given for similar cases in literature. None of those are found to be convincing. It is proposed that the adsorption of Na^+ ion causes greater adsorption of collector species by decreasing the repulsion between the ionic heads of the hydrocarbon chains. Further work on the adsorption of sodium ions is required so that the above mentioned explanation, may be substantiated.

At large additions of NaF no appreciable depression effect was found while adsorption of sodium oleate did decrease. The action of NaF in decreasing adsorption is essentially exchange type,

$$M] \cdot Cl + F^- \rightleftharpoons M]- F + Cl^-$$

over a range of NaF concentration. This has been supported by the constancy of ($\Gamma_{Ol^-} + \Gamma_{F^-}$). Thus, the oleate and fluoride ions have common sites over a range of NaF concentration. At higher NaF concentrations, the fluoride ions seek additional sites for adsorption.

Zeta potential results for the above system can be explained on the basis of the observed adsorption trends. When sodium silicate is used, the depression is quite pronounced and on the basis of adsorption and zeta potential studies, it has been suggested that the neutral H_2SiO_3 is the predominant adsorption species and is responsible for depression. Here also, the constancy of $\Gamma_{Ol} + \Gamma_{Na_2SiO_3}$ within certain Na_2SiO_3 concentration ranges indicates common surface sites for adsorption of oleate and H_2SiO_3.

Sodium fluosilicate also shows a pronounced depression effect which is accompanied by a decrease in collector adsorption. Due to analytical difficulties, adsorption studies could not be made for Na_2SiF_6. It is proposed that Na_2SiF_6 hydrolytically dissociates to give H_2SiO_3 and F^- ions and H_2SiO_3 acts as a predominant depressing species.

In the end it would be worth while to mention in brief about the types of measurements mentioned in the present work and their relevence to the flotation studies. This discussion is meant to be a pointer towards future investigations.

Although quantitative correlations between flotation recovery and adsorption density have been obtained for limited ranges in the zircon-sodium oleate system, no single linear correlation could be obtained. This is partly due to the particle size difference which is inevitable. This point has been discussed in Chapter VII page 153.

In flotation systems, the particle size has to be kept comparatively coarse to avoid slime formation. However, the adsorption studies for the same size range are not possible due to a very small surface area available for adsorption. This would result in such a negligible change in the initial and terminal concentrations that the difference may not be detectable.

In collector-depressor systems, the problem of correlation becomes more complex as the flotation recovery now is a function of collector adsorption density, depressor adsorption, pH etc. The magnitudes of adsorption of the collector as well as the moderator species contribute towards the change in the solid-liquid interfacial free energy which is probably the most relevant parameter determining the flotability of a particle. Gibbs adsorption equation is one of the tools for computing the change in surface free energy (ΔG_s) from the measured adsorption data for all relevant species. However, the applicability of this equation to complex flotation systems

is far from simple, as it involves the requirements of the constancy of the total ionic concentration and reversibility of the adsorption. Upto what magnitude of the heat of adsorption one could assume reversibility is not clear. Added to this one has to take care of the double layer present. It is tempting to suggest that the studies on well defined systems conforming to Gibb's requirements (for the applicability of the equation) may be undertaken and equations on the lines of those developed by Chattoraj (138) incorporating the double layer considerations in Gibb's equation may be applied with advantage.

From a more practical point of view, it may be rewarding to conduct similar studies on the other component minerals of the beach sand, so that best conditions for selective flotation could be established.

The problem of crystal structure-flotability relationships for silicates and other mineral classes is of paramount importance as more and more complex ores of this category would be encountered in future. Only detailed and fundamental studies on individual minerals would unravel rational generalisations in this regard.

REFERENCES

1. P. Somsundaran,:The Relationship Between Adsorption at Different Interfaces and Flotation Behaviour, Trans. SME/AIME, 241, 105 (1968).

2. D.W.Fuerstenau: Correlation of Contact Angles, Adsorption Density, Zeta Potentials and Flotation Rate, Trans. SME/AIME, 208, 1365 (1957).

3. D.W. Fuerstenau:,T.W.Healy and P.Somsundaran: The Role of Hydrocarbon Chain of Alkyl Collectors in Flotation, Trans. SME/AIME, 229, 321 (1964).

4. K.V. Viswanathan, S.K. Shukla and K.K.Majumdar: Adsorption of Long Chain Electrolytes at the Solid-Liquid Interface Part I, Technical Report B.A.R.C.-385 (1968).

5. J. Rogers: Principles of Sulfide Mineral Flotation, Froth Flotation, 50th Anniversary Volume ed. D.W.Fuerstenau AIME Publi, 139, (1962).

6. S.R. Rao: The Collector Mechanism in Flotation, Separation Science, 4(5), 357 (1969).

7. F.F. Aplan and D.W. Fuerstenau: Principles of Nonmetallic Mineral Flotation, Froth Flotation 50th Anniversary Volume ed. D.W. Fuerstenau AIME Publ. 170 (1962).

8. N. Pilpel: Soap Films in Flotation, Dispersion and Lubrication, Chemical Reviews, 66, 29 (1966).

9. A.M. Gaudin, H.L. Miaw and H.R. Spedden: Native Flotability and Crystal Structure, Proc. Second. Intl. Cong. of Surface Activity Vol. III, Butterworth s, London,202,(1957).

10. T.W. Healy, A.P. Herring and D.W. Fuerstenau: The Effect of Crystal Structure on the Surface Properties of a Series of Manganese dioxides, J. Coll. Sci. 22, 599 (1966).

11. P.L. deBruyn and G.E. Agar: Surface Chemistry of Flotation Froth Flotation 50th Anniversary Volume ed. D.W.Fuerstenau AIME, Pub. 91 (1962).

12. A.M. Gaudin: Flotation, McGraw Hill, Pub. (1957).

13. D.W. Fuerstenau: Streaming Potential Studies on Quartz, Sc. D. Thesis, MIT (1957).

14. M. Robinson,: Streaming Potential Studies of Al_2O_3 and MgO in Aqueous Systems, M.Sc. Thesis, Univ. Cali. (1962).

15. H.C. Li: Adsorption of Organic and Inorganic Ions on Quartz, Sc. D. Thesis, MIT (1958).

16. R.M. Garrels: Mineral Equilibria, Harper and Bros., New York (1960).

17. Pourbaix, Atlas of Electrochemical Equilibrium in Aqueous Solutions, Brussels, Centre belge d'etude de la Corrosion.

18. M.C. Fuerstenau and S.D. Miller: The Role of the Hydrocarbon Chain in the Anionic Flotation of Calcite, Trans. AIME/SME 238, 157 (1967).

19. J.M.W. Mackenzie and R.T. O'Brien: Zeta Potential of Quartz in the Presence of Nickel (II) and Cobalt (II), Trans. AIME/SME, 244, 168 (1969).

20. G.A. Parks: The Isoelectric Points of Solid Oxides, Solid Hydroxides and Aqueous Hydroxocomplex Systems, Chemical Reviews, 177, 65 (1965).

21. G.A. Parks Aqueous Surface Chemistry of Oxides and Complex Oxide Minerals, Isoelectric Point and Zero Point of Charge, Adv. Chem. Soc. No. 67, 121 (1967).

22. A.S. Peck and M.E. Wadsworth: Infrared Study of the Depression Effect of Fluoride, Sulphate and Chloride on Chemisorption of Oleate on Fluorite and Barite, VII th International Min. Proc. Cong. Gordon and Reach, New York, 259, (1964).

23. A.S. Peck, L.H. Raby and M.E. Wadsworth: An Infrared Study of the Flotation of Hemalite with Oleic Acid and Sodium Oleate Trans. SME/AIME 235, 304 (1966).

24. A.S. Peck and M.E. Wadsworth: An Infrared Study of the Activation and Flotation of Benyl with Hydrofluoric and Oleic Acid, Trans. AIME/SME, 238, 264 (1967).

25. R.W. Smith: Activation of Beryl and Feldspars by Fluorides in Cationic Collector System, Trans. AIME/SME, 232, 160 (1965).

26. V.I. Klasser and V.A. Mocrousov: An Introduction to the Theory of Flotation, Section V, 289, Butterworths, London (1963).

43. I.N. Plaksin and E.N. Chapligina: Reports of Acad. Sci. (U.S.S.R.), 756, (1958).

44. I.N. Plaksin, R.S. Shafeev, V.A. Chanturia: Izvestia, Akad. Nauk, USSR, 184, (1964).

45. L.V. Kostina, G.N. Nazarova, I.N.Plaksin and V.I. Solnyshkin: Dokl.Acad. Nauk. SSSR, 161, 1382 (1965).

46. I.N. Plaksin: Flotation Properties of Rare Metal Minerals, Primary Sources, New York (1965).

47. J.M. Cases: On the Normal Interaction Between Adsorbed Species and Adsorbing Surface: Trans. SME/AIME, 247, 123, (1970).

48. J.M. Cases: Thesis for Doctorat d'Etat Sciences Physiq University of Nancy (1967).

49. D.Salatic: Intl. Min. Proc. Congr.Leningrad,Vol.II, 468 (1969).

50. D.Salatic: Flotability of Monazite and Zircon Related to Electrochemical Changes on Their Surfaces, Trans. Inst. Min. Met. Bull./Sec. C, C231, 76, (1967).

51. S.G. Dixit and A.K. Biswas: pH-Dependence of Flotation and Adsorption Properties of Some Beach Sand Minerals: Trans. SME/AIME, 244, 173 (1969).

52. R.Goiffon and M. Couchoud: Micro-Determination of Unsaturated Fatty Acids with Nile Blue.,Annal. Boil, Clin (Paris), II, 327 (1953).

53. J. Vance Batty, W.W. Agey and B.F. Andrew: U.S.Bureau of Mines, Report No. 7094 (1968).

54. Electrophoretic Mass Transport Analyser, Numinco Model MIC-1201, Information Manual.

55. J.F. Danielli, K.G.A. Pankhrust and [illegible]. Recent Advances in Surface Science, Vol. 1, Academic Press, New York, 94, (1964).

56. L.H. Little: Infrared Spectra of Adsorbed Species, Academic Press (1966).

57. M.L. Hair: Infrared Spectroscopy in Surface Chemistry, Marcel Dekkar Pub. New York (1967).

58. R. Mecke: Z. Physik, Chem. (Frankfurt) B16, 409,421 (1932).

59. (a) F.C. Cross and J.H. Van Vleck: J. Chem. Phys, 1, 350 (1933).

(b) R.M. Badger: A Relation Between Internuclear Distances and Bond Force Constants, J. Chem. Phys. 2, 128 (1934).

60. G. Herzberg: Infrared and Raman Spectra of Polyatomic Molecules, Van Nostrand Princeton, N.J. (1945).

61. G. Duyckaerts: The Infrared Analysis of Solid Substances Analyst, 84, 201 (1959).

62. M.M. Stimson and M.J. O' Donnell: The Infrared, Ultraviolet Absorption Spectra of Cystosine and Isocystosine in the Solid State, J.Am. Chem. Soc. 74, 1805 (1952).

63. R.O. French, M.E. Wadsworth, M.A. Cook and I.B. Cutler: The Quantitative Application of Infrared Spectroscopy Studies in Surface Chemistry, J. Phys, Chem. 58, 805 (1954).

64. De Sesa and L.B. Rogers: Spectrophotometric and Palarographic Determination of Soluble Salts: Anal. Chem. 26, 1278, (1954).

65. D.T.W. Chow and R.J. Robinson: Forms of Silicates Available for Colorimetric Determination, Anal. Chem. 25, 646 (1953).

66. S. Abbeg: Photometric Determination of Silicon in Ferrous, Ferromanganese, Nickel and Copper Alloys, Anal.Chem. 25, 148 (1953).

67. J.C. McHard: Determination of Silicon in Organo-silicon Compounds, Anal. Chem. 20, 325 (1948).

68. P.G. Jeffery: Geochim, Cosmochim, Acta, 26, 1353 (1962).

69. J.A. Maxwell: Rock and Minerals Analysis, Chemical Analysis, Vol. 27, Interscience, Publishers (1968).

70. a) R. Greenhalgh and J.P. Riley: The Determination of Fluorides in Natural Waters: Anal. Chim. Acta 25, 179, (1961).

b) K.M. Chan and J.P. Riley: The Automatic Determination of Fluoride in Sea Water and Other Natural Waters, Anal. Chim. Acta. 35, 365 (1966).

71. C.H. Giles and S.N. Nakhwa: Studies in Adsorption XVI The Measurement of Specific Surface Areas of Finely Divided Solids by Solution Adsorption, J.Appl.Chem. 12, 266 (1962).

72. S.S. Kajiji and D.M. Desai: Properties of K oleate, Science and Culture (India) 12, 266 (1962).

73. V.L. Schneider, R.T.Holman and G.O.Burr: A Monolayer Study of the Isomerism of Unsaturated and Oxyfatty Acids, J.Phys. and Coll.Chem. 53, 1016 (1949).

74. A.M. Gaudin and D.W. Fuerstenau: AIME Trans.,/SME Sec. 1955, Vol. 202, p. 958.

75. H.R. Kruyt: Colloid Science, Vol. I, Elsevier, Pub. (1952).

76. L. Vegard: a) VI Resultsof Crystal Analysis: Phil, Mag. 32, 65 (1916), b) ibid, (7) 1, 1151 (1926).

77. R.W.G. Wycoff and S.B. Hendricks: Z. Krist, 66, 73 (1927).

78. I.R. Krstanovic: Rdetermination of the Oxygen Parameters in Zircon ($ZrSiO_4$), Acta, Cryst.11, 896 (1958).

79. W. Huckel: Structural Chemistry of Inorganic Compounds, Vol. II, Elsevier, Publ. Co. (1951).

80. W.B. Bluementhal: The Chemical Behaviour of Zirconium, D. Van Nostrand Co. Princ. (1958).

81. L.A. Pauling: Nature of the Chemical Bond: Cornell Univ.Press, Ithaca, N.Y. (1960).

82. H.F. Holmes, C.S. Shoup and C.H. Secoy: Electrokinetic Phenomena at the Thorium Oxide-Aqueous Solution Interface, J.Phys.Chem.69(9), 3148, (1965).

83. O' Connor and A.S. Buchanan: Aust. J.Chem. 7, 245, (1945).

84. (a) O'Connor and A.S. Buchanan: Electrokinetic Properties of Cassiterite, Aust. J. Chem. 6, 278 (1953).

(b) ibid: An Electrokinetic Study by Streaming Potential Method of Ion Exchange at Oxide-Mineral Surfaces, Aust. J. Chem. 10, 393, (1957).

85. N. Street: Zeta Potential of Synthetic Sapphire, Aust. J. Chem. 17, 828, (1964).

86. I.I. Zukov and A.A. Kryukov: Proc. Jubilee Sciences, 1948 Session, Leningrad, Uni. Section 62 (1948.

87. T.W. Healy and V.R. Jellet: Adsorption-Coagulation Reactions of Zn(II) Hydrolysed Species of the Zinc Oxide-Water Interface, J. Coll. Interface Sci. 24, 41 (1967).

88. Buchanan and Heymann: a) J.Coll. Sc. 4, 137 (1949), b) ibid, 4, 151, 1949, c) ibid 4, 157 (1949).

89. D.J. O'Connor: Electrokinetic Properties and Surface Reactions of Scheelite, Proc. IInd Intl. Conf. of Surface, Activity III, Butterworth, London, 319 (1957).

90. M.C. Fuerstenau, G. Gutierrez and D.A. Elgillani: The Influence of Sodium Silicate in Non-Metallic Flotation System, Trans. SME/AIME, 319, (1968).

91. a) Adolf and Pauli: Some Aspects of Solution Chemistry of Zirconium, J. Chem. Soc. 4330, (1952).

b) W.B. Bluementhal: J. Chem. Ed. 26, 472 (1949).

92. J.H. Hildbrand: Some Applications of the Hydrogen Electrode in Analysis Research and Teaching, J.Am. Chem. Soc. 35, 847 (1913).

93. P.D. Cratin: A Quantitative Characterization of pH-Dependent Systems, Ind. and Engg. Chem. V. 61, 35, (1969).

94. P.D. Cratin and A.M. Dean: J. Ala. Acad. Sci. 37,228 (1966).

95. J. Powney and D.O. Jordan: The Hydrolysis of Soap as Determined by Glass Electrode, pH Measurements, Trans. Far. Soc. 34, 366 (1938).

(c) C.H. Giles, T.H. Mac Ewan, S.N. Nakhwa and D.Smith: Studies in Adsorption Part XI, A System of Classification of Solution Adsorption Isotherms, and its Use in Diagnosis of Adsorption Mechanisms and in Measurement of specific Surface Areas of Solids, J. Chem. Soc. (786), 3973 (1960).

96. J.J. Kipling: Adsorption From Solutions of Non Electrolytes, Academic Press, New York, p. 101, (1965).

97. G. Barsky: Trans. AIMME, 112, 236 (1934).

98. I.W. Wark and A.B. Cox: Trans. AIME, 112,189-244 and 267-302, (1934).

99. A.M. Gaudin: Flotation, McGraw Hill Pub. 285, (1957).

100. I.A. Kakovsky and E.J. Salina: Theoretical Studies on Flotation Process, (Papers), O.B.T.I. Mekhanbr Inst. (1955).

101. G.A. Last and M.A. Cook: J. Phys. Chem. 56, 637 (1952).

102. K.L. Sutherland: Collector-Depresent Equilibrium in Flotation, J. Phys. Chem. 63, 1717 (1959).

103. O'Mellgren; Adsorption of Ethyl Xanthate on Pyrite, Ph.D. Dissertation, MIT (1954).

104. S. Mukai and T. Wakamatsu: Electrochemical Study on Flotation, Memoirs of the Faculty of Engg. Kyoto, Uni. Vol. XXIV, Part 4, 389,(1962).

105. Herzberg; Infrared and Raman Spectra of Polyatomic Molecules, Van Nostrand Co. New York, p. 100 (1946).

106. B.D. Saxena, Infrared Absorption Studies of Some Silicate Structures, Trans. Fara. Soc. 57 Part 2, 242, (1961).

107. F. Matossi: J. Chem. Phys. 17, 679 (1949).

108. R.G. Sinclair, et.al.: J. Am. Chem. Soc. 2578, 74 (1952).

109. K.V. Viswanathan and K.K. Majumdar: I.R. Absorption Studies on Beach Sand Minerals Under Conditions of Soap Flotation, Technical Report BARC-391,Bombay India (1969).

110. I.D. Hodgman, R.C. Weast,and S.M. Selby: Handbook of Physics and Chemistry, 42 Ed. The Chem. Rubber Pub. Co. (1961).

111. V.I. Klassen and V.A. Mocrousov; An Introduction to the Theory of Flotation, Section V, Butterworths, London (1963).

112. R.W. Harman: Aqueous Solutions of Sodium Silicates, Part VIII, General Summary and Theory of Constitution, Sodium Silicates as Colloidal Electrolytes, Jour. of Phys. Chem. p. 44, V. 32, (1928).

113. Peskov in Introduction to the Theory of Flotation by Klassen and MoCrousov, (1963).

114. A.G. Rees and J. Hudleston, J. Chem. Soc. 1334, (1936).

115. I.G. Ryss: Hydrolytic Equilibria in Solutions of Sodium Fluosilicate at 11° , J. Gen. Chem. SSSR, 16, 331 (1946).

116. N.I. Crosby: Equilibria of Fluosilicate Solutions with Special Reference to the Fluoridation of Public Water Supplies, J. of Appl. Chem. 19, 100 (1969).

117. J.A. Buslaev, N.S. Nikolaev and M.P. Gustyakova; Investigation of Solutions in the System HF-SiO_2-H_2O, Izvest Sibir, Oldel, Akad. Nauk SSSR, 10, 57 (1960).

118. S.M. Thomsen: High Silica Fluosilicic Acid, J. Am. Chem. Soc. 72, 2798, (1950).

119. C.A. VanderWerf: Acids, Bases and the Chemistry of the Covalent Bond, Reinhold PublishingCorp., New York, (1961).

120. J.R.Cooke and Minski: J. Appl. Chem. 12, 123 (1962).

121. M.A. Eigels: Theoretical Basis of the Flotation of Non-Sulphide Minerals, Metallurgizdat.

122. V.A. Mocrousov: Concentration of Calcite-Fluorite Ores, Using an Aluminum Salt, Min. J. (Moscow) No. 9 (1945).

123. I.N. Shorsher: Flotation of Carbonate Minerals (Cerussite and Malachite), Gostoptekhizdat (1949).

124. K. F. Beloglazov and G.A. Osolodkov; Effect of Alkalinity of the Pulp on Flotation of Appatite, Rep. Leningr. Min. Inst. 9, 1, (1936).

125. A.E. Zakharov in Flotation Properties of Rare Metal Minerals, Primary Sources, New York (1965).

126. Klassen and Mocrousov: Introduction to the Theory of Flotation, RButterworths, London (1963).

127. W. Gordy; A Relation Between Bond Force Constants, Bond Orders, Bond Lengths, and Electronegativities of the Bonded Atoms. J. Chem. Phys., v. 14, No. 5, May 1946, pp. 305-320.

128. G.H. Cartledge: The Ionic Potential as a Periodic ~~Funct~~ Function, J. Am. Chem. Soc., v. 50, No. 11, Nov. 6, 1928, pp. 2855-2863.

129. Hagihara and Sakurai: Proc. IVth Intl. Congr. Surface Activity Substance, Vol. 3, 361 (Gordon and Breach, New York 1967).

130. A.S. Peck, L.H. Raby and M.E.Wadsworth: An Infrared Study of the Flotation of Hematite with Oleic Acid and Sodium Oleate Trans. SME/AIME, 235, 304, (1966).

131. A.S. Peck: Infrared Studies of Oleic Acid and Sodium Oleate Adsorption on Fluorite, Barite, and Calcite, Bureau of Mines Rep. of Investigations 6202, (1963).

132. K.V. Viswanathan and K.K. Majumdar: I.R. Absorption Studies on Beach Sand Minerals Under Conditions of Soap Flotation, Technical Report BARC-391, Bombay, India (1969).

133. I. Satake and R. Matuara: Kolloid. Z. 176, 31 (1961).

134. M.J.D. Low and H. Inoune: Anal. Chem. 2397, 36, (1964).

135. W.A. Bonner and J.I. Degraw (Jr.): J. Chem. Edn. 639, 39 (1962).

136. E. Rosen and A. Maun: J.Am. Cer. Soc., 603, 48 (1965).

137. W.M. Latimer; Oxidation Potentials, Prentice Hall Inc. (1959).

138. D.K. Chattoraj: Models of Electrical Double Layer and Gibbs Equation for Adsorption of Electrolytes, J.Coll. Int. Sci. 399, 29 (1969).

APPENDIX A

CARBONYL STRETCHING FREQUENCY OF METAL OLEATES

Carbonyl (C=O) antisymmetric stretching frequency in the infrared spectra of metal oleate $R - C\begin{matrix}\nearrow O \\ \searrow O - M\end{matrix}$ is characteristic of the oleates and is dependent on the metal cations. The vibration frequency is dependent on the masses of the atoms bonded and force constant and is given by,

$$\nu = 1/2 \sqrt{k(1/m_A + 1/m_B)} \qquad (A.1)$$

where ν - vibration frequency

m_A, m_B - masses of the bonded atoms A and B

k - force constant.

The above equation is true for a system containing two atoms and undergoing simple harmonic motion. However, similar though more complex equations would be followed by the systems containing more than two atoms. Therefore, the vibrational frequency of bonded atoms is directly proportional to the force constant of the bond. In turn, the force constant of the bond is related to bond length by the equation suggested by Gordy (127) which is,

$$k = aN (X_A X_B / L^2)^{3/4} + b \qquad (A.2)$$

where a and b - constants

N - bond order

L - bond length

and X_A and X_B - electronegativity of the atoms, A and B.

Hence, increase in force constant would mean a decrease in bond length. Thus the change in frequency of carbonyl group due to the presence of different cations nearby would also indicate whether the bonds were increasing or decreasing in length. According to Cartledge (128) the extent of polarisation of the anion by the cation is given by the ratio of valence to radius of the cation i.e. Z/R. In case of xanthates the C=S frequency was found to be the function of Z/R and a straight line relationship was obtained ([redacted]). However, when similar plot was attempted [redacted] in case of the Carbonyl stretching frequencies of the metal oleates, no single straight line was obtained. Instead, 3 separate straight lines with cations of the same valency falling on the same straight line were obtained as shown in Fig. 73. The corresponding data finds place in Table V. This clearly indicates that the C=O stretching frequency is not a function of cation valency (Z) but of R only. Accordingly an excellent straight line plot was obtained between frequency and R as shown in Fig. 66. Therefore, it is tempting to suggest that only monovalent compounds of the types,

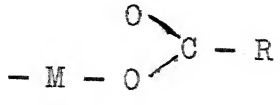

are formed at the solid substrate with other valencies of the metal cations being satisfied at the solid substrate. In case of lead xanthate such a monovalent compound has been suggested(

Table V

Carbonyl Stretching Frequency and R/Z Ratio of Different Metal Oleates

Cation	C=O Anti. sym. Mode	Z	Radius	R/Z	Reference
Be^{++}	1623 cm^{-1}	2	0.31 Å	0.155	130
Na^{+}	1540-1555	1	0.95	0.950	130
Fe^{+++}	1520-1540	3	0.65	0.217	130
Ca^{++}	1560	2	0.99	0.495	131
Ba^{++}	1515	2	1.35	0.675	131
La^{+++}	1530	3	1.15	0.383	132
Ti^{++++}	1510-1595	4	0.68	0.170	132
Cu^{++}	1585	2	0.72	0.360	133
Al^{+++}	1563	3	0.50	0.170	134
Ag^{+}	1560	1	0.89	0.890	135

APPENDIX B

THERMODYNAMIC DATA ON SPECIES OF ZIRCON IN AQUEOUS SOLUTIONS

The thermodynamic data on the species that are likely to be formed while zircon is in contact with water are given in this appendix. The free energy of formation of $ZrSiO_4$ has been calculated indirectly as follows:

Free Energy of Formation of $ZrSiO_4$:

E. Rosen and Arnulf Maun (136) have found out the free energy of the reaction

$$ZrO_2 + SiO_2 = ZrSiO_4$$

in the temperature range between 1180°C to 1366°C. The values reported are,

Temperature °C	1180	1242	1300	1366
$\Delta G^{\circ}_{(r)}$ Kcal/mole	-2.38	-1.98	-1.64	-1.29 ± 0.1

The free energy of reaction at room temperature $\Delta G^{\circ}_{298}(r)$ was found out by linear extrapolation to 25°C to be -9.0 Kcal/mole as shown in Fig. 74. Now, ΔG°_f for ZrO_2 and SiO_2 are -[redacted] -2,582 Kcal/mole and -190.9 Kcal/mole respectively. Hence from the above reaction we have,

$$\Delta G^{\circ}_f \quad (ZrSiO_4) = -444.3 \text{ Kcal/mole.}$$

Table VI

Thermodynamic Data for Individual Species

Species	ΔH°_f Kcal/mole	ΔS°_f cal/deg.mole	ΔG°_f Kcal/mole
F^-	- 78.66	- 2.3	- 66.08
HF(aq)	- 78.66	2.6	- 70.41
HF_2^-(aq)	-153.6	0.5	-137.5
H^+	0.00	0.0	0.00
OH^-(aq)	- 54.957	- 2.519	- 37.595
H_2O(l)	- 68.3174	16.716	- 56.690
$SiF_6^=$ (aq)	-558.5	-12.00	-511.00
NaF (c)	-136.00	14.00	-129.3
Zr^{4+}(aq)	--	--	-142.0
ZrO^{++}(aq)	-223.1	--	-201.5
$HZrO_3$(aq)	--	--	-287.7
$ZrO(OH)_2$ (c)	-338.0	2.2	-311.5
$ZrO(OH)_2$ (h)	--	--	-254.81
$Zr(OH)_4$ (c)	-411.2	31	-370
$Zr(OH)_4$ (h)	--	--	-256.62
$ZrSiO_4$	--	--	-444.3
H_4SiO_4	-349.10	43.40	-312.80
H_4SiO_4	--	--	-300.70
H_4SiO_4	--	--	-300.10
H_2SiF_6 (aq)	-557.20	--	--
H_2SiO_3 (c)	-270.00	--	-244.5
$SiO_3^=$	--	--	-212.0
SiO_2 (anhy.)	-205.4	10.00	-192.4
SiO_2(glass)	-202.5	-190.9	11.2
ZrO_2 (c)	-258.2	12.03	-244.4
ZrO_2 (h)	-283.5	--	--

Table VII

Equilibrium Constants and $\Delta G^{\circ}_{(R)}$ for Various Reactions

Sl.No.	Reaction	$\Delta G^{\circ}_{(R)}$ Kcal/mole	K
1.	$ZrSiO_4 + 4H_2O$ ==		
1.	$ZrSiO_4+4H_2O \rightleftharpoons H_4ZrO_4(H)+H_4SiO_4$	+ 112.74	8.51×10^{-84}
2.	$ZrSiO_4+4H_2O \rightleftharpoons H_4ZrO_4(c)+H_4SiO_4$	- 0.64	2.906
3.	$H_4SiO_4 \rightleftharpoons H_2SiO_3(c)+H_2O$	- 0.49	2.262
4.	$H_4SiO_4 \rightleftharpoons H_2SiO_3(h)+H_2O$	+ 56.20	2.14×10^{-40}
5.	$H_4ZrO_4(c) \rightleftharpoons H_2ZrO_3(c)+H_2O$	+ 1.81	7.633×10^{-1}
6.	$H_4ZrO_4(h) \rightleftharpoons H_2ZrO_3(h)+H_2O$	- 54.88	5.248×10^{-39}
7.	$Zr^{4+}+2H_2O \rightleftharpoons ZrO^{++} + 2H^+$	--	8.71×10^{-3}
8.	$ZrO^{++}+2H_2O \rightleftharpoons HZrO_3^- + 3H^+$	--	$10^{-19.95}$
9.	$H_4ZrO_4 \rightleftharpoons Zr^{4+} + 4OH^-$	--	6×10^{-58}
10.	$H_2ZrO_3 \rightleftharpoons ZrO^{++} + 2H^+$	--	3×10^{-26}
11.	$H_2ZrO_3 \rightleftharpoons HZrO_3^- + H^+$	--	$10^{-17.95}$
12.	$H_2SiO_3 \rightleftharpoons HSiO_3^- + H^+$	--	10^{-10}
13.	$HSiO_3^- \rightleftharpoons SiO_3^= + H^+$	--	10^{-12}
14.	$SiF_6^= + 2H_2O \rightleftharpoons SiO_2 + 4H^+ + 6F^-$	+ 36.50	2×10^{-27}
15.	$SiF_6^= \rightleftharpoons SiF_4 + 2F^-$	19.00	--
16.	$3SiF_4 + 3H_2O \rightleftharpoons 2H_2SiF_6 + H_2SiO_3$	- 14.00	--

APPENDIX C

X-RAY FLUORESCENCE ANALYSIS AND SURFACE AREA DETERMINATION OF ZIRCON SAMPLE

Surface Area Determination of Zircon Samples:

The surface determination of the zircon sample used for adsorption studies was done by a method in which p-nitrophenol is used as an adsorbing species. The details of the method are given by C.H. Giles (71). An adsorption isotherm of p-nitrophenol on zircon was determined. Aqueous solutions of p-nitrophenol of appropriate strength were used. 2 gms of the dry zircon powder were transferred in different glass bottles and 25 ml. of p-nitrophenol solutions were added. After vigorous shaking for half an hour the bottles were kept in a thermostat for about 6 hours after which the supernatent liquid was analysed colorimetrically. The pH was maintained exactly at 7.00 $\pm$ 0.05 and the transmittance as well as absorbance was measured at 400 mμ.

The adsorption isotherm so obtained is given in Fig.75. From the plateau of the curve the surface area of the sample was calculated to be 2.414 meter^2/gm. The cross-sectional area of p-nitrophenol molecule was taken to be 25 Å^2 as per Gile's suggestion.

X-ray Fluorescence Analysis of Zircon:

X-ray fluorescence pattern of zircon was taken with tungston as a target material. The pattern is given in Fig.76. For the sake of comparison literature values of d spacings are tabulated in Table VIII. No impurity except Hf has been detected.

Table VIII

X-Ray Powder Pattern of $ZrSiO_4$ (Tetragonal)

hkl	d(Å)	I	hkl	d(Å)	I
101	4.434	45	532	1.0590	7
200	3.302	100	424	1.0506	7
211	2.650	7	523		
112	2.518	45	620	1.0442	5
220	2.336	10	325	1.0015	1
202	2.217	8	116	0.9745	5
301	2.066	20	631	0.9713	5
103	1.908	14	415	0.9582	1
321	1.751	11	613	0.9532	1
312	1.712	40	701	0.9321	1
400	1.051	14	444	0.9201	2
411	1.547	4	543		
004	1.495	3	640	0.9157	4
420	1.477	8	316		
332	1.381	10	552	0.8994	5
204	1.362	7	712	0.8915	5
431			604	0.8863	7
501	1.290	5	525		
224	1.259	8	624	0.8561	5
413	1.248	3	703	0.8527	2
512	1.1883	11	732	0.8329	4
440	1.1672	2	723		
404	1.1079	5	800	0.8256	1
600	1.1006	5	741		
611	1.0682	1	811	0.8166	3

APPENDIX D

EXPERIMENTAL DATA ON FLOTATION

Table IX

Performance of the Laboratory Glass Flotation Cell

Percent solid - 10

Volume of the Cell - 375 ml

Conditioning time - 4 minutes

Flotation time - 2.5 minutes

Rate of aeration during flotation - 2 litre/min

Mineral calcite

Collector - Sodium oleate

Frother - Dowfroth - 250

Amount of Frother: 4 drops

Sl.No.	Concentration of Na Oleate (mole/lit)	Percent recovery
1.	9.498×10^{-5}	32.23
2.	9.498×10^{-5}	32.30
3.	9.498×10^{-5}	32.23
4.	9.498×10^{-5}	32.43

Table X

Effect of Sodium Oleate Concentration on the Flotation Recovery of Zircon

Sl.No.	Na Oleate Concentration (mole/lit)	(mg/l)	Final pH	Percent Recovery
1.	0.379×10^{-5}	28.60	9.00	62.50
2.	1.875×10^{-5}	57.14	9.15	74.69
3.	2.829×10^{-4}	86.00	9.12	75.71
4.	3.948×10^{-4}	120.00	9.13	87.64
5.	5.168×10^{-4}	157.10	9.02	90.88
6.	6.579×10^{-4}	200.00	9.00	97.00
7.	8.453×10^{-4}	257.00	9.12	98.86
8.	1.060×10^{-3}	322.00	9.12	75.00
9.	1.128×10^{-3}	343.00	9.25	31.03

Table XI

Effect of pH on the Flotation Recovery of Zircon with Sodium Oleate

Sl.No.	NaOl Concentration (mole/lit)	Final pH	Percent Recovery	Flotation Activity
1.	6.579×10^{-4}	4.55	12.18	0.158
2.	6.579×10^{-4}	4.95	19.74	0.203
3.	6.579×10^{-4}	5.35	57.81	0.594
4.	6.579×10^{-4}	5.75	78.52	0.807
5.	6.579×10^{-4}	5.85	79.75	0.820
6.	6.579×10^{-4}	6.85	96.80	0.995
7.	6.579×10^{-4}	8.65	97.31	1.000
8.	6.579×10^{-4}	8.70	95.20	0.978
9.	6.579×10^{-4}	9.80	28.04	0.288
10.	6.579×10^{-4}	9.90	42.84	0.440
11.	3.948×10^{-4}	3.96	3.59	0.038
12.	3.948×10^{-4}	4.70	12.77	0.135
13.	3.948×10^{-4}	5.15	39.86	0.421
14.	3.948×10^{-4}	5.35	60.10	0.634
15.	3.948×10^{-4}	5.90	80.46	0.849
16.	3.948×10^{-4}	6.15	79.62	0.840
17.				

Contd...

Contd...

Sl.No.	NaOl Concentration (mole/lit)	Final pH	Percent Recovery	Flotation Activity
17.	3.948×10^{-4}	6.75	88.04	0.930
18.	3.948×10^{-4}	7.05	94.77	1.000
19.	3.948×10^{-4}	7.55	93.40	0.986
20.	3.948×10^{-4}	8.18	91.22	0.963
21.	3.948×10^{-4}	9.28	42.85	0.452
22.	3.948×10^{-4}	9.90	6.21	0.065
23.	1.875×10^{-4}	4.80	12.71	0.144
24.	1.875×10^{-4}	6.55	85.80	0.972
25.	1.875×10^{-4}	7.50	85.45	0.968
26.	1.875×10^{-4}	7.85	88.28	1.000
27.	1.875×10^{-4}	8.60	66.85	0.757
28.	1.875×10^{-4}	9.20	24.16	0.274
29.	9.397×10^{-5}	4.85	13.84	0.167
30.	9.397×10^{-5}	5.05	8.16	0.098
31.	9.397×10^{-5}	5.35	60.33	0.728
32.	9.397×10^{-5}	6.05	76.42	0.923
33.	9.397×10^{-5}	6.40	82.81	1.000
34.	9.397×10^{-5}	7.09	78.32	0.946
35.	9.397×10^{-5}	7.55	81.62	0.986
36.	9.397×10^{-5}	8.55	26.87	0.324
37.	9.397×10^{-5}	8.95	8.18	0.099

Table XII

Effect of Sodium Fluoride Addition on the Flotation Recovery of Zircon

Sl.No.	NaF Concentration mg/l	NaF Concentration mole/lit	Final pH	Percent Recovery
1.	0.00	0.000	9.70	46.17
2.	28.57	6.803×10^{-4}	9.80	75.44
3.	28.57	6.803×10^{-4}	9.65	79.21
4.	57.44	1.368×10^{-3}	9.68	76.76
5.	100.03	2.381×10^{-3}	9.74	78.96
6.	171.48	4.083×10^{-3}	9.70	82.45
7.	228.64	5.444×10^{-3}	9.65	82.56
8.	357.50	8.513×10^{-3}	9.67	77.67
9.	429.00	1.020×10^{-2}	9.65	76.38

Table XIII

Effect of Sodium Silicate Addition on the Flotation of Zircon

Sl.No.	NaOl Concentration mole/lit	Na_2SiO_3 Concentration		Final pH	Percent Recovery
		mg/l	mole/lit		
1.	6.579×10^{-4}	0.00	0.00	9.00	97.00
2.	6.579×10^{-4}	21.43	1.530×10^{-4}	9.18	94.97
3.	6.579×10^{-4}	28.60	2.042×10^{-4}	9.04	96.65
4.	6.579×10^{-4}	71.43	5.100×10^{-4}	9.06	94.73
5.	6.579×10^{-4}	143.00	1.021×10^{-3}	9.20	65.53
6.	6.579×10^{-4}	185.90	1.327×10^{-3}	9.23	35.91
7.	6.579×10^{-4}	228.80	1.633×10^{-3}	9.29	14.87
8.	4.934×10^{-4}	0.00	0.000	9.47	57.59
9.	4.934×10^{-4}	7.14	5.105×10^{-4}	9.50	64.92
10.	4.934×10^{-4}	14.28	1.021×10^{-4}	9.47	48.23
11.	4.934×10^{-4}	28.57	2.042×10^{-4}	9.48	32.96
12.	4.934×10^{-4}	57.16	4.080×10^{-4}	9.50	19.68
13.	3.948×10^{-4}	0.00	0.000	9.13	87.64
14.	3.948×10^{-4}	14.30	1.021×10^{-4}	9.10	90.91

contd..

Contd....

Sl.No.	NaOl Concentration mole/lit	Na_2SiO_3 Concentration		Final pH	Percent Recovery
		mg/l	mole/lit		
15.	3.948×10^{-4}	21.43	1.530×10^{-4}	9.18	95.48
16.	3.948×10^{-4}	35.71	2.550×10^{-4}	9.14	92.32
17.	3.948×10^{-4}	50.00	3.572×10^{-4}	9.14	92.49
18.	3.948×10^{-4}	114.30	8.160×10^{-4}	9.17	71.88
19.	3.948×10^{-4}	171.43	1.224×10^{-3}	9.28	15.44
20.	2.829×10^{-4}	0.00	0.000	9.12	75.71
21.	2.829×10^{-4}	14.30	1.021×10^{-4}	9.00	80.89
22.	2.829×10^{-4}	21.43	1.530×10^{-4}	8.99	71.58
23.	2.829×10^{-4}	35.71	2.550×10^{-4}	9.01	70.68
24.	2.829×10^{-4}	57.14	4.080×10^{-4}	8.97	49.21
25.	2.829×10^{-4}	114.3	8.160×10^{-4}	9.22	28.19

Table XIV

Effect of Sodium Fluosilicate Addition on the Flotation Recovery of Zircon

Sl.No.	NaOl Concentration mole/lit	Na_2SiF_6 Concentration		Final pH	Percent Recovery
		mg/l	mole/lit		
1.	6.579×10^{-4}	0.00	0.000	9.02	79.77
2.	6.579×10^{-4}	14.30	7.588×10^{-4}	8.98	83.64
3.	6.579×10^{-4}	28.60	1.522×10^{-4}	9.05	88.98
4.	6.579×10^{-4}	57.20	3.042×10^{-4}	9.03	86.62
5.	6.579×10^{-4}	85.80	4.564×10^{-4}	9.01	87.86
6.	6.579×10^{-4}	128.60	6.841×10^{-4}	9.02	78.45
7.	6.579×10^{-4}	157.14	8.356×10^{-4}	8.97	36.38
8.	6.579×10^{-4}	171.60	9.126×10^{-4}	9.05	37.23
9.	3.948×10^{-4}	0.00	0.000	9.13	77.64
10.	3.948×10^{-4}	4.29	2.282×10^{-5}	9.07	84.67
11.	3.948×10^{-4}	8.60	4.564×10^{-5}	9.06	85.59
12.	3.948×10^{-4}	28.60	1.522×10^{-4}	9.02	89.71
13.	3.948×10^{-4}	42.86	2.279×10^{-4}	9.00	84.76
14.	3.948×10^{-4}	100.00	5.319×10^{-4}	9.20	70.39
15.	3.948×10^{-4}	114.30	6.078×10^{-4}	8.97	37.86

Contd....

Contd...

Sl.No.	NaOl Concentration mole/lit	Na_2SiF_6 Concentration		Final pH	Percent Recovery
		mg/l	mole/lit		
16.	3.948×10^{-4}	143.00	7.588×10^{-4}	9.05	36.64
17.	3.948×10^{-4}	171.43	9.116×10^{-4}	9.15	8.01
18.	2.829×10^{-4}	0.00	0.000	9.12	75.71
19.	2.829×10^{-4}	5.72	3.042×10^{-5}	9.10	77.91
20.	2.829×10^{-4}	11.44	6.078×10^{-5}	9.22	79.56
21.	2.829×10^{-4}	17.16	9.110×10^{-5}	9.12	81.36
22.	2.829×10^{-4}	28.60	1.522×10^{-4}	9.10	80.65
23.	2.829×10^{-4}	42.86	2.279×10^{-4}	9.10	78.63
24.	2.829×10^{-4}	78.56	4.178×10^{-4}	9.12	66.25
25.	2.829×10^{-4}	100.00	5.319×10^{-4}	9.16	46.01

Table XV

Effect of H_2SiF_6 Concentration on the Flotation of Some Beach Sand Minerals

Sl. No.	NaCl Concentration mole/lit	H_2SiF_6 Concentration		Final pH	Percent Recovery	Mineral
		mg/l	mole/lit			
1.	4.111×10^{-4}	2.80	1.945×10^{-5}	8.18	64.00	
2.	4.111×10^{-4}	17.35	1.204×10^{-4}	8.16	69.50	
3.	4.111×10^{-4}	40.45	2.808×10^{-4}	8.05	87.80	Zircon (Travancore)
4.	4.111×10^{-4}	57.80	4.076×10^{-4}	8.17	90.00	
5.	4.111×10^{-4}	86.70	6.018×10^{-4}	7.98	63.00	
6.	4.111×10^{-4}	115.60	8.028×10^{-4}	7.84	49.00	
7.	3.453×10^{-4}	11.56	8.028×10^{-5}	10.00	28.70	
8.	3.453×10^{-4}	28.90	2.006×10^{-4}	9.95	47.30	
9.	3.453×10^{-4}	57.80	4.076×10^{-4}	9.85	53.50	Monazite (Travancore)
10.	3.453×10^{-4}	86.70	6.018×10^{-4}	9.85	53.85	
11.	3.453×10^{-4}	115.60	8.028×10^{-4}	9.96	57.40	
12.	3.453×10^{-4}	156.00	1.083×10^{-3}	9.82	35.80	
13.	4.440×10^{-4}	0.00	0.000	10.00	52.00	
14.	4.440×10^{-4}	60.00	4.167×10^{-4}	10.04	63.50	
15.	4.440×10^{-4}	80.00	5.555×10^{-4}	9.94	72.50	Ilmenite (Travancore)
16.	4.440×10^{-4}	120.00	8.333×10^{-4}	9.88	30.00	
17.	4.440×10^{-4}	160.00	1.111×10^{-3}	10.01	18.90	

Table XVI

Effect of Na_2SiF_6 Concentration on the Flotation Recovery of the Minerals (Denver Cell)

Sl. No.	NaOl Concentration mole/lit	Na_2SiF_6 Concentration mole/lit	Final pH	Percent Recovery	Mineral
1.	7.401×10^{-4}	0.00	9.49	87.36	Ilmenite
2.	7.401×10^{-4}	1.862×10^{-4}	9.60	95.19	
3.	7.401×10^{-4}	3.724×10^{-4}	9.48	97.42	
4.	7.401×10^{-4}	9.307×10^{-4}	9.75	68.24	
5.	7.401×10^{-4}	1.489×10^{-3}	9.74	46.70	
6.	7.401×10^{-4}	2.234×10^{-3}	9.54	6.02	
7.	6.579×10^{-4}	0.000	9.73	76.60	Monazite
8.	6.579×10^{-4}	3.724×10^{-4}	9.73	95.10	
9.	6.579×10^{-4}	5.585×10^{-4}	9.62	94.62	
10.	6.579×10^{-4}	7.448×10^{-4}	9.65	96.15	
11.	6.579×10^{-4}	1.303×10^{-3}	9.63	95.55	
12.	6.579×10^{-4}	2.606×10^{-3}	9.60	94.45	

APPENDIX E

EXPERIMENTAL DATA ON ADSORPTION

Table XVII

Adsorption of Na Oleate on Zircon at Constant Initial pH 9.

Sl. No.	Wt. of Solid gm.	Initial Concn. mole/lit.x10^4	Initial pH	Final pH	Final Concn. mole/lit.x10^4	NaOl Adsorbed mole/cm^2
1.	5.0886	4.605	9.15	8.85	1.275	1.355×10^{-10}
2.	2.7436	4.605	8.95	8.81	1.907	2.544×10^{-10}
3.	2.4514	5.262	8.96	8.50	1.858	2.889×10^{-10}
4.	2.8214	7.894	8.95	8.65	2.813	3.747×10^{-10}
5.	2.8101	8.553	9.00	8.93	3.996	3.377×10^{-10}
6.	3.1572	9.210	8.98	8.35	3.322	3.861×10^{-10}
7.	2.5120	9.210	9.04	9.03	4.720	3.724×10^{-10}
8.	2.1656	10.524	9.03	9.18	6.250	4.119×10^{-10}
9.	2.8556	11.190	9.05	9.26	5.970	3.782×10^{-10}
10.	3.9607	12.500	8.98	8.45	5.262	3.785×10^{-10}
11.	2.9206	13.150	9.07	8.95	7.286	4.660×10^{-10}

Table XVIII

Effect of pH on the Adsorption of Sodium Oleate on Zircon

Initial NaOl Concentration: 6.579×10^{-4} mole/lit.

Sl. No.	Wt. of Solid (gms.)	Initial pH	Final pH	Final NaOl Concn. (mole/lit x 10^{4})	NaOl Adsorbed mole/cm^2	(OH^-) Final Concn. mole/lit.	(OH) Adsorbed mole/cm^2
1.	3.0598	8.64	7.75	3.075	2.371×10^{-10}	5.624×10^{-7}	5.151×10^{-11}
2.	2.3511	9.55	9.32	3.898	2.072×10^{-10}	2.095×10^{-5}	2.563×10^{-10}
3.	3.3386	10.3	9.56	3.816	1.714×10^{-10}	9.730×10^{-5}	1.269×10^{-9}
4.	3.8282	10.62	9.94	6.298	1.513×10^{-10}	8.711×10^{-5}	3.568×10^{-9}
5.	4.3162	10.74	10.12	5.640	4.500×10^{-11}	1.318×10^{-4}	3.402×10^{-9}
6.	3.3694	7.00	6.99	5.591	6.066×10^{-11}	1.000×10^{-7}	--
7.	4.0656	9.64	7.16	4.061	1.282×10^{-10}	1.445×10^{-7}	4.299×10^{-11}
8.	3.3456	10.10	8.90	3.618	1.833×10^{-10}	7.941×10^{-6}	1.461×10^{-9}
9.	3.1701	10.55	9.64	6.448	8.600×10^{-11}	4.365×10^{-5}	4.067×10^{-9}
10.	2.8296	10.87	10.58	6.546	2.416×10^{-12}	3.802×10^{-4}	5.430×10^{-9}
11.	3.6828	7.65	7.24	3.537	1.711×10^{-10}	1.740×10^{-7}	2.953×10^{-11}
12.	2.6786	6.55	6.82	4.309	1.756×10^{-10}	--	--
13.	2.4706	5.65	6.70	3.866	2.275×10^{-10}	--	--
14.	2.5704	4.13	5.85	2.470	3.360×10^{-10}	--	--

Table XIX

Effect of pH on the Adsorption of NaOl on Zircon.

Initial NaOl Concentration: 3.29×10^{-4} mole/lit.

Sl. No.	Wt. of Solid (gms.)	Initial pH	Final pH	Final NaOl Concn. (mole/lit. $\times 10^{4}$)	NaOl Adsorbed mole/cm^2	(OH^-) Final Concn. mole/lit.	(OH) Adsorbed mole/cm^2
1.	3.9930	9.30	8.68	1.237	1.064×10^{-10}	4.787×10^{-6}	1.571×10^{-10}
2.	3.2486	9.82	9.14	2.039	7.975×10^{-11}	1.380×10^{-5}	6.665×10^{-10}
3.	2.7596	10.43	10.00	3.204	4.504×10^{-11}	1.000×10^{-4}	2.539×10^{-9}
4.	3.3031	10.62	10.28	2.861	2.681×10^{-11}	1.905×10^{-4}	2.839×10^{-9}
5.	4.1738	7.88	7.26	0.633	1.318×10^{-10}	1.819×10^{-7}	5.731×10^{-12}
6.	3.2802	7.25	6.95	0.929	1.490×10^{-10}	8.914×10^{-8}	1.119×10^{-12}
7.	2.8024	10.13	8.15	0.970	1.714×10^{-10}	1.412×10^{-6}	1.551×10^{-9}
8.	3.1896	8.90	7.80	0.657	1.709×10^{-10}	6.308×10^{-7}	9.495×10^{-11}
9.	3.3176	10.94	10.50	0.306	1.437×10^{-11}	3.163×10^{-4}	6.918×10^{-9}
10.	2.8276	5.95	6.65	1.196	1.314×10^{-10}	--	--

Table XX

Effect of pH on the Adsorption of Na Oleate on Zircon

Initial NaOl Concentration: 4.93×10^{-4} mole/lit.

Sl. No.	Wt. of Solid (gms.)	Initial pH	Final pH	Final NaOl Concn. (Mole/lit. $\times 10^{-4}$)	NaOl Adsorbed mole/cm^2	(OH^-)ions Final Concn. mole/lit.	(OH)ions Adsorbed Mole/cm^2
1.	3.5716	8.53	7.38	1.496	2.050×10^{-10}	2.399×10^{-7}	3.651×10^{-11}
2.	3.6004	9.10	7.72	0.773	2.394×10^{-10}	5.250×10^{-7}	1.388×10^{-10}
3.	3.5126	9.65	8.26	0.882	2.424×10^{-10}	1.819×10^{-6}	5.049×10^{-10}
4.	2.9746	10.18	8.94	2.056	2.004×10^{-10}	8.711×10^{-6}	1.986×10^{-9}
5.	2.6264	10.45	9.26	3.289	1.296×10^{-10}	1.819×10^{-5}	4.159×10^{-9}
6.	3.5196	10.66	9.80	4.111	4.840×10^{-11}	6.308×10^{-5}	4.635×10^{-9}
7.	3.0266	10.85	10.28	3.947	6.753×10^{-11}	1.905×10^{-4}	8.041×10^{-9}
8.	3.9647	6.90	7.00	2.632	1.202×10^{-10}	--	--
9.	3.8324	5.50	6.40	2.302	1.423×10^{-10}	--	--
10.	3.1866	10.28	8.60	1.727	2.084×10^{-10}	3.981×10^{-6}	2.124×10^{-9}

Table XXI

Effect of pH on the Adsorption of Sodium Oleate on Zircon

Initial NaOl Concentration: 2.302×10^{-4} mole/lit.

Sl. No.	Wt.of Solid (gms.)	Initial pH	Final pH	Final NaOl Concn. (mole/lit.x10^{4}	NaOl Adsorbed mole/cm^2	(OH^-)ions Final Concn. mole/lit	(OH) ions Adsorbed mole/cm^2
1.	3.0332	8.00	7.10	0.937	9.324×10^{-11}	1.259×10^{-7}	1.194×10^{-11}
2.	3.3811	8.68	7.28	0.526	1.088×10^{-10}	1.905×10^{-7}	5.626×10^{-11}
3.	4.9411	10.00	8.02	0.773	6.409×10^{-11}	1.047×10^{-6}	8.301×10^{-10}
4.	3.6146	9.05	7.68	0.542	1.008×10^{-10}	4.787×10^{-6}	7.370×10^{-11}
5.	3.7126	10.55	9.84	2.253	2.754×10^{-12}	6.920×10^{-5}	3.187×10^{-9}
6.	3.3206	5.15	6.35	1.365	5.848×10^{-11}	--	--
7.	3.3558	4.32	5.82	1.151	5.641×10^{-11}	--	--
8	2.9720	10.68	9.80	--	--	6.308×10^{-5}	5.792×10^{-9}
9.	2.7578	9.70	7.70	6.907	1.210×10^{-10}	5.012×10^{-7}	7.452×10^{-10}
10.	3.2926	10.35	9.45	2.302	--	2.819×10^{-5}	2.460×10^{-9}

Table XXII

Effect of Temperature on the Adsorption of NaOl on Zircon at Constant Initial pH.

Initial NaOl Concentration: 3.289×10^{-4} mole/lit.

Sl. No.	Weight of sample	Initial pH	Final pH	Temperature $^{\circ}C$	Final NaOl Concn. (mole/lit.$\times 10^{-4}$)	Adsorption mole/cm^2
1.	3.5906	6.02	6.70	25.5	1.431	1.486×10^{-10}
2.	3.6849	8.45	7.18	25.5	0.937	1.322×10^{-10}
3.	3.9624	9.55	7.65	25.5	0.617	1.377×10^{-10}
4.	3.1166	6.02	6.64	30.0	0.773	1.671×10^{-10}
5.	3.0326	8.48	7.26	30.0	0.625x1	1.821×10^{-10}
6.	3.8300	9.52	7.61	30.0	0.724	1.385×10^{-10}
7.	3.3361	6.02	6.72	35.0	2.237	9.191×10^{-11}
8.	3.2730	8.48	7.52	35.0	1.266	1.035×10^{-11}
9.	3.8836	9.60	8.00	35.0	1.809	1.098×10^{-10}
10.	3.4630	8.52	7.40	40.0	1.513	6.292×10^{-11}
11.	4.0706	9.55	7.75	40.0	1.345	6.947×10^{-11}

Table XXIII

Adsorption of NaF on Zircon at Constant Initial pH 9.1 ± 0.5

Sl. No.	Weight of zircon (gms)	Initial pH	Final pH	NaF concentration (mole/lit)	(mg/l)	NaF Adsorbed (mole/cm^2)
1.	2.5582	9.10	7.35	2.381×10^{-4}	2.191×10^{-4}	1.543×10^{-11}
2.	2.5056	9.10	7.10	5.526×10^{-4}	9.048×10^{-4}	3.938×10^{-11}
3.	2.8239	9.12	7.65	1.191×10^{-3}	1.131×10^{-3}	4.351×10^{-11}
4.	2.9051	9.08	7.35	2.381×10^{-3}	2.191×10^{-3}	1.358×10^{-10}
5.	2.2438	9.14	7.49	2.858×10^{-3}	2.286×10^{-3}	5.278×10^{-10}
6.	2.9433	9.15	7.44	3.572×10^{-3}	2.619×10^{-3}	6.702×10^{-10}

Table XXIV

Adsorption of Sodium Fluoride at Constant Sodium Oleate Concentration

Initial Sodium Oleate Concentration: 4.934×10^{-4} mole/lit

Sl. No.	Weight of solid (gms.)	Initial pH	Final pH	NaF Concentration (mole/lit)	NaOl Adsorbed (mole/cm^2)	NaF Adsorbed (mole/cm^2)
			Initial pH Constant at 10.3 ± 0.1			
1.	2.9746	10.18	8.94	0.00	2.004×10^{-10}	0.00
2.	3.7234	10.34	8.18	2.381×10^{-4}	2.082×10^{-10}	--
3.	3.4836	10.18	8.15	4.762×10^{-4}	1.926×10^{-10}	2.123×10^{-11}
4.	2.2572	10.40	9.25	9.526×10^{-4}	1.736×10^{-10}	2.185×10^{-11}
5.	3.4600	10.34	9.15	1.191×10^{-3}	1.525×10^{-10}	4.986×10^{-11}
6.	2.9381	10.30	9.83	1.666×10^{-3}	7.308×10^{-11}	1.174×10^{-11}
			Initial pH Constant at 10.5 ± 0.1			
7.	2.6264	10.45	9.26	0.00	1.296×10^{-10}	0.00
8.	2.1848	10.52	9.84	7.145×10^{-4}	1.450×10^{-10}	7.740×10^{-11}
9.	2.8452	10.55	9.52	9.526×10^{-4}	1.308×10^{-10}	--
10.	2.5543	10.53	9.62	1.429×10^{-3}	1.096×10^{-10}	2.898×10^{-11}
11.	2.7755	10.53	9.52	1.905×10^{-3}	6.223×10^{-11}	1.423×10^{-10}
12.	2.7872	10.45	9.50	2.143×10^{-3}	7.638×10^{-11}	2.124×10^{-10}
13.	2.4154	10.60	9.36	2.381×10^{-3}	5.250×10^{-11}	3.146×10^{-10}

Table XX

Adsorption of Sodium Oleate and Sodium Fluoride at Constant Final pH 9.7 ± 0.15

Initial Sodium Oleate Concentration: 4.934×10^{-4} moles/lit

Sl. No.	Weight of the solid (gms.)	Initial	Final	NaF Concentration (mole/lit)	NaOl Adsorption (mole/cm^2)	NaF Adsorbed (mole/cm^2)
1.	3.5196	10.66	9.80	0.00	4.840×10^{-11}	0.00
2.	3.2867	10.62	9.76	2.381×10^{-4}	5.445×10^{-11}	4.765×10^{-11}
3.	2.4871	10.60	9.58	4.762×10^{-4}	7.257×10^{-11}	--
4.	2.1848	10.52	9.84	7.145×10^{-4}	1.450×10^{-10}	4.740×10^{-11}
5.	2.8452	10.55	9.52	9.526×10^{-4}	1.308×10^{-10}	--
6.	2.5543	10.53	9.62	1.429×10^{-3}	1.096×10^{-10}	2.898×10^{-11}
7.	2.9381	10.30	9.83	1.666×10^{-3}	7.308×10^{-11}	1.174×10^{-10}
8.	2.7731	10.53	9.52	1.905×10^{-3}	6.223×10^{-11}	1.443×10^{-10}

Table XXVI

Adsorption of Sodium Silicate on Zircon at Constant Initial pH 9.2 ± 0.05

Sl. No.	Weight of solid (gms.)	Initial pH	Final pH	Na_2SiO_3 Concentration (mole/lit)	Na_2SiO_3 Adsorbed (mole/cm^2)
1.	1.9806	9.21	6.88	7.142×10^{-5}	2.465×10^{-11}
2.	2.4262	9.23	6.96	2.142×10^{-4}	4.634×10^{-11}
3.	2.6162	9.23	7.14	4.285×10^{-4}	6.061×10^{-11}
4.	2.8206	9.23	7.16	6.427×10^{-4}	6.087×10^{-11}
5.	2.1270	9.25	7.36	8.570×10^{-4}	6.153×10^{-11}
6.	2.8554	9.25	7.64	1.142×10^{-3}	7.463×10^{-11}
7.	4.0029	9.25	7.42	1.429×10^{-3}	8.582×10^{-11}

Table XXVII

Adsorption of Sodium Oleate and Sodium Silicate at Constant Initial pH 9.0 ± 0.05

Initial Sodium Oleate Concentration: 3.289×10^{-4} mole/lit

Sl. No.	Weight of Solid (gms.)	Initial pH	Final pH	Na_2SiO_3 Concentration (mole/lit)	NaOl Adsorbed (mole/cm^2)	Na_2SiO_3 Adsorbed (mole/cm^2)
1.	3.5219	8.96	7.52	0.00	1.249×10^{-10}	0.00
2.	3.0347	9.00	7.74	7.142×10^{-4}	1.155×10^{-10}	8.078×10^{-11}
3.	3.2811	9.05	7.90	1.429×10^{-3}	1.038×10^{-10}	6.313×10^{-11}
4.	4.2748	8.95	7.52	7.142×10^{-5}	8.966×10^{-11}	3.806×11^{-9}
5.	3.2669	9.05	7.75	2.142×10^{-4}	1.113×10^{-10}	3.442×10^{-11}
6.	3.3514	8.98	7.67	3.572×10^{-4}	1.009×10^{-10}	3.403×10^{-11}
7.	3.3279	9.03	7.85	4.999×10^{-4}	1.034×10^{-10}	2.246×10^{-11}
8.	3.4584	9.06	8.42	2.142×10^{-3}	3.942×10^{-11}	--
9.	3.2016	9.04	8.54	2.857×10^{-3}	3.726×10^{-11}	1.769×10^{-1}
10.	3.8392	9.01	8.28	2.500×10^{-3}	--	--
11.	3.7630	9.05	8.50	3.572×10^{-3}	--	4.811×10^{-9}

Table XXIX

Adsorption of Sodium Oleate and Sodium Silicate at Constant Initial pH 10.00 + 0.1

Initial Sodium Oleate Concentration: 4.934×10^{-4} mole/lit

Sl. No.	Weight of Solid (gms)	Initial pH	Final pH	Na_2SiO_3 Concentration (mole/lit)	NaOl Adsorbed (mole/cm^2)	Na_2SiO_3 Adsorbed (mole/cm^2)
1.	2.9746	10.08	8.94	0.00	2.004×10^{-10}	0.00
2.	3.0739	10.01	8.60	2.142×10^{-4}	1.857×10^{-10}	1.013×10^{-10}
3.	2.9198	9.91	9.07	3.572×10^{-4}	1.339×10^{-10}	1.554×10^{-10}
4.	3.4062	10.14	9.65	4.285×10^{-4}	1.050×10^{-10}	--
5.	2.1946	10.04	9.59	5.714×10^{-4}	1.242×10^{-10}	--
6.	2.6526	9.99	9.81	7.142×10^{-4}	9.632×10^{-11}	2.052×10^{-10}

Table XXX

Adsorption of Sodium Silicate and Sodium Oleate at Constant Final pH

Initial Na Oleate Concentration: 4.93×10^{-4} mole/lit

Sl. No.	Wt. of Solid (gms)	Initial pH	Final pH	Na_2SiO_3 Concentration (mole/lit)	NaOl Adsorbed (mole/cm^2)	Na_2SiO_3 Adsorbed (mole/cm^2)
			Final pH 9.45 ± 0.1			
1.	2.5836	10.79	9.44	0.00	1.701×10^{-10}	0.00
2.	3.0146	10.49	9.46	7.142×10^{-5}	1.835×10^{-10}	1.403×10^{-11}
3.	2.1946	10.04	9.50	5.714×10^{-4}	1.242×10^{-10}	0.00
4.	2.6486	9.90	9.303	8.570×10^{-4}	1.222×10^{-10}	1.823×10^{-10}
5.	2.4961	9.92	9.43	1.285×10^{-3}	1.293×10^{-10}	0.00
6.	2.6652	10.00	9.52	1.429×10^{-3}	0.00	1.999×10^{-10}
			Final pH 9.85 ± 0.1			
7.	3.5196	10.66	9.80	0.00	4.840×10^{-11}	0.00
8.	3.3380	10.46	9.77	1.429×10^{-4}	1.181×10^{-10}	0.00
9.	2.9790	10.34	9.91	2.142×10^{-4}	9.603×10^{-11}	5.389×10^{-11}
10.	2.6526	9.99	9.80	7.142×10^{-4}	9.632×10^{-11}	2.052×10^{-10}
11.	3.1590	10.00	9.89	1.071×10^{-3}	1.106×10^{-10}	2.061×10^{-10}

Table XXXI

Adsorption of Sodium Oleate in the Presence of Sodium Fluosilicate at Constant Initial pH 9.0±0.1

Initial Sodium Oleate Concentration: 4.94×10^{-4} mole/lit.

Sl. No.	Wt. of Zircon (gms.)	Initial pH	Final pH	Na_2SiF_6 Concentration (Mole/lit)	Na Oleate Adsorbed (Mole/cm^2)
1.	3.6004	9.10	7.72	0.00	2.39×10^{-10}
2.	2.8080	9.08	8.48	5.319×10^{-5}	2.184×10^{-10}
3.	3.2166	9.02	8.60	1.064×10^{-4}	1.271×10^{-10}
4.	3.0429	9.00	8.30	1.596×10^{-4}	1.426×10^{-10}
5.	2.8916	8.95	7.70	2.128×10^{-4}	1.272×10^{-10}
6.	2.4266	8.96	8.30	2.659×10^{-4}	1.152×10^{-10}
7.	2.5574	9.00	8.04	3.192×10^{-4}	7.379×10^{-11}

APPENDIX F

ELECTROKINETIC MEASUREMENTS

Table XXXII

Effect of pH on the Electrokinetic Properties of Zircon

Variable Total Ionic Concentration

Sl.No.	Initial pH	Electrophoretic mobility (microns)	Zeta Potential (m volts)
1.	3.67	--1.928	- 25.05
2.	4.00	- 1.232	- 15.94
3.	4.22	- 0.8307	- 10.79
4.	4.40	- 0.4291	- 5.575
5.	4.62	- 1.113	- 14.45
6.	5.45	- 0.9471	- 12.31
7.	6.40	- 0.727	- 9.454
8.	7.16	- 1.452	- 18.87
9.	9.06	- 1.616	- 21.01
10.	9.73	- 6.017	- 78.21
11.	9.90	-11.24	-146.2
12.	10.06	-11.60	-150.7
13.	10.10	- 9.131	-106.4
14.	10.20	-11.68	-151.8
15.	10.42	-13.96	-181.4
16.	10.55	-12.78	-166.2

The electrophoretic mobility is expressed as microns sec^{-1}/volts cm^{-1}. It will be referred as 'microns' in subsequent chapters.

Table XXXIII

Effect of pH on the Electrokinetic Properties of Zircon at Constant KCl Concentration

Sl. No.	Final pH	Electrophoretic Mobility (microns)	Zeta Potential (m volts)
	KCl Concentration:	1.0×10^{-3} M	
1.	2.64	- 8.407	-109.30
2.	3.75	- 3.527	- 45.85
3.	4.30	- 2.916	- 37.90
4.	6.15	- 1.959	- 25.46
5.	9.45	- 2.969	- 38.59
6.	9.43	- 4.93	- 64.08
7.	10.00	- 5.96	- 77.46
8.	10.41	- 6.57	- 85.45
	KCl Concentration:	5.0×10^{-3} M	
9.	6.91	- 9.084	-118.10
10.	8.01	- 7.257	- 94.34
11.	8.10	- 7.466	- 97.05
12.	9.81	- 9.954	-129.30
13.	10.31	-13.16	-171.10

Table XXXIV

Effect of KCl Addition on the Electrokinetic Properties of Zircon

Sl. No.	Concentration of KCl (mole/lit.)	Final pH	Electro-phoretic mobility (microns)	Zeta Potential (m Volts)
1.	0.00	6.55	-0.312	- 4.062
2.	2.0×10^{-4}	6.50	-3.859	-50.17
3.	1.0×10^{-3}	6.60	-4.188	-54.44
4.	5.0×10^{-3}	6.50	-5.616	-73.00
5.	1.0×10^{-2}	6.32	-6.630	-86.18

Table XXXV

Effect of NaF Addition on the Electrokinetic Properties of Zircon at Constant pH.

Final pH - 9.00

Sl. No.	NaF Concentration	Final pH	Electrophoretic Mobility (microns)	Zeta Potential (m volts)
1.	0.00	9.02	- 1.608	- 20.90
2.	4.005×10^{-4}	9.05	- 1.698	- 22.07
3.	2.381×10^{-3}	9.00	- 3.521	- 45.77
4.	2.858×10^{-3}	8.95	- 4.440	- 57.72
5.	3.573×10^{-3}	9.05	-10.33	-134.3
6.	4.762×10^{-3}	8.98	-12.27	-159.5

Table XXXVI

Effect of the Concentration of Na_2SiO_3 on the Electrokinetic Properties of Zircon at Constant pH.

Final pH - 9.04 ± 0.05

Sl. No.	Na_2SiO_3 Concentration	Final pH	Electrophoretic Mobility (microns)	Zeta Potential (m volts)
1.	0.00	9.02	-1.608	-20.90
2.	1.429×10^{-4}	9.08	-1.684	-21.89
3.	2.859×10^{-4}	9.09	-1.682	-21.65
4.	7.142×10^{-4}	9.04	-3.973	-51.64
5.	1.071×10^{-4}	9.06	-5.685	-73.99
6.	1.429×10^{-3}	9.06	-5.255	-68.31

Table XXXVII

Effect of the Concentration of Na_2SiF_6 on the Zeta Potential of Zircon

Sl. No.	Na_2SiF_6 Concentration	Final pH	Electro-phoretic Mobility (micron)	Zeta Potential (m volts)
1.	0.00	9.02	-1.608	- 20.90
2.	7.945×10^{-5}	8.95	-1.918	- 24.93
3.	1.117×10^{-4}	8.98	-2.434	- 31.64
4.	1.595×10^{-4}	9.00	-2.353	- 30.59
5.	2.390×10^{-4}	8.96	-2.794	- 36.32
6.	3.190×10^{-4}	8.98	-3.351	- 43.30

Table XXXVIII

Effect of Na Oleate Concentration on the Electrokinetic Properties of Zircon at Constant pH 9.0 ± 0.05

Sl. No.	Na Oleate Concentration (mole/lit.)	Final pH	Electrophoretic Mobility (Microns)	Zeta Potential (m volts)
1.	0.000	09.02	- 1.638	- 21.30
2.	0.000	9.06	- 1.643	- 21.35
3.	4.111×10^{-5}	9.04	- 3.040	- 39.52
4.	1.052×10^{-4}	9.06	- 2.874	- 37.36
5.	2.056×10^{-4}	8.98	- 5.078	- 66.01
6.	4.111×10^{-4}	9.05	- 7.649	- 99.43
7.	6.167×10^{-4}	8.99	- 8.554	-111.20
8.	1.028×10^{-3}	9.02	-10.620	-138.00
9.	2.056×10^{-3}	8.97	- 8.35	-108.60
10.	3.467×10^{-3}	9.04	- 7.004	- 91.03

Table XXXIX

Effect of Na Oleate Addition on the Electrokinetic Properties of Zircon at Constant pH

pH : 9.95 ± 0.05

Sl. No.	Na Oleate Concentration Mole/lit	Final pH	Electrophoretic Mobility (microns)	Zeta Potential (m volts)
1.	0.000	9.94	- 5.645	- 73.38
2.	4.111×10^{-5}	9.98	- 5.761	- 74.85
3.	2.056×10^{-4}	9.94	-10.350	-134.6
4.	6.167×10^{-4}	9.95	-12.850	-167.0
5.	1.028×10^{-3}	9.92	-13.03	-169.3
6.	1.253×10^{-3}	10.00	-10.40	-135.2
7.	1.644×10^{-3}	9.92	- 8.782	-114.1

Table XL

Effect of pH on the Electrokinetic Properties of Zircon at Constant Sodium Oleate Addition

Sl. No.	Final pH	Electrophoretic Mobility (microns)	Zeta Potential (m volts)
		NaOl Concentration: 6.579×10^{-4} mole/lit	
1.	7.90	- 6.351	- 82.55
2.	9.25	- 8.722	-113.40
3.	8.50	- 7.563	- 98.28
4.	9.02	- 8.828	-114.8
5.	9.03	- 8.660	-112.6
6.	9.53	- 9.196	-119.5
7.	9.98	-13.96	-181.4
8.	10.58	-14.38	-186.8
9.	10.72	-15.33	-199.4
10.	10.10	-11.33	-147.3
11.	9.82	-10.79	-140.3
12.	10.59	-14.32	-186.1
		NaOl Concentration: 4.111×10^{-4} mole/lit.	
13.	8.67	- 5.766	- 74.94
14.	9.00	- 7.500	- 97.47
15.	9.35	- 8.708	-113.2
16.	9.90	- 9.987	-129.8
		NaOl Concentration: 1.973×10^{-4} mole/lit.	
17.	8.35	- 4.634	- 60.24
18.	9.20	- 5.559	- 72.26
19.	10.10	- 7.625	- 99.10
20.	10.28	-13.93	-181.09
21.	10.20	- 8.843	-114.9
22.	10.42	-12.36	-160.6

Table XLI

Effect of Sodium Fluoride Addition on the Electrokinetic Properties of Zircon at Constant Sodium Oleate Addition.

Sl. No.	NaF Concentration (mole/lit)	pH	Electrophoretic Mobility (Microns)	Zeta Potential (m volts)
	NaOl Concentration: 6.579×10^{-4} mole/lit.			
		Initial pH		
1.	0.000	9.00	- 6.601	- 85.80
2.	2.977×10^{-4}	8.92	- 7.295	- 94.82
3.	5.954×10^{-4}	8.88	- 7.433	- 96.63
4.	7.619×10^{-4}	8.98	- 7.696	-100.02
5.	1.286×10^{-3}	9.00	- 7.702	-100.1
6.	1.905×10^{-3}	8.88	- 7.711	-100.23
7.	3.810×10^{-3}	8.97	- 7.766	-100.95
8.	5.954×10^{-3}	9.00	- 9.988	-129.84
	NaOl Concentration: 4.934×10^{-4} mole/lit.			
		Final pH		
9.	4.762×10^{-4}	9.70	-10.49	-136.3
10.	9.524×10^{-4}	9.68	-11.85	-154.00
11.	1.905×10^{-3}	9.74	-15.24	-198.4
12.	3.095×10^{-3}	9.72	-20.21	-262.7

Table XLII

Effect of Sodium Silicate Addition on the Electro-Kinetic Properties of Zircon at Constant Sodium Oleate Addition.

Sl.No.	Concentration of Na_2SiO_3 (mole /lit.)	Final pH	Electro-phoretic Mobility (Microns)	Zeta Potential (m volts)
	NaOl Concentration: 4.934×10^{-4} mole/lit.			
1.	0.000	9.51	-12.35	-160.5
2.	5.714×10^{-5}	9.53	-13.02	-169.5
3.	1.429×10^{-4}	9.53	-16.55	-215.0
4.	5.716×10^{-4}	9.46	-14.28	-185.6
5.	7.142×10^{-4}	9.54	-13.72	-182.4
6.	8.568×10^{-4}	9.52	-12.31	-160.0
7.	9.998×10^{-4}	9.58	-11.45	-148.8
8.	1.285×10^{-3}	9.55	-11.62	-151.1
	NaOl Concentration: 6.579×10^{-4} mole/lit.			
9.	0.00	9.00	- 6.601	- 85.80
10.	7.142×10^{-5}	8.98	- 7.013	- 91.16
11.	2.142×10^{-4}	9.00	- 8.782	-114.10
12.	4.284×10^{-4}	9.04	- 9.290	-120.10
13.	7.142×10^{-4}	9.00	- 8.281	-107.65
14.	1.428×10^{-3}	9.00	- 8.151	-105.95

Table XLIII

Effect of Sodium Fluosilicate Addition on the Electro-Kinetic Properties of Zircon at Constant Na Oleate Concentration.

Sl. No.	Na_2SiF_6 Concentration (mole/lit)	Final pH	Electrophoretic Mobility (microns)	Zeta Potential (m volts)
	NaOl Concentration: 3.948×10^{-4} mole/lit.			
1.	0.000	9.00	- 6.601	- 86.00
2.	7.979×10^{-6}	9.04	- 9.204	-119.65
3.	1.595×10^{-5}	9.06	- 9.988	-129.84
4.	1.117×10^{-4}	9.02	- 9.221	-119.86
5.	1.595×10^{-4}	9.01	- 8.151	-105.95
6.	3.989×10^{-4}	8.95	- 7.780	-101.12
	NaOl Concentration: 6.579×10^{-4} mole/lit.			
7.	0.00	9.06	- 7.163	- 93.09
8.	4.255×10^{-5}	9.06	-11.91	-154.6
9.	8.510×10^{-5}	9.05	-18.69	-243.0
10.	1.489×10^{-4}	9.05	-13.20	-171.6
11.	2.553×10^{-4}	9.03	-11.92	-155.0
12.	7.446×10^{-4}	9.01	- 6.412	- 83.52

APPENDIX G

FREQUENCY ASSIGNMENTS FOR OLEIC ACID AND SODIUM OLEATE

Table XLIV

Sl. No.	Adsorption bands s Oleic Acid	Sodium Oleate	Assignment
1.	1708	--	C=O stretching of COOH group dimer.
2.	--	1545	Anti-symmetrical C=O of salt oleic acid
3.	--	1450	Symmetrical C=O of salts of oleic acid.
4.	920-960	930-940	OH deformation out of plane
5.	720	720	Rocking Mode of CH_2 groups.
6.	Not resolved	1180-1350	Band Progression series due to wagging of CH_2 groups.
7.	3100	3100	Stretching vibrations of C=C-H carbon-hydrogen bond.
8.	2920	2920	CH_3 Methylene vibration.

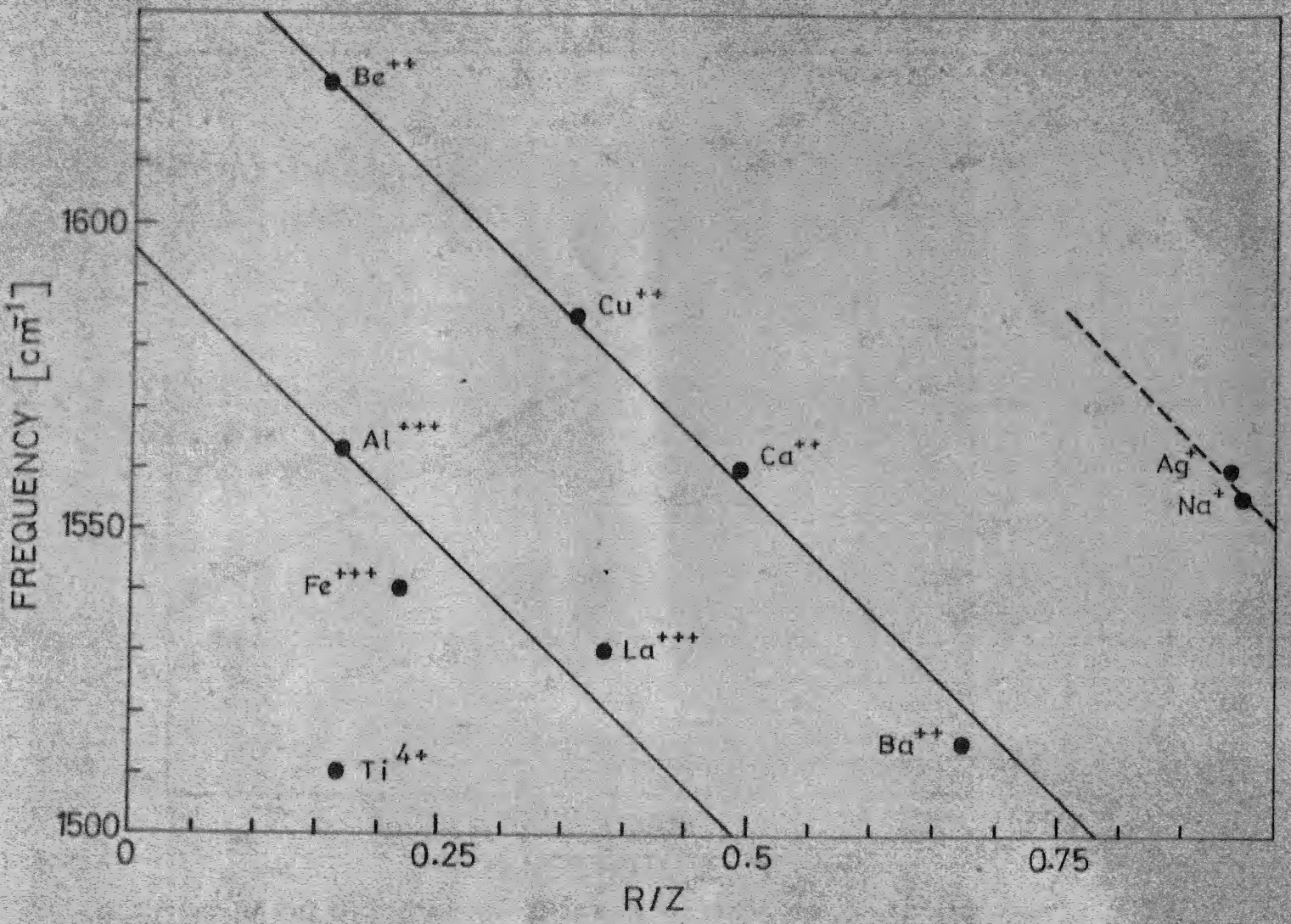

FIGURE 73 VARIATION OF C=O STRETCHING FREQUENCY WITH R/Z RATIO OF METAL CATIONS IN OLEATES

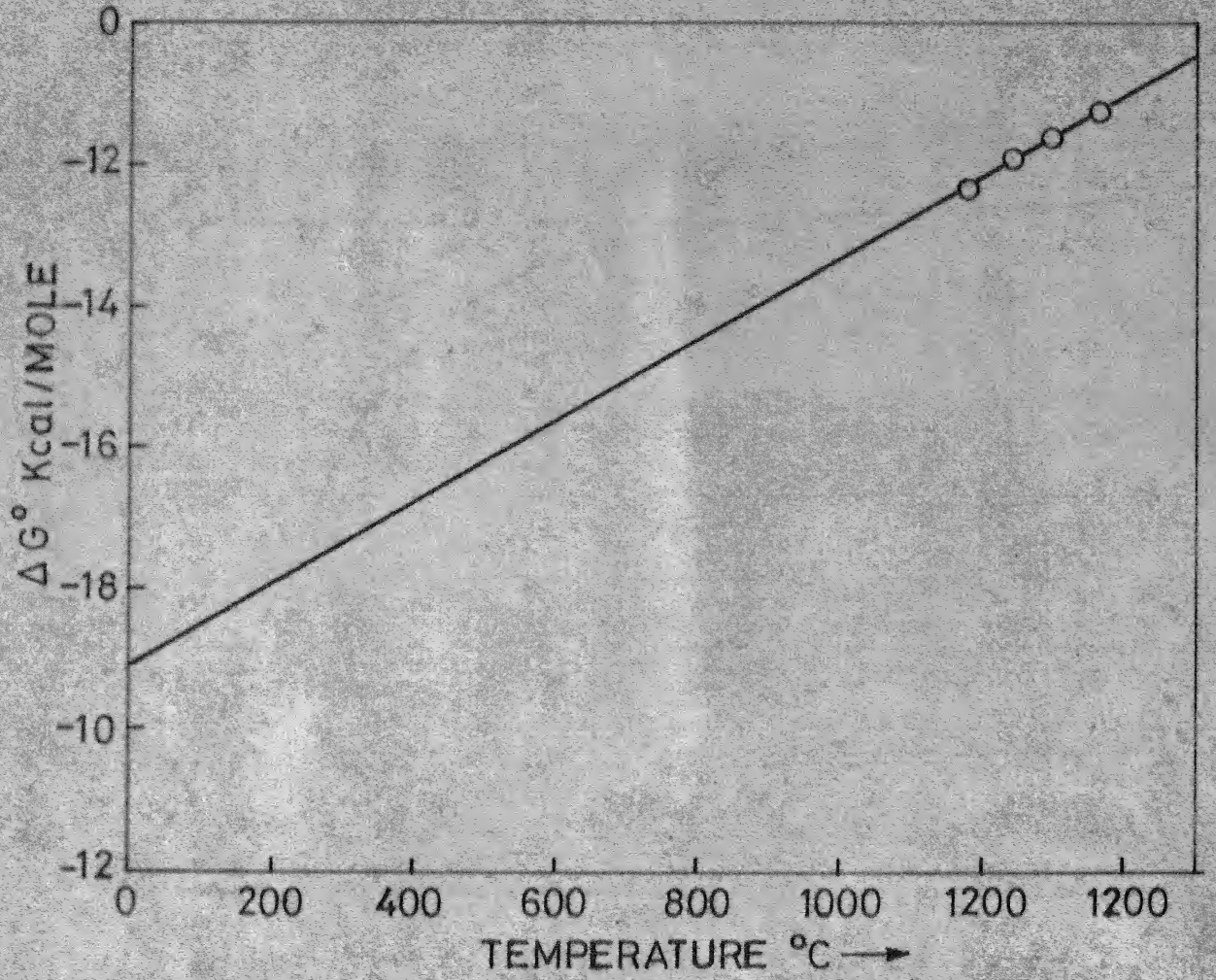

FIGURE 74 VARIATION OF FREE ENERGY CHANGE OF THE REACTION $ZrO_2 + SiO_2 = ZrSiO_4$ WITH TEMPERATURE

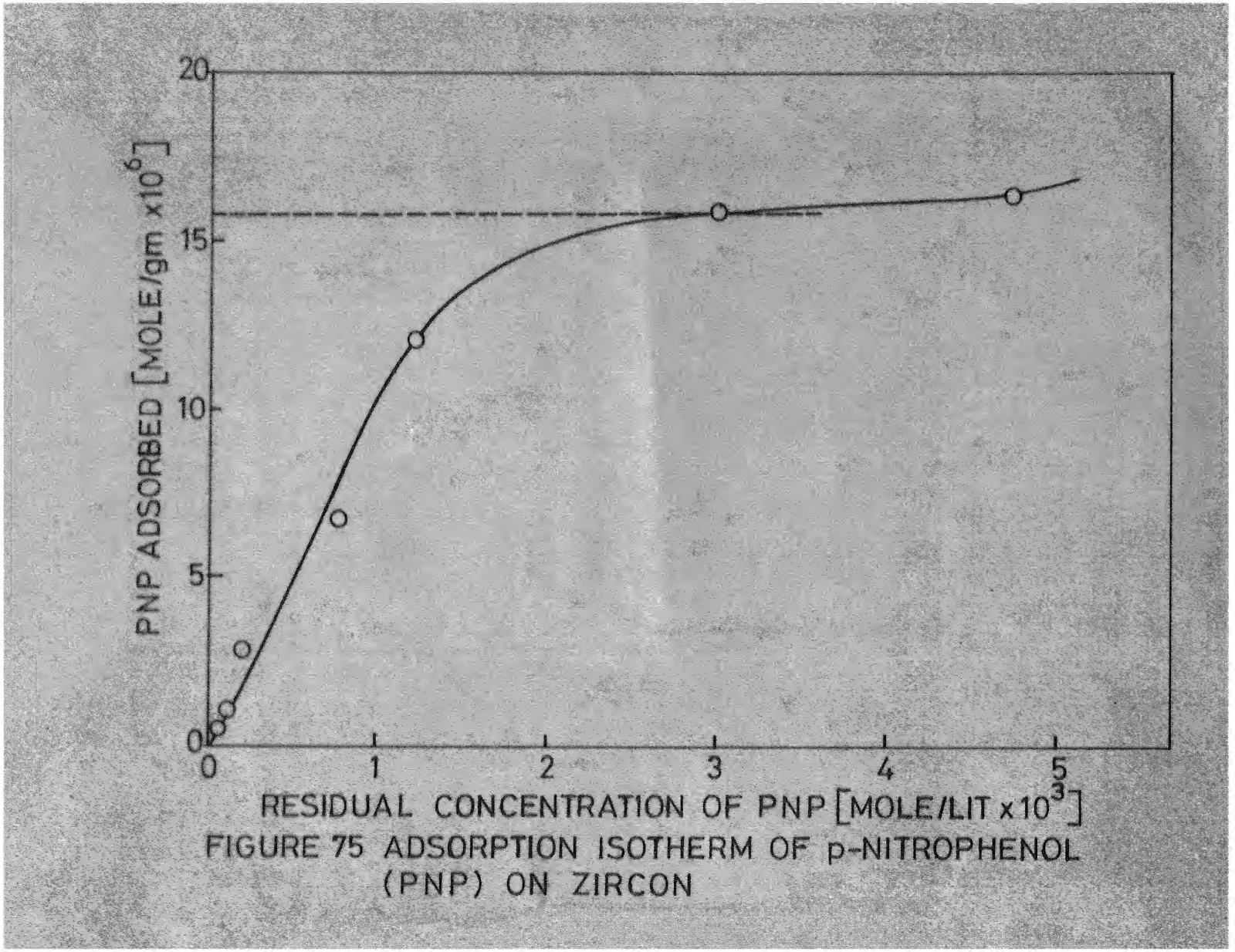

FIGURE 75 ADSORPTION ISOTHERM OF p-NITROPHENOL (PNP) ON ZIRCON

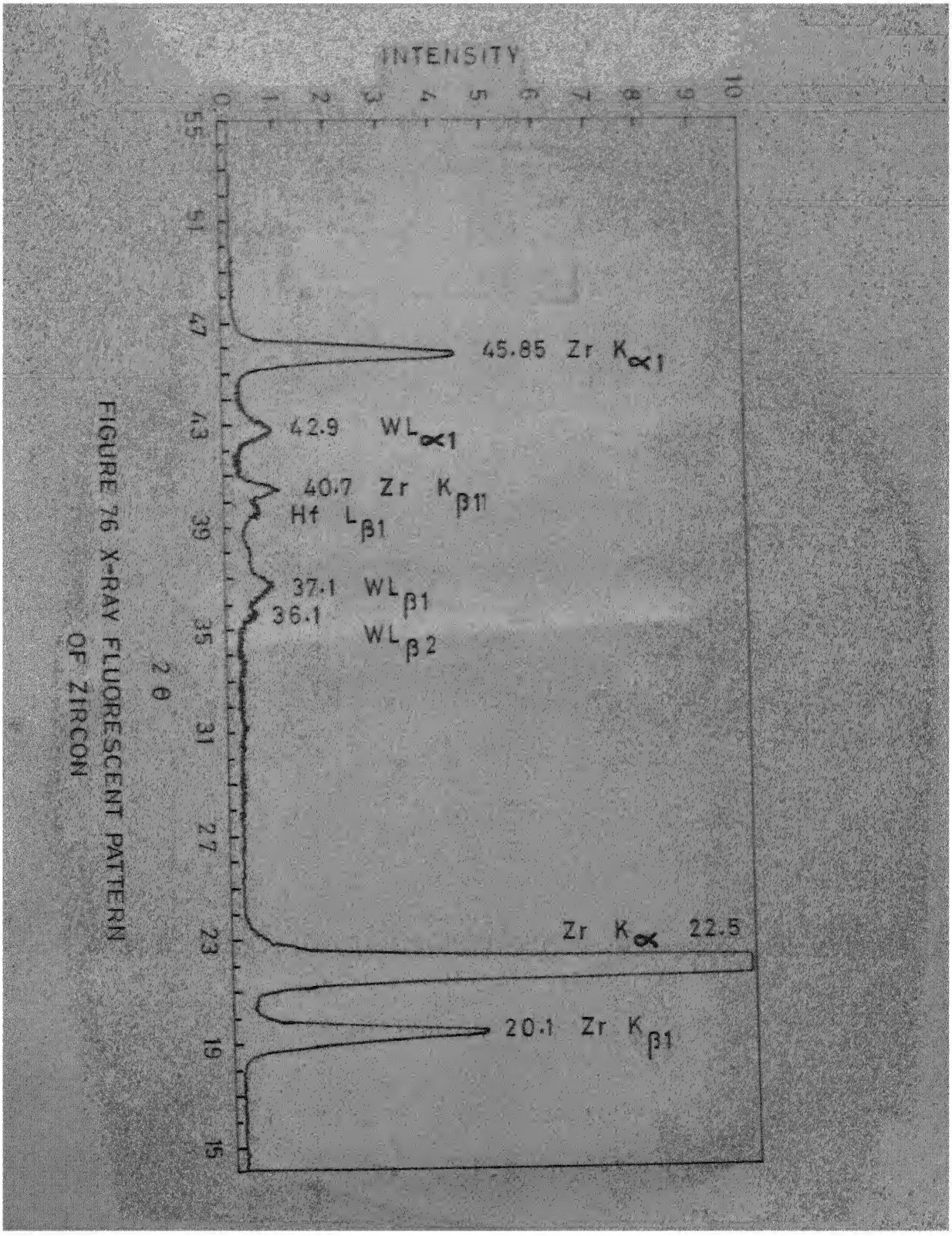

FIGURE 76 X-RAY FLUORESCENT PATTERN OF ZIRCON